

# Northumbria Research Link

Citation: Bassarab, Paul (2010) Novel approaches to the controlled release of Quaternary ammonium-based biocides. Doctoral thesis, Northumbria University.

This version was downloaded from Northumbria Research Link:  
<http://nrl.northumbria.ac.uk/id/eprint/36302/>

Northumbria University has developed Northumbria Research Link (NRL) to enable users to access the University's research output. Copyright © and moral rights for items on NRL are retained by the individual author(s) and/or other copyright owners. Single copies of full items can be reproduced, displayed or performed, and given to third parties in any format or medium for personal research or study, educational, or not-for-profit purposes without prior permission or charge, provided the authors, title and full bibliographic details are given, as well as a hyperlink and/or URL to the original metadata page. The content must not be changed in any way. Full items must not be sold commercially in any format or medium without formal permission of the copyright holder. The full policy is available online: <http://nrl.northumbria.ac.uk/policies.html>



# **Novel Approaches to the Controlled Release of Quaternary Ammonium-based Biocides**

Paul Bassarab

A thesis presented to Northumbria  
University for the degree of Doctor of  
Philosophy

Northumbria University  
Newcastle Upon Tyne

September 2010

*“There is no form of prose more difficult to understand and tedious to read than the average scientific paper.”*

Francis Crick (1995) *The Astonishing Hypothesis: The Scientific Search for the Soul*

# Abstract

The major economic and environmental consequences of unfettered growth of marine organisms (fouling) on any substrate immersed in the marine environment have a global reach. Currently biocidal antifouling coatings are the most widely employed method to control this growth on vessels. These coatings are under increasing legislative scrutiny because they release primarily metal-based biologically active agents (biocides) to deter the fouling, and hence have the potential to persist in some form in the environment.

This thesis explores the potential use of organic salt-based biocides, quaternary ammonium compounds (quats), as new marine biocides which are considered to be environmentally benign due to their short environmental half-lives. Detailed are methodologies to control the release of the quats as well as a new liquid chromatography (LC) mass spectroscopy (MS) analytical method to quantify the quats in seawater.

The primary focus of the controlled release research has been the development of novel quat-polymer systems, which hydrolyze in the presence of seawater to generate biocidal quats *in-situ*. The quat-polymers are synthesised via a free radical polymerisation from different monomers, which are a blend of commercial available film forming monomers and a novel quat-monomer. The preparation of the quat-monomer is also detailed within this thesis. The quat-polymers have been shown to be stable in a prototype antifouling paint formulation and several coatings have been developed which exhibit significantly better antifouling performance than a current commercial product, Intersmooth 460, even after over 1 year with the testing continuing.

The developed LC-MS method utilizes a sample pre-treatment solid phase extraction (SPE) process and is capable of quantifying quats to low parts-per-trillion (ppt) levels in seawater. The method is exceptionally flexible and able to detect a range of commercially available quats simultaneously. The application of this method to the determination of the release rates of the quats from antifouling coatings under standard laboratory conditions is also outlined.

# List of Contents

<b>Abstract</b> .....	<b>i</b>
<b>List of Contents</b> .....	<b>ii</b>
<b>List of Figures</b> .....	<b>vi</b>
<b>List of Schemes</b> .....	<b>xiii</b>
<b>List of Tables</b> .....	<b>xiv</b>
<b>List of Equations</b> .....	<b>xvi</b>
<b>List of Abbreviations</b> .....	<b>xvii</b>
<b>Acknowledgements</b> .....	<b>xxiii</b>
<b>Declaration</b> .....	<b>xxiv</b>
<b>1 Introduction</b> .....	<b>1</b>
<i>1.1 Antifouling</i> .....	<i>1</i>
1.1.1 Overview.....	1
1.1.2 Fouling .....	1
1.1.3 History of Antifoulings .....	6
1.1.4 Organotin Antifoulings .....	9
1.1.5 TBT Ban.....	11
1.1.6 Contemporary Tin-Free Antifoulings .....	12
1.1.7 Organic Booster Biocides .....	17
1.1.8 Alternatives and Future Developments.....	20
<i>1.2 Quaternary Ammonium Compounds</i> .....	<i>23</i>
1.2.1 Introduction.....	23
1.2.2 Antimicrobial Activity .....	24
1.2.3 Environmental Fate and Biodegradation.....	35
1.2.4 Toxicology .....	38
1.2.5 Analysis/Detection.....	41
<i>1.3 Objectives</i> .....	<i>49</i>

<b>2</b>	<b>Quaternary Ammonium-Polymers.....</b>	<b>50</b>
2.1	<i>Post-Quaternisation Polymer Synthesis.....</i>	52
2.1.1	Background.....	52
2.1.2	Quat Methylcarbonate Synthesis.....	53
2.2	<i>Polymer Synthesis.....</i>	54
2.2.1	Development.....	54
2.2.2	Synthesis.....	56
2.3	<i>Paint manufacture.....</i>	56
2.4	<i>Mechanical and Antifouling Testing.....</i>	58
2.4.1	Semi Rapid Boot-Top Cycling.....	58
2.4.2	Polishing Trials.....	60
2.4.3	Antifouling Performance.....	61
2.4.4	Storage Stability.....	64
2.5	<i>Conclusions.....</i>	66
<b>3</b>	<b>Sequential Preparation of Monomer then Polymer 1.....</b>	<b>67</b>
3.1	<i>Monomer Synthesis.....</i>	68
3.2	<i>Polymer Syntheses.....</i>	69
3.3	<i>Paint Formulation and Manufacture.....</i>	71
3.4	<i>Paint Testing.....</i>	72
3.4.1	Semi Rapid Boot-Top Cycling.....	72
3.4.2	Polishing Rate Determination.....	73
3.4.3	Antifouling Performance.....	73
3.4.4	Storage Stability.....	76
3.5	<i>Second Generation Polymers.....</i>	77
3.5.1	Polymer Glass Transition Temperature Determination.....	78
3.6	<i>Second Generation Paint Formulation and Manufacture.....</i>	82
3.7	<i>Second Generation Paint Testing.....</i>	82
3.7.1	Semi Rapid Boot-Top Cycling.....	82
3.7.2	Polishing Rate Determination.....	84
3.7.3	Antifouling Performance.....	86
3.7.4	Storage Stability.....	92

3.8	<i>Conclusions</i> .....	95
<b>4</b>	<b>Sequential Preparation of Monomer then Polymer 2</b> .....	<b>97</b>
4.1	<i>Monomer Synthesis</i> .....	98
4.2	<i>Polymer Syntheses</i> .....	99
4.2.1	Polymer Glass Transition Temperature Determination .....	102
4.2.2	Polymer Free Surface Energy Determination .....	103
4.3	<i>Paint Formulation and Manufacture</i> .....	106
4.4	<i>Paint Testing</i> .....	106
4.4.1	Semi Rapid Boot-Top Cycling.....	106
4.4.2	Polishing Rate Determination .....	107
4.4.3	Antifouling Performance.....	115
4.4.4	Storage Stability .....	129
4.5	<i>Conclusions</i> .....	130
<b>5</b>	<b>Analytical Method Development</b> .....	<b>132</b>
5.1	<i>Initial Instrumentation Evaluation</i> .....	133
5.2	<i>LC-MS Method Development</i> .....	134
5.2.1	Mass Spectrometer Tuning and Ion Identification .....	134
5.2.2	Liquid Chromatography Set up.....	136
5.3	<i>Solid Phase Extraction Development</i> .....	140
5.3.1	Surface Adsorption Test.....	145
5.4	<i>LC-MS Development for Other Quats</i> .....	147
5.5	<i>Development of Leaching Protocol</i> .....	151
<b>6</b>	<b>Quat Leaching Experiment</b> .....	<b>155</b>
6.1	<i>Coating Development</i> .....	155
6.1.1	AMPSQ(I)v10 Paint.....	155
6.1.2	AMPSQ(I)v10 Polymer .....	155
6.1.3	Free Association Didecyl-Quat Paint.....	156

6.1.4	AMPSQ(I)v10 FB Paint.....	157
6.2	<i>Leaching Panel Preparation</i> .....	158
6.3	<i>Leaching Experiment</i> .....	158
6.4	<i>Leach Rate Results</i> .....	160
6.5	<i>Conclusions</i> .....	164
<b>7</b>	<b>Conclusions</b> .....	<b>165</b>
<b>8</b>	<b>Future Work</b> .....	<b>168</b>
<b>9</b>	<b>Appendix 1: Scientific Publication Detailing Analytical Method for the Quantification of Quaternary Ammonium Compounds in Seawater.</b> .....	<b>170</b>
<b>10</b>	<b>Experimental</b> .....	<b>176</b>
10.1	<i>Monomer Precursor Syntheses:</i> .....	176
10.2	<i>Monomer Syntheses:</i> .....	177
10.3	<i>Polymer Syntheses:</i> .....	180
10.4	<i>Paint Manufacture</i> .....	185
10.5	<i>Test Methodology/Procedure</i> .....	188
<b>11</b>	<b>References</b> .....	<b>256</b>

# List of Figures

Figure 1:1: Schematic of fouling growth from Wahl M. (1989).....	2
Figure 1:2: Global ocean surface water temperature .....	4
Figure 1:3: Historical development of antifouling methods .....	7
Figure 1:4: Release profile of free association paint from Gitlitz M, (1981).....	9
Figure 1:5: TBT-SPC biocide release profile from Gitlitz M, (1981) .....	10
Figure 1:6: Representation of biocide release from contact leaching antifouling system <sup>23</sup> .....	13
Figure 1:7: Representation of biocide release from soluble matrix antifouling system <sup>23</sup> .....	14
Figure 1:8: Leach layer development in a soluble matrix system.....	14
Figure 1:9: Representation of biocide release from a tin-free SPC antifouling system <sup>23</sup> .....	15
Figure 1:10: Film thickness depletion and leach layer development of an SPC system.....	15
Figure 1:11: Biocide release profile for contact leaching, soluble matrix and SPC antifouling systems. The “minimum threshold value” indicates the limit below which the release of biocide is too low to prevent fouling <sup>5</sup> .....	16
Figure 1:12: Prolifometry showing the relative smoothness of foul release (left) coating compared to tin free-SPC (right) .....	17
Figure 1:13: Structures zinc/copper pyrithione (1-1 and 1-2) and the five registered organic antifouling biocides - tolylfluanid (1-4), dichlofluanid (1-5), zineb (1-6), irgarol 1051 (1-7) and seanine-211 (1-3) .....	19
Figure 1:14: Structures of diuron (1-8) and chlorothalonil (1-9).....	20
Figure 1:15: Schematic of a generic SPC system .....	23
Figure 1:16: Generic formula of quaternary ammonium compounds.....	23
Figure 1:17: Structure of hexamethylenetetramine (1-20).....	24
Figure 1:18: Generic formula of alkyldimethylbenzylammonium chloride (1-21) .....	25
Figure 1:19: Effect of chain length on the bactericidal activity of benzalkonium chloride <sup>49</sup> .....	25
Figure 1:20: Structures of alkyldimethylethylbenzylammonium chloride (1-22) and dialkyldimethylammonium halide (1-23) .....	26
Figure 1:21: a) General formula of bis-quaternary ammonium salts, b) example of releasable polymeric quat, c) example of a tethered polymeric quat and d) example of a tethered polymeric quat. ....	27
Figure 1:22: Structure of dodecyldimethylbenzylammonium chloride (1-24) .....	28
Figure 1:23: Germicidal activity of linear homologues of alkyldimethylbenzylammonium chloride and octadecenyldimethyl- and dioctylmethyl- modified quat at 20 °C <sup>69</sup> .....	29
Figure 1:24: Structures of alkyldimethylallylammonium (1-25) and alkytrimethylammonium bromides (1-26).....	29
Figure 1:25: Structures of octyldimethylbenzylammonium chloride (1-27) and octadecyldimethylbenzylammonium chloride (1-28) .....	30

Figure 1:26: Structure of poly(vinylbenzyl ammonium chloride) (1-29) .....	32
Figure 1:27: Structures of alkylated poly(4-vinylpyridine) (1-30) and alkylated polyethylenimine (1-31) .....	33
Figure 1:28: Structures of linear alkylbenzene sulphonates (1-32) and alkyl ethoxylates (1-33).....	35
Figure 1:29: Structures of octadecyltrimethylammonium chloride (1-34), hexadecyltrimethylammonium bromide (1-36) and ditallowdimethylammonium halide (1-35) .....	37
Figure 1:30: Structures of hexadecylbenzyltrimethylammonium halide (1-37), hexadecyltrimethylammonium halide (1-38) and dioctadecyltrimethylammonium halide (1-39) .....	40
Figure 1:31: Hofmann degradation .....	42
Figure 1:32: Structures of paraquat (1-40), diquat (1-41) and chlormequat (1-43) .....	46
Figure 2:1: Structure of didecyltrimethylammonium halide (2-1) .....	50
Figure 2:2: Examples of mediated ion exchange reaction of SPCs systems i) copper SPC, and ii) quat SPCs .....	51
Figure 2:3: Structure of trioctyltrimethylammonium halide (2-2) .....	52
Figure 2:4: Structures of didecyltrimethylamine (2-3) and trioctylamine (2-4).....	53
Figure 2:5: Structures of didecyltrimethylammonium (2-5) and trioctyltrimethylammonium (2-6) methylcarbonates .....	54
Figure 2:6: i) <sup>1</sup> H NMR of didecyltrimethylammonium methylcarbonate (2-5) (red) and ii) <sup>1</sup> H NMR of didecyltrimethylamine (2-3) (blue) .....	54
Figure 2:7: Chart displaying change in percentage reaction and reaction temperature profile.....	56
Figure 2:8: Crosslinking of two polymer chains by cupric ion.....	58
Figure 2:9: Example of 'cold flow' from the port side of a commercial vessel.....	60
Figure 2:10: Laser profilometry of two strips from a polishing disk after 60 days testing. The right strip has remained intact and can be analysed. The left strip has become deformed due to cold flow and cannot be analysed. ....	61
Figure 2:11: Example of Latin square antifouling board .....	61
Figure 2:12: RC957 coating polished through to underlying primer .....	63
Figure 2:13: Test Paint antifouling results after 14 weeks immersion. 2483 is RC957Q(I) paint, 2428 is RC957 paint, 2571 is RC957Q(II) paint, 2422 is the matched paint formulation and the standard is Intersmooth 460. ....	63
Figure 2:14: Test Paint antifouling results after 46 weeks immersion. 2483 is RC957Q(I) paint, 2428 is RC957 paint, 2571 is RC957Q(II) paint, 2422 is the matched paint formulation and the standard is Intersmooth 460. ....	64
Figure 2:15: Storage stability of RC957 and RC957Q(I) at 23 and 45 °C. ....	65

Figure 3:1: Schematic of the requirement of a ‘linker’ between the quaternised acid functionality and the functionality for polymerisation. ....	67
Figure 3:2: Structures of mono-2-(methacryloyloxy)ethyl succinate (3-1) and 2-acrylamido-2-methyl-1-propanesulfonic acid (3-2) monomers identified as suitable for quaternisation. ....	68
Figure 3:3: Structures of biocidal MESQ(I) (3-3) and non-biocidal MESQ(II) (3-4) monomers ....	69
Figure 3:4: i) <sup>1</sup> H NMR of final didecyldimethyl quat-monomer solution in xylene (green) (3-3) and its starting materials ii) didecyldimethylammonium methylcarbonate (red) (2-5) and iii) MES acid (blue) (3-1) .....	69
Figure 3:5: Structure of isobornyl methacrylate (3-5) .....	70
Figure 3:6: Example of <sup>1</sup> H NMR of final quat-polymer xylene solution, MESQ(I)v25.....	71
Figure 3:7: Photograph of MESQ(I)25 coating which failed after 6 cycles. The picture shows the corrosion of the coated steel substrate through the extensive cracking of the test coating. ....	72
Figure 3:8: Total film loss over 60 (blue), 90 (yellow) and 120 (white) days immersion .....	73
Figure 3:9: Example of an immersed ‘clear’ Latin square antifouling board .....	73
Figure 3:10: Test Polymers antifouling results. Biocidal polymers 1827 and 1828 are MESQ(I)v25 and MESQ(I)v30 respectively. Non-biocidal polymers 1829 and 1830 are MESQ(II)v25 and MESQ(II)v30 respectively after 16 weeks immersion.....	74
Figure 3:11: Cracking of biocidal polymers MESQ(I)25 .....	74
Figure 3:12: Test Paint antifouling results. Biocidal paints 1772 and 1769 are MESQ(I)v25 and MESQ(I)v30 respectively. Non-biocidal paints 1771 and 1770 are MESQ(II)v25 and MESQ(II)v30 respectively after 27 weeks immersion.....	75
Figure 3:13: Test Paint antifouling results. Biocidal paints 1772 and 1769 are MESQ(I)v25 and MESQ(I)v30 respectively. Non-biocidal paints 1771 and 1770 are MESQ(II)v25 and MESQ(II)v30 respectively after 47 weeks immersion.....	76
Figure 3:14: Test Paint antifouling results. Biocidal paints 1772 and 1769 are MESQ(I)v25 and MESQ(I)v30 respectively. Non-biocidal paints 1771 and 1770 are MESQ(II)v25 and MESQ(II)v30 respectively after 105 weeks immersion.....	76
Figure 3:15: Changes in viscosity of test paints while on storage. ....	77
Figure 3:16: Structures of 2-ethylhexyl methacrylate (3-6), butyl methacrylate (3-7) and lauryl methacrylate (3-8).....	78
Figure 3:17: DSC chart displaying unpronounced and multiple transitions for MESQ(VI)v4 and v7. ....	80
Figure 3:18: Structure of octadecyl methacrylate .....	80
Figure 3:19: MESQ(I)25v4 after 12 semi rapid cycles showing enhanced mechanical properties compared to the first generation coatings, which failed after 6 cycles. ....	83

Figure 3:20: Post test LMA (3-8) paints polishing disk which has the six strips of MESQ(I)25v8, the softest coating, removed also displaying the effects of ‘cold flow’ on MESQ(I)25v9, the first 6 strips. ....	84
Figure 3:21: Total film loss over 60 (blue), 90 (yellow) and 120 (white) days immersion of EHMA (3-6) containing coatings: MESQ(I)25v3 and v4.....	85
Figure 3:22: Total film loss over 60 (blue), 90 (yellow) and 120 (white) days immersion of BMA (3-7) containing coatings: MESQ(I)25v6 and v7.....	85
Figure 3:23: Total film loss over 60 (blue), 90 (yellow) and 120 (white) days immersion of LMA (3-8) containing coatings: MESQ(I)25v10 .....	86
Figure 3:24: EHMA containing polymers antifouling results. Polymer 1827 is MESQ(I)v25 and 2029, 2030 and 2031 are MESQ(I)25v2, 3 and 4 respectively after 17 weeks immersion.....	87
Figure 3:25: BMA containing polymers antifouling results. Polymer 1827 is MESQ(I)v25 and 2032, 2033 and 2034 are MESQ(I)25v5, 6 and 7 respectively after 17 weeks immersion.....	88
Figure 3:26: LMA containing polymers antifouling results. Polymer 1827 is MESQ(I)v25 and 2035, 2036 and 2037 are MESQ(I)25v8, 9 and 10 respectively after 17 weeks immersion.....	88
Figure 3:27: LMA containing polymers antifouling results. Polymer 1827 is MESQ(I)v25 and 2035, 2036 and 2037 are MESQ(I)25v8, 9 and 10 respectively after 24 weeks immersion.....	89
Figure 3:28: Test EHMA paints antifouling results. Paint 2019 is MESQ(I)v25 and 2020, 2021 and 2022 are MESQ(I)25v2, 3 and 4 respectively after 17 weeks immersion .....	89
Figure 3:29: Test BMA paints antifouling results. Paint 2019 is MESQ(I)v25 and 2023, 2024 and 2025 are MESQ(I)25v5, 6 and 7 respectively after 17 weeks immersion .....	90
Figure 3:30: Test LMA paints antifouling results. Paint 2019 is MESQ(I)v25 and 2026, 2027 and 2028 are MESQ(I)25v8, 9 and 10 respectively after 17 weeks immersion .....	90
Figure 3:31: Test EHMA paints antifouling results. Paint 2019 is MESQ(I)v25 and 2020, 2021 and 2022 are MESQ(I)25v2, 3 and 4 respectively after 53 weeks immersion. ....	91
Figure 3:32: Test BMA paints antifouling results. Paint 2019 is MESQ(I)v25 and 2023, 2024 and 2025 are MESQ(I)25v5, 6 and 7 respectively after 53 weeks immersion. ....	92
Figure 3:33: Test LMA paints antifouling results. Paint 2019 is MESQ(I)v25 and 2026, 2027 and 2028 are MESQ(I)25v8, 9 and 10 respectively after 53 weeks immersion. ....	92
Figure 3:34: Chart showing the temperature dependence of the change in viscosity of the LMA. ..	93
Figure 3:35: IR spectra of the new particulate material in the paint (red) and the spectra of the non defective coating (blue). Ovals indicate significant differences between the two IR spectra at 1450 and 900-800 $\text{cm}^{-1}$ . ....	93
Figure 3:36: Comparison between the calculated spectra of the ‘lumps’ (green) and that of copper pyrithione (1-2) (red). Ovals indicate significant differences between the two IR spectra at 1450-1400 and 1150-1100 $\text{cm}^{-1}$ . ....	94
Figure 3:37: Cleavage of MESQ through transesterification.....	94

Figure 3:38: <sup>1</sup> H NMR displaying the degradation of the MESQ(I) monomer (3-3) overtime.....	95
Figure 4:1: Structures of biocidal AMPSQ(I) (4-1) and non-biocidal AMPSQ(II) (4-2) monomers .....	98
Figure 4:2: i) <sup>1</sup> H NMR of final didecyldimethyl quat-monomer (black) (4-1) and its starting materials ii) didecyldimethyl quat-methylcarbonate (red) (2-5) and iii) AMPS acid (blue) (3-2) .....	99
Figure 4:3: Experimental design triangle of AMPSQ(I) polymers .....	100
Figure 4:4: Example of <sup>1</sup> H NMR of final quat-polymer solution in xylene:butanol 3:1, AMPSQ(I)v4 .....	102
Figure 4:5: Schematic of a surface droplet and its contact angle .....	104
Figure 4:6: Correlation between theoretical and experimental hydrophobicities of the AMPSQ(I) polymer .....	106
Figure 4:7: Daily polishing rate of AMPSQ(I)v3, v8 and v10 .....	109
Figure 4:8: Correlation between changes in mass and hydrophilicity of AMPSQ(I) coatings .....	112
Figure 4:9: Picture of a polishing disk with varying surface deformations and their distances from the centre of the disk .....	113
Figure 4:10: Apparent correlation between the speed threshold of the AMPSQ(I) paints and the theoretical T <sub>g</sub> and percentage of AMPSQ(I) monomer.....	114
Figure 4:11: Apparent correlation between the speed threshold of the AMPSQ(I) paints and the percentage mass of water absorbed and theoretical hydrophilicity.....	114
Figure 4:12: Test Polymers antifouling results. Biocidal polymers 2664, 2665, 2666 and 2667 are AMPSQ(I)v1, v2, v3 and v4 respectively. Standard (ST) is non-biocidal polymers AMPSQ(II)v4 after 8 weeks immersion .....	116
Figure 4:13: Test Polymers antifouling results. Biocidal polymers 2667, 2668, 2669 and 2717 are AMPSQ(I)v4, v5, v6 and modified AMPSQ(II)V4 respectively. Standard (ST) is non-biocidal polymer AMPSQ(II)v4 after 8 weeks immersion .....	117
Figure 4:14: Test Polymers antifouling results. Biocidal polymers 2669, 2670, 2671 and 2672 are AMPSQ(I)v6, v7, v8 and v9 respectively. Standard (ST) is non-biocidal polymer AMPSQ(II)v4 after 8 weeks immersion .....	117
Figure 4:15: Test Polymers antifouling results. Biocidal polymers 2668, 2673, 2674 and 2675 are AMPSQ(I)v5, v10, v11 and v12 respectively. Standard (ST) is non-biocidal polymer AMPSQ(II)v4 after 8 weeks immersion .....	118
Figure 4:16: Test Polymers antifouling results. Biocidal polymers 2667, 2668, 2669 and 2717 are AMPSQ(I)v4, v5, v6 and modified AMPSQ(II)V4 respectively. Standard (ST) is non-biocidal polymer AMPSQ(II)v4 after 14 weeks immersion.....	118

Figure 4:17: Test Polymers antifouling results. Biocidal polymers 2664, 2665, 2666 and 2667 are AMPSQ(I)v1, v2, v3 and v4 respectively. Standard (ST) is non-biocidal polymer AMPSQ(II)v4 after 14 weeks immersion .....	119
Figure 4:18: Test Polymers antifouling results. Biocidal polymers 2669, 2670, 2671 and 2672 are AMPSQ(I)v6, v7, v8 and v9 respectively. Standard (ST) is non-biocidal polymer AMPSQ(II)v4 after 14 weeks immersion .....	120
Figure 4:19: Test Polymers antifouling results. Biocidal polymers 2668, 2673, 2674 and 2675 are AMPSQ(I)v5, v10, v11 and v12 respectively. Standard (ST) is non-biocidal polymer AMPSQ(II)v4 after 14 weeks immersion .....	120
Figure 4:20: Test Paints antifouling results. Biocidal paints 2652, 2653, 2654 and 2655 are AMPSQ(I)v1, v2, v3 and v4 respectively. Standard (ST) is Intersmooth 460 after 14 weeks immersion .....	121
Figure 4:21: Test Paints antifouling results. Biocidal paints 2657, 2658, 2659 and 2660 are AMPSQ(I)v6, v7, v8 and v9 respectively. Standard (ST) is Intersmooth 460 after 14 weeks immersion .....	122
Figure 4:22: Test Paints antifouling results. Biocidal paints 2656, 2661, 2662 and 2663 are AMPSQ(I)v5, v10, v11 and v12 respectively. Standard (ST) is Intersmooth 460 after 14 weeks immersion .....	122
Figure 4:23: Test Paints antifouling results. Biocidal paints 2655, 2656 and 2657 are AMPSQ(I)v4, v5 and v6 respectively. Non-biocidal paint 2676 is AMPSQ(II)V4. Standard (ST) is Intersmooth 460 after 14 weeks immersion .....	123
Figure 4:24: Test Paints antifouling results. Biocidal paints 2652, 2653, 2654 and 2655 are AMPSQ(I)v1, v2, v3 and v4 respectively. Standard (ST) is Intersmooth 460 after 59 weeks immersion .....	124
Figure 4:25: Test Paints antifouling results. Biocidal paints 2655, 2656 and 2657 are AMPSQ(I)v4, v5 and v6 respectively. Non-biocidal paint 2676 is AMPSQ(II)V4. Standard (ST) is Intersmooth 460 after 59 weeks immersion .....	124
Figure 4:26: Test Paints antifouling results. Biocidal paints 2657, 2658, 2659 and 2660 are AMPSQ(I)v6, v7, v8 and v9 respectively. Standard (ST) is Intersmooth 460 after 59 weeks immersion .....	125
Figure 4:27: Test Paints antifouling results. Biocidal paints 2656, 2661, 2662 and 2663 are AMPSQ(I)v5, v10, v11 and v12 respectively. Standard (ST) is Intersmooth 460 after 59 weeks immersion .....	125
Figure 4:28: Viscosity measurements of various AMPSQ paints.....	130
Figure 4:29: Photographs of the stern (right) and bow (left) starboard sections of the test patching vessel. Yellow circles indicate AMPSQ coating test patches .....	130

Figure 5:1: Potential routes to formation the major fragmentation ions of the quats .....	135
Figure 5:2: Initial calibration plot: 50-1000ppb benzyl-quat (1-21) .....	137
Figure 5:3: Structure of internal standard compound - tetra n-butylammonium nitrate (5-4) .....	138
Figure 5:4: Chromatogram of tetra-butylammonium nitrate (5-4) (1.38 mins) and benzyl-quat (1-21) (1.93mins).....	138
Figure 5:5: Calibration plot: 5-100 ppb benzyl-quat (1-21) using internal standard (5-4) .....	140
Figure 5:6: Amalgamated calibration plot: 5-100 ppb trioctyl-(2-2) and didecyl-quat (2-1) with Internal Standard (5-4).....	147
Figure 5:7: Calibration plot: dual quat method .....	149
Figure 5:8: Structure of dodecyltrimethylammonium halide (5-5).....	149
Figure 5:9: Average recoveries from 'loaded' SPE cartridges stored for 3, 7 and 10 days. Error bars are 95 % confidence limits.....	153
Figure 5:10: Trial leach rate profiles for didecyl-, trioctyl- and benzyl-quat polymers together with a didecyl-quat paint formulation .....	154
Figure 6:1: Example of mediated ion exchange reaction of different SPCs systems i) quat SPC and ii) anion SPC .....	156
Figure 6:2: Structure of 2, 2, 3, 4, 4, 4 – Hexafluorobutyl methacrylate (6-1) .....	157
Figure 6:3: Photograph of four types of final leaching panel .....	158
Figure 6:4: Photograph of leaching storage tank .....	159
Figure 6:5: Photograph of a leach rate experiment using bubble agitation.....	159
Figure 6:6: Leach rate profiles for AMPSQ(I)v10 polymer (red) and AMPSQ(I)v10 paint (blue), inlay is a blown up view of the same chart .....	161
Figure 6:7: Leach rate profiles for AMPSQ(I)v10 paint (blue), free association didecyl-quat paint (yellow) and an alternative free association biocide paint (brown), inlay is a blown up view of the same chart .....	163
Figure 6:8: Leach rate profiles for AMPSQ(I)v10 paint (blue) and AMPSQ(I)v10 FB paint (fluorinated monomer, green), inlay is a blown up view of the same chart.....	164

## List of Schemes

Scheme 1:1: Ion exchange reaction of TBT-SPC copolymer <sup>6</sup> .....	10
Scheme 1:2: Release of Cu <sup>2+</sup> ion in seawater <sup>25</sup> .....	13
Scheme 1:3: Polishing reactions for TBT and tin-free SPCs <sup>25</sup> .....	16
Scheme 1:4: Anode reaction of chloride ions .....	21
Scheme 2:1: Synthetic sequence for the preparation of quat methylcarbonates .....	53
Scheme 3:1: Two step synthetic sequence for the preparation of didecyldimethylammonium quat- monomer .....	68
Scheme 4:1: Two step synthetic sequence for the preparation of didecyldimethylammonium quat- monomer-AMPSQ(I) (4-1) .....	98

# List of Tables

Table 1:1: Selected properties of commonly used organic biocides <sup>36</sup> (a)-Solubility in seawater; (b)-ISO method .....	19
Table 1:2: Classification of quaternary ammonium compounds .....	27
Table 1:3: Quat liquid chromatography analytical methods .....	44
Table 1:4: LC-MS applications.....	45
Table 1:5: SPE methods.....	47
Table 2:1: Example of paint formulation for RC957Q(I) .....	57
Table 2:2: Semi rapid boot-top results for the RC957 coatings series (+) – delamination of the test coating from the substrate. ....	59
Table 3:1: Example of paint formulation for MESQ(I)v25 .....	71
Table 3:2: Semi rapid boot-top results for both biocidal and non-biocidal coatings .....	72
Table 3:3: Mol% breakdown of second generation polymers .....	78
Table 3:4: Polymer code names with corresponding mol% of third comonomer.....	78
Table 3:5: Published T <sub>g</sub> data for comonomers used in second generation polymers.....	79
Table 3:6: T <sub>g</sub> data for the EHMA (3-6), BMA (3-7) and LMA (3-8) polymers .....	80
Table 3:7: Second generation polymer T <sub>g</sub> s.....	81
Table 3:8: Semi rapid boot top data for paints, omitting the first 2 cycles as pass, fail and test coatings were all rated 5. ....	82
Table 3:9: SRBT results for polymers, (-) - corresponds to complete failure of polymer by detached from the substrate, (*) - corresponding to sagging at waterline.....	83
Table 4:1: Table of AMPSQ Polymers and their monomer compositions .....	101
Table 4:2: Measured T <sub>g</sub> s for the AMPSQ polymers .....	102
Table 4:3: Published T <sub>g</sub> for co-monomers used in AMPSQ polymers <sup>180</sup> .....	103
Table 4:4: AMPSQ percentage and average surface energies (n = 6) .....	104
Table 4:5: Computationally derived logK <sub>ow</sub> of the co-monomers of the AMPSQ polymers.....	105
Table 4:6: Theoretically derived logK <sub>ow</sub> for the AMPSQ(I) polymers.....	105
Table 4:7: Semi rapid boot-top results for AMPSQ coatings .....	107
Table 4:8: Gravimetric and Profilometry changes in AMPSQ coatings.....	111
Table 4:9: Speed limit above which the test paints displayed surface defects.....	113
Table 4:10: Antifouling performance of AMPSQ(I) polymers ranked statistically against the non-biocidal AMPSQ(II)v4 polymer. Yellow and green indicates statistically superior and inferior antifouling performance respectively.....	127

Table 4:11: Antifouling performance of AMPSQ(I) paints ranked statistically against the standard product paint (Intersmooth 460). Yellow and green indicates statistically superior and inferior antifouling performance respectively.....	128
Table 4:12: Antifouling performance of AMPSQ(I) paints ranked statistically against the non-biocidal AMPSQ(II)v4 paint. Green indicates statistically inferior antifouling performance. ....	128
Table 5:1: Quats' mass ions and major fragmentation ions.....	135
Table 5:2: RSDs calculated detection settings from five repeat injections of 500 ppb sample .....	139
Table 5:3: 10 and 100 ppb injection data.....	139
Table 5:4: SPE extractions.....	141
Table 5:5: SPE eluent and stationary phase search; (✓) – analyte successfully recovered, (✗) – no analyte recovered .....	142
Table 5:6: Elution eluent 90:10 ACN 5 % acetic acid:water 0 % acetic acid.....	142
Table 5:7: Elution eluent 90:10 ACN 5 % acetic acid:water 5 % acetic acid.....	142
Table 5:8: Elution eluent 90:10 ACN 10 % acetic acid:water 10 % acetic acid.....	142
Table 5:9: SPE protocol.....	143
Table 5:10: Recovery results from initial attempts to improve SPE process.....	143
Table 5:11: Recovery results from initial attempts to improve seawater SPE process.....	144
Table 5:12: Recovered benzyl-quat (1-21) from volumetric flasks made of different materials....	145
Table 5:13: Results for the recovery of benzyl-quat (1-21) with glassware pre-soaked with benzyl-quat (1-21).....	147
Table 5:14: Results for the recovery of didecyl-quat (2-1) with glassware pre-soaked with didecyl-quat (2-1).....	148
Table 5:15: Calculated limits of the developed analytical methods .....	149
Table 5:16: Repeat SPE results with glassware soaked with pre-saturation-quat.....	150
Table 5:17: Measured concentrations of both benzyl- and didecyl-quat in treated and untreated 2 l beakers .....	152
Table 6:1: Final dried paint mass on each leaching panel .....	158

# List of Equations

Equation 3:1: Fox Equation .....	78
Equation 3:2: Manipulated Fox equation for the calculation of the $T_g$ of a monomer from a blended polymer. ....	79
Equation 4:1: Proposed equation to derive the theoretical hydrophilicity of a blended polymer ( $\log K_{ow, p}$ ), where $x_i$ is the co-monomer's weight fraction within the polymer and ( $\log K_{ow, i}$ ) is the co-monomer's hydrophilicity .....	105
Equation 4:2: Hydrodynamical rating, where $H$ is the hydrodynamical rating, $d_i$ the fouling drag factor and $c_i$ the fouling type's percentage coverage of the test square. ....	126

# List of Abbreviations

ACN	Acetonitrile
AE	Alkyl ethoxylates
AMBN	2,2'-Azobis-(2-methylbutyronitrile)
AMPS	2-Acrylamido-2-methyl-1-propanesulfonic acid
AMPSQ	Quaternary ammonium salt of 2-Acrylamido-2-methyl-1-propanesulfonic acid
AMPSQ(I)	Didecyldimethylammonium cation salt of 2-Acrylamido-2-methyl-1-propanesulfonic acid
AMPSQ(II)	Trioctylmethylammonium cation salt of 2-Acrylamido-2-methyl-1-propanesulfonic acid
amu	Atomic mass unit
ASTM	American standard test method
benzyl-quat	Alkylbenzyltrimethylammonium halide
BMA	Butyl methacrylate
BPD	Biocidal Product Directive
Bu	Butyl group
Bz	Benzyl group
°C	Celsius
C	Equilibrium solution concentration
<i>c</i>	Fouling type's percentage coverage
C <sub>6</sub>	6 carbon alkyl chain
C <sub>8</sub>	8 carbon alkyl chain/Octyl stationary phase
C <sub>10</sub>	10 carbon alkyl chain
C <sub>12</sub>	12 carbon alkyl chain
C <sub>14</sub>	14 carbon alkyl chain
C <sub>16</sub>	16 carbon alkyl chain
C <sub>18</sub>	18 carbon alkyl chain/Octadecyl stationary phase
CE	Capillary electrophoresis
cm	Centimetre
cm <sup>-1</sup>	Wavenumber
cm <sup>2</sup>	Square centimetre
cm <sup>3</sup>	Cubic centimetre
CMC	Critical micelle concentration
CN	Cyano stationary phase

<i>d</i>	Fouling type's drag coefficient factor
Da	Daltons
DCM	Dimethyl carbonate
deg	Degree
dialkyl-quat	Quaternary ammonium compound with two alkyl chains which contains greater than 2 carbon atoms
didecyl-quat	Didecyldimethylammonium halide
DMA	Dynamic mechanical analyser
DNA	Deoxyribonucleic acid
DSC	Differential scanning calorimetry
dwt	Dead weight tonnes
EDTA	Ethyldiaminetetraacetic acid
EHMA	2-Ethylhexyl methacrylate
ELS	Evaporative light scattering
Enviro	Environmental
EU	European Community
FI	Flame ionisation
FPSO	Floating production storage and offload
g	Grams
GC	Gas chromatography
GPC	Gel permeation chromatography
GSI	Global shipping industry
<sup>1</sup> H	Proton (NMR)
H	Proton/hydrodynamic rating
h/hrs	Hour(s)
halo	Halogenated compound
HFBMA	2, 2, 3, 4, 4, 4 – Hexafluorobutyl methacrylate
HMS	His/Her Majesty's ship
HSD	High speed dispersion
iBoMA	Isobornyl methacrylate
IMO	International Maritime Organisation

Int	International
IR	Infrared
K	Kelvin/thousand
K <sub>d</sub>	Sorption co-efficient
Km	Kilometre
kV	Kilovolts
l	Litre
LAS	Linear alkylbenzene sulphonates
LC	Liquid chromatography
LD <sub>50</sub>	Median lethal dose
LMA	Lauryl methacrylate
LOD	Limit of detection
logK <sub>ow</sub>	Log of the octanol-water partition coefficient
LOQ	Limit of quantification
M	Molar
m	Multiplet (NMR); metre
m/z	Mass to charge ratio
Me	Methyl group
MEPC	Maritime Environment Protection Committee
MES	Mono-2-(methacryloyloxy)ethyl succinate
MESQ	Quaternary ammonium cation salt of mono-2-(methacryloyloxy)ethyl succinate
MESQ(I)	Didecyldimethylammonium cation salt of mono-2-(methacryloyloxy)ethyl succinate
MESQ(II)	Trioctylmethylammonium cation of mono-2-(methacryloyloxy)ethyl succinate
MFO	Mixed function oxygenase
mg	Milligram
MIC	Minimum inhibition concentration
micron	Micrometre
min(s)	Minute(s)
ml	Millilitre
mM	Millimolar
M <sub>n</sub>	Number average molecular weight

mN/m	Millinewton per metre
mol%	Molar percentage
monoalkyl-quat	Quaternary ammonium compound with one alkyl chain which contains greater than 2 carbon atoms
MRM	Multiple reaction monitoring
MS	Mass spectroscopy
MS <sup>2</sup>	Secondary mass spectroscopy on molecular ion
MW	Molecular weight
M <sub>w</sub>	Weight average molecular weight
N <sup>+</sup> cm <sup>-2</sup>	Ammonium groups per square centimetre
ng	Nanogram
NMR	Nuclear magnetic resonance
NP	Nitrogen-phosphorus
NVC	Non-volatile content
Occupat	Occupational
PDMS	Polydimethylsiloxane
PEI	Polyethylenimines
PFA	Perfluoroalkoxyl copolymer
PMP	Polymethylpentene
PP	Polypropylene
ppb	Part per billion
ppm	Part per million
ppt	Part per trillion
psi	Pounds per square inch
PTFE	Polytetrafluoroethylene
QA	Quality Analysis
quat	Quaternary ammonium compound
R	Organic carbon bonded group
RC956Q	Quaternary ammonium cationic salt of RC957 polymer
RC957	Acid functionalized acrylic polymer
RC957Q(I)	Didecyldimethylammonium cationic salt of RC957 polymer
RC957Q(II)	Trioctylmethylammonium cationic salt of RC957 polymer

REACH	Regulation on Registration, Evaluation, Authorisation and Restriction of Chemicals
RNA	Ribonucleic acid
S	Concentration of surfactant adsorbed onto solid phase
s	Singlet (NMR)
SBL-D	Styrenedivinylbenzene phase
sec	Second
SFE	Supercritical fluid extraction
SG	Specific gravity
Si	Silica phase
SIM	Single ion monitoring
SPC	Self polishing co-polymer
SPE	Solid phase extraction
SPME	Solid phase micro-extraction
TBT	Tributyl tin
T <sub>g</sub>	Glass transition temperature
THF	Tetrahydrofuran
trioctyl-quat	Trioctylmethylammonium halide
USP-NF	United States Pharmacopeia – National Formulary
USS	United States Ship
UV	Ultraviolet
v	Version
V	volts
WCX	Weak cation exchange
WFD	Water framework directive
X-CW	Mixed-mode weak cation exchange
Visc	Viscosity
δ	Chemical shift (NMR)
μg	Microgram

$\mu\text{l}$	Microlitre
$\mu\text{m}$	Micrometre
$\rho$	Probability

# Acknowledgements

I would like to thank Dr Justin Perry for all his support, advice, guidance and encouragement during the three years of this research. I would also to thank Dr David Williams without whom the opportunity to undertake this research would never have presented itself and for his boundless enthusiasm especially when handed reams of text to proof at the last minute. I am also grateful to Professor John Dean for his guidance provided during the development of the quat analytical method.

My grateful thanks also to the Royal Commission for the Exhibition of 1851 without whose financial support this research would not have occurred.

To Ed Ludkin, I owe a special and big thank you for his wizardry in keeping the LC-MS instrumentation running and his constant advice to “stop faffing!”, and to John Sellers who was always at the end of a phone when I needed instrumentation advice and his general encouragement.

Thank you to all the members of International Paint who have help make this research run as smoothly as possible:

- Dr Clayton Price and Richard Ramsden, for all their advice and experience with the polymer synthesis and experimental design.
- Dr Adrian Downer for keeping me motivated to write up quickly, his extensive knowledge of leach rate method development and supply comparable leach rate data.
- Gina Jones and Neil Oxtoby for their assistance in paint manufacture and especially Harry Joyce for manufacturing paints and preparing panels ridiculously quickly.
- Dr Simon Welsh, Vickie White and Vickie Elliot for their NMR analysis and their patience with my continuous demands for NMR re-integrations.
- Paul Robins, Mina Dadgostar and Steph Mallam for their GPC analysis.
- Dave Clark for IR microscopy analysis.
- Dr Jeremy Thomason for his statically analysis of the antifouling data.
- Dr Ian Millichamp for his long memory and patience with all my questions.
- All the members of International Paint based in Newton Ferrers for their assistance with the antifouling testing.

And last but not least, my family members for their never-ending supported and encouragement. In particular Nick Bassarab and Robbie Grogan who read, and read through this tome without any thought to their own sanity.

## **Declaration**

This thesis has not been submitted for a degree in this or any other university. Except where acknowledgement is given, all work described is original and carried out by the author alone. This thesis is confidential and therefore cannot be borrowed or copied.

# 1 Introduction

## 1.1 Antifouling

### 1.1.1 Overview

The global shipping industry (GSI) is the primary conveyor for raw materials, commodities and other products around the globe. At its peak in 2009, the GSI numbered some 113, 307<sup>1</sup> vessels facilitating the movement of 1, 317 million tonnes of cargo<sup>1</sup>, enabling the growth and expansion of the global economy over the recent decades. During this period the impact of human activities on the environment both locally and globally have come to the fore, most notably as the major cause of Global Warming.

It is now widely accepted that gases such as carbon dioxide, sulphur dioxide and nitrous oxides are responsible for the Greenhouse Effect and Climate change. Recent assessments suggest that the GSI now emits more greenhouse gases from the consumption of fuel than the aviation industry; long believed to be the primary source<sup>2</sup>. It is estimated that 1 billion tonnes of carbon dioxide are released annually<sup>2</sup> by the GSI, which is under increasing scrutiny as the European Union aims to cut carbon dioxide emissions by 20 % by 2020<sup>3</sup>.

A vessel consumes fuel to overcome the drag forces it experiences as it passes through water. A major component of the drag is due to the frictional resistance<sup>4</sup> of the water passing over the surface of the hull. Any process, which increases the amount of drag experienced by a vessel, will ultimately lead to the release of a greater quantity of greenhouse gases. Fouling is the principal process through which this happens. It has been estimated that fouling could cost the GSI \$3 billion annually through increases in fuel, dry-docking and maintenance costs<sup>5</sup>. Antifouling coatings are currently the most cost effective method for preventing fouling and as such have major financial and environmental implications.

### 1.1.2 Fouling

#### 1.1.2.1 Definition

Fouling is the process of adsorption, colonisation and development of living and non-living material on immersed substratum<sup>6</sup>.

This natural process is not a new phenomenon. It has dogged mankind's movement by water over the millennia and is still a pertinent problem today. Plutarch, as early as the 1<sup>st</sup> century AD stated that it was usual to scrape the weeds, ooze, and filth from the ships sides to make them go more easily through the water<sup>7</sup>.

Currently there are at least 4000 recognised fouling species which are broadly classified into two groups<sup>6</sup>:

- Microfouling
- Macrofouling

Microfouling includes bacteria, diatoms, algae and protozoa. In the field, without magnification, identification can be difficult and these are usually collectively known as slime fouling<sup>8</sup>.

Macrofouling broadly refers to invertebrate and plant species, identified in the field as either weed and hard or soft bodied animal fouling. Plant species, such as weeds and kelp, have a prescriptive distribution, solely being located in the top few metres on the submerged substrate, due to the deteriorating penetration of light. The invertebrate species such as barnacles, tubeworms and hydroids are less restricted as they do not require light to grow and can proliferate in areas of low light levels, such as flat bottom of hulls. Barnacles are the most common fouling species, the larvae of which actively seek out their mature forms for cross fertilisation, resulting in large infestations. The gooseneck barnacle is even capable of attaching to moving vessels in open water<sup>8</sup>. Hydroids are colonial invertebrates, which resemble plants in appearance. They are frequently found on the flat bottom of hulls; where due to the low ambient light levels do not compete with plant species. Another major fouling organism is tubeworms, whose larvae actively

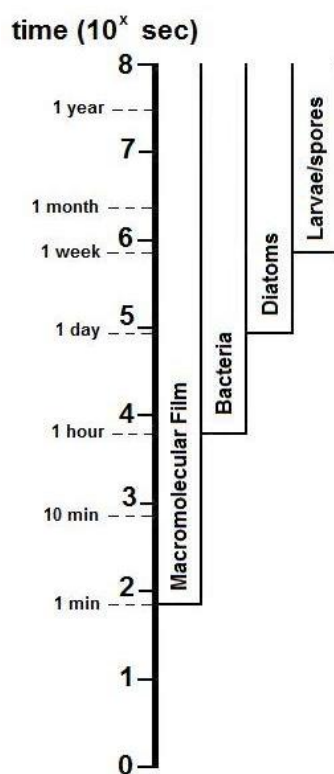


**Figure 1:1: Schematic of fouling growth from Wahl M. (1989)**

seek out their mature forms resulting in large colonies. These species tend to infect vessels which spend long periods stationary, such as in ports.

It is widely accepted that there are four stages in the fouling process<sup>9</sup>:

- 1) Conditioning
- 2) Colonisation of pioneer species
- 3) Colonisation of other microorganisms
- 4) Accumulation

Conditioning occurs within seconds of the substrate being immersed through the adsorption of both organic and inorganic material from the seawater to form a film, **Figure 1:1**. This organic-inorganic material forms a macromolecular film over the substrate altering the substrate-water interface and its composition influences the type of colonisation that follows<sup>6</sup>.

Within several hours pioneering bacteria begin to colonise the substrate. Initially the bacterial attachment is reversible but once a suitable location is found they

secrete a polysaccharide adhesive and become sessile. Unlike other fouling organisms the bacterial population will grow endlessly from this point<sup>10</sup>. The attachment of the bacteria again alters the interface as they begin to gather nutrients, deposit cellular material and debris into the film<sup>6</sup>. As the film develops other microorganisms such as diatoms and microalgae begin to become incorporated. Diatoms are particularly important as they represent the majority of the biomass of the developing film, reaching the surface through hydrodynamical means and attach via secretion of an adhesive.

The last and longest stage is accumulation, which can last days to weeks. At this point the larvae and spores of multicellular organisms begin to colonise the substrate. Algal spores are brought to the substrate by the motion of the surrounding water and are retained in the biofilm. Invertebrate larvae require the right set of physical and chemical cues prior to final attachment. These cues include food source, light, water velocity, temperature and other established adult forms. It is possible for invertebrate larvae to explore a surface by reversibly attaching and move on before final attachment<sup>6</sup>. The surrounding waters can be almost a soup of spores and larvae due to the vast numbers that are capable of being produced. A single filament of weed is capable of producing 100 million spores<sup>11</sup> while a single barnacle is capable of producing 10, 000 larvae<sup>12</sup> in a single season.

The type and degree of fouling a vessel experiences is also dependent upon additional factors to those mentioned above, such as local environment, seasonal variations and vessel critical factors. Local environments can have marked differences in the degree of fouling i.e. close-water areas, such as estuaries and harbours, from open-water, such as oceans and seas, where there can be large ranges in salinity, pollution and silts levels which can have a major impact on the diversity of fouling species.

Overarching these local variations are also limitations imposed by seasonal variations. For example both light levels and rainfall fluctuate during the year. Light levels are crucial for the rate of photosynthesis of plants and thus control the nutrient levels available. Consequently light levels are responsible for the vertical zonation of fouling. Plant species are dominant in the first few metres of water with a gradual shift to the domain of invertebrate species as the penetration of light diminishes<sup>13</sup>. Rainfall will also have a direct effect on the salinity of close-water systems. Salinity levels have been shown to have an effect on breeding behaviour of invertebrate species, in particular oysters<sup>14</sup>.

Water temperature however, appears to be the principle limiting condition for the geographical distribution of marine fouling organisms and determines their breeding periods<sup>14</sup>, **Figure 1:2**.

**Polar Zone (Blue coloured regions).** Less than 5 °C.

Fouling will occur for a short time period typically for a few weeks either side of midsummer.

**Temperate Zone (Green coloured regions).** 5 – 20 °C.

Fouling will occur throughout the year, peaking in spring to early autumn.

**Tropical/Sub-tropical Zone (Red coloured regions).** +20 °C.

Fouling continuous throughout the year with a multitude of species

In short, the breeding season starts later and terminates earlier at higher latitudes<sup>14</sup>.

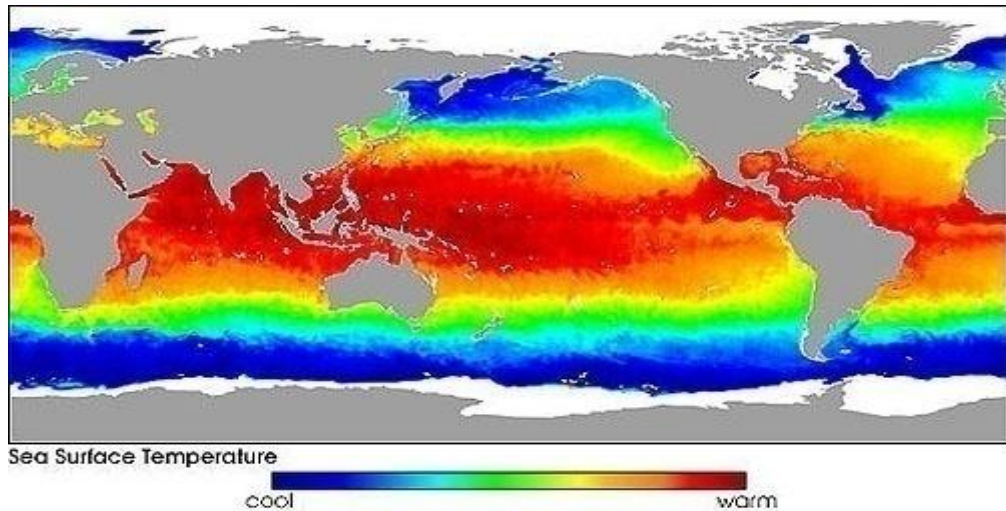


**Figure 1:2: Global ocean surface water temperature<sup>15</sup>**

Additional to the environmental factors there are also vessel specific factors which affect the degree of fouling, such as trade route, activity levels and speed of the vessel. Barnacles for example have a velocity threshold of 1 knot, above which it is not possible for the larvae to attach<sup>16</sup>. Vissler, in 1928, established that a vessel in constant use tends to be less heavily fouled than those which spend a greater percentage of time in port<sup>16</sup>.

Slow vessels trading exclusively in tropical waters are subject to the most severe fouling, particularly in shallow waters where light, heat and nutrients levels are high. However, fast moving active deep-sea vessels are also at risk in tropical environments depending upon the frequency and percentage of time they are in port<sup>8</sup>.

Collectively all these fouling stimuli combine to create the fouling challenge. An appreciation of which is crucial for antifouling immersion testing (field trials). 25 months foul free performance in the Arctic for example, is not deemed as successful as 6 months performance in Singapore due to their vastly different fouling challenges. Therefore the location at which the antifouling immersion testing is conducted is an important variable which needs to be controlled and carefully considered.

### 1.1.2.2 Impact

As stated earlier, the consequences of fouling have been known since ancient times. The primary effect of the growth of fouling is to dramatically increase in the roughness of the hull. A pristine freshly painted hull can increase in roughness from 130 to over 1000  $\mu\text{m}^5$ .<sup>17</sup> This results in an increase in the frictional resistance experienced by the vessel as it passes through water. Frictional resistance together with residual resistance are the forces more commonly known as drag<sup>4</sup>. Increasing drag impacts on the operational efficiency of a vessel in two significant ways; namely reducing the maximum speed and increasing fuel consumption. Fouling can also affect propellers, greatly reducing their efficiency resulting in an increased power requirement to maintain a given speed.

The *USS America* while on operation in the Indian Ocean was subject to heavy barnacle growth which reduced its maximum speed from 30 to 23 knots resulting in an average daily fuel penalty of \$53, 000. Across the US navy as a whole, the annual fuel costs have been estimated at \$500 million of which \$75 – 100 million is due to fouling<sup>6</sup>. By way of a non-military example the fuel costs for a 250, 000 dwt tanker with 5 % of the vessel's hull covered with fouling will increase by 17 % or \$1 million annually<sup>18</sup>.

Fouling can also substantially increase the weight of a vessel, further impacting its power requirements. For example 225 tonnes of mussels were removed from a floating production storage and offloading (FPSO) vessel which was static in the North Sea without antifouling protection for 65 months<sup>18</sup>.

Fouling may also adversely affect the substrate to which it is attached by effecting the local electrochemical environment causing corrosion. This can happen in a number of ways<sup>10</sup>:

- The adhesion of slime fouling creates disparities between fouled and non-fouled regions. As the microorganisms utilise oxygen they establish different aeration cells leading to localised corrosion.
- The microorganisms can concentrate several biological by-products at the surface of the metal e.g. sulphuric and carboxylic acids, sulphur ions and surfactants.
- Microfouling in anaerobic conditions can oxidise the metal by stripping hydrogen from the surface or by the production of metal sulphides.
- Production of polymers which are good chelating agents for metals.

All these processes can result in the metal becoming structurally unsound and will require increasingly frequent maintenance. It has been estimated that antifoulings have other financial

savings over and above fuel savings. For the GSI the benefits of antifoulings can be expressed as four main areas<sup>5</sup>:

- 1) Extended dry-docking \$400 million
- 2) Reduced Maintenance \$800 million
- 3) Indirect Savings \$1000 million
- 4) Fuel Savings \$500 million

This equates to total savings in the order of \$3 billion annually.

Clearly, the financial and operational consequences of fouling are on a vast scale but there are also major environmental aspects, particularly emissions associated with fouling. It has been estimated that effective uses of an antifouling can reduce the GSI fuel consumption by 7 million tonnes. This unburned fuel would be equivalent to an additional 22 million tonnes of carbon dioxide and 0.6 million tonnes of sulphur dioxide emitted<sup>5</sup>, both known greenhouse gases.

Another environmental consequence of fouling is the possibility of a fouled vessel acting as a vector for species migration. Specific examples of invasive species migration are well established in the literature. For example *Balanus eburnes* (barnacle) from the eastern American seaboard is now found in the Mediterranean Sea and *Elminius modestus* (barnacle) has been imported from Australasia to the northern temperate zone<sup>19</sup>.

### 1.1.3 History of Antifoulings

The protracted nature of mankind's struggle with fouling has resulted in numerous and varied attempts to solve the problem, **Figure 1:3**. In ancient times civilisations from the Phoenicians and Carthaginians to the Romans and Greeks used substances such as pitch, asphaltum, tar and wax to coat the undersides of their boats<sup>7</sup>. An Aramaic record from 412 BC states that arsenic and sulphur mixed in oil was used to coat ships' hulls<sup>20</sup>. These remedies, while in part were attempts to prevent fouling, will also have been applied to achieve water-tightness and other structural enhancements.

In the 3<sup>rd</sup> century BC, Greeks nailed lead plates onto ships with copper nails<sup>5</sup>. This lead sheathing remained the most frequently trialled form of protection right up to the 18<sup>th</sup> century. Other rudimentary attempts to prevent fouling involved covering the hull with a mixture of tallow and pitch<sup>20</sup>, as used by the fleet of Christopher Columbus, or charring the outer surface of the ship's hull to a depth of several inches<sup>7</sup> as favoured by Portuguese sailors.

Ancient:	Resistant wooden ship -coating coal tar, oil and wax -wooden and metallic sheathing
1850 - 1900:	Resistant wood and iron ship -copper sheathing, galvanic protection of iron -“patent paints” almost ineffective -“Italian Moravian” hot plastic paint, fairly effective
1900 - 1950:	Antifouling paint -various binders and copper oxide -hot plastic paint, followed by cold plastic paint
1950 - present:	Antifouling paint -Insoluble or soluble matrices used, containing copper oxide and mercuric oxide as biocides -organotin and copper combinations -(1974) organotin polymer antifoulant (TBT self-polishing copolymer antifoulant)
Present - future:	Paint and system -low and non toxic paint -electrolysis technology of seawater by electroconductive coating systems -use of copper alloy etc. -low surface-energy paint

In 1625 William Beale filed the first patent for an antifouling composition of iron powder, copper and cement for protection against fouling<sup>17</sup>. However, it was not until 1758 and the trial of copper sheathing on *HMS Alarm* that copper was recognised as the first successful antifouling<sup>6</sup>. The report of this experiment established the antifouling properties of copper sheathing to such an extent that for the next 40 years there was negligible interest in alternative methods. In the years that followed the success of copper was such that two boats were built in England ‘entirely of copper’<sup>7</sup>. In 1805 at the battle of Trafalgar Horatio Nelson is quoted as saying, “See how Collingwood takes his ship (*HMS Royal Sovereign*) into action”<sup>21</sup>. This is in reference to *HMS Royal Sovereign* engaging the joint Spanish-French fleets ahead of Nelson’s *HMS Victory* reputedly because Collingwood’s ship had new antifouling as the ship had recently been refitted<sup>22</sup>.

**Figure 1:3: Historical development of antifouling methods**

Although copper was the best antifouling surface, it was by no means perfect. Its antifouling action was not always certain and its corrosive effects on iron nearly caused it to be discarded by the British Navy, who sought the advice of the Royal Society<sup>7</sup>. In 1824 Sir Humphrey Davy proved that zinc, tin and iron all corroded in the presence of copper sheathing. These experiments were probably the first to relate the antifouling of copper to its rate of solution<sup>5</sup>.

With the exponential growth in the use of iron hulls, the corrosive problems of copper were exacerbated<sup>7</sup>. The main benefit of the corrosion crisis was to intensify efforts to create effective antifouling compositions. By 1870 over 300 patents had been registered<sup>6</sup> which would ultimately lead to the modern antifouling paint industry. These early compositions, for the most part, were entirely worthless. However, their poor performance was not necessarily due to a lack of knowledge on the part of the manufacturers. Robert Mallet stated that his paint failed because he could not control the dissolution rate of the toxins within useful limits and because of abrasion<sup>7</sup>.

Astute observations; the solutions to which are still the subject of much scientific and industrial research.

The first practical composition to come into widespread use was “McInnes” in 1860. It used copper sulphate as a biocide in a metallic soap composition, which was applied hot over a quick drying anticorrosive primer<sup>20</sup>. This hot plastic was very similar to the “Italian Moravian” paint, which used rosin (a natural tree resin) and copper compounds, developed concurrently in Italy<sup>17</sup>. By the close of the 19<sup>th</sup> century patents were being granted in the US and Japan for antifoulings. These compositions relied on copper, arsenic, mercury and their various compounds as toxins. Solvents included turpentine, naphtha and benzene with either linseed oil, shellac, tar and various resins as the matrix<sup>7</sup>.

In 1906 the US navy began its own experiments into antifouling compositions based on shellac and hot plastics that culminated in 1926 with their own hot plastic formulation using cuprous and mercuric oxides, which could provide greater protection than the 9 months of the commercial alternatives<sup>7</sup>. Owing to the inherent difficulties in applying hot plastics, which required specialist equipment and heating facilities at the shipyard, cold plastic compositions were created. These were easier to apply, drying through solvent evaporation but still provided thick films similar to that of the hot plastics with 18 months of service lifetime<sup>7</sup>.

From the late 1940’s onward the paint industry benefited from the appearance of new industrial chemicals. However, the lifetime of ‘conventional’ antifoulings remained limited because the release rate of the biocide could not be adequately controlled<sup>20</sup>. During the 1960s, broad-spectrum biocidal organotin compounds emerged and were incorporated into existing paint formulations as co-biocides. One in particular, tributyltin (TBT) halide, was so effective that only a fraction of the weight of copper was required to achieve full algal and barnacle control<sup>5</sup>.

A further significant advance took place in the 1970s with the development of organotin copolymer paints. In these, the copolymer provides both biocide and the acrylic binder for the paint<sup>6</sup>. Crucially, this finally provided a mechanism through which the release rate of the biocide was controlled. These antifouling paints were hailed as a “wonder weapon” because they provided 2-3 years fouling free performance<sup>5</sup>, extending dry-docking intervals and providing a significant contribution to the fuel efficiency of the global shipping industry<sup>20</sup>. However, in the early 1980s it became clear that organotin (TBT) not only killed fouling organisms, but also had toxic effects on non-target organisms<sup>17</sup>, which subsequently led to a total ban on TBT containing paints that came into effect on 1 January 2008<sup>23</sup>. This loss of TBT, whose performance still serves as a benchmark for all subsequent antifouling paints, reinvigorated the paint industry. Today there are both

biocidal and foul release (non-biocidal) products that offer performance levels comparable to that of TBT systems.

### 1.1.4 Organotin Antifoulings

In 1958 experimental work by van der Kerk established the broad spectrum biocidal activity of organotin compounds, general formula  $R_nSnX_{(4-n)}$ , where  $R$  is a carbon bonded organic group,  $X$  is an inorganic substituent and  $n = 1-4$ <sup>5</sup>. The work demonstrated that the maximum efficacy of this class of compounds occurred with the triorganotin compounds,  $R_3SnX$ . As the length of the  $R$ -group increases the maximum efficacy occurs with ethyl-groups. However, at butyl-groups the potency for mammals is at a minimum, without compromising the efficacy to other species<sup>5</sup>. This resulted in tributyltin (TBT) compounds becoming the most widely used organotin compounds.

During the 1960's the broad spectrum activity and compatibility of TBT compounds with other paint components<sup>24</sup> resulted in their incorporation into conventional antifoulings. Initially this was as a co-biocide with copper but later as a sole biocide, due to its greater efficacy, being ten times more potent than copper<sup>5</sup>. In these paints the TBT was not reacted into the paint binder but existed in a "free association form"<sup>25</sup>. Coupled with this was the known instability of triorganotin compounds which undergo degradation in the environment. This can occur through a number of mechanisms, namely UV light, microbial or chemical degradation all of which result in the cleavage of the tin-carbon bond<sup>5</sup>.

The release of the biocide from these "free association" paints occurs through the ingress of seawater that dissolves the TBT compound and subsequently diffuses out of the coating carrying the biocide with it. This results in an initial rapid and uncontrolled release of biocide but also

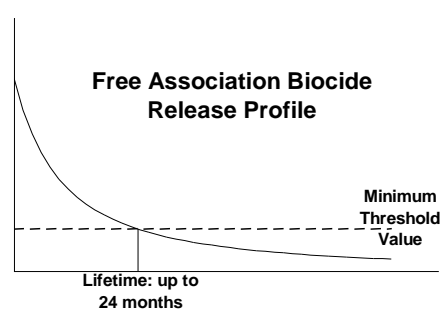


**Figure 1:4: Release profile of free association paint from Gitlitz M, (1981)**

creates a depleted region of biocide in the paint film, known as a leached layer. Subsequent biocide release declines steadily as the solubilised biocide has to traverse further and further because of the growing leached layer, producing a logarithmical release profile<sup>24</sup>, **Figure 1:4**. Consequently the antifouling performance therefore diminished with time<sup>5</sup>. Once the release rate has decreased below a critical level,  $1\mu\text{gcm}^{-2}\text{day}^{-1}$  for TBT, the antifouling coating is no longer effective. Free association

paints were capable of providing 24-36 months<sup>26</sup> performance, because of the logarithmical relationship, to double the lifetime of the coating would require four times the initial biocide loading<sup>24</sup> which was not practical.

Milne and Hails in 1974 revolutionised the antifouling industry with the innovative TBT-Self Polishing Copolymers (SPCs)<sup>27, 28</sup>. These systems crucially bound the TBT moiety to an acrylic polymer, which also served as the binder for the paint. The main advantage of TBT-SPC antifouling was that the release of the biocide was now controlled and constant with time, above the critical  $1\mu\text{gcm}^{-2}\text{day}^{-1}$  level<sup>5</sup>, **Figure 1:5**. This constant release rate meant that the lifetime of the antifouling was now predictable and proportional to the film thickness of coating applied to the vessels hull<sup>24</sup>.

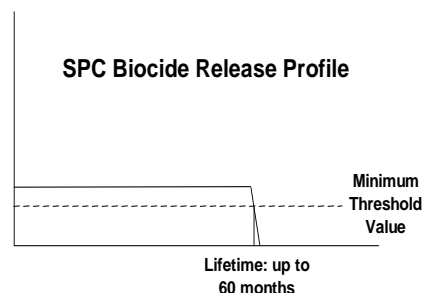
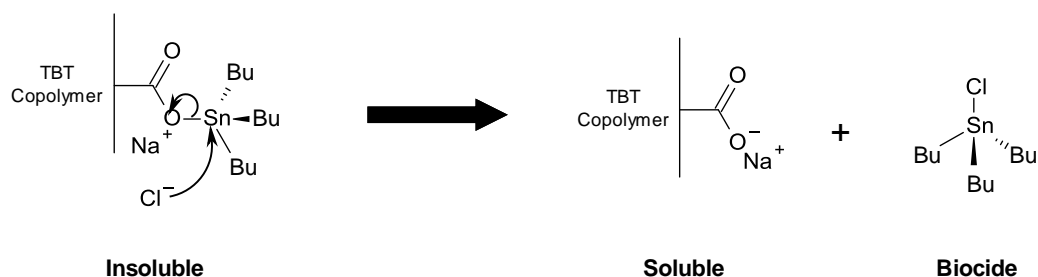


**Figure 1:5: TBT-SPC biocide release profile from Giltitz M, (1981)**

The TBT biocide was released from TBT-SPC systems through an ion exchange reaction of the tin-ester linkage, which readily occurred in slightly alkaline seawater ( $\text{pH} \sim 8.2$ )<sup>29</sup>, **Scheme 1:1**. This reaction caused a switch to occur from insoluble TBT-SPC polymer to a soluble carboxylate functional polymer that had little integral strength and was easily eroded by moving seawater, exposing fresh TBT-SPC polymer<sup>24</sup>, a process known as polishing<sup>26</sup>. This reaction was confined to a surface layer of  $20\ \mu\text{m}$ <sup>26</sup>, substantially smaller than a leached layer for conventional free association paints.



**Scheme 1:1: Ion exchange reaction of TBT-SPC copolymer<sup>6</sup>**

Apart from the constant release of the biocide, this action also generated fuel savings by reducing hull roughness, as peaks of roughness polished preferentially with consequential reductions in hull friction<sup>26</sup>. This polishing rate, because of its chemical nature, could also be optimised by varying the chemical properties of the TBT-SPC polymer providing tailored products for each particular vessel and up to 60 months fouling protection<sup>29</sup>. High activity, high speed vessels needed a slower polishing product than slower vessels that remained stationary for long periods<sup>29</sup>.

The advantages of predictable performance combined with additional fuel savings, over and above the general saving from the use of an antifouling resulted in TBT-SPCs becoming the dominant technology in the antifouling market. It is estimated that at its peak usage 70 to 80 % of the global shipping industry used TBT-SPCs<sup>25, 30</sup>. However, by the early 1980s adverse environmental

impacts of TBT were being reported globally. By 1999, faced with overwhelming evidence the International Maritime Organisation (IMO) passed a resolution banning TBT<sup>23</sup>; in part bolstering the legislation of proactive nations such as Japan, and other European countries.

### **1.1.5 TBT Ban**

Following the unprecedented success of TBT antifoulings in the 1970s, an increasing number of ecological problems began to be noticed in the early 1980s. *Crassostrea gigas* (oyster) populations on the west coast of France began to decline and showed increasing instances of shell deformities<sup>5</sup>, resulting in commercial shellfisheries becoming unviable<sup>23</sup>. Analysis showed elevated larvae mortality together with abnormally high levels of TBT in the shellfish tissue<sup>23</sup>. On the south coast of England the *Nucella lapillus* (dog whelk) populations were also declining. Studies showed that the females were developing male sexual organs and becoming sterile, a condition known as imposex<sup>23</sup>.

By 1982, France prohibited the use of TBT-based antifoulings on vessels less than 25 m in length and other countries followed suit including UK and Japan, who in 1997 prohibited the production of TBT containing antifoulings.

Since that time, substantial research has been undertaken worldwide, focusing on the environmental levels of TBT, toxicity assays and degradation rates. Studies showed that the “hotspots” of adverse TBT effects were closely associated with high densities of recreational craft in regions of limited water exchange, such as harbours and marinas<sup>6</sup>. There was also a correlation with dockyards, where vessels were cleaned, repaired and repainted<sup>6</sup>. Marine mammals and fish also showed evidence of accumulation of TBT, prompting fears of bioaccumulation of TBT in the food chain<sup>23</sup>, but none were as susceptible as shellfish<sup>6</sup>. The marine mammals and fish have the ability to metabolise the organotin compound via the relatively effective mixed function oxygenase (MFO) system providing protection against the toxicity of TBT<sup>6</sup>. However, shellfish have very low MFO activity and this correlated well with their limited ability to metabolise TBT and its subsequent accumulation in their tissue<sup>6</sup>. The toxicity of TBT arises because it acts as an endocrine disruptor leading to disorders, such as imposex<sup>5</sup>, even at low concentrations, 1 ng/l<sup>6</sup>.

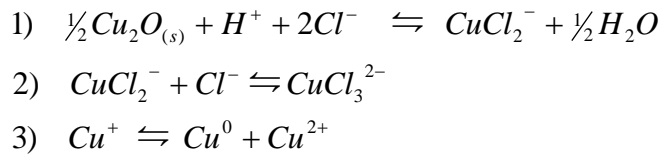
The principal problem with TBT was its persistence in the marine environment, in particular in sediment. Originally organotin compounds were thought to be relatively safe as they sequentially degraded to inorganic tin with a half-life of several days. Unfortunately once incorporated into marine sediments, deprived of oxygen and UV light, the half-life increases to several years<sup>23</sup>.

The proactive approach by France was shown to pay dividend as tin levels were 5-10 times lower in 1985 than 1982 with the *Crassostrea gigas* (oyster) population showing signs of recovery. Similar findings were also matched in the UK's *Nucella lapillus* (dog whelk) populations<sup>6</sup>. Studies on marine sediment cores showed the flux of TBT to the surface sediment was also decreasing<sup>5</sup>. In 1988 the problem of TBT was brought to the attention of the Marine Environment Protection Committee (MEPC) of the IMO. By 1990, the MEPC adopted a resolution recommending governments take steps to eliminate antifoulings with TBT; based on prohibiting TBT on vessels less than 25 m in length and eliminating antifoulings with an average leach rate above  $4 \mu\text{gcm}^{-2}\text{day}^{-1}$ . In 1999, the MEPC passed another resolution targeting, ultimately, the global ban on TBT. This was a two-stage phased process. Firstly a ban on new applications of TBT on vessels by 1<sup>st</sup> January 2003 was instituted and the second phase involved complete prohibition on the presence of organotin compounds on ships came into force on the 1<sup>st</sup> January 2008.

This legislation resulted in the development of tin-free antifoulings. These formulations again rely on copper compounds as the primary biocide but also require a secondary, booster, biocide to control weed<sup>31</sup> and algae to optimise their performance<sup>6</sup>. These booster biocides are based on organic compounds and are perceived to be environmentally benign. The TBT ban also set a precedent for future biocides. Metal based biocides, such as copper compounds are now coming under increasing worldwide scrutiny over concerns about their environmental safety. Sweden has banned copper antifoulings on its east coast with similar bans in effect in other Scandinavian countries<sup>26</sup>. The Netherlands no longer approves copper-based antifoulings<sup>26</sup> while Canada has implemented a limit on copper leach rates of less than  $40 \mu\text{gcm}^{-2}\text{day}^{-1}$ <sup>26</sup>. There are also restrictions on the booster biocides in the form of the Biocidal Product Directive (BPD), introduced in 2000. The directive requires each biocide to be registered, with its use justified and safety approved<sup>31</sup>. These tin-free antifoulings are the mainstay of the current antifouling industry.

### 1.1.6 Contemporary Tin-Free Antifoulings

Currently there are two main types of TBT-free antifoulings, which are broadly classified as biocidal and foul release. The foul release systems are non-biocidal and rely on coatings with low surface energies creating a “non-stick” surface. The biocidal systems mainly rely on copper oxide as the primary biocide, which is supplemented by the addition of a secondary booster biocide. Copper oxide is well known for controlling barnacles and other animal fouling species, but there are forms of algal fouling which are resistant to copper and these are controlled by the booster biocide. The antifouling properties of copper, as first demonstrated by Sir H. Davies in 1824, is via the release of cupric ions ( $\text{Cu}^{2+}$ ), formed by a disproportion reaction of cuprous ions ( $\text{Cu}^+$ , reaction 3) once they are released from the coating (reaction 1 and 2)<sup>6</sup>, **Scheme 1:2**.



**Scheme 1:2: Release of  $Cu^{2+}$  ion in seawater<sup>25</sup>**

The release of copper into the environment is considered negligible because only 3000 tonnes/year of copper are release from antifoulings compared to 250, 000 tonnes/year from natural weathering processes<sup>25</sup>. The low solubility of copper also acts to reduce further its bioavailability as it readily precipitates and becomes incorporated into sediments<sup>25</sup>.

There are three main types of biocidal coatings<sup>26</sup>:

- 1) Contact leaching
- 2) Soluble matrix
- 3) Self-Polishing Copolymer (SPC)

Both the soluble matrix and contact leaching coating systems are “free association” or conventional paints in which the biocide is physically dispersed within the paint matrix<sup>26</sup>.

### 1.1.6.1 Contact Leaching Systems

Contact leaching systems have a high dry film volume of biocide in the paint. This ensures that there is contact between the biocidal particles in the dry film<sup>26</sup>. The matrix of these coatings are based on chlorinated rubber or vinylic resins which have much higher mechanical strength than soluble biocidal particles<sup>6</sup> and do not erode, **Figure 1:6**.

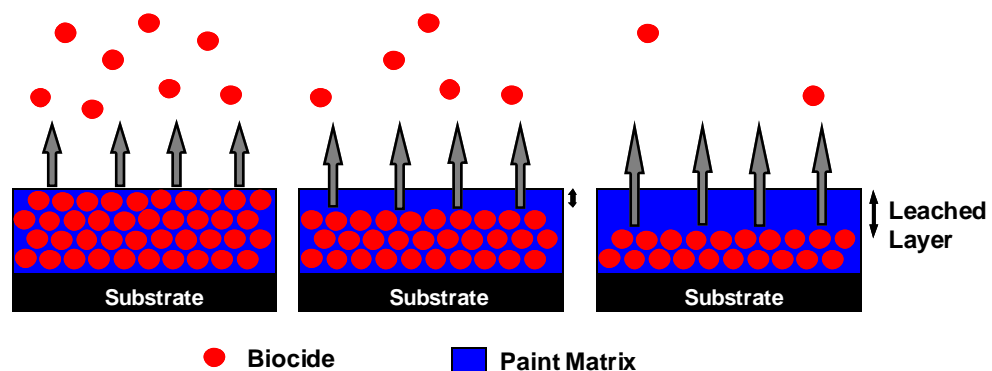


**Figure 1:6: Representation of biocide release from contact leaching antifouling system<sup>23</sup>**

Due to contact between the particles, as the water ingresses and dissolves a biocidal particle the next one is exposed<sup>26</sup>, creating micro-channels through the coating, ensuring a continuous flux of biocide. The main problem with this coating system is that the initial biocide release is excessive<sup>26</sup> and uncontrolled, **Figure 1:11**. The mechanical strength of the matrix results in a substantial leach layer being formed, in which the micro-channels may become blocked with insoluble precipitate<sup>26</sup>.

These coatings frequently provide up to 24 months protection, but are generally considered to be obsolete.

### 1.1.6.2 Soluble Matrix Systems

The biocides of the soluble matrix coatings are released by the physical dissolution of the paint binder, **Figure 1:7**, the rate of which is controlled by the different resins that make up the binder<sup>31</sup>.

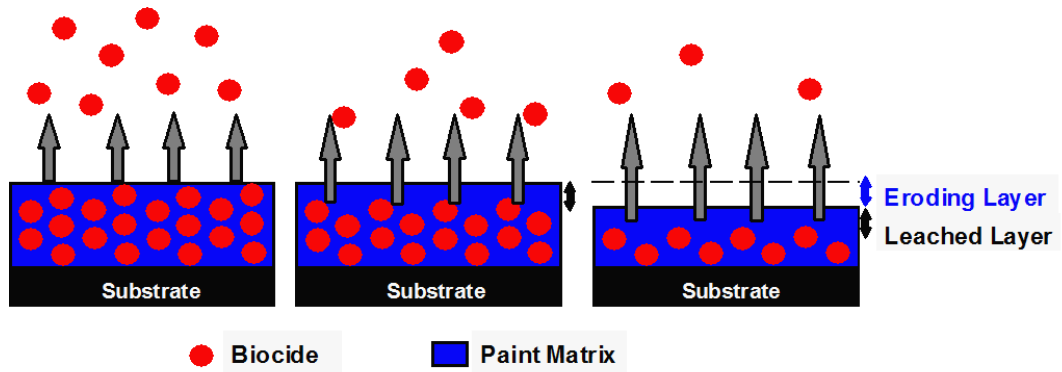


**Figure 1:7: Representation of biocide release from soluble matrix antifouling system<sup>23</sup>**

The main component of the binder is a natural tree resin (> 50%)<sup>32</sup> that is slightly soluble in water<sup>26</sup>, called rosin. Unfortunately rosin is unstable to oxidation<sup>6</sup> which can cause brittle coatings<sup>17</sup>. Therefore the binder is modified by the addition of polyacrylics, polyvinyls, polyesters or polyamides. However, too higher percentage of modifier can result in the binder becoming insoluble<sup>17</sup>. Rosin also does not prevent the penetration of water into the coating<sup>17</sup>, which through dissolution and diffusion carries the biocide out of the coating. The longer the immersion, the thicker the leach layer, because the erosion of the coatings surface is slower than the leaching out of the biocide<sup>31</sup>. Consequently the leach layer is the primary means for controlling the biocide release<sup>17</sup>. As the leach layer grows the rate of biocide release decreases as the solubilised biocide has a thicker layer to pass through<sup>31</sup>, **Figure 1:8** and **Figure 1:11**.

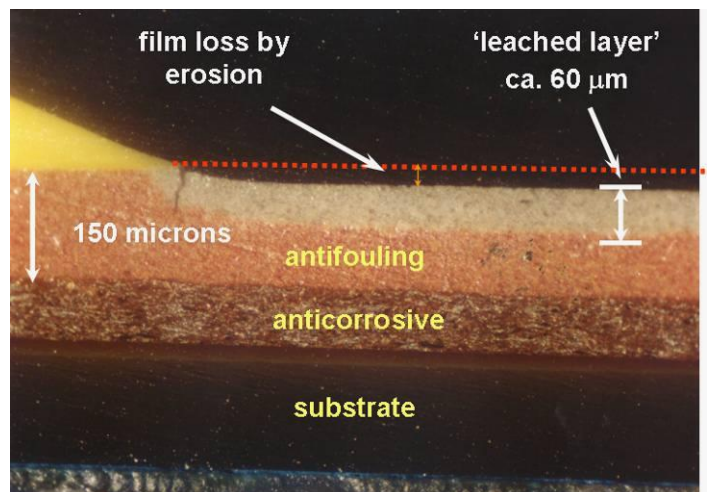


**Figure 1:8: Leach layer development in a soluble matrix system**

Soluble matrix coatings can provide up to 36 months antifouling performance<sup>26</sup>. However, they suffer from a number of drawbacks such as inconsistent dissolution rates of the biocide caused by the development of insoluble precipitates within the coating preventing biocide release. The leach

layer is also problematic and must be removed to regain antifouling performance or prior to repainting<sup>26</sup>.

### 1.1.6.3 Self-Polishing Copolymer (SPC) Systems

There are currently three types of SPCs in the market, which use either copper, zinc or silyl moieties to replace TBT in the acrylate polymer<sup>26</sup>. The surface of these systems is continually polished away, thereby exposing a fresh surface layer, which repeats until the whole thickness of the coating has eroded away<sup>31</sup>, **Figure 1:9**. This polishing ensures that the leach layer is consistently small with time ( $< 30 \mu\text{m}$ )<sup>32</sup>, **Figure 1:10**, and so the biocide can be released more efficiently, **Figure 1:11**.

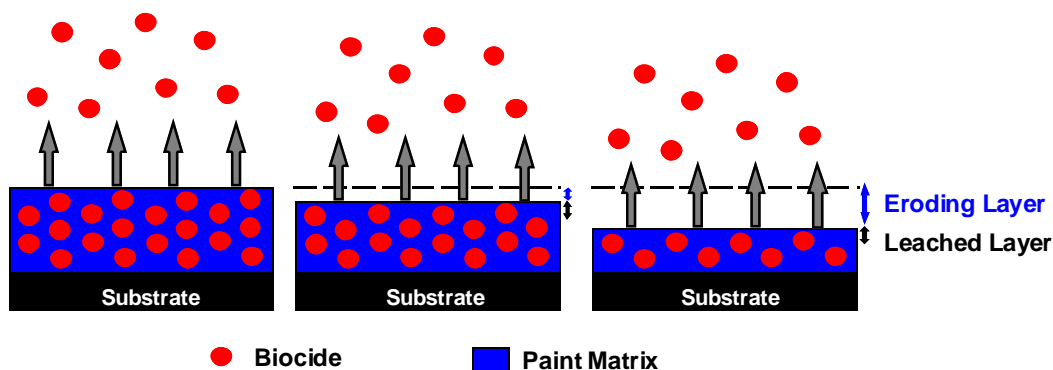


**Figure 1:9:** Representation of biocide release from a tin-free SPC antifouling system<sup>23</sup>

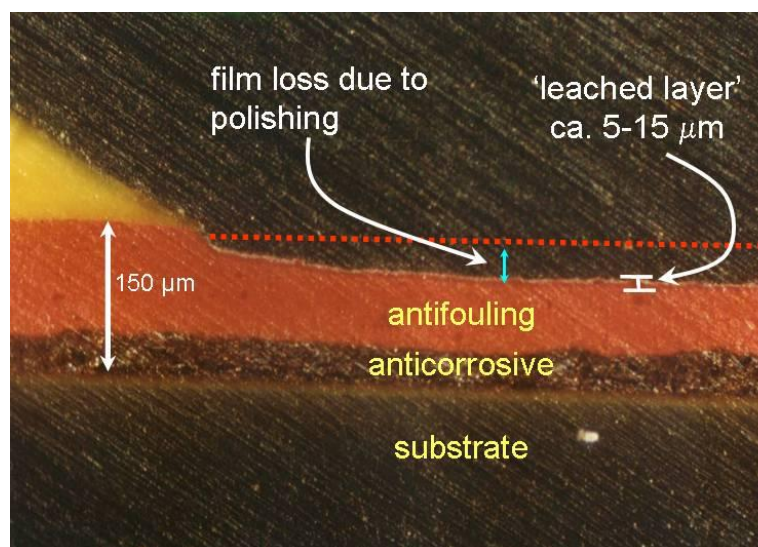
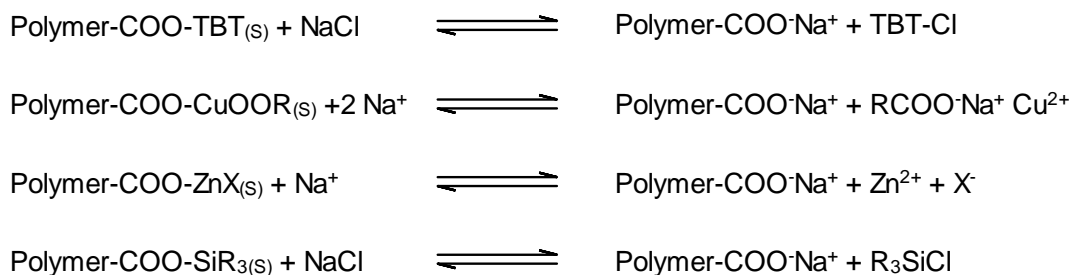


**Figure 1:10:** Film thickness depletion and leach layer development of an SPC system

The polishing mechanism for all types of SPC is similar to that of TBT-SPC involving an ion exchange reaction, **Scheme 1:3**.



**Scheme 1:3: Polishing reactions for TBT and tin-free SPCs<sup>25</sup>**

Copper/acrylate was the first tin-free SPC, introduced in 1990<sup>17</sup>. Again these systems primarily use copper oxide but the release of copper alone is not sufficient to prevent fouling. Therefore booster biocides are used which have half-lives in the order of a few hours<sup>31</sup> and are thought to be environmentally benign. The biocidal package combined with the polishing characteristic provides up to 60 months foul free performance, comparable with TBT-SPCs.

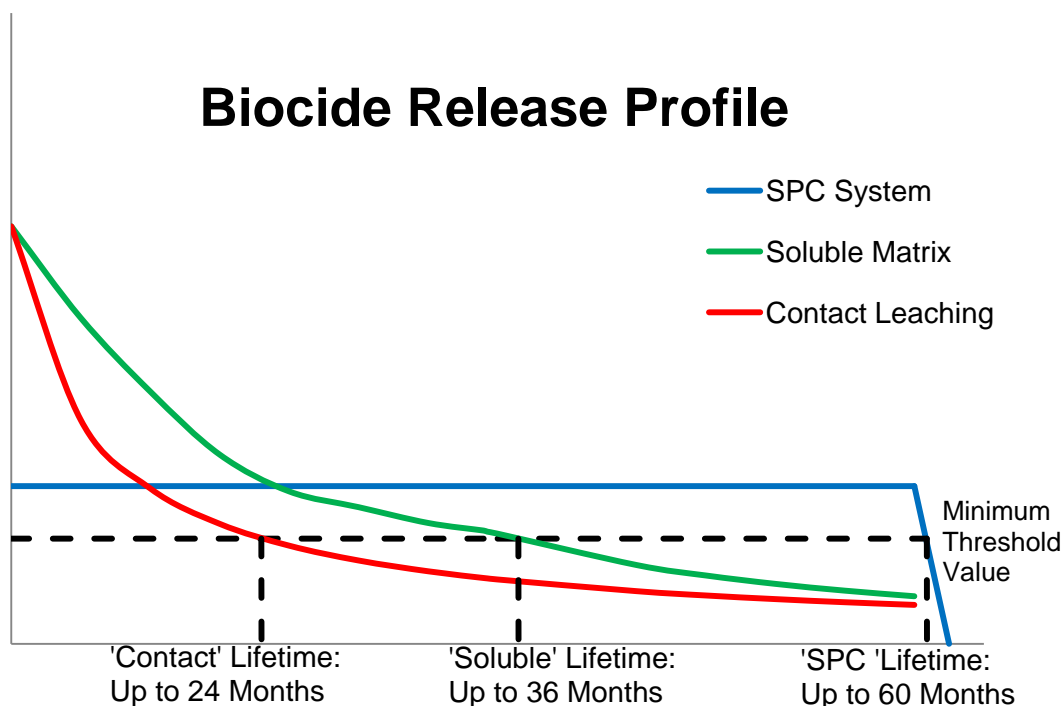


**Figure 1:11: Biocide release profile for contact leaching, soluble matrix and SPC antifouling systems. The "minimum threshold value" indicates the limit below which the release of biocide is too low to prevent fouling<sup>5</sup>.**

#### 1.1.6.4 Foul Release Systems

These systems have no biocidal component and their antifouling performance is derived solely from the smoothness of their hydrophobic surface, which have low surface energies. Fouling, except slime, cannot attach securely to these low energy surfaces because their adhesives cannot "wet-out" and spread over the coating<sup>26</sup>. This compromised adhesion results in the fouling being

easily removed either by its own weight or the motion of the water over the coating. Slime can remain attached, even at speeds of 35 knots<sup>17</sup>, because it has a low profile and can exist within the laminar layer of water at the coatings interface, without being washed off. These “non-stick” surfaces were originally modelled on Teflon®, using fluoropolymers, such as poly(tetrafluoroethylene) but because of irregularities in the surface microstructure fouling could securely attach<sup>6</sup>. Current foul release coatings are based on silicon elastomers, in particular polydimethylsiloxane (PDMS)<sup>26</sup>, which has an extremely flexible backbone allowing the polymer to adopt the lowest energy configuration<sup>32, 33</sup>. However, this surface energy can increase with time immersed, although taking years<sup>6</sup>. It has been postulated that this change in surface energy is due to rearrangements in the PDMS polymer chains close to the surface of the coating. The driving force for this change is the drive to increase the hydrogen bonding between water and the oxygen atoms in the polymer chain<sup>6</sup>. Foul release coatings draw favourable comparisons with tin free-SPCs. Foremost is that there is no biocidal component to cause environmental problems and secondly they provide similar fuel savings, even with slime fouling<sup>17</sup> over 60 months service. Foul release coatings are initially smoother than tin free-SPCs, **Figure 1:12**, and so initially provide enhanced fuel savings, compared with the SPCs, which are ultimately equalled out over the 60 months in operation.

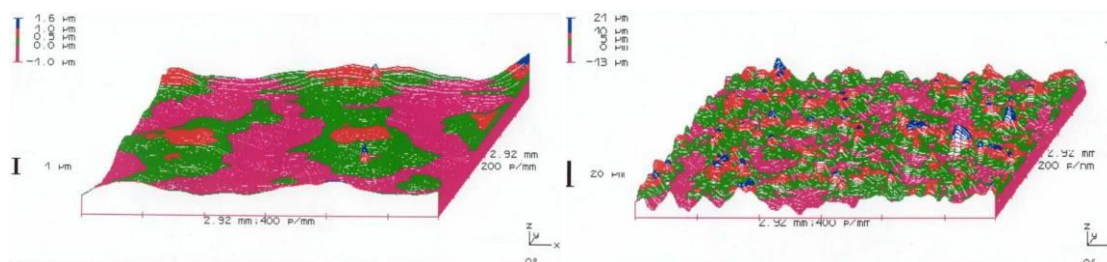


**Figure 1:12: Prolifometry showing the relative smoothness of foul release (left) coating compared to tin free-SPC (right)**

Another advantage of these coatings is they simply need to be cleaned with high-pressure water washing to remove the slime to regenerate the coating, reducing time lost with costly dry-docking. The main disadvantages of these coatings is that they have a lower speed threshold, 18 knots<sup>29</sup>, below which the coatings are ineffective and so are only suitable for fast or constant moving vessels. The elastomeric nature of the coatings also makes them susceptible to mechanical damage, which dramatically reduces their effectiveness<sup>26</sup>. However, recent advancements of incorporation of fluoro-polymer additives into silicon elastomers have reduced this lower speed threshold to below 10 knots<sup>34</sup>.

### 1.1.7 Organic Booster Biocides

During the introduction of the TBT ban, the IMO whilst considering copper to be significantly less harmful than TBT also sought to introduce environmental risk assessment criteria for future organic biocides to “avoid one harmful substance being replaced with another”<sup>23</sup>. Rather than the

TBT ban resulting in a plethora of new organic biocides becoming available the existing biocides were consigned to a secondary role as co-biocides because antifouling paint manufactures reverted to copper compounds. This was because organic biocide manufacturers were reluctant to register new products. For organic biocide manufacturers, the relatively small size of the global antifouling market makes it difficult to recoup the very high cost of developing and registering new antifouling organic biocides<sup>32</sup>, estimated to be \$10 million for the US alone<sup>26</sup>.

Following the precedent set by the IMO's TBT-ban, the European Union (EU) introduced further legislation in the form of the Biocidal Product Directive (BPD) 98/8/EC<sup>35</sup> which set out minimum standards that biocidal products must conform to. The BPD operates through a mechanism of risk assessments, which evaluate the substance's chemistry and toxicity to both humans and the environment<sup>32</sup>. The Directive classifies the products by their intended end-uses of which there are twenty three recognised end-uses. Antifouling products are covered by product type 21.

Globally there are approximately eighteen organic biocides used in antifouling<sup>36</sup>, which are largely, existing biocides used in other industries, such as agriculture<sup>37</sup>. Of these, five are permitted for use in the EU under the BPD, which also permits 5 metal-based biocides. The vast majority of these metal-based biocides are copper compounds, the one exception zinc pyrithione (PT) (**1-1**). However, zinc pyrithione (**1-1**) has been shown to convert to copper pyrithione (**1-2**); also on the BPD list<sup>36</sup>, **Figure 1:13**. The five organic biocides are<sup>37</sup>: Seanine-211 (**1-3**), Tolyfluanid (**1-4**), Dichlofluanid (**1-5**), Zineb (**1-6**), and Irgarol 1051 (**1-7**), **Figure 1:13**.

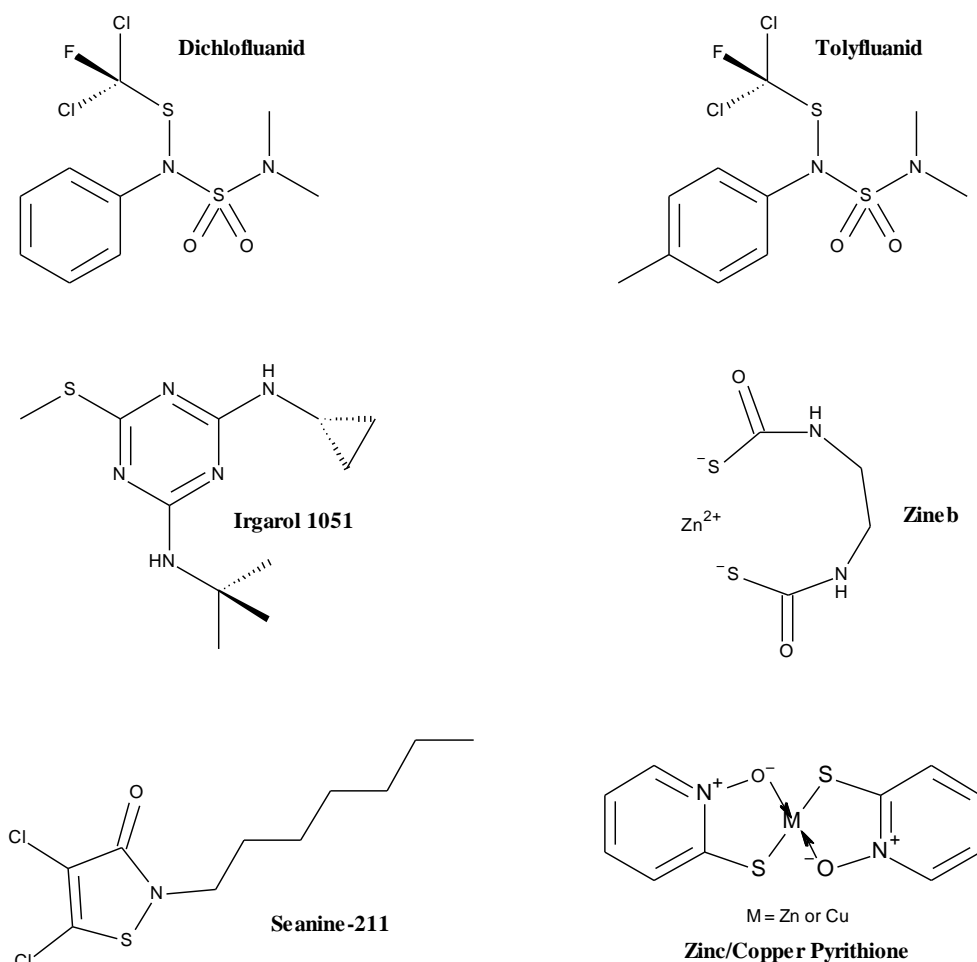


**Figure 1:13: Structures zinc/copper pyrithione (1-1 and 1-2) and the five registered organic antifouling biocides - tolylfluamid (1-4), dichlofluamid (1-5), zineb (1-6), irgarol 1051 (1-7) and seanine-211 (1-3)**

These biocides have varying chemical properties of which solubility; release and degradation rates are the most pertinent for their use as antifoulants, other than their efficacy, see **Table 1:1**.

Biocide	Solubility <sup>a</sup> (mg l <sup>-1</sup> )	Release Rate <sup>b</sup> ( $\mu\text{gcm}^{-2}\text{day}^{-1}$ )	Degradation Data	
			Half-life in Seawater	Principal Degradation Process
<b>Irgarol 1051 (1-7)</b>	7	5.0	100 days	-
<b>Zineb (1-6)</b>	0.07 - 10	-	96 h	Hydrolysis
<b>Seanine-211 (1-3)</b>	14	2.9	< 24 h	Biotic
<b>Dichlofluamid (1-5)</b>	1.3	0.6	18 h	-

**Table 1:1: Selected properties of commonly used organic biocides<sup>36</sup> (a)-Solubility in seawater; (b)-ISO method**

As a consequence of TBTs effects, environmental monitoring has become commonplace, with organic biocides becoming the main focus. This analytical vigilance highlighted Irgarol 1051 (1-7) as an environmental contaminant as early as 1993<sup>36</sup>; with concentrations being highest near marinas with high yachting activity and sporting harbours<sup>36, 38</sup>. Similar results have been reported

worldwide. The accumulation in fish of this compound has even been reported<sup>39</sup>. Prompted by these observations and concerns over its safety the Health and Safety Executive (HSE) has banned Irgarol (**1-7**) as an antifoulant<sup>40</sup> in the UK. The persistent nature of Irgarol (**1-7**) and other older organic biocides, such as Diuron (**1-8**) and Chlorothalonil (**1-9**), **Figure 1:14**, is due to a combination of their slow degradation rates and widespread use during the early years of the post TBT-ban.

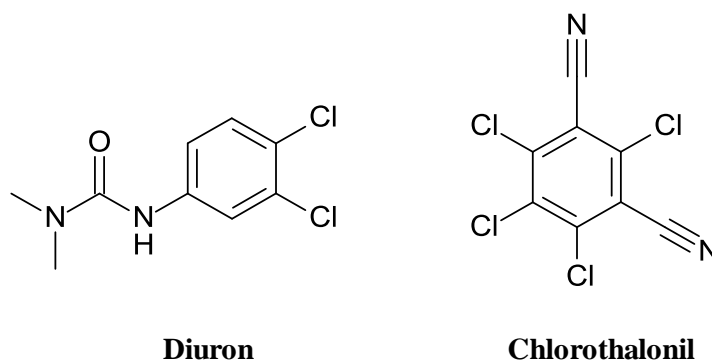


**Figure 1:14: Structures of diuron (1-8) and chlorothalonil (1-9)**

These first phase TBT replacement biocides have degradation half-lives in the order of 100 days<sup>36</sup>. The second generation/newer biocides, such as Seanine-211 (**1-3**) and copper/zinc pyrithione (**1-2** and **1-1**) have characteristically shorter half-lives, less than 24 hrs<sup>36</sup>, which reflects the move by antifouling paint manufactures to use rapidly degrading broad spectrum biocides. There is a belief that these fast degradation rates will prevent the build up of environmentally hazardous levels of biocides and are thought to be environmentally benign. Unfortunately, even given the quantity and quality of data required for registration, there are still large gaps in our understanding of the fate of organic biocides in the environment. In particular that of flakes/particles of antifouling paint, which become incorporated into sediments. Each particle can be considered as a new site for biocide release, which is likely to be very different in sediment than on a vessel<sup>36</sup>. The quantity and quality of the data amassed for the organic biocides needs to be matched by a similar dataset and analysis for their degradation products to ensure these new biocides are truly environmentally benign. Until such time as these omissions are filled the validity of environmental predictions will remain questionable. Therefore an overtly precautionary approach rather than unfettered use of the organic biocides is the overriding consensus<sup>25, 36, 41</sup>.

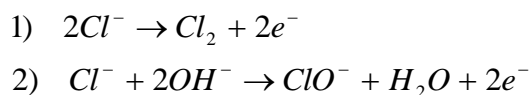
### 1.1.8 Alternatives and Future Developments

The increased level of legislation and the prohibitive cost of registering new biocides have created a diverse range of possible solutions to the fouling problem, which range from new concepts to trialled methods.

Currently vessels periodically undergo hull cleaning<sup>23</sup>. This requires high pressure water washing during dry-docking or a diver using a rotating brush. It is believed that a more regimented cleaning schedule could prevent fouling. However, this can also increase the fouling problem, because fouling residues left behind can promote further colonisation<sup>8</sup> and is costly.

The most tested concept is metallic sheathing. Although this has frequently been tested with varying results, the use of new copper alloys that offer improved corrosion resistance combined with the known antifouling properties of copper may provide a solution. These alloys are already used in “splash zones” on oil platform legs and from 1970-1998; seventeen ships were coated with copper-nickel alloys<sup>6</sup>. The drawbacks are the substantial initial cost compared to antifouling paint alternatives and the need to regularly remove the accumulate fouling by scrubbing to regenerate the coating.

Other tested alternatives include electricity, radiation and ultrasound. The use of electricity to develop a charge on the surface of the hull to deter fouling has long been known. In 1891 Thomas Edison patented an antifouling system using direct current<sup>5</sup>. Subsequently it was shown that alternating current systems were more effective. Unfortunately the electrical power required has proved to be uneconomic<sup>5</sup>. Another method uses the abundant supply of ions in seawater and electrolysis to create a “cloud” of chlorine and hypochlorite ions to cover the hull<sup>42</sup>, **Scheme 1:4**.



**Scheme 1:4: Anode reaction of chloride ions**

However the practical problems involved in creating a uniform dispersion of chlorine and hypochlorite ions combined with concerns over increased corrosion, makes implementation difficult<sup>5</sup>.

Other trialled solutions which have subsequently been commercially unsuccessful include ultrasonic antifouling systems<sup>43</sup>, radioactive coatings<sup>19, 43</sup> and coatings composed of long free flowing fibres<sup>23</sup>. Concepts in the early stages of research that might develop into effective antifouling include micro-textured surfaces<sup>23</sup> and the incorporation of enzymes into coatings<sup>43</sup>. The morphology of fish and marine mammals’ skin has been the focus of recent research, specifically for advanced sportswear<sup>44</sup> but also because it does not foul. One particular example, Sharklet<sup>TM</sup><sup>45</sup>, mimics sharks skin to create a foul resistant surface. Another approach has been to create surfaces, which mimic the hydrophobic nature of the lotus leaf. These super-hydrophobic surfaces repel water and trap a layer of air at the surface, which prevents fouling larvae and spore

reaching the surface. However, it is unclear as to whether these super-hydrophobic surfaces will ultimately prove practical.

Another area of current research is into natural products. Marine organisms already produce antifouling substances to prevent the surfaces of their bodies becoming fouled without causing environmental problems. This research has also broadened to include terrestrial plants such as wasabi, green tea<sup>5</sup> and chilli. The active ingredients in these plants and animals have been isolated and generally are large molecules with high levels of functionality and numerous stereo-centres<sup>46</sup>. Their production on an industrial scale at an economically viable price represents a significant challenge for synthetic chemists. Although these compounds are derived from natural sources they will require the same rigorous and expensive testing as a synthetic biocide before their registration.

Improvements in currently available coating systems can also be anticipated. The drawbacks of mechanical strength and speed threshold for foul release systems are likely areas for improvement. For biocidal coatings the new legislation and restrictions on leach rate have created a requirement for the release of the biocides to be controlled and sustainable<sup>39</sup>. This controlled release would eliminate the initial excessive flux of biocide and result in extending the coating's lifetime. There are a number of ways this can be achieved including:

- **Reservoir Membranes**<sup>39</sup>. Two layer coating systems where the base layer is composed of pure or nearly pure antifoulant. Over which a polymeric topcoat is applied and acts as a membrane to control the diffusion of the antifoulant to the surface.
- **Microencapsulation**<sup>39</sup>. A pure or highly concentrated solution of antifoulant is encased in a polymeric capsule that is incorporated into the paint binder. The release rate will depend on the slow or controlled diffusion through the capsule wall and the rapid diffusion through the binder.
- **TBT-SPC mimic**. In this case the TBT moiety is replaced by a new biocidal cation, **Figure 1:15**, having broad spectrum activity combined with a short half-life. Ideally such a biocide would previously be registered, for example in other product types of the BPD, which would dramatically reduce the cost for antifouling registration.

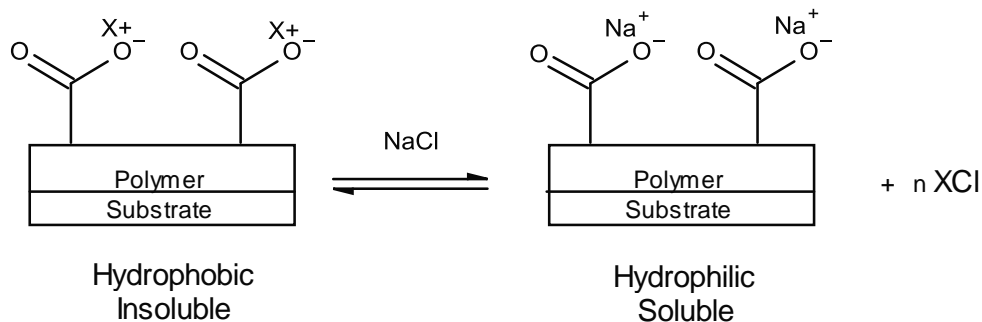


**Figure 1:15: Schematic of a generic SPC system**

One such group of chemicals are quaternary ammonium compounds, which are widely used and exhibit the required activity and environmental profile.

## 1.2 Quaternary Ammonium Compounds

### 1.2.1 Introduction

Quaternary ammonium compounds (quats) are surfactants, in particular cationic surfactants<sup>47</sup>. Characteristic of these surfactants is the presence of a hydrophilic group which carries a positive charge. Cationic surfactants are almost exclusively based on nitrogen, but examples of phosphonium<sup>48</sup> cations are available. Nitrogen centred cations can be divided into two categories quats and amines, which require protonation of the nitrogen to form a cationic moiety.

Quats are the product of a nucleophilic substitution reaction of alkyl halides or alcohols with tertiary amines. Chemically, they have four carbon atoms bonded directly to the nitrogen cation through covalent bonds, while the anion in the original alkylating agent becomes associated with the nitrogen cation through an ionic bond<sup>49</sup>. Menschutkin, in 1890 first reported the synthesis of quats via a nucleophilic substitution<sup>50</sup> and the ‘Menschutkin reaction’ is still regarded as the best method for their preparation.

The general formula for a quat is represented as follows, **Figure 1:16**:

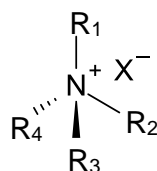


**Figure 1:16: Generic formula of quaternary ammonium compounds**

$R_1$ ,  $R_2$ ,  $R_3$  and  $R_4$  are alkyl groups that may be alike or different, saturated or unsaturated, branched or unbranched and cyclic or acyclic, and may be aromatic or substituted aromatic groups. The nitrogen atom plus the attached alkyl groups form the singly positively charged portion, the cation,

which is the functional part of the molecule. The portion attached to the nitrogen by an electrochemical bond, the anion, is usually chloride, bromide or hydroxide<sup>49</sup>.

As a result of the localisation of a positive charge, in conjunction with the organic nature of the R groups, quats have both hydrophilic and hydrophobic domains within their structure and as such have the ability to be soluble in both aqueous and/or organic solvents. Therefore quats have a broad spectrum of applications, including ophthalmic formulations<sup>51</sup>, anti-electrostatics<sup>52</sup>, phase transfer catalysts<sup>53</sup>, ionic liquids<sup>54, 55</sup>, disinfectants/antimicrobial agents<sup>56</sup>, herbicides<sup>57</sup>, molluscicides<sup>58</sup> and other antifouling products<sup>59</sup>.

## 1.2.2 Antimicrobial Activity

### 1.2.2.1 History

In Merianos' comprehensive review, *Quaternary Ammonium Antimicrobial Compounds* (1991)<sup>49</sup>, he attributes the growth in the commercialisation of quats as antimicrobial agents to two important publications that described their antimicrobial activity and related their structure and activity.

The first publication by Jacobs *et al*, (*circa* 1915)<sup>49</sup>, centred on different series of quats based on hexamethylenetetramine (**1-20**), **Figure 1:17**, detailed their preparation and correlated their structure to antimicrobial efficacy. Quat derivatives from other nitrogen containing molecules such as pyridine, quinoline and other ring structures were also the subject of study.

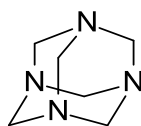
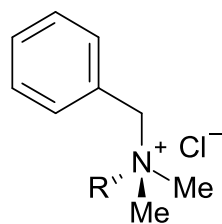


**Figure 1:17: Structure of hexamethylenetetramine (1-20)**

The second publication by Domagk in 1935<sup>49</sup> detailed the antimicrobial activity of the long chain quats. The report described the effect on germicidal activity that occurred when the chain length of an aliphatic residue attached to the quaternary nitrogen atom was varied.

Since then, there have been several iterations of commercially significant antimicrobial quats. The first, benzalkonium chloride<sup>49</sup> (**1-21**), is unusual as it is a mixture of alkyldimethylbenzylammonium chlorides (**1-21**), which possess different physical, chemical and microbiological properties depending on the length of the alkyl chain portion, **Figure 1:18**: where R = n-C<sub>8</sub>H<sub>17</sub> to n-C<sub>18</sub>H<sub>37</sub><sup>60</sup>. The C<sub>12</sub>, C<sub>14</sub> and C<sub>16</sub> chains comprise the major proportion of the alkyl mixture. This diverse range of possible compositions also has a direct influence on the efficacy of the compositions; the major determining factor of which is bioactivity which is controlled by the hydrophilic/hydrophobic balance of the product. The optimal of biocidal activity for this homolog series occurs with a fourteen carbon chain, as illustrated in **Figure 1:19**.



R = Alkyl

Figure 1:18: Generic formula of alkyldimethylbenzylammonium chloride (1-21)

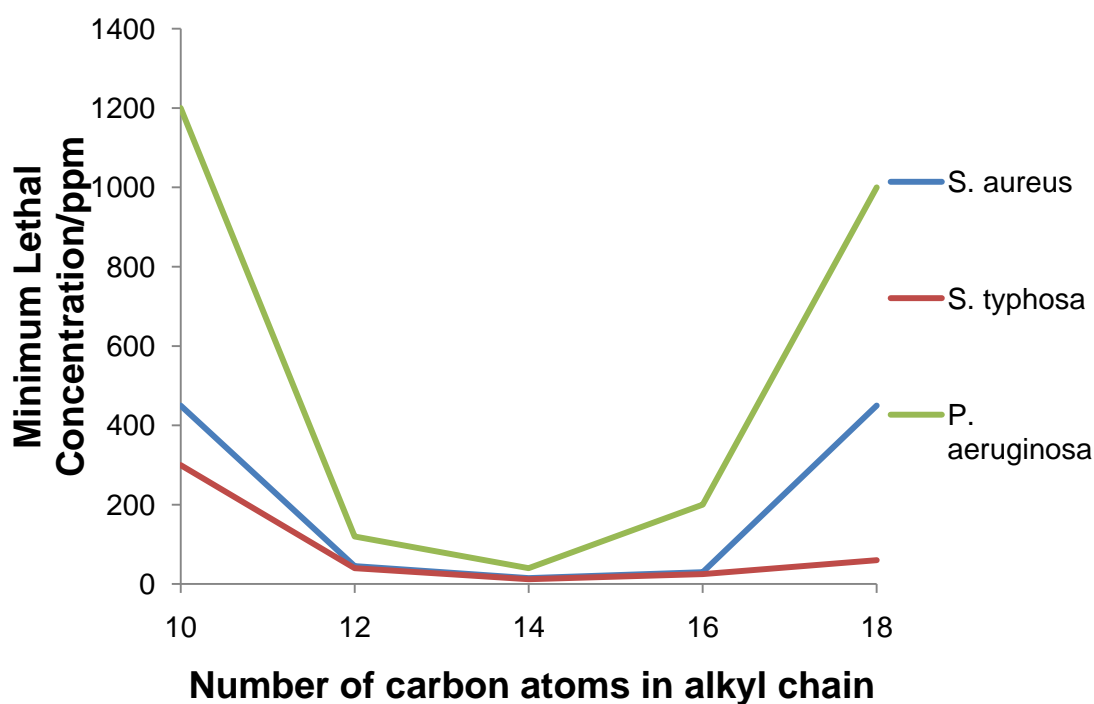


Figure 1:19: Effect of chain length on the bactericidal activity of benzalkonium chloride<sup>49</sup>

It is clear that the homologs do not possess identical bactericidal activity; therefore, the United States Pharmacopeia – National Formulary (USP-NF) sets forth guidelines for the content of benzalkonium chloride (**1-21**) as cited in Prince *et al*<sup>61</sup>:

“On anhydrous basis, the content of the  $n\text{-C}_{12}\text{H}_{25}$  homolog is not less than 40 % and the content of the  $n\text{-C}_{14}\text{H}_{29}$  homolog is not less than 20 % of the total alkyldimethylbenzylammonium chloride content. The amount of  $n\text{-C}_{12}\text{H}_{25}$  and  $n\text{-C}_{14}\text{H}_{29}$  homologs comprises together not less than 70 % of the total alkyldimethylbenzylammonium chloride content”.

Incorporation of substitutions for the aromatic ring hydrogens with chlorine, methyl or ethyl groups resulted in the next iteration of quats, being exemplified by alkyldimethylethylbenzylammonium chloride (**1-22**), **Figure 1:20**.

In 1965 catalytic amination of long alkyl chain alcohols brought about another iteration of quats, dialkyldimethylammonium halides<sup>49</sup>(1-23), **Figure 1:20**. These compounds display outstanding germicidal performance, unusual tolerance for anionic surfactants, hard water and low-foaming characteristics. Commercially these products are almost exclusively composed of even number alkyl chains owing to the high cost of odd numbered alkyl alcohols.

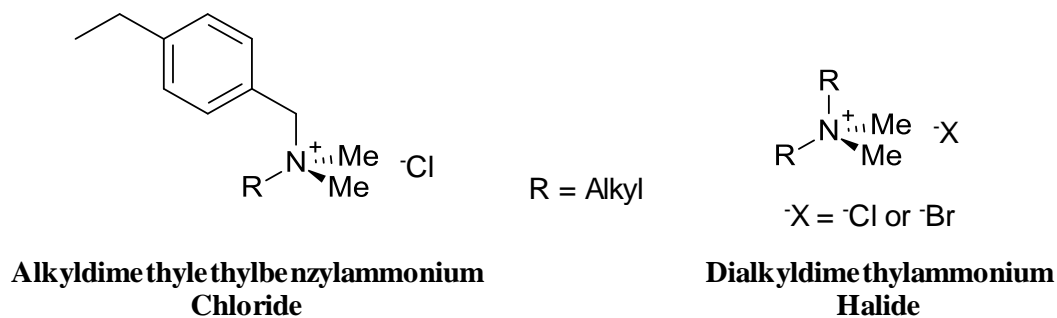


**Figure 1:20: Structures of alkyldimethylethylbenzylammonium chloride (1-22) and dialkyldimethylammonium halide (1-23)**

In the 1980's, with the growth in environmental awareness, research into quats was driven by the safety of the biocide rather than their efficacy. This more focused research led to the latest iteration, polymeric quats<sup>49</sup>. These are milder, being less toxic than benzalkonium chlorides (1-21) and safer than all previous classes of quats based on LD<sub>50</sub> and cytotoxicity.

### 1.2.2.2 Classification

In Merianos' comprehensive review<sup>49</sup>, quats may be classified depending on the nature of the R groups, the anion and the number of quaternary ammonium nitrogen atoms present in the molecule,

**Table 1:2:**

Type	R groups	Synthesis
<b>Monoalkyltrimethyl ammonium salts</b>	1xLong-chain alkyl group 3xShort-chain alkyl groups	Long-chain alkyldimethylamine with methyl halide. Or Trimethylamine with long-chain alkyl halide.
<b>Monoalkyldimethyl benzylammonium salts</b>	1xLong-chain alkyl group 1xBenzyl group 2xShort-chain alkyl groups	Long-chain alkyldimethylamine with benzyl halide.
<b>Dialkyldimethyl ammonium salt</b>	2xLong-chain alkyl groups 2xShort-chain alkyl groups	Long-chain alkyldimethylamine with long-chain alkyl halide. Or Dialkylmethylamine with methyl halide.
<b>Heteroaromatic ammonium salts</b>	1xLong-chain alkyl group 3 remaining groups form an aromatic system with the nitrogen atom e.g. pyridine or quinoline	Aromatic amine with long-chain alkyl halide.
<b>Bis-Quaternary ammonium salts</b>	R groups are as described previously, Z is an alkyl chain, <b>Figure 1:21a</b> .	Bis-tertiary amine with alkyl halide. Or Di-halo compound with a tertiary amine.
<b>Polymeric quaternary ammonium salts:</b>  1) <i>Releasable quat</i>  2) <i>Tethered<sup>62</sup> quat</i>	<u>Releasable quat</u> R groups are as described previously. Quat is bound to polymer architecture by ionic bond, <b>Figure 1:21b</b> .  <u>Tethered quat</u> Minimum of one group forming a covalent bond with the polymer architecture. The remaining groups are alkyl or aryl residues as described previously, <b>Figure 1:21c and d</b> .	<u>Releasable quat</u> Quaternary ammonium halide with alkali metal salts of a polymeric species or polymerisation of an ionic quaternary ammonium containing monomer.  <u>Tethered quat</u> c) Tertiary alkylamine with chlorinated polymer e.g. poly(3-chloropropyl)methylsiloxane <sup>63</sup> . Or d) Tertiary alkylamine with oxyethylene bromide <sup>64</sup> .

**Table 1:2: Classification of quaternary ammonium compounds**

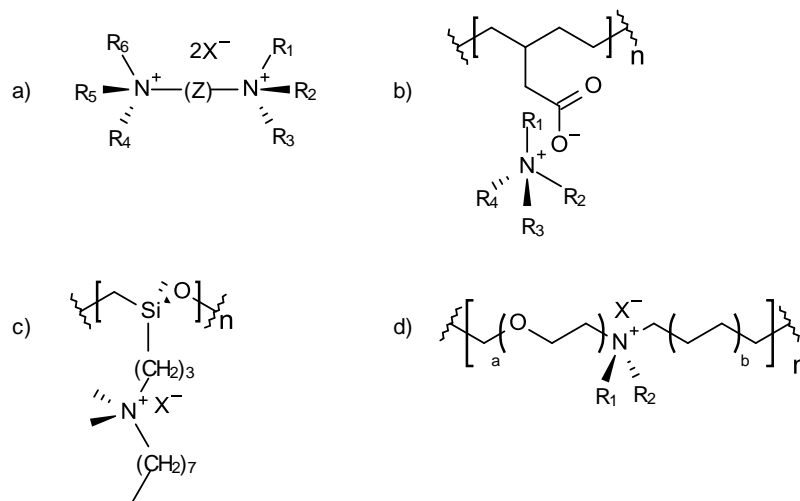


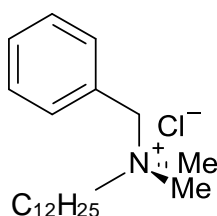
**Figure 1:21: a) General formula of bis-quaternary ammonium salts, b) example of releasable polymeric quat, c) example of a tethered polymeric quat and d) example of a tethered polymeric quat.**

### 1.2.2.3 Mode of Action

It is long been accepted that water-soluble cationic biocides, such as quats, operate through a lethal electrostatic-hydrophobic interaction with bacterial cell membranes<sup>65, 66, 67, 68</sup>, which has a number of key stages, summarised as follows:

- 1) Adsorption onto the bacterial cell surface (electrostatic)
- 2) Diffusion through the membrane (hydrophobic)
- 3) Binding to the cytoplasmic membrane
- 4) Disruption of the cytoplasmic membrane
- 5) Release of cytoplasmic constituents, such as potassium ions, DNA and RNA
- 6) Cell death

However, the degree of activity of the cationic biocides is sharply dependent upon their chemical structure. Valko and Dubois<sup>69</sup> highlighted this structural dependency in 1945. Their study centred on a series of compounds closely related to dodecyldimethylbenzylammonium chloride (**1-24**), **Figure 1:22**, and their germicidal activity towards two strains of bacteria *Staphylococcus aureus* and *Eberthela typhi*. The study showed that in the series linear homologous of alkyldimethylbenzylammonium chloride (**1-21**), **Figure 1:23**, the maximum potency is reached with a carbon chain length of 12 and 14, which have practically the same efficacies. They also noted the decrease in efficacy from the C<sub>12</sub>/C<sub>14</sub> maxima is not symmetrical, being steeper towards the shorter chain species as well as the marked disparity in activity shown towards the two bacterial strains. Minor structural modifications to some of the linear homologs produced major differences in the efficacy of the quats. The introduction of unsaturation greatly increased the efficacy of 9-octadecenyl dimethyl compound to *S. aureus* compared to its octadecyl analogue while the enhancement in efficacy was not as marked for *E. typhi*. Substitution of a methyl group for an octyl alkyl chain enhanced the efficacy of dioctylmethyl compound compared to its octyldimethyl analogue for both the bacteria.



**Dodecyldimethylbenzylammonium Chloride**

**Figure 1:22: Structure of dodecyldimethylbenzylammonium chloride (1-24)**

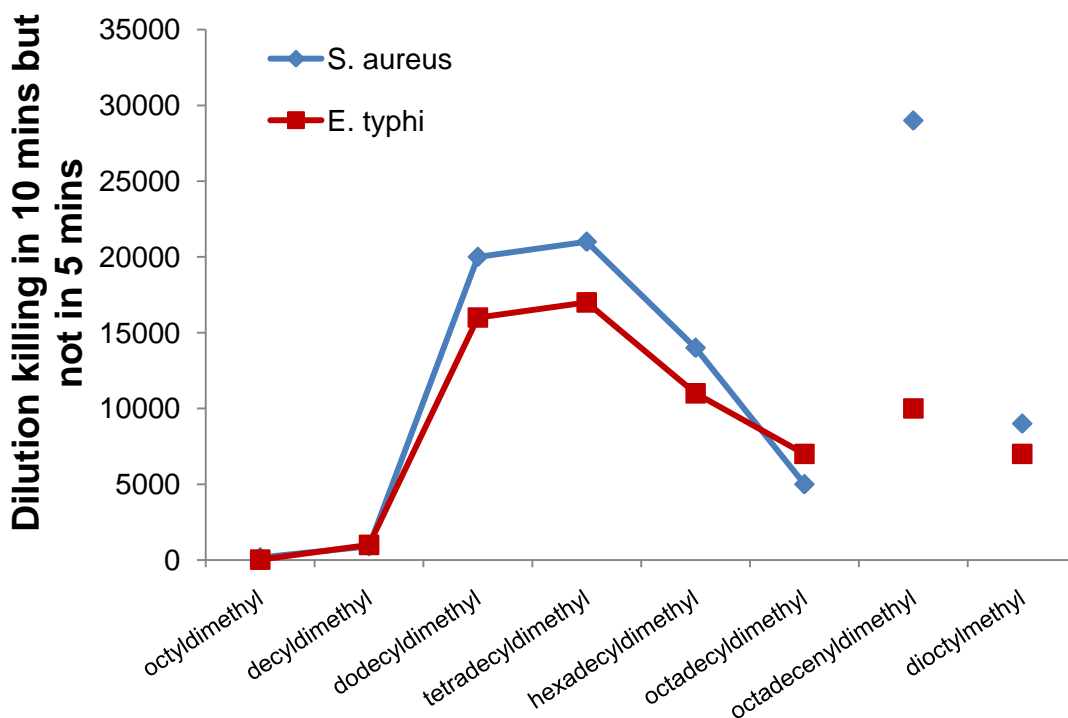


**Figure 1:23: Germicidal activity of linear homologues of alkyldimethylbenzylammonium chloride and octadecenyl dimethyl- and dioctylmethyl- modified quat at 20 °C<sup>69</sup>**

Similar results were also gained for series based on alkyldimethylethylbenzylammonium (**1-22**), alkyldimethylallylammonium (**1-25**) and alkyltrimethylammonium bromides (**1-26**) species, **Figure 1:24**, with the notable exception that exchange of the benzyl group for an allyl, ethylbenzyl or third methyl group resulted in the maximum potency shifting towards the higher chain lengths C<sub>14</sub>/C<sub>16</sub>.

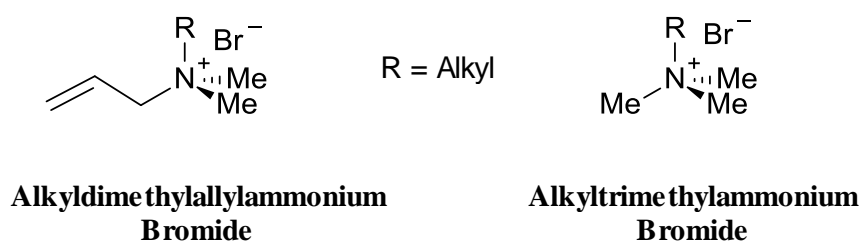


**Figure 1:24: Structures of alkyldimethylallylammonium (1-25) and alkyltrimethylammonium bromides (1-26)**

Responding to the fact that commercially available quat biocides are sold as mixtures of chain lengths, Valko and Dubois briefly explored the efficacy of a mixed quat systems. Commercial quats are synthesised from natural fats/alcohols and hence that molecular distribution is transposed onto the quats. The efficacy of a 3:2 mixture of octyldimethylbenzylammonium chloride (**1-27**), with octadecyldimethylbenzylammonium chloride (**1-28**), **Figure 1:25**, was compared to that of dodecyldimethylbenzylammonium chloride (**1-24**), which can be considered as the single

molecular species which has the equivalent alkyl chain length as that of the mixture. The killing dilutions were 1:2000 for the mixture and 1:20 000 for the dodecyldimethylbenzylammonium chloride (**1-24**). The result indicated that the determining factor in antimicrobial activity is not the average composition of the mixture but the independent contribution of each individual component and hence determining the average chemical composition is of no value.

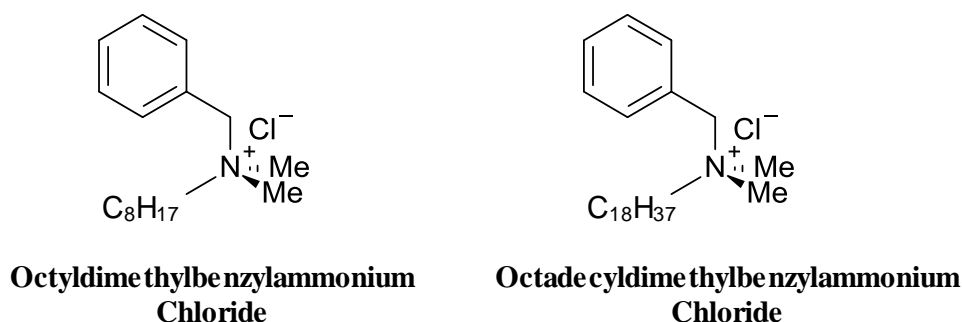


**Figure 1:25: Structures of octyldimethylbenzylammonium chloride (1-27) and octadecyldimethylbenzylammonium chloride (1-28)**

The efficacy of the cationic biocide is also dependent upon the target organisms. Several studies have published reports detailing the differences in activity of quats to gram-positive and negative bacteria<sup>70, 71, 72</sup> fungi<sup>73</sup> and algae<sup>74</sup>.

It is well documented that gram-negative bacteria show a greater resistance to quats than gram-positive. A major difference between gram-positive and gram-negative bacteria, fungi and yeasts is their cell membrane. In gram-positive bacteria the cell membrane is covered by a thick layer composed of peptidoglycan. Gram-negative bacteria have additional outer membrane found above the peptidoglycan wall. Yeast and fungi have a single membrane covered by a thick layer composed of glucan and chitin, similar to gram-positive bacteria<sup>75</sup>. These outer components of the cell perimeter can be considered as a series of aqueous and hydrophobic domains and this analogy has been invoked to explain the differences in efficacy<sup>49</sup>.

Kouvai *et al*<sup>76</sup> in 1989 reported on the relationship between hydrophobicity of the bacterial cell surface and their susceptibility to quats. The partition coefficient of bacterial cells between n-hexadecane and physiologic saline was proposed as the best pairing to investigate the hydrophobicity of the cell surface. The hydrophobicity of the gram-negative bacteria was always higher than that of the gram-positive. This relative ordering was also exhibited in their quat susceptibility.

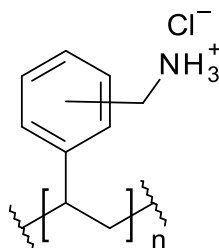
Daoud *et al*<sup>77, 78</sup> in 1983, demonstrated that the chain length for optimal activity varies from organism to organism. The lower chain lengths, C<sub>10</sub>-C<sub>12</sub> were more active against yeast and fungi,

whereas gram-negative bacteria were susceptible towards the longer more hydrophobic C<sub>16</sub> species. The authors suggested this was a consequence of the complex alternating hydrophobic/aqueous layers of their cell membranes and the difficulties encountered by molecules traversing it. That is, molecules of low water solubility would be unable to penetrate the aqueous regions of the cell perimeter and would accumulate within the hydrophobic region; conversely those compounds of low organic solubility would be unable to cross the hydrophobic barrier. Therefore compounds between these two extremes, such as quats, exhibit the optimum balance between the hydrophobicity and hydrophilicity for traversing the cell barrier. As a result gram-negative bacteria with their more complex cell structure are the most resistant to quats.

Quats, due to their surfactant nature, are thermodynamically driven to form micelles once a specific threshold is reached in their concentration, the Critical Micelle Concentration (CMC). Tomlinson *et al* (1977)<sup>79</sup> has explored how the Minimum Inhibition Concentration (MIC) of quats is affected by their CMC and changing salinity of the test conditions. The salinity proved critical as it altered the CMC and resulted in lower efficacious results for quats once passed their CMC. Consequently, the authors questioned the result of MIC toxicity tests simulating physiological conditions because they might not represent a true reflection of the intrinsic activity of the compounds due to the presence of salt altering the CMC.

Since the 1980s with the switch in focus to quats which have shorter environmental residence half-lives, research has centred on polymeric quats and specifically those which can be chemically bonded to a host surface. These new quats have a number of advantages compared to non-polymeric quats. Namely the biocidal centre is permanently attached to the surface and as a result is not released. This therefore negates the possibility of the target organism(s) developing resistance to the quats by virtue of preventing 'over medication'. The fact that the quats are chemically attached to the host surface results in a permanent biocidal surface that can withstand repeated washing and maintain its biocidal performance and hence extend the commercial lifetime of these surfaces.

Early in the development of these polymeric quats it was noted that they exhibit greater antimicrobial activity than their monomeric precursors<sup>80</sup>. It was assumed that they followed the same mode of action as the non-polymeric quats but their enhanced activity was instead molecular weight (MW) dependent. In 1986 Ikeda *et al* using water soluble poly(vinylbenzyl ammonium chloride) (1-29), **Figure 1:26**, investigated the MW dependency.



**Poly(vinylbenzyl ammonium chloride)**

**Figure 1:26: Structure of poly(vinylbenzyl ammonium chloride) (1-29)**

The polymer was chromatographically fractionated into defined MW distributions and their activity was determined through the release of potassium ions from the target organism, *S. aureus*. The activity was shown to be strongly MW dependent and that there existed an optimal MW range,  $5 \times 10^4$  to  $10 \times 10^4$  Da. The authors concluded that increasing the MW of the quats increased the charge density of the cationic centres, which would enhance the adsorption of the polymeric quats onto the negatively charged cell surface. Likewise the polymer would interact more strongly with the cytoplasmic membrane due to the many negatively charged species present in the membrane causing greater disruption and ultimately cell death. On the other hand the diffusions through the cell membrane of the polymers would be suppressed as the MW of the diffusing species increased. Therefore the observed optimal MW range for antimicrobial activity can be considered as the sum of two competing factors, namely the increasing interaction of the positively charged cations centres with the negatively charged constituents of the cell and the decreasing potential for the molecule to diffuse through the cell membrane.

Klibanov *et al* have also demonstrated, based on tethered quats, similar MW dependencies in their comprehensive succession of publications. The underlying premise of their work has been to try to develop persistent antimicrobial surfaces for example on glass<sup>81</sup>, polyethylene<sup>82</sup> and textiles<sup>83</sup>. Not only, have they investigated two types of polymeric quats<sup>82, 83</sup> but have also endeavoured to offer insights into the mechanism of the mode of action of these quats<sup>83</sup>. Through their initial work alkylating poly(4-vinylpyridine) (**1-30**), **Figure 1:27**, they again demonstrated the parabolic efficacy of quats with a maximum for a six carbon chain alkyl residue attached to the pyridine<sup>81</sup>. They suggested that this relationship was due to the sum of two competing factors, the increasing efficacy with chain length but also the decreasing availability of the chains at the surface due to increasing intramolecular hydrophobic interaction between chains. Therefore the optimal efficacy occurred with a C<sub>6</sub>-alkyl residue. At this chain length the hydrophobic interaction is counter-balanced by the electrostatic repulsion between vicinal pyridinium cations allowing the C<sub>6</sub>-alkyl residue to present itself from the host surface. They also further demonstrated that the C<sub>6</sub>-alkyl

residue represents the optimum activity for alkylated polyethylenimines (PEIs)<sup>84</sup> (**1-31**), **Figure 1:27**.

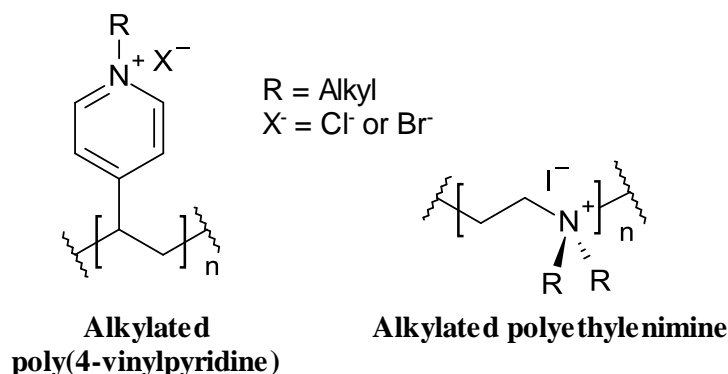


**Figure 1:27: Structures of alkylated poly(4-vinylpyridine) (1-30) and alkylated polyethylenimine (1-31)**

Through the utilization of commercially available PEIs with different MW they also demonstrated the MW dependency of quat systems, showing that high MW alkylated PEIs are substantially more active than low MW species<sup>84</sup>. They estimated the linear lengths of the PEIs and compared these to typical bacterial cell dimensions. The low MW PEIs, 0.8K and 2K Da have estimated linear length of 0.007 and 0.02  $\mu\text{m}$  respectively, which are too short to penetrate the cell membrane (1-2  $\mu\text{m}$ ). However, the 750K Da has an estimated length of 6  $\mu\text{m}$  and could easily penetrate the cell and cause cell death. The authors questioned previous publications relating surface bound quats with the historically accepted mode of action; diffusion through the membrane and lethal interaction with the cytoplasm. Unlike water-soluble quats, which may be able to penetrate the cell membrane, surface bound quats are constrained by their molecular length and can only penetrate the cell membrane if they extend far enough away from the surface. In these earlier publications the polymeric quats were substantially shorter than the 0.8K Da in Klivanov's work and hence would have great difficulty penetrating the cell membrane.

Sambhy *et al* further elaborated on the understanding of the alkylated poly(4-vinylpyridine) (**1-30**) by investigating the spatial relationship between the alkyl residue and the cationic centre<sup>85</sup>. The 4-vinylpyridine was co-polymerised with either hexyl acrylate or methyl acrylate monomers allowing the position of the C<sub>6</sub>-alkyl residue to vary from the pyridinium centre to the acrylate group. It was observed that spatial positioning of the positive charge and the alkyl tail has a significant effect on the antibacterial activity of the polymer, decreasing markedly when the alkyl residue is positioned other than on the cationic centre.

Since Klivanov's assertion regarding the inconsistencies with the theory of the mode of action of the quats, it has gradually become accepted that the historically accepted mode of action of

polymeric quats is too simplistic. It fails to fully explain the broad spectrum activity they exhibited, killing viruses to fungi even though the different microbes have dramatically different membrane properties and structures.

Several studies have established that surface density of the quat units is a critical element in the activity of surface bound polymeric quats<sup>66, 86, 87</sup>. Kügler *et al*<sup>66</sup> investigated the activity of the quats towards bacteria in different metabolic states, either growth or quiescent condition. They demonstrated that the electrostatic attraction between the negative charge bacterial membrane and the positive charged substrate is also applicable to bacteria in dividing conditions. However, the efficacy is very dependent upon experimental conditions and rate of cell division. In experiments which use large volumes of solutions the probability of a bacteria, subjected to Brownian motion, encountering the quat surface, if it is more than 100  $\mu\text{m}$  away is very small. Under these conditions the rate of cell division can outpace the rate of cell death and hence appear to result in low efficacies. They also discovered that there is a threshold above which the rate of cell death is dramatically increased. For *S. epidermidis* in the growth state the threshold is  $10^{13} \text{ N}^+ \text{ cm}^{-2}$  (ammonium groups per cm) and  $10^{14} \text{ N}^+ \text{ cm}^{-2}$  in the quiescent state. For *E. coli* the thresholds are  $10^{12} \text{ N}^+ \text{ cm}^{-2}$  in the growth state and  $10^{14} \text{ N}^+ \text{ cm}^{-2}$  in the quiescent. Bacteria have in the order  $10^5$  negative charge sites over their surfaces; this is equivalent to  $10^{13} \text{ N}^+ \text{ cm}^{-2}$ . This convergence of numbers between charge density of the cell surface and the charge density threshold may be significant. Murata *et al*<sup>86</sup> and Cen *et al*<sup>87</sup> have reported similar results. These results suggest that tethered quats become biocidal when their number of cationic sites is large enough to replace all the stabilising counter ions surrounding the bacterial membrane in solution. Their observations have helped establish an alternative mechanism explaining the broad spectrum activity of polymeric quats. This mechanism conjectures that the highly charged polymeric quats can induce an ion exchange reaction between the cationic centres of the polymer and the structurally critical cations within the cell membrane. The loss of these structural cations results in the loss of membrane integrity. In aqueous solution the negatively charged cell membrane is surrounded by many low-valency cationic counter ions that ensure electroneutrality. It has gradually been realised that the adsorption of the polymeric quats is driven by the release into solution and replacement of these low-valency cationic counter ions. Their release leads to a large entropy increase which, more than compensates the loss of entropy associated with the polymer immobilization and that this release leads to non-viable cells and ultimately death.

For gram-positive bacteria the outer membrane is stabilised by magnesium and calcium ions. If these are expelled by the polymeric quats the outer membrane is destabilised leading to cell death. Similar effects have also been noted in solution with the addition of multivalent complexing agents such as EDTA<sup>88</sup>. However, it is unclear as to whether this mechanism is applicable to gram-

negative bacteria as their cell membrane is different, having a peptidoglycan layer as an outer membrane. It is significant that a higher charge density threshold is required for gram-negative bacteria.

### 1.2.3 Environmental Fate and Biodegradation

The environmental fate of quats is of great interest due to the fact that they are widely employed as pesticides and fabric softeners/detergents, which readily pass into the water system, whether by discharge or runoff. The research into quats has largely focused on the most commercially available species. At the outset, it must be noted that cationic surfactants, of which quats are the main examples, are not the major constituent of detergents and this is reflected in the literature, being studied less than linear alkylbenzene sulphonates (LAS) (1-32) and alkyl ethoxylates (AE) (1-33), **Figure 1:28**. The main focus of research in the literature has been wastewater treatment facilities and waterways, which represent possible repositories for surfactants, with very few considering the marine environment.

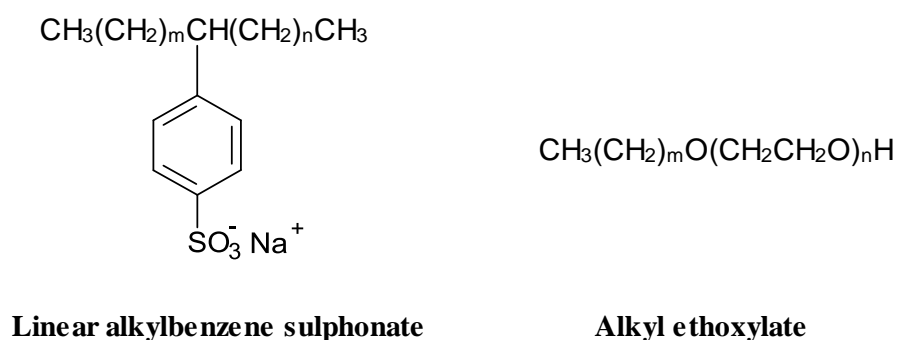


**Figure 1:28: Structures of linear alkylbenzene sulphonates (1-32) and alkyl ethoxylates (1-33)**

There are two main processes by which quats are removed from the environment, biodegradation and sorption onto particulate matter/sediments.

Balson and Felix<sup>89</sup> defined biodegradation as the destruction of a chemical by the metabolic activity of microorganisms. During biodegradation microorganisms can either utilise quats as substrates for energy and nutrients or co-metabolise the surfactants by microbial metabolic reactions. There are many chemical and environmental factors that affect biodegradation of surfactants in the environmental. The most important influencing factors are chemical structure and physiochemical conditions of the aqueous environmental media<sup>90</sup>. The literature concerning the degradation of surfactants mainly quotes primary and/or ultimate biodegradation. Primary degradation can be defined as to have occurred when the structure has changed sufficiently for a molecule to lose its surfactant properties<sup>91</sup>. Ultimate degradation is said to have occurred when a surfactant molecule has been rendered to carbon dioxide, methane, water, mineral salts and biomass<sup>91</sup>.

Under aerobic conditions Nishiyama *et al*<sup>92</sup> proposed a degradation pathway for alkyltrimethylammonium halides (**1-26**) as a process of N-dealkylation followed by N-demethylation. According to this pathway alkyltrimethylammonium salts are initially degraded to trimethylamine by N-dealkylation. The trimethylamine is then degraded to dimethylamine via N-demethylation and then through another iteration to methylamine. The trimethylamine, dimethylamine and methylamine have been identified as the intermediates of alkyltrimethylammonium halides (**1-26**) in sewage treatment plants<sup>90</sup>.

In 1991, van Ginkel *et al*<sup>93</sup>, studied the oxidation rates of alkyl substituted quats by microbial cultures to assess their rates of biodegradation. It was elucidated that the biodegradation rates decrease with increasing alkyl-chain length and suggested that this may be caused by steric hindrance of the quaternary nitrogen atom, a theory postulated by Yoshimura *et al*<sup>94</sup> in 1980. It was also noted that the decrease in rate of biodegradation was more pronounced with increasing numbers of alkyl-chains attached to the nitrogen. This is in agreement with the biodegradation susceptibility ladder proposed by Swisher *et al*<sup>95</sup> in 1987:



Moreover replacement of a methyl group with a benzyl group can further decrease biodegradation. Viewed as a series based on reducing steric hindrance of the nitrogen cationic centre, the susceptibility ladder could be considered consistent with the biodegradation pathway proposed by Nishiyama. Reducing steric hindrance allows the N-dealkylation and subsequent N-demethylation reactions to proceed quicker, allowing an increased rate of degradation.

Garcia *et al*<sup>96</sup> in 2001 reported half-lives for different quats in various media including seawater ranging from three to eight days. The degradation of these compounds in coastal water was associated with an increase in bacterioplankton density suggesting that the degradation is due to the compounds being utilised as a growth substrate. Conversely, Games *et al*<sup>97</sup> reported half-lives as short as 2.5 hrs for octadecyltrimethylammonium chloride (**1-34**) in wastewater, **Figure 1:29**.

Unfortunately, literature concerning the fate of quats under anaerobic conditions is scarce. Garcia *et al*<sup>98</sup> in 1999 stated that under anaerobic conditions there was no evidence of ultimate degradation was found for alkyltrimethylammonium (**1-26**) and alkylbenzyltrimethylammonium halides (**1-21**) and that for both homologs the primary degradation after 125 days of anaerobic testing was 20-30 %. Topping and Waters (1982) cited in Garcia *et al*<sup>98</sup> noted that there was no evidence for the degradation of ditallowdimethylammonium halides (**1-35**), **Figure 1:29** (a dialkyldimethylammonium homolog in which the alkyl portion contains 65 % octadecyl, 30 %

hexadecyl and 5 % tetradecyl) under anaerobic conditions. Battersby and Wilson<sup>99</sup> observed that concentrations of 200 mg l<sup>-1</sup> hexadecyltrimethylammonium bromide (**1-36**), **Figure 1:29**, inhibited the production of methane, suggesting that at that concentration the quat is inhibitory to the microbes. Garcia *et al*<sup>98</sup>, showed that the toxicity to methanogenesis decreased with increasing alkyl-chain length, reported similar observations.

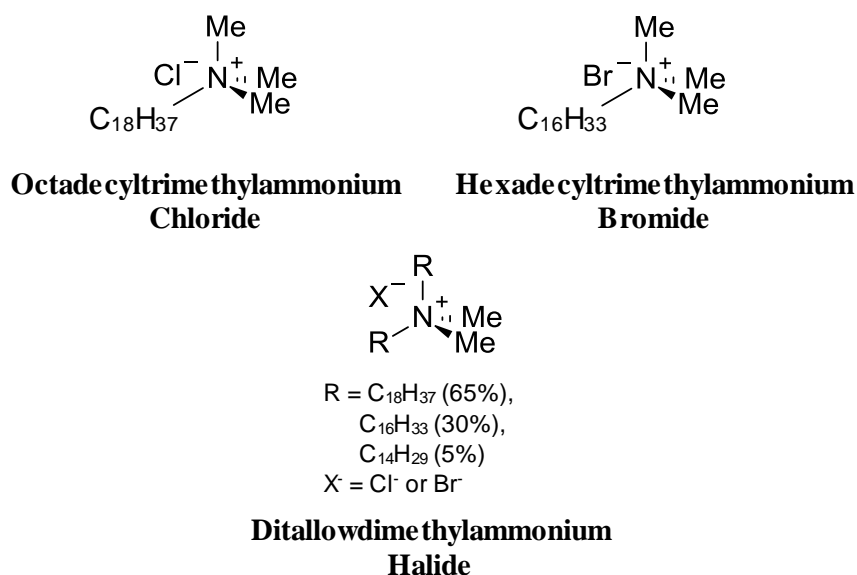


**Figure 1:29: Structures of octadecyltrimethylammonium chloride (1-34), hexadecyltrimethylammonium bromide (1-36) and ditalowdimethylammonium halide (1-35)**

No pathway for anaerobic degradation exists within the literature. The initial N-dealkylation of the quats cannot take place without the presence of molecular oxygen. Therefore, it can be assumed that quats are not anaerobically biodegradable either because of a lack of appropriate metabolic pathways, and/or a possible toxic effect of the quats upon the relevant anaerobic microbes. Under these conditions sorption of quats is the primary route to removal from the water system.

Several studies have reported that sorption of quats is a major removal pathway from water systems<sup>100, 101, 102, 103</sup>. Quats, having a positive charge, have a strong affinity for the surface of particulate matter, which is predominately negatively charged. Sorption can be described by the Freundlich equation which defines the relationship between the amount sorbed and the equilibrium solution concentration:

$$S = K_d C$$

Where  $S$  is the concentration of a surfactant sorbed by the solid phase (mg/kg);  $K_d$  is the sorption coefficient (l/kg); and  $C$  is the equilibrium solution concentration (mg/l).  $K_d$  is frequently used to characterise the sorption of a chemical in sediment/soil<sup>90</sup>.

Games *et al*<sup>97</sup> reported the  $K_d$  for octadecyltrimethylammonium chloride (**1-34**) was 66, 000 l/kg which was substantially larger than the  $K_d$ s for anionic and non-ionic surfactants which were respectively one and two orders of magnitude lower. The authors asserted that this large range in  $K_d$  reflected the different mechanisms of sorption for different surfactants, electrostatic for quats and a hydrophobic mechanism for LAS and AE. Games *et al* also reported that 98% of quats were removed within 90 mins after an initial dosage of 20 mg/l. Larson *et al*<sup>100</sup> found that quats sorb strongly to natural sediments with an equilibrium being reached within hours and that the  $K_d$  values are higher for monoalkyl- than dialkyl-quats, being 226, 000 and 12, 000 l/kg respectively. This further suggests that the sorption of the quats is via an electrostatic interaction and that the more sterically hindered dialkyl-quats interact more weakly than the monoalkyl-quats.

The biodegradation of monoalkyl-quats was found to be inhibited in the presence of montmorillonite, a clay mineral, in two separate studies by Weber *et al*<sup>101</sup> and Barbaro *et al*<sup>102</sup>. Moraru<sup>103</sup> has shown that the monoalkyl-quats can intercalate into the clay lattice forming two layers having parallel orientations of alkyl-chains. The intercalation can protect the quats from microbial attack by adsorption on the inner surfaces of the clay lattice. Therefore sorption is the primary mechanism for removal of quats from the environment.

#### **1.2.4 Toxicology**

There are substantially fewer toxicological studies dealing with cationic surfactants/quats than other types of surfactants due to their lower levels of commercialisation. Therefore the available data is mostly for commercially available quats. The fact that quats frequently enter the water system through sewage systems or agricultural run-off has resulted in cationic surfactants being the subject of a number of studies, most notably in a trilogy of reviews by Lewis<sup>104, 105, 106</sup>. The first review by Lewis<sup>104</sup> considered the effects of surfactants on algae. After a comprehensive review of the published scientific data, Lewis concluded; the only consistent finding was the hierarchical succession of efficacy with cationic surfactants being the most effective followed by anionic and non-ionic surfactants respectively against algae. Also evident was that the toxicity of all surfactant was less when determined for natural algal communities under natural conditions. Inconsistencies such as surfactant type, tests species, effect parameters and lack of analytical verification of effect concentration hampered any further general conclusions being drawn. Lewis also queried the practise of using species specific laboratory tests as predictive tools for environmental toxicology due to the over estimation of laboratory tests when compared to results derived from natural communities. The reported effect concentrations for quats were greater than the environmental concentrations indicating an unlikelihood of an adverse effect of quats on algae.

The second review<sup>105</sup> considered the effect of surfactants on aquatic animals. Similarly with the previous review, conclusions for cationic surfactants were severely limited due to their limited data-set with the main focus again being ditallowdimethylammonium chloride (**1-35**). However, results for standard toxicology tests on fish had an effect range of 0.05-0.46 mg/l compared with 0.05-28 mg/l and 0.05-50 mg/l for anionic and non-ionic respectively. For invertebrates the trend was the same: 0.009-1.27 mg/l for cationic and 0.04->10 mg/l and <0.1-20 mg/l for anionic and non-ionic. These results again emphasised the greater efficacy of cationic surfactants and mirror the trend seen with algae.

The third review<sup>106</sup> of the series concerned the toxic effects of surfactants on aquatic life and environmental modifying factors. It is accepted that a variety of environmental characteristics can affect the toxicity of surfactants; these include species type, life stage, temperature, water hardness, dissolved oxygen and particulate content. The dearth of published data again reflects limited commercialisation. Of all the mitigating effects, suspended solid/particulates concentrations have the greatest effects on cationic surfactant toxicity. The presence of suspended particulates significantly reduces the bioavailability of quats due to their adsorption to the particles, thereby reducing their efficacy. Throughout all three reviews Lewis questioned the tendency to predict environmental toxicities using models which do not adequately account for a significant number of the environmental variables. However, it was also acknowledged that these tests would be labour intensive and long term.

Utsunomiya *et al* (1997) cited in Ying *et al*<sup>90</sup> reported the effects of three quats and one anionic surfactant on green algae, *Dunaliella spp.* The most effective was alkyltrimethylammonium halides (**1-26**). Substitution of a methyl group from the alkyltrimethylammonium halides (**1-26**) for a benzyl group reduced the efficacy and a further substitution of the benzyl group for a secondary alkyl group reduced the efficacy further. The efficacy of the dialkyldimethylammonium halides (**1-23**) was notably lower than anionic surfactant. These results are contrary to those of Garcia *et al* (1999)<sup>98</sup>. In the 1999 study it was concluded that there was no difference in the toxicity of quats to methogenic gas production with the substitution of a methyl group for a benzyl group i.e. alkyltrimethylammonium halides (**1-26**) were as effective as alkyldimethylbenzylammonium chlorides (**1-21**). There was however a correlation with increased inhibition of gas production with increasing alkyl chain length. However in Garcia *et al* (2001)<sup>96</sup> the conclusions were different. This study determined the toxic effect of quats to bacteria, planktonic crustacean (*Daphnia magna*), and marine bacteria, (*Photobacterium phosphoreum*), in the concentration range 0.1-1.0 mg/l. The quats were C<sub>12</sub>-C<sub>16</sub> alkyltrimethylammonium (**1-26**) and the alkyldimethylbenzylammonium (**1-21**) homologs. Here there appeared to be no effect on *D. magna* from increasing alkyl chain length, which was possibly due to reduced bioavailability of the quats because of reducing solubility.

However, there was an increase in toxicity with the substitution of a benzyl for a methyl group. It was also concluded that no important toxic effects of cationic surfactants on marine bacteria population was detected.

In a comparable study by Leal *et al* (1994)<sup>107</sup>, the conclusions were again different with hexadecylbenzyltrimethylammonium halide (**1-37**), **Figure 1:30**, the most efficacious, six times greater than hexadecyltrimethylammonium halide (**1-38**), **Figure 1:30**, which was four times more effective than dioctadecyldimethylammonium halide (**1-39**), **Figure 1:30**, against *D. magna*. While overall the efficacy of the quats was greater for *P. phosphoreum* the same order was evident; reflecting the high toxicity resulting from the benzyl moiety and the poorer transmission of the dioctadecyldimethylammonium halide (**1-39**) through the biological membranes of the bacteria.

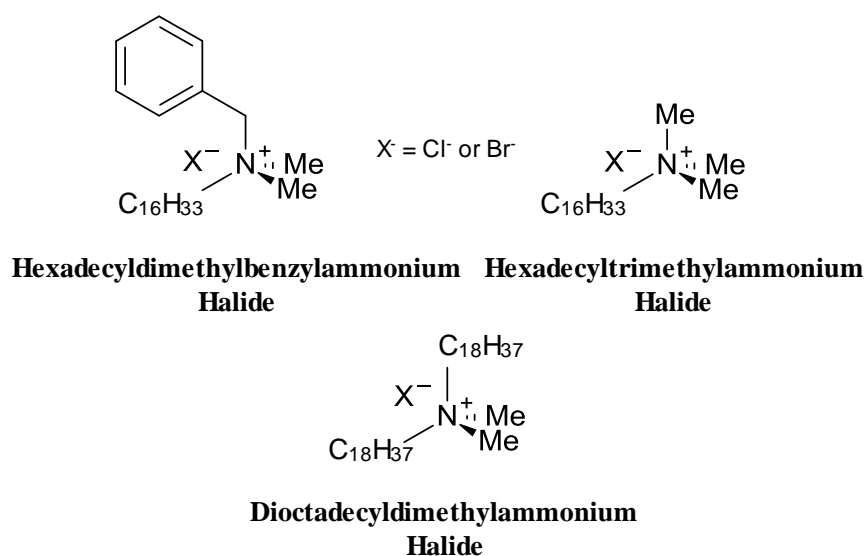


**Figure 1:30: Structures of hexadecylbenzyltrimethylammonium halide (1-37), hexadecyltrimethylammonium halide (1-38) and dioctadecyldimethylammonium halide (1-39)**

Baudrion *et al* (2000)<sup>108</sup> specifically investigated the effects of quats on a marine bacterial community. It was concluded that cationic surfactants, while using a similar mode of action as organotin compounds were far less toxic. The efficacy of quats was predominately determined by the number of carbon atoms in the alkyl chain, with the optimum length dependent upon the remaining three groups on the nitrogen atom, but in general C<sub>8</sub>-C<sub>16</sub> carbon atoms gave the maximum potency. Substitution of a methyl group with a ring structure, such as a benzyl or phenolic, increased efficacy with a phenolic structure being greater. The effect of the halide counter ion was also investigated. The toxicity of the iodide quats was greater than either chloride or bromide quats, which had similar potency.

Ferks *et al* (2007)<sup>109</sup> compared the toxicity of alkyldimethylbenzylammonium chlorides (**1-21**) with dialkyldimethylammonium halides (**1-23**) on DNA of both mammalian and plant cells. The results indicated that both the quats induced a moderate but significant genotoxic effect in eukaryotic cells at environmentally relevant concentrations. The toxicity of the dialkyl-quat was greater than the benzyl-quat. This appeared to be the first study using dioctadecyldimethylammonium bromide (**1-39**) while dioctadecyldimethylammonium chloride (**1-39**) had been previously reported in the scientific literature and gave negative genotoxic results.

The lack of consistency in a number of key test parameters, as well as target species used combine to hinder definitive conclusions for the toxicity of quats from being drawn<sup>105</sup>. The dominance of toxicological data for freshwater species reflects the ease of culture techniques and available standard test methods, which contrasts negatively with that for marine species. Consequently the toxicological of quats on marine aquatic life has largely been estimated from effects derived from freshwater life<sup>105</sup>. It is difficult to know whether marine strains of bacteria are more resistant than other strains (terrestrial or lake) because of the variety of strains and compounds used by different authors<sup>108</sup>. Until sufficient data is generated with regards the toxicity of quats in the marine environment, a precautionary approach should be used. However, the likelihood of accumulation of quats is limited due to their biodegradation and their ready adsorption to particulates reducing their bioavailability.

### 1.2.5 Analysis/Detection

The main focuses of quat analytical methods have been characterisation and/or quantification. These methods are as numerous and varied as the plethora of possible analytes encompassed by the term quat. These methods reflect the diversity and multifaceted natures of quats: harnessing either the presences/absences of a chromophore, the hydrophobic/hydrophilic domains and either the cationic/neutral regions of the molecule. The use of quats as antimicrobial, herbicidal and softening agents has resulted in their application in products as broad as cosmetic formulations, cleaning and disinfectant products, pharmaceutical preparations as well as textile softeners. Analysis of these products along with biological, sewage treatment and environmental samples, both aqueous and sedimentary, represents a significant and varied array of analytical matrices. Together with the nature of the quats, the analytical matrix exerts a major influence over the development of a method and subsequently its range of applications. Methods utilising UV detectors will be unsuitable for analytes which lack a chromophore. Likewise analytes in a predominately aqueous matrix would be unsuitable for a GC-based method.

Historically quats were analysed using colorimetric<sup>110</sup> and titration<sup>111</sup> methods. These procedures were long, tedious and lacked the specificity to distinguish between different homologs. These

issues have largely been addressed with the use of modern analytical instrumentation such as Capillary Electrophoresis (CE)<sup>112</sup>, Gas Chromatography (GC)<sup>113</sup> and Liquid Chromatography (LC)<sup>114</sup> which have automated and enhanced the procedures.

The application of CE has largely focused on pharmaceutical<sup>115, 116, 117</sup> and biological samples<sup>118</sup>, but there are examples of applications for cleaners/disinfectants<sup>119</sup> as well as irrigation water<sup>120</sup> analysis. CE separates analytes based on charge, via the application of a potential difference across a capillary column with a continuous flow of buffered aqueous eluent. Detection is primarily based on UV absorbance<sup>115, 116</sup> but conductivity and fluorescence<sup>121</sup> detectors have also been used. Detection limits are in the range of low parts per million (ppm; mg/l)<sup>122</sup>. However, CE analysis of quats is problematic because of their ability to adsorb strongly to the capillary walls<sup>118</sup> and their tendency to form micelles at low concentrations<sup>122</sup>. This can result in peak tailing, poor separation and reproducibility. The solubility of higher alkyl-group containing quats is also problematic as it is substantially reduced in the aqueous eluent<sup>123</sup>. Attempts to improve the problems have focused on coated capillaries<sup>124</sup> to deactivate the walls and the addition of varying modifiers<sup>125</sup> such as tetrahydrofuran (THF), acetonitrile (ACN) and cyclodextrins<sup>121</sup> to reduce the tendency of the quats to aggregate into micelles.

The main focus of GC analysis has been towards biological and clinical samples<sup>126, 127</sup>. GC analysis requires the analyte to be sufficiently volatile to enable it to pass through the column to the detector. Direct GC analysis of quats is not possible due to their ionic nature and hence their low volatility. However, by converting the quat to a tertiary amine through an Hofmann degradation<sup>113</sup>, **Figure 1:31**, the resultant amine is sufficiently volatile for GC analysis and suitable for a broad range of detectors such as flame ionisation (FI), nitrogen-phosphorous (NP) and mass spectrometry (MS).

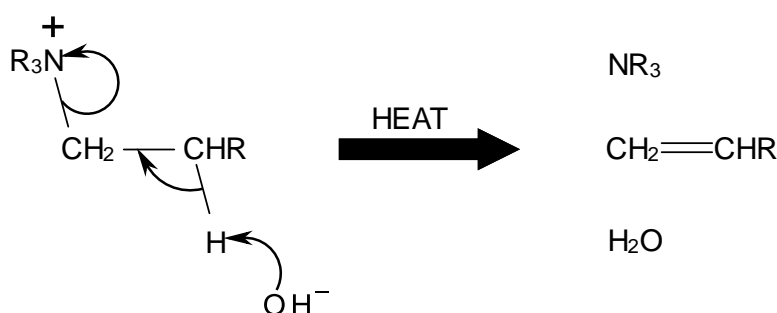


**Figure 1:31: Hofmann degradation**<sup>128</sup>

The degradation process, while enabling GC analysis, also unavoidably results in the loss of structural information of the original quat during the formation of the tertiary amine. Of the

published methods, GC-MS<sup>129</sup> analysis is the most sensitive providing the lowest detection limits frequently in the parts per billion range (ppb;  $\mu\text{g/l}$ ) and the most structural information about the tertiary amine. The application of GC methods is further limited by the analyte matrix because analysis of aqueous samples is not possible without extensive sample preparation, such as solid phase extraction (SPE) or solid phase micro-extraction (SPME).

LC applications, by contrast are the most numerous and diverse in the scientific literature. The range of published applications encompasses not only the pharmaceutical and biological analyses<sup>130, 131, 132</sup> but there is also a wealth of literature concerned with environmental samples<sup>133, 134, 135</sup>. This is in part due to the ease with which LC systems can harness various detection types such as UV<sup>61</sup>, conductometric<sup>136</sup>, evaporative light scattering (ELS)<sup>137</sup> and MS<sup>133</sup> but also to the various different separation techniques possible with an LC system such as ion chromatography<sup>137</sup>, normal phase<sup>138</sup> and reverse phase<sup>139</sup> chromatography, see **Table 1:3**. Analysis of quats in seawater is problematic by ion chromatography, as the concentration of sodium ions and other cations in the matrix will swamp the conductometric detector, greatly reducing its sensitivity for the quats. Conversely, reverse phase chromatography has largely established itself as the standard technique for LC systems because of the broad array of stationary phases available facilitating a more powerful chromatographic technique. Due to this broad range there is very little consensus in the scientific literature as to the optimum column for quat analysis. This diversity reflects the serendipitous way analytical methods are developed. Current research has primarily focused on quat analytes which contain aryl or pyridinium groups which are good chromophores, **Figure 1:32** (*see page 46*). Consequently this has a major influence over the most suitable detector and is reflected in the published analytical methods with the primary detection method being UV spectroscopy, see **Table 1:3**. In general all the methods use acidified buffered eluents. The buffers usage, rather than affecting the ionization state of the quat, is instead to improve the peak shape by reducing the interaction of the quat with the residual uncapped silanol groups present in the stationary phase<sup>139</sup>.

<b>Author (Year)</b>	<b>Analyte</b>	<b>Matrix</b>	<b>Column Phase Type</b>	<b>Detector</b>	<b>Limit of Detection</b>
Nakae (1997) <sup>140</sup>	Benzalkonium Chloride (1-21)	-	Poly(styrene-divinylbenzene)	UV	-
Ambrus (1986) <sup>141</sup>	Benzalkonium Chloride (1-21)	Ophthalmic solution	CN	UV	-
Valladao (1994) <sup>142</sup>	Various	Milk	C <sub>18</sub>	UV	1.0 ppm
Parhizkari (1995) <sup>143</sup>	Benzalkonium Chloride (1-21)	Ophthalmic solution	Phenyl	UV	25 ppb
Ibáñez (1997) <sup>57</sup>	Paraquat (1-40) and Diquat (1-41)	Water	Hypercarb PCB	UV	0.1 ppb
Itagaki (1997) <sup>132</sup>	Paraquat (1-40) and Diquat (1-41)	Serum and Urine	Si	UV	2.5 ppb
Taylor (1997) <sup>144</sup>	Hexadecylpyridinium Chloride (1-42)	Lozenges	CN	UV	5.0 ppm
Shibukawa (1999) <sup>145</sup>	Alkyltrimethylammonium Chloride (1-20)	Water	Polymeric	Conductometric	-
Liu (2006) <sup>137</sup>	Various	-	Acclaim® Surfactant	ELSD	-
Restek Application Note <sup>146</sup>	Paraquat (1-40) and Diquat (1-41)	Water	Ultra Quat	UV	6 ppb

**Table 1:3: Quat liquid chromatography analytical methods**

Similar to GC methods, LC-MS based analysis offers the best levels of detection with limits of detection, frequently in the range of low ppb. However, the greater sensitivity of the MS detector can also be problematic if the sample analytical matrix is not matched with that of the analytical standards, because trace levels of contamination can adversely affect the analyte ion enters the MS detector which will be reflected in the reproducibility of the method<sup>147</sup>. Again the LC-MS methods show a similar level of diversity to that of the LC methods. There is a general consensus on the use of ammonium salts as buffer along with ACN as the primary organic solvent together with the uses of hydrophobic stationary phases. However, the degree of hydrophobicity varies from very weak, “CN” to the most hydrophobic “C<sub>18</sub>”, **Table 1:4**.

<b>Author (Year)</b>	<b>Analyte</b>	<b>Matrix</b>	<b>Column Phase Type</b>	<b>Eluent</b>	<b>Buffer</b>	<b>Sample Preparation</b>	<b>Limit of Detection</b>
Kambhampati (1994) <sup>148</sup>	Paraquat (1-40) and Diquat (1-41)	Water	Cation exchange and C <sub>18</sub>	ACN	Ammonium Acetate	Manual Column	5.3 µgml <sup>-1</sup>
Fernández (1996) <sup>149</sup>	Dialkyldimethyl ammonium chloride (1-23)	Marine Sediment	Aminopropyl	Chloroform, Methanol	Acetic Acid	SFE	80 ng
van der Hoeven (1996) <sup>150</sup>	Various	Plasma	Poly(styrene-divinylbenzene)	ACN	Ammonium Acetate	-	1.0 ngml <sup>-1</sup>
Marr (1997) <sup>135</sup>	Paraquat (1-40) and Diquat (1-41)	Water	C <sub>8</sub>	ACN	Heptafluorobutyric Acid	-	1.0 µg <sup>-1</sup>
Vahl (1998) <sup>151</sup>	Chlomequat (1-43)	Grain	C <sub>18</sub>	ACN, Methanol	Ammonium Acetate	SPE	0.7 ngml <sup>-1</sup>
Radke (1999) <sup>152</sup>	Dialkyldimethyl ammonium chloride	Sewage	Partisil PAC	Chloroform, Methanol, ACN	-	Liquid-Liquid Extraction	0.4 ngml <sup>-1</sup>
Castro (1999) <sup>153</sup>	Paraquat (1-40) and Diquat (1-41)	Water	Lichromshper 60	ACN	Ammonium Formate	SPE	0.05 µg <sup>-1</sup>
Ferrer (2001) <sup>154</sup>	Benzalkonium Chloride (1-21)	Enviro. Water	C <sub>18</sub>	ACN	Ammonium Formate	SPE	5.0 ng <sup>-1</sup>
Ford (2002) <sup>155</sup>	Benzalkonium Chloride (1-21)	Occupat. Hygiene	CN	ACN	Ammonium Formate	SPE	3.0 ng <sup>-1</sup>
Merino (2003) <sup>156</sup>	Benzalkonium Chloride (1-21)	Sewage	C <sub>8</sub>	Methanol	Ammonium Formate	Cloud Point Extraction	40 mgg <sup>-1</sup>
Martinez-Vidal (2004) <sup>157</sup>	Paraquat (1-40) and Diquat (1-41)	Enviro. Water	C <sub>8</sub>	Methanol	Heptafluorobutyric Acid	SPE	0.02 µg <sup>-1</sup>
Núñez (2004) <sup>158</sup>	Benzalkonium Chloride (1-21)	Various	C <sub>18</sub>	ACN	Ammonium Formate	-	0.1 µg <sup>-1</sup>
Martínez-Carballo (2007) <sup>159</sup>	Benzalkonium Chloride (1-21)	Enviro. Water	C <sub>18</sub>	ACN, Isopropanol	Ammonium Formate	Liquid-Liquid Extraction	0.5 ngml <sup>-1</sup>

**Table 1-4: LC-MS applications**

Crucial to several methods is a preparation step for the analytical sample prior to analysis. These methods usually have extremely turbid or highly particulate sample matrices which without the preparation step could not be analysed efficiently. Frequently this preparation step is in the form of a solid phase extraction (SPE) process, see **Table 1:4**. The reasons for this are twofold. Firstly, to clean or purify the sample and secondly to concentrate the sample reducing the limit of detection. There are two types of SPE; off-line<sup>151, 153, 160</sup> or on-line<sup>57, 134</sup>. This refers to whether the SPE process is connected directly to the analysis instrumentation (on-line) or performed remotely by a manual procedure from which an aliquot is then transferred for analysis (off-line). In general on-line SPE provides the highest levels of recovery and lowest detection limits, but requires major alterations to the instrumentation, while for off-line SPE recoveries of over 80 % are frequently possible and require minimal capital expenditure. However, both processes are essentially another chromatographic technique which requires the optimisation of a number of steps: preconditioning, wash, elution and sorbent, **Table 1:5**. The selection of the right sorbent is crucial<sup>161</sup>. This requires an appreciation of the types of interaction the sorbent exerts not only with the target analyte but also the contamination to ensure that it will retain the analyte in preferences to the contaminant, but not to such an extent that the analyte cannot be easily released<sup>161</sup>. To aid this, the elution eluent must have the right balance of polarity, pH and hydrophobicity to successfully reclaim the analyte from the sorbent<sup>161</sup>. The opposite criteria are required for a wash step, that is, the target analyte is retained while the contaminants are successfully removed. Prior to these steps the sorbent also needs to be activated to ensure maximum interaction with the analyte. On top of these are also practical issues such as flow rate, sorbent bed volume and elution volume. The development of an SPE method is a non-trivial task and requires the successful resolution of all these separate issues and consequently there is a diverse range of published methods, **Table 1:5**.

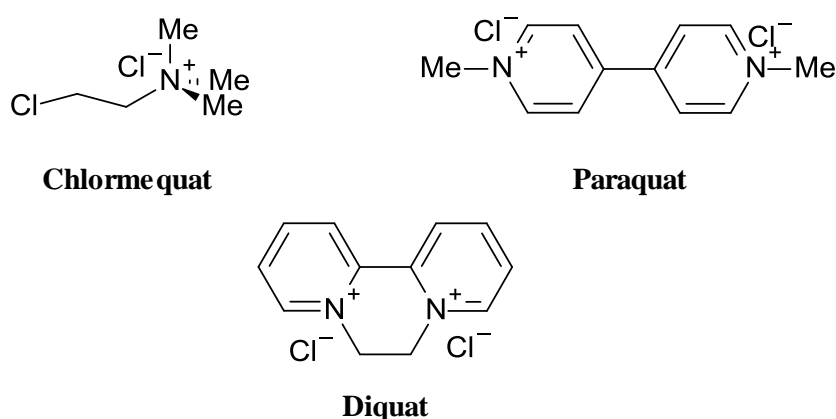


**Figure 1:32: Structures of paraquat (1-40), diquat (1-41) and chlormequat (1-43)**

<b>Author (Year)</b>	<b>Analyte</b>	<b>Cartridge Type</b>	<b>Precondition Step</b>	<b>Wash Step</b>	<b>Elution Step</b>	<b>Recovery (%)</b>
Vahl (1998) <sup>151</sup>	Chlomequat (1-43)	C <sub>18</sub>	1)Methanol 2)50mM ammonium acetate in elution solvent	-	Methanol:water: acetic acid (75:24:1)	89
Castro (1999) <sup>153</sup>	Paraquat (1-40) and Diquat (1-41)	Si	-	-	6M HCl-8% methanol	85
Carnerio (2000) <sup>162</sup>	Paraquat (1-40) and Diquat (1-41)	Si or PGC	1)Methanol 2)Water 3)Methanol	water	TFA:ACN (20:80)	89
Ferrer (2001) <sup>154</sup>	Benzalkonium Chloride (1-21)	C <sub>18</sub>	1)ACN 2)Water	-	ACN-50mM ammonium formate (aqueous solution)	Online
Núñez (2002) <sup>163</sup>	Paraquat (1-40) and Diquat (1-41)	PGC	1)Methanol 2)Methanol:water (1:1) 3)Water	-	TFA:ACN (20:80)	40
Konstantinou (2002) <sup>38</sup>	Antifouling Biocides	Poly(styrene-divinylbenzene) or C <sub>18</sub>	1)Acetone 2)2xEthyl acetate 3)Methanol	-	Ethyl acetate: dichloromethane (50:50)	75
Martinez-Vidal (2004) <sup>157</sup>	Paraquat (1-40) and Diquat (1-41)	Si	-	-	6M HCl-methanol (9:1 v/v)	90

**Table 1.5: SPE methods**

While it is important to monitor levels of environmental contaminants, such as biocides, under the current legislative climate it is also mandatory that the release rates of such contaminants be measured. For antifouling products the release rates of the biocides contained within the coatings is called the leach rate. There are recognised international standard test methods which enable leach rates in artificial seawater to be calculated, such as ASTM D6903-07<sup>164</sup>. These methods stipulate the internationally accepted analytical procedures for each target biocide, including the analytical instrumentation (e.g. LC) and detection (e.g. UV) as well as their limits of detection (LOD). The target analytes/biocides are those currently permitted for use in antifouling products including Seanine-211 (**1-3**) and copper/zinc pyrithione (**1-2** and **1-1**), which have LODs of 7.8, 0.6 and 0.6 ppb<sup>164</sup> respectively. These LODs are far lower than comparable LC-UV methods for the detection of quats, **Table 1:3**, notwithstanding differences in analytical matrices, and are therefore only achievable via LC-MS analysis, **Table 1:4**. Currently there is no international standard for the calculation of quat leach rates.

## 1.3 Objectives

There are a number of aims for this thesis:

1. Assess the potential efficacy of quats as marine biocides and determine whether the release rates of these compounds needs to be controlled.
2. Develop a method to control release quats based on tethering the quats into a polymeric system via an electrovalent bond, such that the bond is labile in seawater.
3. The quat-polymeric systems should be suitable for use as a new type of binder for an antifouling paint by demonstrating good mechanical and antifouling properties.
4. Develop an analytical protocol to measure the release rate of quats into seawater.

Chapter 2 will initial explore the possible routes to quat-polymers and then use the method of post-quaternisation of an existing polymer to prepare a range of quat-polymers. The potential of these polymers to be used as a candidate binder of an antifouling paint is investigated using a series of assays to determine their mechanical and chemical properties. The antifouling performance of these systems is assessed through field immersion trials at International Paint's immersion facility.

Chapter 3 explores an alternative route to quat-polymer by the sequential preparation of a quat-monomer and then quat-polymer. The quat-monomer preparation uses a commercially available acid functionalized monomer to retain the quat moiety. The synthesised quat polymers are used to prepare analogous antifouling paints to those of Chapter 2 and are subject to the same physical, chemical and antifouling testing.

Chapter 4 continues the exploration of the same route as Chapter 3 but using an alternative commercially available acid functionalized monomer. The coatings prepared within this chapter enabled the potential of quats as marine biocides to be assessed.

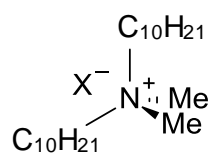
Chapter 5 details the development of the analytical method for the quantification of quats in seawater.

Chapter 6 utilizes the developed analytical method to measure the release rates of quats from a range of the antifouling paints prepared in Chapter 4 to assess whether the release of the quats has been controlled.

Chapters 7 and 8 are a final discussion of the results and their implications for potential future work.

## 2 Quaternary Ammonium-Polymers

As elucidated earlier in the introductory literature review, research into alternatives to metal-based antifouling compounds has highlighted quats as potential candidates, specifically alkylbenzyltrimethylammonium (1-21) and didecyldimethylammonium (2-1) halides, **Figure 2:1**. These compounds need to be fully evaluated for their efficacy towards fouling species and stability within antifouling coating formulations prior to any commercial deployment. This assessment will consist of the development of novel polymeric systems which will act as a vehicle for the delivery of the quats enabling them to deter the settlement of marine fouling organisms. Suitable polymers would demonstrate sustained antifouling activity, be stable into prototype antifouling paint formulations and the subsequent coatings should be mechanically robust to immersion within the marine environment.



X<sup>-</sup> = Cl<sup>-</sup> or Br<sup>-</sup>

### Didecyldimethylammonium Halide

**Figure 2:1: Structure of didecyldimethylammonium halide (2-1)**

Synthesis of polymers containing these quats can be achieved through two alternative routes:

- 1) Post-quaternisation of a pre-formed acid-functionalized polymer.
- 2) Sequential synthesis of a quat-monomer then polymerisation.

Both routes have their advantages and disadvantages, namely; route 1 is more synthetically succinct and hence the most attractive. However, the quat-monomer production step of route 2 would result in complete quaternisation of the acid-functionality in the final polymer which, due to steric hindrance, is less likely to be achieved with the post-quaternisation route. ‘Free’ acid-functionality can be problematic in antifouling coatings due to its interactions with other components, such as copper ions, in the coating formulation causing severe detrimental effects<sup>165</sup>. These effects can range from increases in the grind (size of particulate material) of the paint to causing cross linking between polymer chains resulting in the paint forming a gel.

The sequential synthesis of quat-monomer and polymer of route 2 represents a route with more synthetic flexibility. This would present the opportunity for optimisation of the quat-polymer, through a combination of manipulation of the polymerisation conditions, altering the co-monomers and their ratios within the polymer, which is not possible when using a preformed polymer as in route 1. Conversely, route 1 would use existing polymers which have been selected due to their

predetermined mechanical properties, which is not the case in route 2. It would be possible to use an acid-functionalized polymer, in route 1, which has previously been used in other antifouling systems and shown to release a biocide and demonstrated the desired polishing effect, which is characteristics of SPC antifoulings. One such polymer is the acrylic polymer used in copper self-polishing antifoulings. Copper/acrylic-SPC polymers possess the required acid-functionality for the quat-polymers. This functionality is used to bind the biocidal copper moiety into the SPC-polymer and operates in an analogous way to the envisioned quat-polymers, **Figure 2:2**. Incorporation of a quat-cation moiety into this polymer would result in a novel quat-polymer which has, in the copper system, demonstrated the desired performance, facilitating a direct comparison of the antifouling performance between copper and quat-biocides. In these polymers the biocide (copper or quat) is released through an ion exchange reaction with the cations present in seawater,  $\text{Na}^+_{(\text{aq})}$ ,  $\text{Mg}^{2+}_{(\text{aq})}$  etc, which readily occurs in slightly alkaline seawater ( $\text{pH} \sim 8.2$ ). This reaction causes a switch to occur from insoluble biocide-SPC polymer to a soluble carboxylate functional polymer that has little integral strength and is easily eroded by moving seawater, exposing fresh biocides-SPC polymer, **Figure 2:2**. Therefore self-polishing copolymers (SPCs) due to their polishing mechanism provide a unique opportunity to control the release of quat-biocides from antifouling coating.

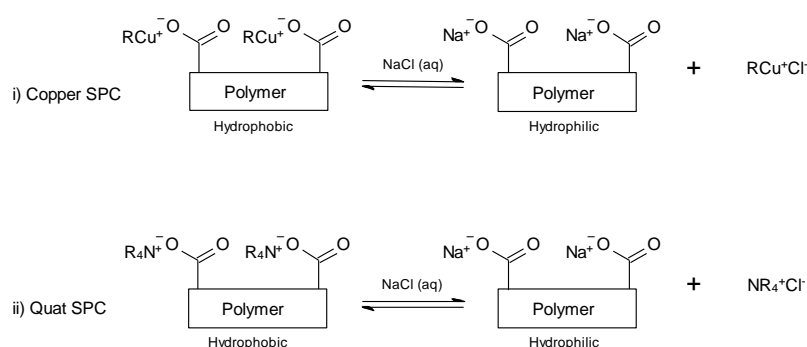
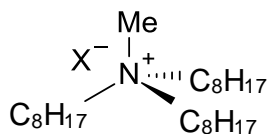


**Figure 2:2: Examples of mediated ion exchange reaction of SPCs systems i) copper SPC, and ii) quat SPCs**

The post-quaternisation route was the initially attempted because it is shorter than route 2 and used a polymer which has, in previous forms, demonstrated the required antifouling performance.

The biocidal quat which was the focus of this research was didecyldimethylammonium halide (**2-1**) selected for its well established biocidal activity and commercial potential with trioctylmethylammonium analogue (**2-2**), **Figure 2:3**, used as a non-biocidal control. It should be noted that, as a consequence of the mechanism through which the quats were released from the polymer, a seawater mediated cation-exchange reaction, the exact chemical identity of the anion of the quat cannot be precisely identified. The specific identity of the counter-anion will be governed

by the composition of the anions present in the seawater into which the quat is released, chiefly chlorides or bromides.



### **Trioctylmethylammonium Halide**

*Figure 2:3: Structure of trioctylmethylammonium halide (2-2)*

## **2.1 Post-Quaternisation Polymer Synthesis**

### **2.1.1 Background**

The quaternisation reaction of the acid-functionalized polymer is, in essence, a cation exchange reaction and due to its ionic nature, results in the formation of ionic by-products created from the cation of the acid-functionalized polymer, protons or alkali metal ions, and the anion of the quat. Although there is a wide array of quats commercially available, this diversity is not reflected when the quats are categorized via their counter anions. Commercially only halides and hydroxides are available, which translate into water or simple alkali metal salts as potential by-products. These by-products would be problematic in a coating system causing corrosion to a vessel's steel substrate or adversely affecting the mechanical performance of the coating. The effects of water would also provide another unknown variable, especially its limited compatibility with the polymer synthesis process due to the types of organic solvents used. The removal of these by-products although simple on a laboratory scale, through undemanding manipulations such as liquid-liquid extractions, acid/base washes or use of drying agents, can be far from straightforward on a tonne scale. Therefore an alternative to the utilisation of commercially available quats is their synthesis with more synthetically useful anions, such as methylcarbonates. The methylcarbonate anions, in the presence of acids, reacts to form methanol and carbon dioxide which, as by-products, are far less problematic than those previously identified because they can be readily removed *in vacuo*. Synthesis of quat methylcarbonates can be achieved through an N-methylation reaction of tertiary amines with dimethyl carbonate under conditions of elevated temperature and pressure<sup>166</sup>. For the aforementioned quat methylcarbonates synthesis the only suitable tertiary amines commercially available were didecylmethylamine (2-3) and trioctylamine (2-4), **Figure 2:4**. The synthesis of a suitable synthetic synthon for the alkylbenzyltrimethylammonium cation (1-21) was beyond the scope of this thesis and hence benzyl-quat SPC polymers were not extensively studied.

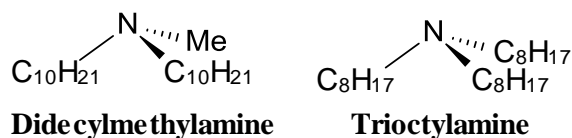
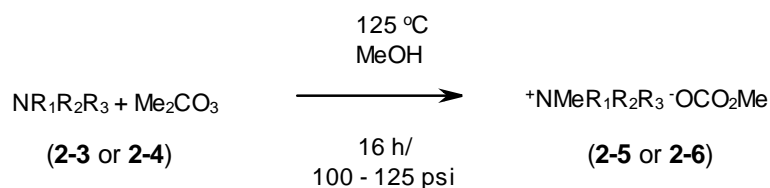


**Figure 2:4: Structures of didecylmethylamine (2-3) and trioctylamine (2-4)**

A suitable initial polymer to use as the vehicle for the quats was RC957, a proprietary acrylic acid functionalized polymer which was mass produced by International Paint and forms the basis of a copper/acrylate SPC system, hence its chemical and physical properties were well documented within the company.

### 2.1.2 Quat Methylcarbonate Synthesis

Didecyltrimethylammonium methylcarbonate (**2-5**), **Figure 2:5**, was synthesised by N-methylation of didecylmethylamine (**2-3**) with excess dimethyl carbonate (DMC) after 16 hours in methanol at elevated temperature and pressure, 125 °C and 100 – 125 psi. Upon cooling and removal of methanol by evaporative distillation a brown viscous liquid was obtained. Any residual DMC was removed as an azeotrope by the addition of methanol and further distillation, **Scheme 2:1**.



Where:

- a)  $\text{R}_1 = \text{Me}$  and  $\text{R}_2, \text{R}_3 = \text{C}_{10}\text{H}_{21}$  [Didecylmethylamine]  
 b)  $\text{R}_1, \text{R}_2$  and  $\text{R}_3 = \text{C}_8\text{H}_{17}$  [Trioctylamine]

**Scheme 2:1: Synthetic sequence for the preparation of quat methylcarbonates**

The success of the reaction was confirmed by  $^1\text{H}$  NMR with the appearances of a singlet at  $\delta$  3.20 (s, 6H) corresponding to the two methyl-groups directly bonded to the positively charged nitrogen cation which was absent in the  $^1\text{H}$  NMR of the amine starting reagent, **Figure 2:6**. Trioctylmethylammonium methylcarbonate (**2-6**), **Figure 2:5**, was obtained by an analogous N-methylation of trioctylamine (**2-4**) using the same procedure outlined above, **Scheme 2:1**. The success of this reaction was also confirmed by the presence of the singlet at  $\delta$  3.20 (s, 3H) corresponding to a methyl group directly bonded to the ammonium centre.

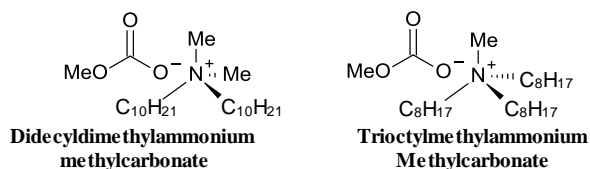


**Figure 2:5: Structures of didecyldimethylammonium (2-5) and trioctylmethylammonium (2-6) methylcarbonates**

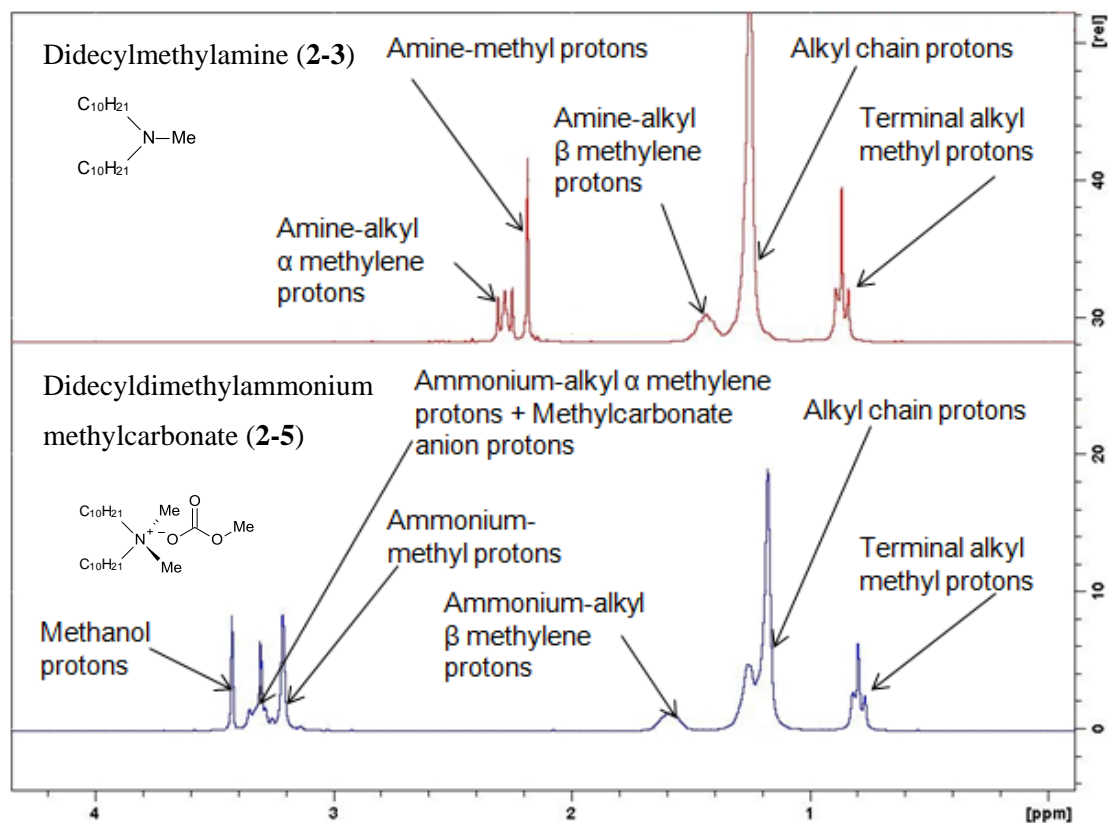


**Figure 2:6: i) <sup>1</sup>H NMR of didecyldimethylammonium methylcarbonate (2-5) (red) and ii) <sup>1</sup>H NMR of didecylmethylamine (2-3) (blue)**

## 2.2 Polymer Synthesis

### 2.2.1 Development

In an attempt to ensure complete quaternisation of RC957 (acid functionalized polymer) a small stoichiometric excess of quat methylcarbonate was used (1 mole acid:1.1 moles methylcarbonate).

As the RC957 polymer was supplied as a polymer solution obtaining its molecular molar mass was problematic. Since the quaternisation reaction only occurred between the acid functionality of the polymer and the quat methylcarbonate, determining the number of moles of the acid functional group within a certain mass of the RC957 polymer served as an alternative to determining its molar mass. The acid value of RC957 was measured in triplicate by titration with a standardized solution of potassium hydroxide (0.1 M in toluene:propan-2-ol 1:1) with phenolphthalein as indicator. To ensure accuracy a Metrohm® 809 Titrando autotitrator was used to perform the titrations and

calculation of the end point. The mean acid value of RC957 was calculated as 62.4 mg KOH/g ( $1.11 \times 10^{-3}$  mol KOH/g).

Therefore 50 g (0.1197 mol) of quat methylcarbonate required 107.8 g RC957 polymer solution for a 1:1 stoichiometric reaction. For 1.1:1 reaction 55 g of quat methylcarbonate would be required for 107.8 g polymer solution.

The RC957 polymer solution was supplied at 50 % non-volatile content (NVC), which was the target for the final quat-polymer. Consequently the prepared quat methylcarbonates were not dissolved in solvent to aid their addition because extra solvent would depress the % NVC further from the targeted 50 % NVC. Addition of the quat methylcarbonates in a drop wise fashion was therefore problematic due to their high viscosities. To resolve this issue it was decided to reverse the addition process i.e. add the liquid polymer solution drop wise to the quat methylcarbonates.

The validity of this synthetic process was determined by adding RC957 (107.8 g) drop wise over 1 hour to mechanically stirred didecyldimethylammonium methylcarbonate (55.0 g, 0.1317 moles) at 25 °C. The progress of the reaction was checked at regular intervals by monitoring the acid value of the reaction liquor. Visually the reaction was confirmed by the effervescence of the reaction liquor upon the addition of the acid, corresponding to the anticipated carbon dioxide production associated with the decomposition of the methylcarbonate anion.

The first measurement of the reaction was 2.5 hrs after the addition of RC957 was completed, **Figure 2:7**. At this point the reaction was found to be 78 % complete. Given the concerns about the possibility of the unquaternised acid functionality reacting with the copper compounds in the antifouling paint formulation the reaction temperature was increased to 73 °C. The reaction was then maintained at this temperature for a further 17 hrs with the reaction monitored at several stages. At the end of this 17 hr period the reaction was found to be 91 % complete. Since it took 17 hrs at an elevated temperature to achieve only an additional 13 % reaction, the reaction temperature was then further increased to 95 °C to try and force the reaction to completeness. After maintaining the reaction at this temperature for a further 6 hrs the reaction was found to be only 93 % complete, **Figure 2:7**. At this stage it was decided the benefit of further increases in percentage completeness were outweighed by increased reaction costs both in term so of increased temperature and reaction time, so the experiment was stopped. It was hoped that the remaining 7 % unreacted acid-functionality, which by virtue of its unreactive nature was likely to be the most sterically hindered, and hence would be sufficiently shielded to prevent any such adverse reactions with the copper compounds in the paint formulation.

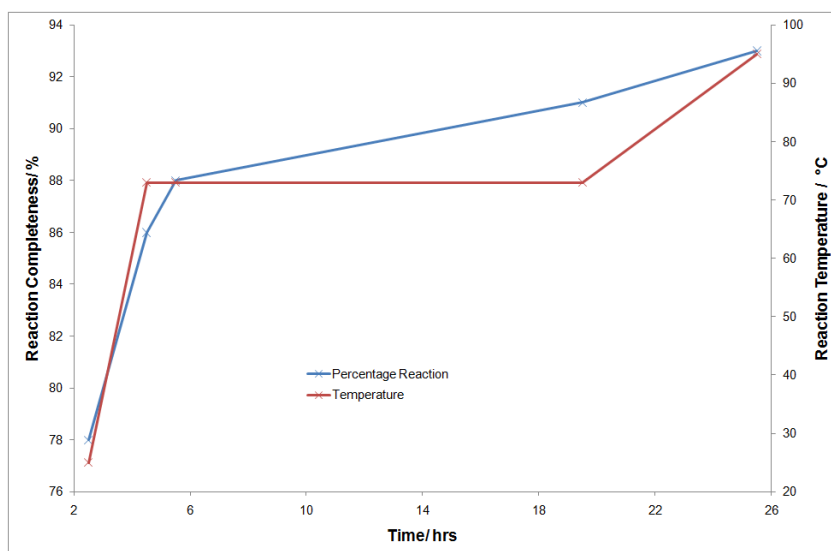


**Figure 2:7: Chart displaying change in percentage reaction and reaction temperature profile**

In an attempt to reduce the reaction time the above reaction was repeated but with the temperature set to 100 °C. When monitored after 24 hrs the reaction was again found to be 93 % complete. Subsequent monitoring showed no benefit for prolonged reaction time and so no further development of this synthetic method was performed and was used without further modification for the production of the quat-polymers.

### 2.2.2 Synthesis

Two polymers were prepared RC967Q(I) and RC967Q(II). The RC957Q stem reflecting the acid-functionalized monomer, RC957 where the acid-functionality had been capped by a quat cation, Q. The Roman numeral reflected which quat cation was present in the polymer, I, for didecyldimethylammonium cation and II for trioctylmethylammonium cation. Polymer RC967Q(I) was prepared by the drop wise addition over 1 hour of RC957 polymer solution (470.4 g) to mechanically stirred didecyldimethylammonium methylcarbonate (230.4 g, 0.5746 moles). The reaction was maintained at 100 °C for 24 hours. Following this the acid value of the resulting polymer was checked and ensured to be 7 % of the original acid value of RC957. RC967Q(II) was synthesised by the above process but trioctylmethylammonium methylcarbonate was used instead. Each polymer was characterised in terms of  $^1\text{H}$  NMR, viscosity<sup>167</sup>, percentage non-volatile content<sup>168</sup> (NVC), specific gravity<sup>169</sup> (SG), number average molecular weight ( $M_N$ ), weight average molecular weight ( $M_W$ ) and polymer polydispersity (data presented in the Experimental Chapter).

## 2.3 Paint manufacture

Two different paints were prepared according to a paint formulation created (using specialist paint formulation software) namely: RC957Q(I) and RC957Q(II). These were prepared by systematic replacement of the binder of the prototype formulation with the synthesised polymers, ensuring that

the test paints were equivalent in terms of volume solids and co-biocide content, **Table 2:1**. Each component of the formulation provided the paint with specific physical characteristic. The binder/test polymer imparted the general mechanical properties to the film and crucially, for SPC coatings, the polishing characteristic, which facilitated the controlled release of the quats in seawater. Copper oxide provided a broad spectrum of biocidal activity against animal fouling species<sup>170</sup>, whereas copper pyrithione (**1-2**) was effective against plant species<sup>171</sup>. Solvents, such as xylene, affected the application properties of the paint.

<i>Raw Material</i>	<i>Weight %</i>
<i>RC957Q(I)</i>	25.7
<i>Copper Oxide</i>	44.8
<i>Copper Pyrithione</i>	6.7
<i>Rheology Modifier</i>	2.3
<i>Pigmentation</i>	7.1
<i>Plasticiser</i>	2.4
<i>Xylene</i>	11.0

**Table 2:1: Example of paint formulation for RC957Q(I)**

The paints were manufactured by creating a uniform dispersion of the raw materials in the polymer solutions using a high speed disperser (HSD). The particle size distribution or “grind<sup>172</sup>” was monitored and ensured to be 60 µm or less by visual inspection of a grind gauge. The final paints were also tested for viscosity (data presented in the Experimental Chapter).

Alongside the test coatings, RC957Q(I) and RC957Q(II), an additional coating was also manufactured which used the unmodified acid functionalized polymer, RC957, as the binder. Due to the unreacted acid functionality of this polymer the paint formulation was altered to replace the copper compounds, copper oxide and copper pyrithione (**1-2**), with alternatives calcium sulphate and Seanine-211 (**1-3**). Paints formulated with ‘free’ acid functionalized polymer and copper compound are known to be unstable on storage<sup>165</sup>. The acid functionalized polymers can form carboxylate anions, which can act as bidentate ligands and react with the cupric cations, chemically linking two polymer chains together or crosslinking, **Figure 2:8**. Should this reaction occur between enough chains then a macro crosslinked polymer network would result which is manifested macroscopically in the paint formulations as the paint gelling.

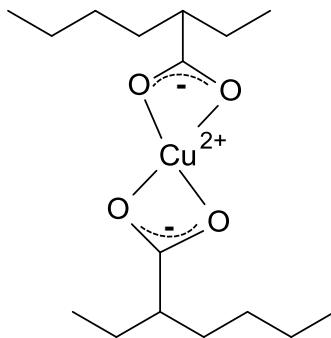


**Figure 2:8: Crosslinking of two polymer chains by cupric ion**

## **2.4 Mechanical and Antifouling Testing**

The paints were tested with regards to their antifouling performance, stability of a prototype paint formulation and mechanical robustness to immersion in the marine environment. These key characteristics were assessed by four performance assays:

### **2.4.1 Semi Rapid Boot-Top Cycling**

#### **2.4.1.1 Background**

The section of the hull of ocean going vessels between the waterline when fully loaded and unloaded is commonly referred to as the boot top. This region is subject to continual variations in exposure to seawater and the atmosphere depending on the loading of the ship. The effect of adsorption of water into the coating during immersion, followed by ‘drying out’ while exposed to the atmosphere, causes internal film stresses to develop resulting in the loss of film integrity, which is observed as cracking. The aim of a semi rapid boot top test, which is a well established test method for antifouling coatings<sup>173</sup>, is to accelerate and exacerbate these stresses by cycling coated panels through conditions which would be environmentally extreme. Panels coated with test paints are subjected to excessive mechanical stresses by repeated cycling between immersion in seawater at 35 °C and storage at -5 °C. These conditions are more extreme than those the coatings would naturally experience in the marine environment, and consequently those that perform well are expected to have the required mechanical robustness to survive in the marine environment. Examined alongside the test coatings are ‘pass’ and ‘fail’ standard coatings which are commercial products with proven in field performance and as such are used to ‘calibrate’ the performance of the test coatings when subjected to the semi rapid boot top testing. The ‘pass’ standard indicate the desired level of performance and the longer the test coatings perform comparably with this standard the better the test coatings are deemed to have performed. The ‘fail’ standard indicates the minimum desired performance level and once the test coatings are perform below that of the ‘fail’ standard they are deemed to have failed the test.

### 2.4.1.2 Assessment

Steel panels were prepared with anticorrosive primer, and once dried, coated with the test paints. Panels were also coated with the ‘pass’ and ‘fail’ standards. After drying at ambient temperature for 48 hours the coated panels were pre-immersed for 1 week in seawater at 25 °C after which they were cycled between immersion in seawater at 35 °C and storage at -5 °C. One rotation consisted of a 24 hour period during which the panels were half immersed in seawater at 35 °C after which they were immediately transferred to a temperature controlled environmental cabinet, programmed for 12 hours at -5 °C followed by 12 hours at 10 °C. After this 48 hour period the panels were inspected at ambient conditions and assessed as to the deterioration of the integrity of the coating. A 5 point rating system was used to assess the film integrity:

- 5 No cracking
- 4 Hairline cracking just visible to the naked eye
- 3 Cracking clearly visible
- 2+1 Progressively worse levels of cracking
- 0 Gross cracking over the whole film

The pass standard coating after 8 cycles was showing no deterioration of the coatings’ film integrity being rated 5. This performance was matched by both test coatings RC957Q(I) and RC957Q(II), both rated 5. After 8 cycles the test coatings were outperforming the fail standard, the performance of which rapidly deteriorated over the first 3 cycles to a rating of 3, due to increased levels of cracking in the paint film. However after these first 3 cycles the performance of the fail standards plateaus out and remained consistently rated 3, which corresponded to no further deterioration in the films integrity. Interestingly, the RC957 paint did not display the same performance as its quaternised analogues. Following the pre-immersion week, the film integrity deteriorated to such an extent that after 1 cycle the coating fully detached from the primed steel panel, resulting a zero rating, **Table 2:2**.

PAINT	CYCLE							
	1	2	3	4	5	6	7	8
<i>Pass Std</i>	5	5	5	5	5	5	5	5
<i>Fail Std</i>	5	5	4	3	3	3	3	3
<i>RC957Q(I)</i>	5	5	5	5	5	5	5	5
<i>RC957Q(II)</i>	5	5	5	5	5	5	5	5
<i>RC957</i>	0*	-	-	-	-	-	-	-

**Table 2:2: Semi rapid boot-top results for the RC957 coatings series (\*) – delamination of the test coating from the substrate.**

The semi rapid testing was suspended after 8 cycles as both RC957Q(I) and RC957Q(II) paints were thought to have demonstrated sufficient mechanical robustness to withstand in-field antifouling testing.

## 2.4.2 Polishing Trials

### 2.4.2.1 Background

Polishing is a technical term used to describe the reduction in film thickness of SPC antifouling coatings. Experimental determination of polishing rate<sup>174</sup> is a necessary test protocol for antifouling paints and is key to the calculation of film thicknesses depletion and hence the prediction of in-service lifetime. Knowledge of the polishing rate also aids understanding of the mode of action of the paint (*i.e.* whether the paint is a self-polishing system or an eroding system). In practice, polishing rates are known to vary with vessel speed, vessel activity, water temperature and salinity<sup>174</sup>. All these factors need to be taken into account when determining the polishing rate of antifouling systems. To properly characterise polishing behaviour it is essential to determine the loss of film thickness as a function of immersion time. This test mimics the hydrodynamical shear experienced by a coating as a vessel moves through the water. This is achieved by the application of the coating to disks which are rotated at high speeds in seawater to mimic the shear. Film loss is calculated by the difference in thickness of the dry pristine coating and dry post-test thickness.

### 2.4.2.2 Assessment

Polishing disks were prepared which had strips of each of the three test coatings and 2 strips of the polishing standard coating, Interswift 655. It was envisioned that a number of disks would be prepared and the polishing rate determined for a series of different tested periods; 60, 90 and 120 days. Unfortunately, even after an extended drying period of 60 days, the test coatings were deemed by visual inspection to be too soft for testing.

Coatings which are too soft do not have sufficiently mechanical robustness to survive the hydrodynamical shear forces created at the surface of the coatings, during the high speed rotation of the polishing disk during testing, resulting in 'cold flow'. In such cases the surface layer of these coatings can 'creep' and tear due to the forces exerted on it, **Figure 2:9**.



**Figure 2:9: Example of 'cold flow' from the port side of a commercial vessel**

Such occurrences on polishing disks would render them unusable in terms of polishing rate determination, as the surface of the paint strips would be deformed to such an extent that no

meaningful data could be recorded when the disks are analysed by using laser profilometry, **Figure 2:10**.

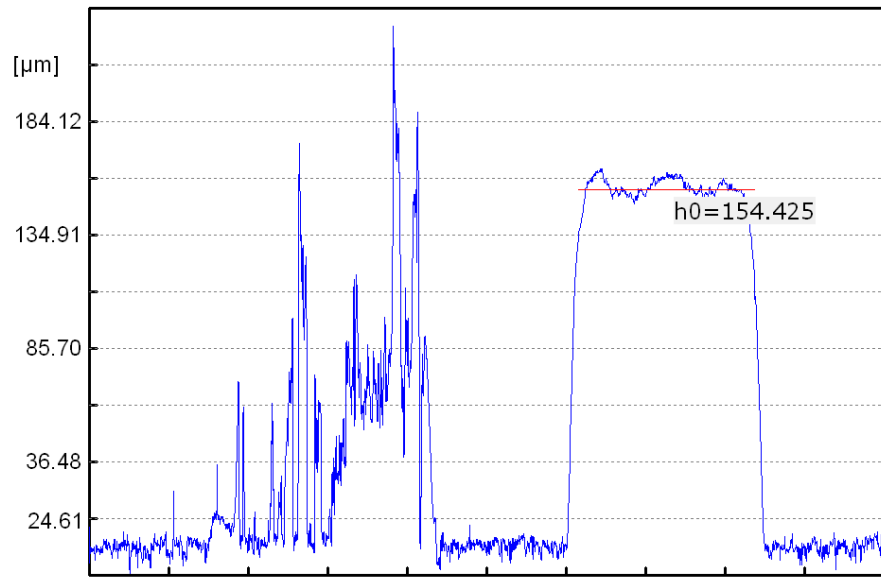


**Figure 2:10: Laser profilometry of two strips from a polishing disk after 60 days testing. The right strip has remained intact and can be analysed. The left strip has become deformed due to cold flow and cannot be analysed.**

The fact that these test coatings were very soft and unsuitable for polishing rate determination was consistent with the good performance demonstrated during the semi rapid boot top testing. Both quats used to cap the acid functionality of the RC957 polymer had multiple long alkyl chains. These long alkyl chains could have internally plasticised the polymers. This plasticisation would have enabled the coatings to cope with the stresses induced during the semi rapid boot top testing, resulting in their good performance; however it could also have resulted in soft coatings which were unsuitable for polishing rate determination.

## 2.4.3 Antifouling Performance

### 2.4.3.1 Background



**Figure 2:11: Example of Latin square antifouling board**

Antifouling performance testing is performed by immersing painted panels under static conditions in the marine environment<sup>175</sup>. Static conditions are considered to be the most severe situation for antifouling paints, as many systems rely on hydrodynamical shear to aid their antifouling performance, as the shear can dislodging fouling from the coatings surface. As this test immerses panels in the marine environment, the antifouling activity exhibited by the test coatings is a true indication of their real performance under the most extreme fouling conditions, and is not an approximation of their performance. The test panels are

prepared using a Latin square statistical arrangement of 36 individual squares which allows for the testing of 6 coatings simultaneously, **Figure 2:11**, with multiple panels immersed at the same location this assay allows the testing of a large number of coatings in parallel. The Latin square arrangement minimises the potential effect of uncontrollable factors such as: light distribution and sporadic fouling growth, improving the quality of the data<sup>176</sup>. Of the 6 possible coatings, 4 are test coatings and the remaining 2 are a blank and a control standard antifouling coating. The control standard being Intersmooth 460, a standard SPC antifouling product from International Paint and the blank coating a non-antifouling coating, Primocon, an International Paint primer coating which provides no antifouling protection, allowing assessment of the level of the fouling challenge to which the test coatings are subjected. Each square is evaluated by visual inspection for the percentage fouling coverage of 4 types of fouling: micro, weed, soft and hard fouling. Antifouling boards are immersed at International Paint's immersion facility, Newton Ferrers, Devon (Longitude: 04° 03' west, Latitude: 50° 19' north) and assessed throughout the UK marine fouling season (March-August)<sup>177</sup>. Successful test coatings could be further evaluated on a larger scale as tests patches on appropriate vessels, to fully mimic real life conditions.

#### **2.4.3.2 Assessment**

The initial immersion testing was carried out to determine whether quats displayed antifouling properties. The test coatings were: RC957Q(I) to test didecyldimethylammonium halide which had previously shown biocidal properties in other non-antifouling applications, RC957Q(II) to test trioctylmethylammonium halide which was selected as a non-biocidal control and RC957 to determine any antifouling performance of the polymer architecture used to create both RC957Q(I) and RC957Q(II). These coatings were compared against two biocidal antifoulings and a non-biocidal control (Primocon). The biocidal antifoulings were Intersmooth 460 and an alternative biocidal SPC antifouling.

In general after 14 weeks immersion at Newton Ferrers, there was no discernable difference in terms of antifouling performance between any of the test and standard biocidal coatings, **Figure 2:13**. Both the biocidal (RC957Q(I) – 2483) and non-biocidal (RC957Q(II) – 2571) coatings seemed to have, on average, less coverage of microfouling (red bar), than the standard product, Intersmooth 460, however the enhanced performance was not as pronounced due to the poor separation of the 95 % confidence error bars. The excellent performance of the unquaternised acid functionalized coating (2428) was, however, anticipated. This enhanced performance was due to the RC957 polymer being more hydrophilic than its quaternised analogues, due to its uncapped acid functionality enabling it to polishing quicker and resulted in its better performance over the biocidal quat system (RC956Q(I) – 2483) and the biocidal standards (Intersmooth 460 and coating 2422). Given this anticipated accelerated polishing, it was expected that the antifouling

performance of this coating would diminish with extended periods of immersion as the film thickness steadily decreased. However, after 14 weeks immersion the coating had already ‘polished’ through to the underlying primer on the antifouling board, **Figure 2:12**, highlighting the excessive polishing. All subsequent inspections of this panel showed deteriorating antifouling performance of RC957, as no test coating remained to deter fouling.

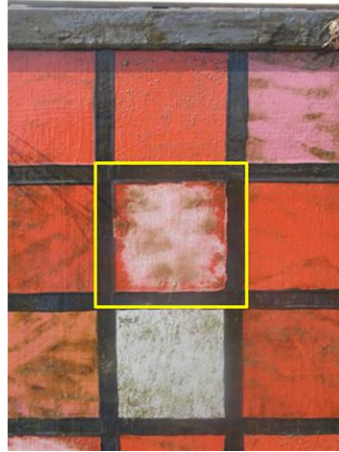


**Figure 2:12: RC957 coating polished through to underlying primer**

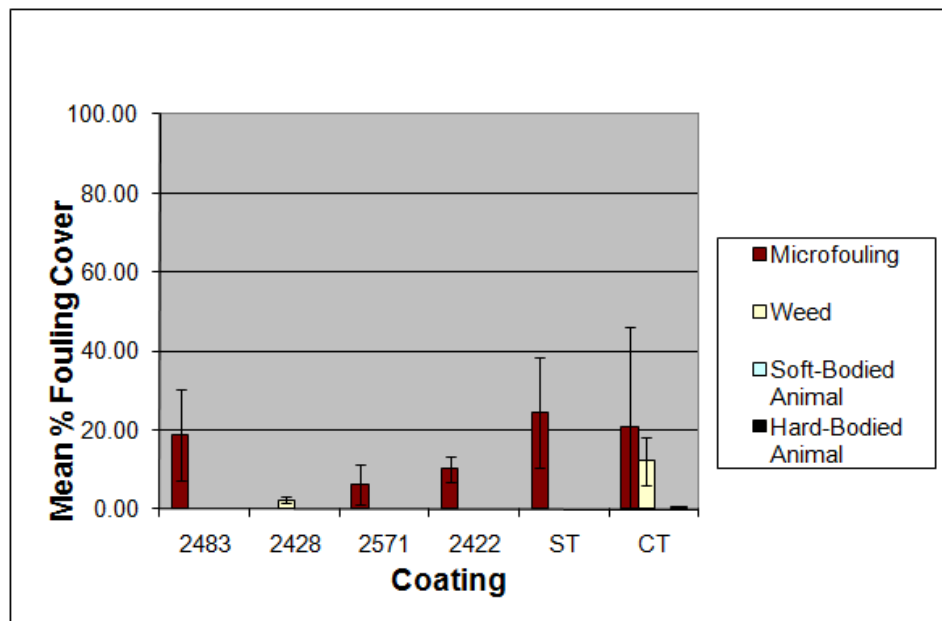


**Figure 2:13: Test Paint antifouling results after 14 weeks immersion. 2483 is RC957Q(I) paint, 2428 is RC957 paint, 2571 is RC957Q(II) paint, 2422 is the matched paint formulation and the standard is Intersmooth 460.**

After 46 weeks immersion the anticipated deteriorated performance of the RC957 (2428) coating was clear, as there was a significant shift in the dominant fouling type on its surface from microfouling (red bar) to soft-bodies animal fouling (sky blue bar), **Figure 2:14**. The performance of the quat containing coatings (2483, 2571) were still comparable to that of the standard biocidal coating, as there was no discernable difference in terms of the microfouling mean percentage coverage on these coatings. However, the comparable performance between both the biocidal

(RC957Q(I) – 2483) and non-biocidal (RC957Q(II) – 2571) quat containing coatings was unanticipated, **Figure 2:14**. Given the prolonged testing period, 46 weeks, a difference in performance would have been expected. The lack of differentiation could have been caused by a number of factors. Either the underlying performance of the quat-polymers was masked by the performance of the co-biocides in the paint formulation, or the difference in performance between the two quats as antifoulants was not as marked as the scientific literature would have suggested.

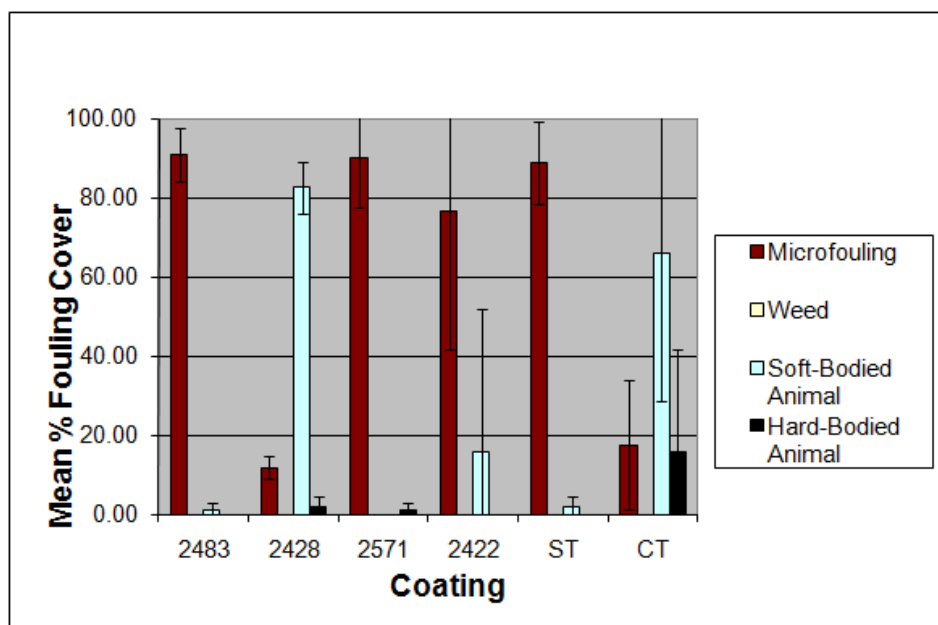


**Figure 2:14: Test Paint antifouling results after 46 weeks immersion. 2483 is RC957Q(I) paint, 2428 is RC957 paint, 2571 is RC957Q(II) paint, 2422 is the matched paint formulation and the standard is Intersmooth 460.**

## 2.4.4 Storage Stability

### 2.4.4.1 Background

The global nature of the fouling problem requires that antifouling paints are shipped from their place of manufacture to their point of sale. Consequently, the antifouling paints must be stable during shipping and storage<sup>178</sup>, often for prolonged periods at high/tropical temperatures. Storage stability trials allow the stability of the chemically complex wet paint to be assessed.

### 2.4.4.2 Assessment

Three paints were placed on storage at 5, 23 and 45 °C and their grind and viscosity was repeatedly checked. The three paints were RC957Q(I), RC957 (the unquaternised acidic polymer) and a standard SPC coating. Viscosity measurements after 30 days storage for all the coatings at all storage temperatures were higher than those recorded post manufacture, **Figure 2:15**. This change in viscosity, especially since it affects all the paints and at all temperatures suggested that there was a source of systematic error within the experiment. After the calibration records of the cone and plate viscometer were checked it was identified that it was out of calibration when used to record the 30 day measurement, and hence, a likely source for the error. For all subsequent measurements

the instrument was within calibration. A direct comparison between the paint RC957 and its quaternised analogue RC957Q(I) clearly demonstrated that the addition of a quat into the polymeric architecture reduced the viscosity of the paint from 6 poises for RC957 to 1 poises for RC957Q(I), **Figure 2:15**. This change was not unanticipated because incorporation of didecyldimethylammonium cations into the polymer resulted in increased proportion of alkyl groups in the polymer reducing its polarity by capping the acid functionality. A less polar polymer would be better solvated by the non-polar solvent, xylene, resulting in the lowered viscosity. In general the measured viscosities of RC957 showed good stability producing consistent results over the 245 days test period. There was no correlation between viscosity and storage temperature, further suggesting stability within the coating system. This trend was also confirmed by measurements of the grind of the coatings which were constant at less than 40  $\mu\text{m}$ . However, the RC957Q(I) paint was unstable. There was a clear trend of increased viscosity and grind over the 245 days which was temperature dependent. This was clearly exemplified by the failed viscosity measurement at 60 days because the liquid paint, while on storage, had gelled, meaning no further viscosity measurements were possible, **Figure 2:15**. The source of this instability was likely to be due to the known problem of ‘free’ acid functionality reacting with the copper compounds in the paint formulation resulting, in crosslinked polymer chains which was manifested as gelling. Although the likelihood of this instability was known prior to manufacturing the paints, it was hoped that sufficient acid functionality has been quaternised in the polymer for the paint to be stable, clearly the 7 % unreacted acid functionality was sufficiently accessible to cause gelling.

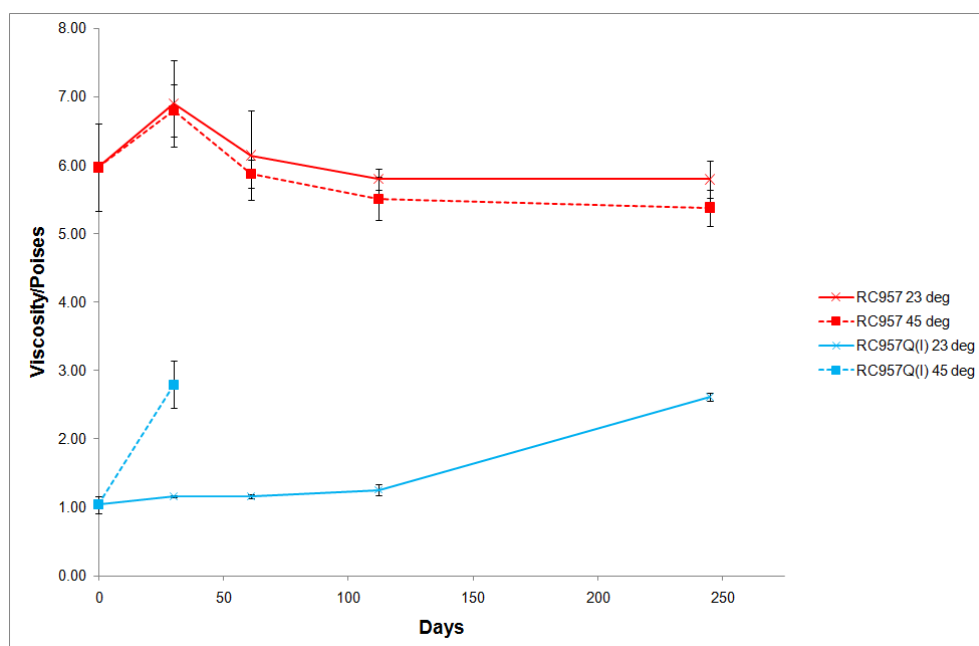


**Figure 2:15: Storage stability of RC957 and RC957Q(I) at 23 and 45 °C.**

## 2.5 Conclusions

There were a number of critical issues associated with the quat-polymers synthesised via this synthetic route, which meant that this route could not be fully evaluated. The paints formulated using the synthesized polymers, RC957Q(I) and RC957Q(II) were very soft, which although resulted in favourable semi rapid boot top test results, crucially meant that the coatings were insufficiently robust for polishing rate testing. To create 'harder' coatings would require major alterations to the polymeric structure of the framework polymer, RC957, used to create the quat-polymers. From a practical view point this would require the synthesis of a new polymer from its constituent monomers. However, to achieve this would negate all the benefits associated with the post quaternisation synthetic route, namely that the framework polymer had previously demonstrated performance and, crucially, no synthesis was required. The synthesis of a suitable replacement framework polymer to enable this route to be fully evaluated would be beyond the scope of this thesis, and hence an alternative route to a quat-polymer is required.

Another major flaw of this route was the acid functionality of the framework polymer could not be fully quaternised. This resulted in a latent instability in the paint formulation which was ultimately exposed during the storage trials. This issue could be resolved if the remaining acid functionality was capped. Should this be achieved it would be likely that stable paint formulations could be produced. A suitable paint industry technique to achieve this is to incorporate small tertiary amines and/or small quats into the paint formulations<sup>165</sup>. These small compounds would be less sterically hindered and could interact with the unquaternised carboxylic functionality. However, this would only resolve the stability issues of the formulation and not the softness of the final coating. A single solution to successfully resolve both issues would be using the alternative synthetic route of sequential synthesis of quat-monomer followed by polymerisation. This facilitates full control over the polymeric mechanical properties while ensuring no 'free' acid functionality.

### 3 Sequential Preparation of Monomer then Polymer 1

The previously attempted route to produce suitable polymers via the post-quaternisation was largely unsuccessful due to its prescriptive nature. The major drawback of the ‘one pot’ nature of this synthesis was that, it does not provide the necessary flexibility to control the final polymer’s properties which were fundamentally dictated by the initial choice of framework polymer. There was no capacity to tailor the synthesis to alter the polymer’s mechanical properties. Hence the ‘soft’ nature of the RC957Q polymers could not be remedied without alterations to the monomeric composition of the framework polymer. To do this would have created a new untested polymer and negated all the advantages of the post-quaternisation route. Route 2, the sequential synthesis of quat-monomer then polymer, on the other hand would be more synthetically flexible affording the possibility of tailoring the polymer through the suitable choice of co-monomers and their proportions in the final polymer. This route could also provide the opportunity to ensure that the acid-functionality of the polymer was completely quaternised via the isolation of the quat-monomer prior to polymerisation. Preparation of the quat-monomer could be achieved via an analogous reaction to the one used, to form the quat-polymers of the post-quaternisation route, but with the replacement of the RC957 polymer with an acid-functionalized monomer. Unfortunately the identification of a suitable acid-functionalized monomer was problematic. Earlier work within International Paint had demonstrated the reluctance of quaternised acid-functionalized monomers to polymerise<sup>179</sup>. This was attributed to the steric hindrance of the quat cations, which when in close proximity to the polymerisable functionality, was sterically shielded preventing polymerisation. This work therefore established the requirement for any potential monomers, used for quaternisation, to have the acid-functionality spatially displaced by a ‘linker’ from the polymerisable functionality of the monomer to enable polymerisation<sup>179</sup>, **Figure 3:1**.

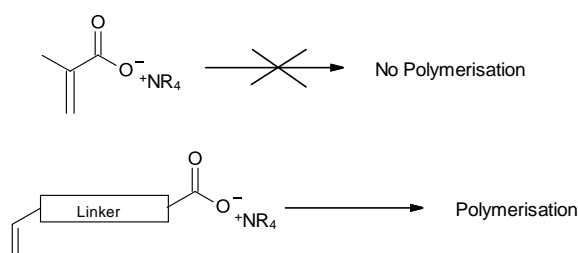


**Figure 3:1: Schematic of the requirement of a ‘linker’ between the quaternised acid functionality and the functionality for polymerisation.**

It can be inferred that the acid-functional monomer of RC957 was not suitable for further polymer development due to insufficient spacing between the acid and polymerisable functionalities and hence an alternative was required. A search of acidic monomeric compounds which are available in industrial quantities highlighted mono-2-(methacryloyloxy)ethyl succinate (MES, **3-1**) and 2-

acrylamido-2-methyl-1-propanesulfonic acid (AMPS, **3-2**) as potential alternatives, **Figure 3:2**, with MES favoured due to its lower unit cost.

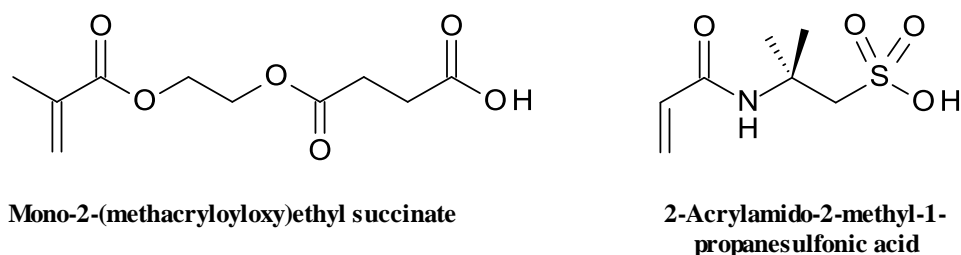
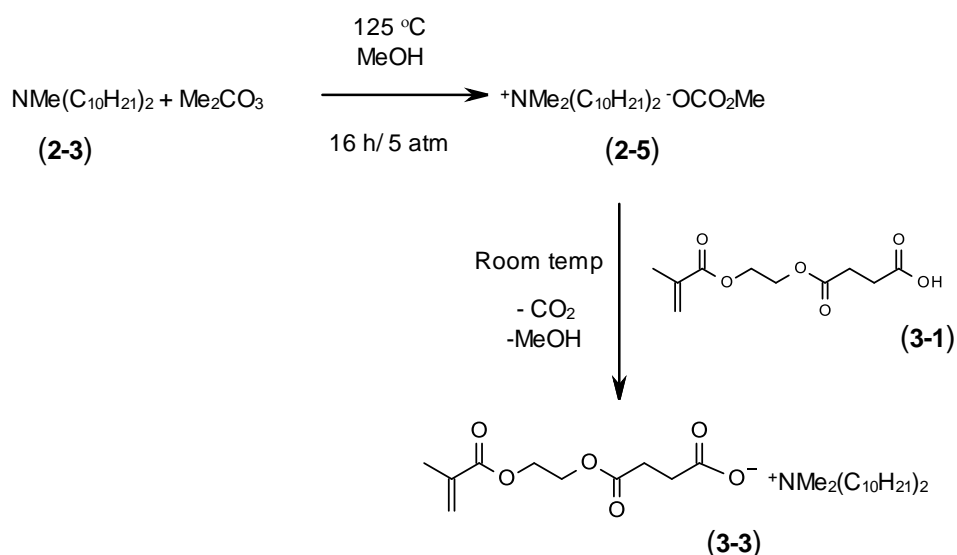


**Figure 3:2: Structures of mono-2-(methacryloyloxy)ethyl succinate (3-1) and 2-acrylamido-2-methyl-1-propanesulfonic acid (3-2) monomers identified as suitable for quaternisation.**

### 3.1 Monomer Synthesis

Only didecyldimethylammonium (**2-1**) and trioctylmethylammonium halides (**2-2**) were grafted onto the acid-functionalized monomer for the reason established during the post-quaternisation route, namely only suitable tertiary amines could be found for these quats. This required the pre-synthesis of their respective quat methylcarbonate. Both didecyldimethylammonium methylcarbonate (**2-5**) and trioctylmethylammonium methylcarbonate (**2-6**) were prepared as previously elucidated without any alteration to the previously detailed methodology. The respective quat salts of MES were obtained by a cation exchange reaction between the quat methylcarbonates and MES (**3-1**) in xylene after 12 hours continuous stirring, **Scheme 3:1**. These compounds were used for the following reactions without purification or evaporation of reaction solvent.



**Scheme 3:1: Two step synthetic sequence for the preparation of didecyldimethylammonium quat-monomer**

The success of the reaction was confirmed firstly by the evolution of carbon dioxide during synthesis, and secondly by  $^1\text{H}$  NMR post synthesis, which exhibited signals for both MES (**3-1**)

and the relevant quat cation. No signal was observed for the methylcarbonate anion as the corresponding signal was absent from the multiplet at  $\delta$  3.38 (m, 4H), post reaction. Of particular note was the changed shift of the methylene protons adjacent to the carbonyl groups of MES (**3-1**),  $\delta$  2.59 (m, 4H), which changed their environments following the reaction and split to form  $\delta$  2.68 (m, 2H) and  $\delta$  2.50 (m, 2H). Additionally the integration per proton was the same for both the quat cation and MES (**3-1**) protons confirming a 1:1 reaction, **Figure 3:4**. The monomer containing the biocidal didecylmethylammonium cation was named MESQ(I) (**3-3**), **Figure 3:3**, and that of the non-biocidal trioctylmethylammonium cation was named MESQ(II) (**3-4**), **Figure 3:3**. The MESQ stem reflected the acid-functionalized monomer, MES where the acid-functionality had been capped by a quat cation, Q. The Roman numeral referenced which quat cation was present in the monomer, I, for didecylmethylammonium cation and II for trioctylmethylammonium cation.

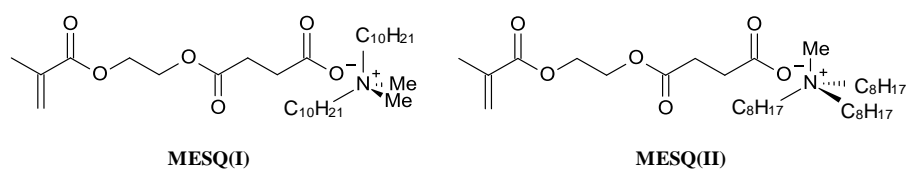


**Figure 3:3: Structures of biocidal MESQ(I) (3-3) and non-biocidal MESQ(II) (3-4) monomers**

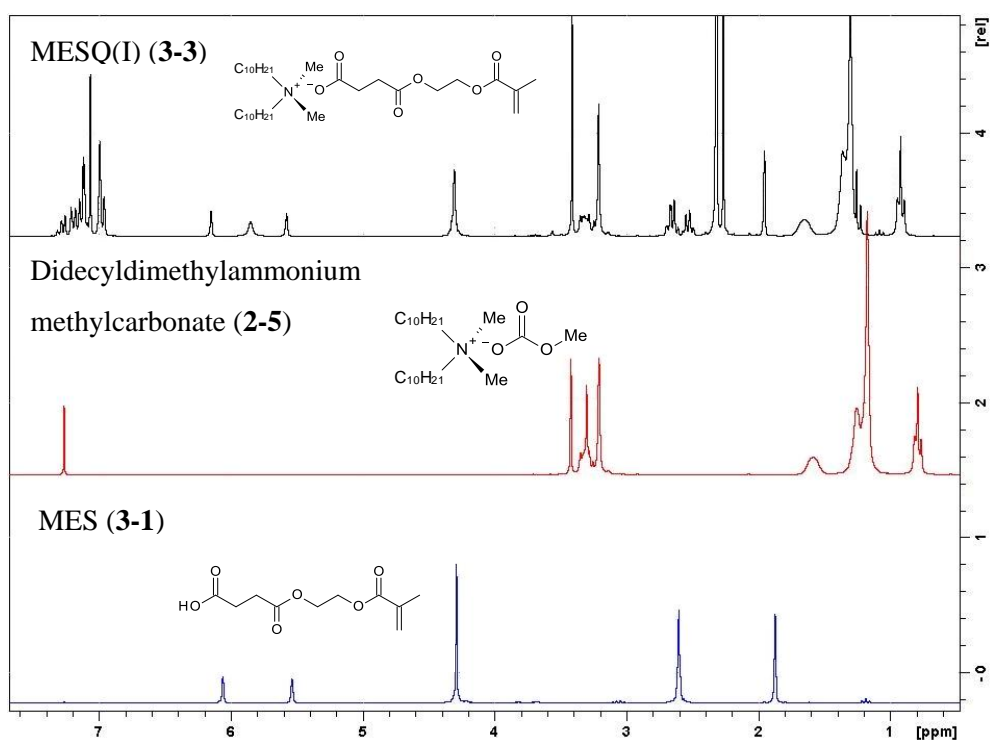
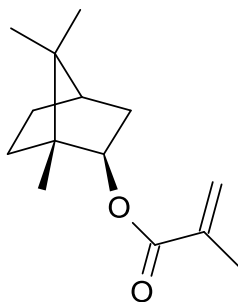


**Figure 3:4: i) <sup>1</sup>H NMR of final didecylmethyl quat-monomer solution in xylene (green) (3-3) and its starting materials ii) didecylmethylammonium methylcarbonate (red) (2-5) and iii) MES acid (blue) (3-1)**

## 3.2 Polymer Syntheses

The cation exchange reaction, which releases the quat cations from the polymer, causes a hydrophobic-hydrophilic switch in the surface chemistry of the coating, resulting in the cycle of

polishing and controlled release of the quats. The development of an SPC polymer therefore required the correct balance between the hydrophobic and hydrophilic functionality within the polymer. Both the synthesised MESQ monomers were highly hydrophilic due to their ester-, and acid-functionalities. Incorporation of these monomers in SPC polymers required a balancing hydrophobic comonomer to give the resultant polymers the desired film hydrophobicity and mechanical properties. Isobornyl methacrylate (iBoMA, **3-5**), **Figure 3:5**, a commercially available hydrophobic monomer, was used to achieve this.



**Isobornyl methacrylate**

**Figure 3:5: Structure of isobornyl methacrylate (3-5)**

Four polymers were synthesised using either the biocidal MESQ(I) (**3-3**) or non-biocidal MESQ(II) (**3-4**) monomers. The polymers were named MESQ(I)v25 and MESQ(I)v30 for the biocidal systems and MESQ(II)v25 and MESQ(II)v30 for the non-biocidal analogues. MESQ(I)v25 was produced by free radical polymerisation of MESQ(I) (**3-3**) and iBoMA (**3-5**) at 85 °C with a 3.5 hour monomer feed after which 0.5 mol% initiator was added and the temperature maintained at 95 °C for a further 30 mins. The monomer feed composition was 25 mol% MESQ(I): 75 mol% iBoMA which was added drop wise into the reactor over 3.5 hours in an attempt to limit any possible compositional drift of the final polymer due to differing reactivities of the different monomers. The final polymer was formulated to be 50 % solids in xylene to create a simple polymeric solution which could be incorporated in a prototype paint formulation. MESQ(I)v30 was produced by the same method, however the monomer feed composition was 30 mol% MESQ(I): 70 mol% iBoMA. As a contrast to these biocidal polymers the equivalent non-biocidal polymers were also produced using MESQ(II) (**3-4**). These polymers were MESQ(II)v25 and MESQ(II)v30 with 25 and 30 mol% MESQ(II) (**3-4**) respectively. Each polymer was characterised in terms of <sup>1</sup>H NMR, **Figure 3:6**, viscosity, percentage non-volatile content (NVC), specific gravity (SG), total unreacted monomer molar percentage and unreacted monomer molar percentage, number average molecular weight ( $M_N$ ), weight average molecular weight ( $M_W$ ) and polymer polydispersity, (data presented in the Experimental Chapter).

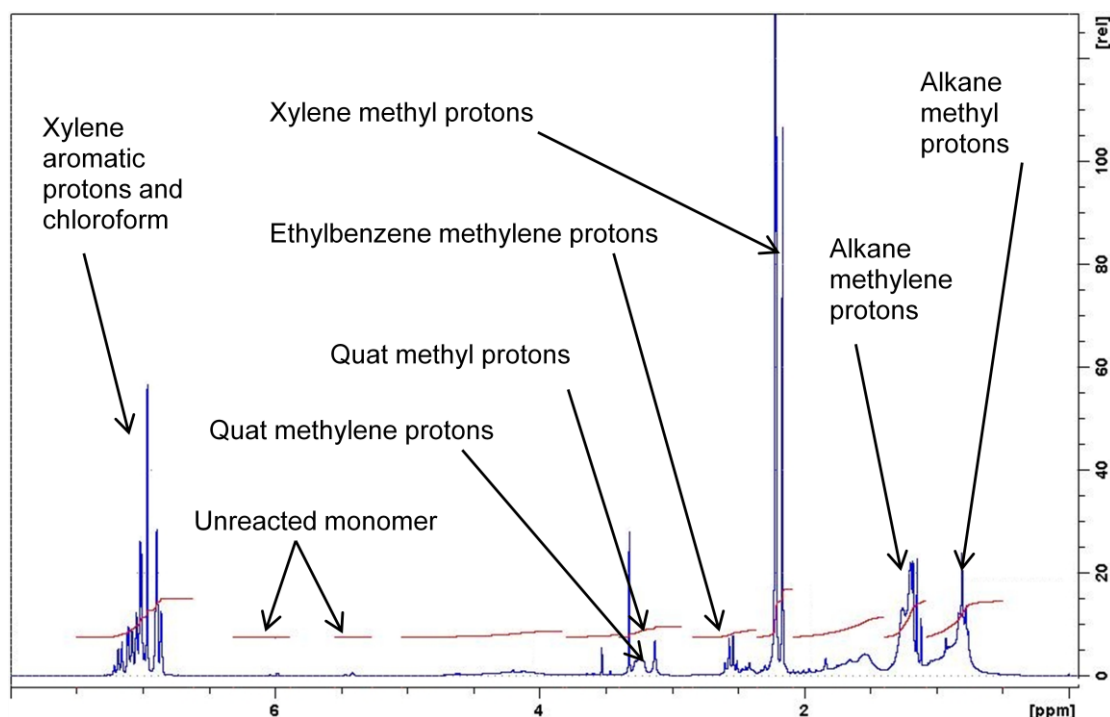


Figure 3:6: Example of  $^1\text{H}$  NMR of final quat-polymer xylene solution, MESQ(I)v25

### 3.3 Paint Formulation and Manufacture

Four different paints were prepared in an analogous fashion to those prepared to evaluate the experimental polymers of Chapter 2; i.e. systematic replacement of the binder of the prototype formulation with the synthesised polymers, ensuring that the test paints were equivalent in terms of volume solids and co-biocide content, **Table 3:1**. These new test paints were: MESQ(I)v25; MESQ(I)v30; MESQ(II)v25 and MESQ(II)v30.

<i>Raw Material</i>	<i>Weight %</i>
<i>MESQ(I)v25</i>	25.7
<i>Copper Oxide</i>	44.8
<i>Copper Pyrithione</i>	6.7
<i>Rheology Modifier</i>	2.3
<i>Pigmentation</i>	7.1
<i>Plasticiser</i>	2.4
<i>Xylene</i>	11.0

Table 3:1: Example of paint formulation for MESQ(I)v25

The final paints were monitored for grind and viscosity (data presented in the Experimental Chapter).

### 3.4 Paint Testing

The coatings developed via this route were evaluated using the same test methods as previously used with the paints produced via the post-quaternisation route.

#### 3.4.1 Semi Rapid Boot-Top Cycling

After 6 cycles the worst performing coatings were MESQ(I)v25 and MESQ(I)v30 both of which contained the biocidal monomer, MESQ(I) (3-3), Table 3:2 and Figure 3:7. There was no discernable difference in performance with increasing the active biocidal monomer level from 25 to 30 mol%, and since their performance was below that of the fail standard were removed from test. Conversely, after 8 cycles, both the non-biocidal coatings performance was substantially better, especially MESQ(II)30 (3-4), which showed a greater level of performance than the fail standard, being rated 4 compared to 2 for the fail standard. However this performance was inferior to that of the pass standard, a current International Paint biocidal antifouling coating, Intersmooth 460. It was therefore evident that replacement of the didecyl-quat with the trioctyl-quat greatly improved the mechanical performance of the coatings. The inclusion of the three octyl-chains comparatively increased the proportions of alkyl residues in the coating film. This increased alkyl residue could act to internally plasticise the film. Extra plasticisation could help the coating survive longer when cycled.

PAINT	CYCLE							
	1	2	3	4	5	6	7	8
<i>Pass Std</i>	5	5	5	5	5	5	5	5
<i>Fail Std</i>	3	3	3	3	3	3	2.5	2
<i>MESQ(I)v25</i>	5	4	4	3	3	2.5	-	-
<i>MESQ(I)v30</i>	5	4	3	3	3	2.5	-	-
<i>MESQ(II)v25</i>	5	5	4	4	4	3.5	3	3
<i>MESQ(II)v30</i>	5	5	4	4	4	4	4	4

Table 3:2: Semi rapid boot-top results for both biocidal and non-biocidal coatings



Figure 3:7: Photograph of MESQ(I)25 coating which failed after 6 cycles. The picture shows the corrosion of the coated steel substrate through the extensive cracking of the test coating.

### 3.4.2 Polishing Rate Determination

There appeared to be no discernable trend when the test coatings were subjected to the Polishing trials assay. When compared to the polishing standard coating (Interswift 655) both the biocidal and non-biocidal test coatings showed limited and sporadic polishing/film thickness depletion for the first 60 days, **Figure 3:8**. By 90 days the film thickness decrease was much smaller than expected and in general was nonexistent. When monitored at 120 days a clear and quantifiable film thickness loss was evident for the standard, Interswift 655, however this behaviour was absent from the MESQ coatings which, in general, showed a film thickness increase, **Figure 3:8**. This trend was unexpected and maybe related to the cause of the premature failure of the coatings when subjected to semi rapid boot top testing.

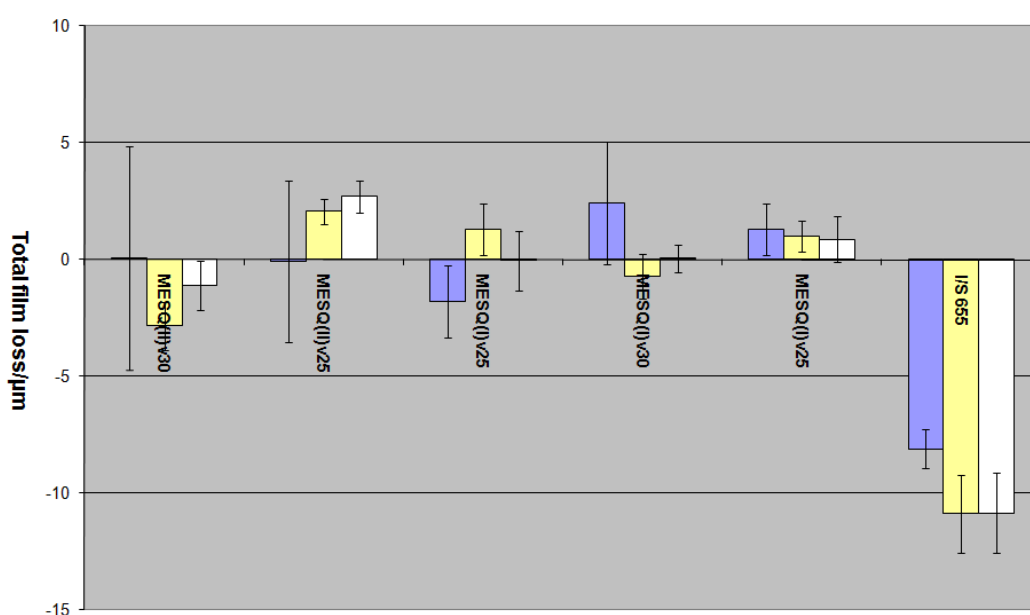


Figure 3:8: Total film loss over 60 (blue), 90 (yellow) and 120 (white) days immersion

### 3.4.3 Antifouling Performance



Figure 3:9: Example of an immersed 'clear' Latin square antifouling board

Together with the 6×6 Latin square antifouling boards which were coated with the test paints, 'clear' polymer boards were also immersed simultaneously, **Figure 3:9**. The 'clear' polymer test coatings were an attempt to speed up the differentiation between the biocidal and non-biocidal quats. The 'clear' polymer test coatings were the corresponding polymers used in the test paints (MESQ(I)v25 and 30 and MESQ(II)v25 and 30), but without the additional compounds present in the paint formulation, in particular the biocides copper oxide and copper pyrithione (1-2). MESQ(I)v25 and 30 were

specifically engineered to release a biocidal quat and hence were anticipated to exhibit an enhanced level of antifouling performance. This performance was, however, unlikely to be as sustained as for the corresponding paints which contained other additional boosting biocides. Hence these ‘clears’ boards were anticipated to give an early indication of the underlying antifouling performance of the polymers.

### 3.4.3.1 Clear Polymer Results

After 16 weeks immersion at Newton Ferrers there was clearly differentiated performance between the biocidal and non-biocidal ‘clear’ polymer test coatings, as demonstrated from the separation of the 95 % confidence error bars, **Figure 3:10**. Both the biocidal polymers (1827 and 1828) had little or no coverage of microfouling (red bar) and a small percentage of soft bodied fouling (sky blue bar). The non-biocidal polymers had a high coverage of microfouling but no soft bodied fouling.

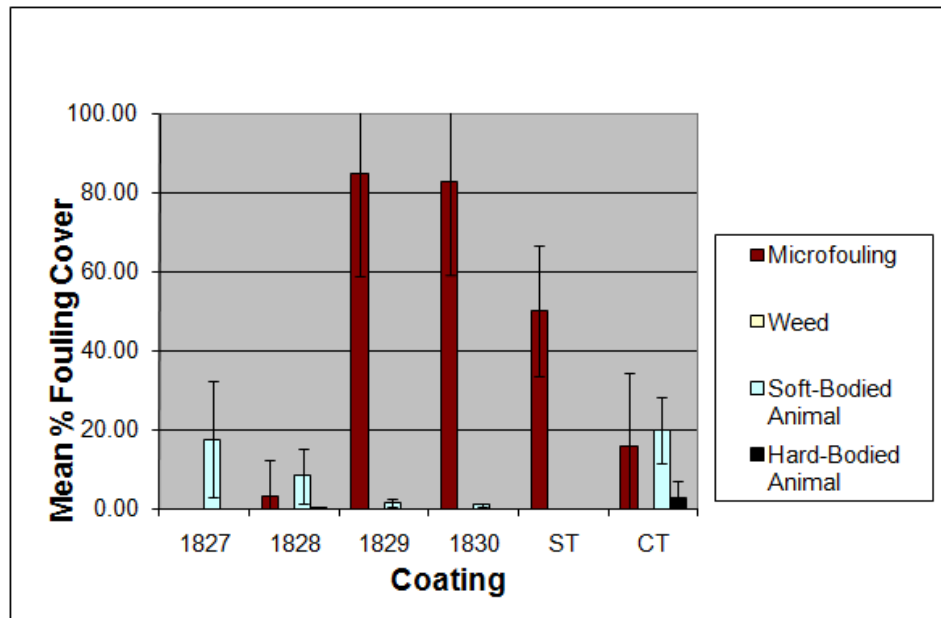


**Figure 3:10: Test Polymers antifouling results. Biocidal polymers 1827 and 1828 are MESQ(I)v25 and MESQ(I)v30 respectively. Non-biocidal polymers 1829 and 1830 are MESQ(II)v25 and MESQ(II)v30 respectively after 16 weeks immersion**

The counter intuitive accumulation of a small percentage of soft bodied fouling on the biocidal rather than the non-biocidal polymers was possibly due to the comparative difference in mechanical properties of the polymers. The mechanical performance of the non-biocidal polymers was sufficient to resist extensive cracking, unlike the corresponding biocidal polymers, which cracked soon after immersion (**Figure 3:11**). These highly cracked



**Figure 3:11: Cracking of biocidal polymers MESQ(I)25**

polymers could have provided the correct surface textures to allow settlement of soft bodied fouling, while the uncracked non-biocidal polymer deterred settlement. Subsequent inspection of this panel at 37 weeks found that there was no longer differentiated performance between the test polymers, as they were too heavily fouled. The panel was therefore removed from tests.

### 3.4.3.2 Paint Results

Conversely, after 27 weeks immersion, the formulated paints were not showing such a marked difference in performance. The biocidal paints (1772 and 1769) appeared to show a smaller percentage coverage of microfouling and hence better performance than the non-biocidal coatings (1771 and 1770), however the enhanced performance was not as pronounced, due to the poor separation of the 95 % confidence error bars, **Figure 3:12**.

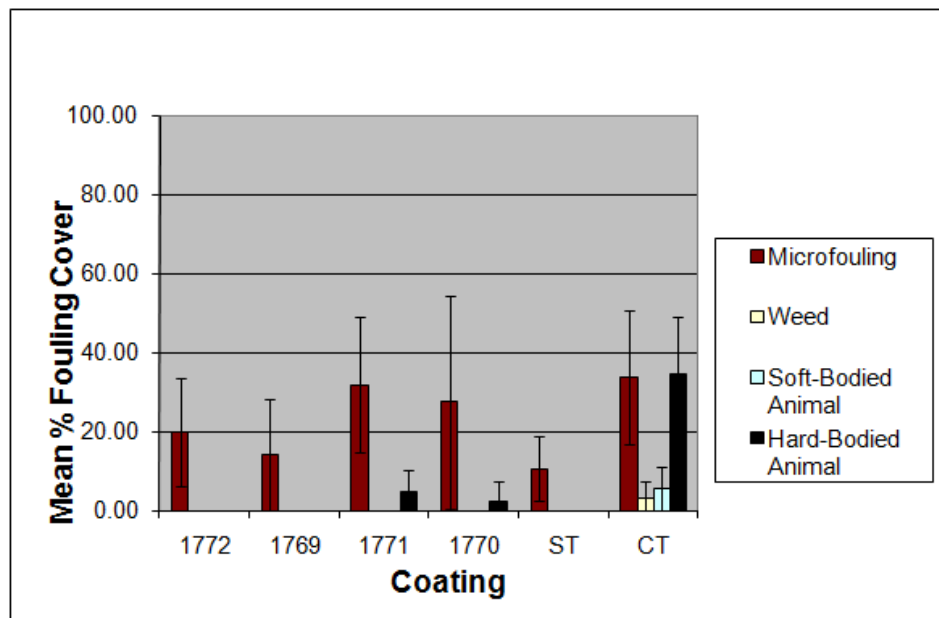


**Figure 3:12: Test Paint antifouling results. Biocidal paints 1772 and 1769 are MESQ(I)v25 and MESQ(I)v30 respectively. Non-biocidal paints 1771 and 1770 are MESQ(II)v25 and MESQ(II)v30 respectively after 27 weeks immersion**

By 47 weeks the percentage coverage of microfouling had substantially increased, being over 80 % for the biocidal MESQ(I) coatings and the standard coating, **Figure 3:13**. Interestingly the non-biocidal coating, MESQ(II)v25 (1771) outperformed all the coatings with an average microfouling coverage of approximately 45 %. Compared with the control coating all the test coatings displayed antifouling performance as these coatings prevented the growth of both soft and hard bodied fouling species. At 105 weeks, **Figure 3:14**, there was no longer differentiated performance, as all the coatings were fouled with similar levels of all the fouling types. The test was suspended after this inspection.

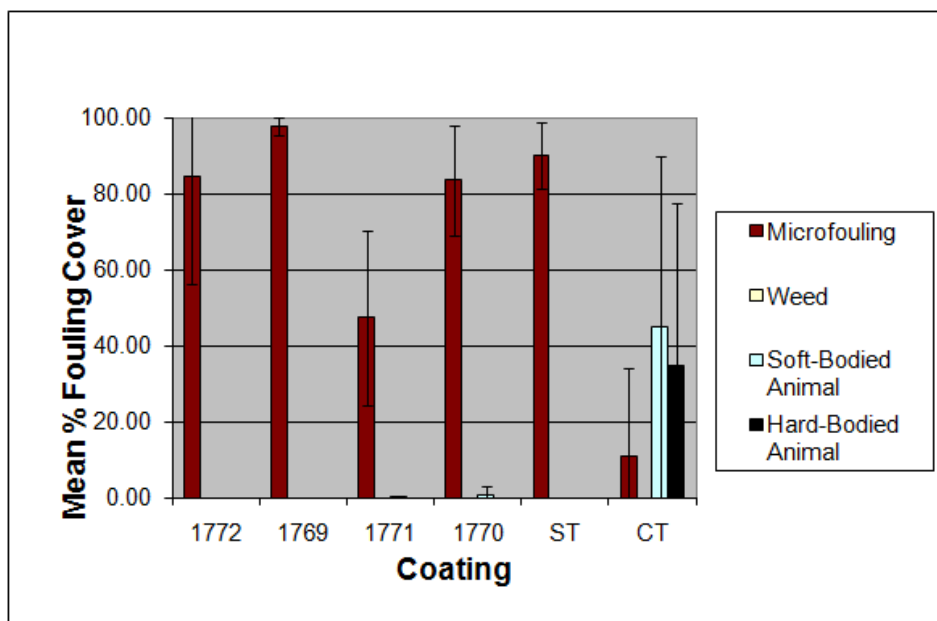


**Figure 3:13: Test Paint antifouling results. Biocidal paints 1772 and 1769 are MESQ(I)v25 and MESQ(I)v30 respectively. Non-biocidal paints 1771 and 1770 are MESQ(II)v25 and MESQ(II)v30 respectively after 47 weeks immersion.**

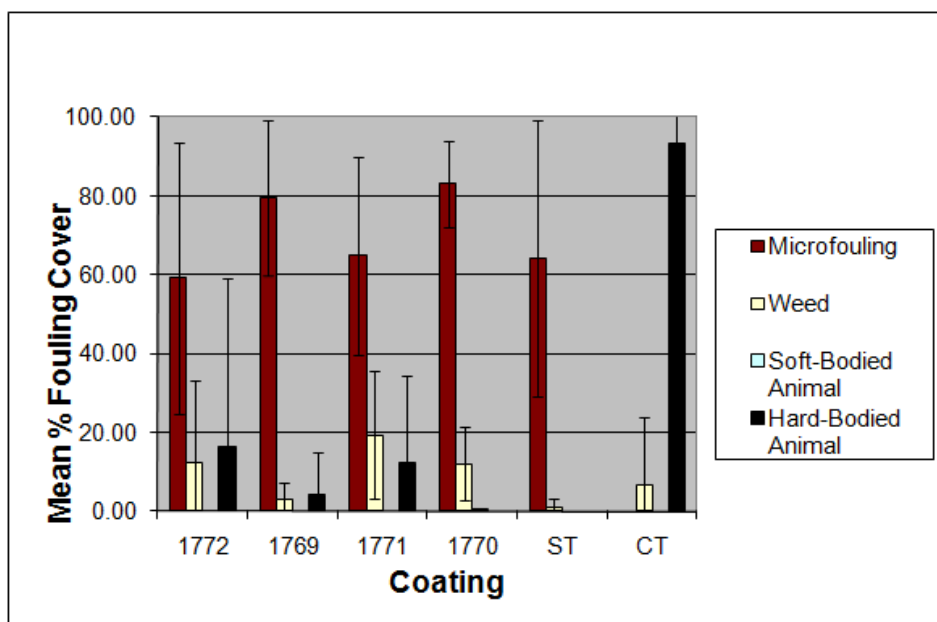


**Figure 3:14: Test Paint antifouling results. Biocidal paints 1772 and 1769 are MESQ(I)v25 and MESQ(I)v30 respectively. Non-biocidal paints 1771 and 1770 are MESQ(II)v25 and MESQ(II)v30 respectively after 105 weeks immersion.**

### 3.4.4 Storage Stability

All paints while stored at 23 °C showed no change in viscosity or grind for the duration of the test. However, during storage at the elevated temperature, 45 °C, the viscosity decreased rapidly and then gradually began to increase, **Figure 3:15**. This dramatic change in viscosity clearly demonstrated that the paints were unstable. The change in viscosity was also matched with a progressive increase in grind. Simultaneous changes in grind and viscosity could be symptomatic of an undesired chemical reaction between components of the paint formulation, which resulted in

the growth of particulate material over and above the average particulate matrix, manifested as increased grind. The instability in the formulation was clearly temperature dependent as the effects were only manifested at elevated temperatures and therefore was likely due to a chemical reaction, which due to the complex chemical composition of the paint was extremely problematic to identify, (see section 3.7.4).

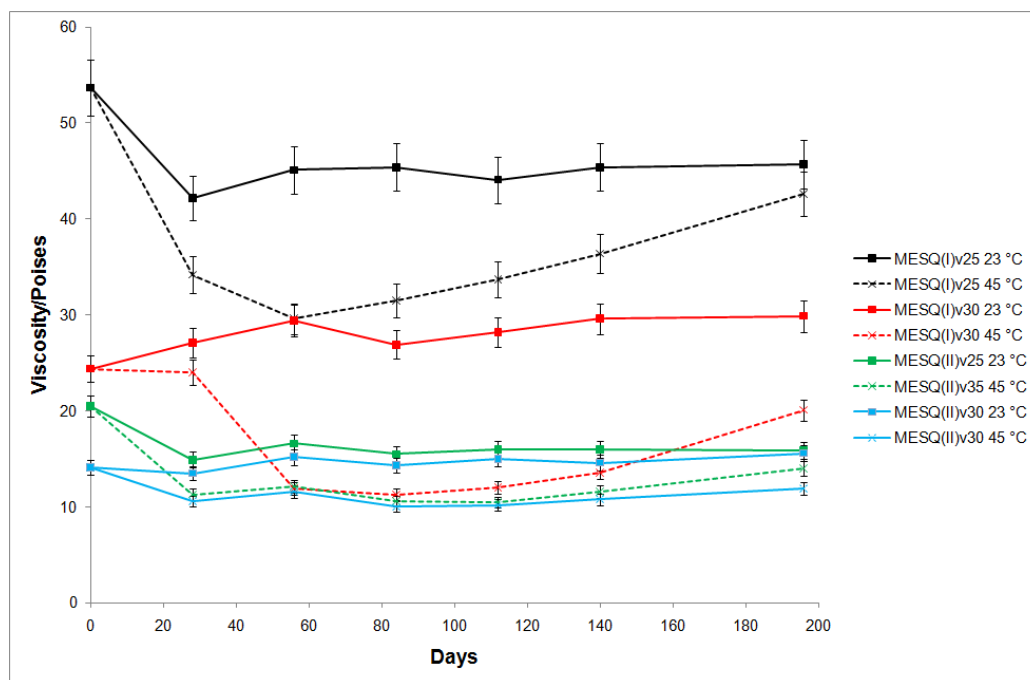
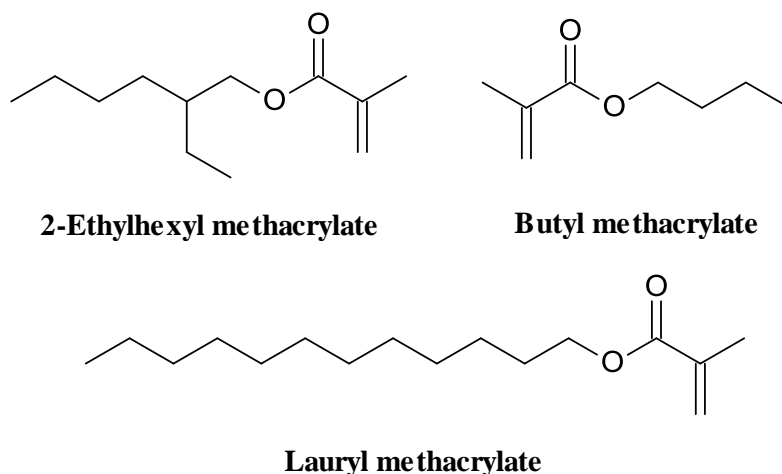


Figure 3:15: Changes in viscosity of test paints while on storage.

### 3.5 Second Generation Polymers

For the second generation polymers a third hydrophobic monomer was incorporated into the polymer to dually balance the hydrophilicity of MES (3-1) and reduce the percentage of iBoMA (3-5) creating less brittle polymers. Quat-monomer content was maintained at 25 mol% to ensure a comparable level of biocidal component with the 1<sup>st</sup> generation polymers to facilitate a direct comparison. The remaining 75 % was reciprocally split between iBoMA (3-5) and the third comonomer, with the smallest percentage arbitrarily set at 15 mol%, Table 3:3. The third monomer was chosen to be one of; 2-ethylhexyl methacrylate (EHMA, 3-6), butyl methacrylate (BMA, 3-7) or lauryl methacrylate (LMA, 3-8), Table 3:4. This series varied the length of the hydrophobic alkyl chain and hence the degree of hydrophobicity of the monomers and plasticisation of the final polymers, Figure 3:16.



**Figure 3:16: Structures of 2-ethylhexyl methacrylate (3-6), butyl methacrylate (3-7) and lauryl methacrylate (3-8)**

Synthetic methodology for the synthesis of the second generation quat-polymers was analogous to that in *section 3.2*. Each polymer was characterised in terms of <sup>1</sup>H NMR, viscosity, percentage non-volatile content (NVC), specific gravity (SG), total unreacted monomer molar percentage and unreacted monomer molar percentage, number average molecular weight (M<sub>N</sub>), weight average molecular weight (M<sub>W</sub>) and polymer polydispersity, (data presented in the Experimental Chapter).

<i>MESQ(I)</i> mol%	<i>iBoMA</i> mol%	<i>Third comonomer mol%</i>		
		<i>EHMA</i> (3-6)	<i>BMA</i> (3-7)	<i>LMA</i> (3-8)
25	15	60	60	60
25	37.5	37.5	37.5	37.5
25	60	15	15	15

**Table 3:3: Mol% breakdown of second generation polymers**

<i>mol%</i>	<i>EHMA (3-6)</i>	<i>BMA (3-7)</i>	<i>LMA (3-8)</i>
60	MESQ(I)v2	MESQ(I)v5	MESQ(I)v8
37.5	MESQ(I)v3	MESQ(I)v6	MESQ(I)v9
15	MESQ(I)v4	MESQ(I)v7	MESQ(I)v10

**Table 3:4: Polymer code names with corresponding mol% of third comonomer**

### 3.5.1 Polymer Glass Transition Temperature Determination

From the Fox equation the glass transition temperature (T<sub>g</sub>) of a polymer can be considered an aggregated sum of the T<sub>g</sub>s of its component homopolymers, **Equation 3:1**:

$$\frac{1}{T_g} = \sum \frac{x_i}{T_{g,i}}$$

**Equation 3:1: Fox Equation**

Since T<sub>g</sub> of a homopolymer is specific to that polymer and a homopolymer is an aggregation of the same monomer, it can therefore be inferred that the monomers when in a mixed monomer copolymer system will contribute to the overall T<sub>g</sub> of that final polymer depending upon their weight

percentage. Therefore, if the  $T_g$  of a polymer is known, the  $T_g$  contribution of any monomer in the polymer can be calculated by simple manipulation of the Fox equation. The second generation MESQ(I) polymers were synthesised using monomers, which have published values of  $T_g$ , **Table 3:5**. The only unknown  $T_g$  was that of MESQ(I) (3-3), which can therefore be calculated using the rearranged Fox equation, **Equation 3:2**:

<i>Monomer</i>	<i><math>T_g/K</math></i>
<i>iBoMA (3-5)</i>	383
<i>EHMA (3-6)</i>	263
<i>BMA (3-7)</i>	293
<i>LMA (3-8)</i>	208

**Table 3:5: Published  $T_g$  data for comonomers used in second generation polymers<sup>180</sup>.**

$$T_{g,A} = \frac{x_A}{\left[ \frac{1}{T_g} - \frac{x_B}{T_{g,B}} - \frac{x_C}{T_{g,C}} \right]}$$

**Equation 3:2: Manipulated Fox equation for the calculation of the  $T_g$  of a monomer from a blended polymer.**

The  $T_g$ s for one of each of the EHMA (3-6), BMA (3-7) and LMA (3-8) containing polymers were measured using differential scanning calorimetry (DSC)<sup>181</sup>, **Table 3:6**, and used to calculate the  $T_g$  of MESQ(I) (3-3), **Table 3:6**.

The identification of the  $T_g$ s were problematic due to the poor responses obtained. Frequently, the transition occurred over a large temperature range, *circa* 20 °C or more and this, combined with the low change in energy at the transition temperature resulted in long diffuse transitions making identification problematic, **Figure 3:17**. This is an inherent problem of acrylic polymers, which commonly give unpronounced responses when analysed by DSC<sup>182</sup>. Unfortunately the nature of the polymer samples meant that it was not possible to analyse them using alternative analytical techniques, such as dynamic mechanical analyser (DMA) as this required samples/flakes which are consistent in their thickness and width across their length. Identification was further complicated by the presence of what appeared to be a second transition temperature, **Figure 3:17**.

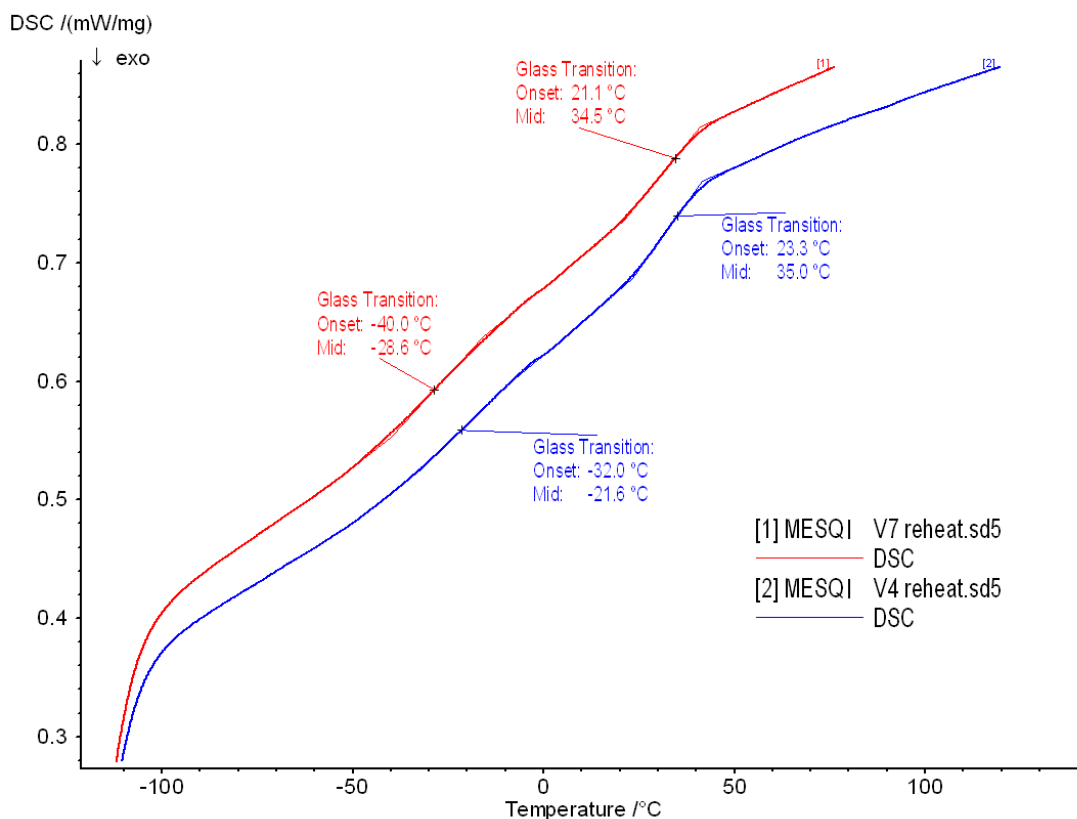
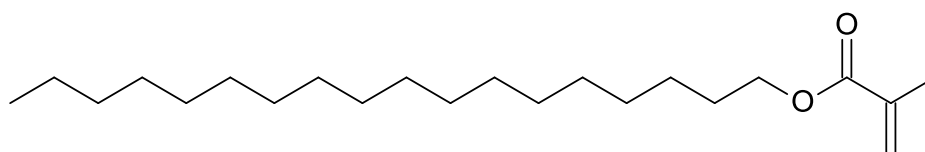


Figure 3:17: DSC chart displaying unpronounced and multiple transitions for MESQ(VI)v4 and v7.

Polymer	Measured Transition Temperature/ K	Calculated $T_g$ of MESQ(I)/ K
MESQ(I)v3	298	263
MESQ(I)v6	307	250
MESQ(I)v9	222	145

Table 3:6:  $T_g$  data for the EHMA (3-6), BMA (3-7) and LMA (3-8) polymers

The two transitions would correspond to MESQ(I) having a  $T_g$  of 125 and 220 K. The structure of MESQ(I) (3-3) consisted of a linear chain of 11 atoms of the MES framework-monomer which was then capped with the didecyldimethylammonium cation. There was limited functionality within the molecule to restrict rotation within the molecule and so it was extremely unlikely that the monomer would produce a polymer network which was brittle (high  $T_g$ ). Comparable structures to MESQ(I) (3-3), having long aliphatic chains, such as LMA (3-8) and octadecyl methacrylate (3-9), Figure 3:18, have  $T_g$ s well below 273 K, at 210 and 173 K<sup>180</sup> respectively.



Octadecyl methacrylate

Figure 3:18: Structure of octadecyl methacrylate

Conversely, a  $T_g$  of 125 K seemed too low; it would be anticipated that polymers containing such a low  $T_g$  monomer at 25 mol% would be far more plasticised than these polymers appeared by visual inspection. In light of its close proximity to  $T_g$ s published for similar structures, the  $T_g$  of 220 K appeared the most likely to represent the  $T_g$  of MESQ(I) (3-3) and was used to predict the  $T_g$ s of the remaining polymers, **Table 3:7**.

<i>Polymer</i>	<i>Predicted <math>T_g</math>/ °C</i>	<i>Measured <math>T_g</math>/ °C</i>
<i>MESQ(I)v2</i>	-11	1
<i>MESQ(I)v3</i>	9	25
<i>MESQ(I)v4</i>	32	34
<i>MESQ(I)v5</i>	6	16
<i>MESQ(I)v6</i>	21	34
<i>MESQ(I)v7</i>	38	36
<i>MESQ(I)v8</i>	-47	-55
<i>MESQ(I)v9</i>	-18	-51
<i>MESQ(I)v10</i>	19	33

**Table 3:7: Second generation polymer  $T_g$ s**

The correlation between the predicted and measured  $T_g$ s was poor. However, it was possible to discern general trends, such as the increased  $T_g$  with increased iBoMA percentage within each group of third comonomer. Of the three polymers with the lowest  $T_g$ s, MESQ(I)v2, v8 and v9; two contained LMA (v8 and v9), which would be anticipated given that LMA (3-8) had the lowest  $T_g$  of all the monomers used, and they also conformed to the order of the polymers based on their predicted  $T_g$ .

The measured  $T_g$ s correlated well with the observed physical characteristics of the polymers. Given that the  $T_g$ s were close to room temperature, the polymers physical state seemed to correspond qualitatively with this, being neither extremely soft/fluid nor very hard/brittle. The poor correlation between the predicted and measure  $T_g$  could be attributed to the inherent difficulties in obtaining accurate values for the  $T_g$ s of acrylic polymers, especially given the 20 °C temperature range for the transitions.

Coatings formulated with low  $T_g$  polymers were unlikely to display the required mechanical performance. This was because seawater temperatures, which vary between 5 and 20 °C, are close to or above the  $T_g$ s of these polymers and as such the coatings would be extremely plasticised or softened. These ‘soft’ coatings would not have sufficient mechanical robustness to survive damage incurred during in-service usage, such as cold flow (*see Chapter 2, section 2.4.2.2, Figure 2:9*).

## 3.6 Second Generation Paint Formulation and Manufacture

Synthetic methodology for paint formulation and manufacture was analogous to that in section 3.3. The paints were monitored for grind and viscosity (data presented in the Experimental Chapter).

## 3.7 Second Generation Paint Testing

### 3.7.1 Semi Rapid Boot-Top Cycling

The mechanical properties of the second generation paints were substantially improved compared with the first generation, with several of the test films outperforming the fail standard and displayed comparable performance with the pass standard. The previous iteration of paints failed after 6 cycles, while this set of paints survived to 12 cycles, at which stage the test was suspended, **Table 3:8** and **Figure 3:19**. The test was suspended after 12 cycles as the coatings were deemed to have sufficiently robust mechanical properties for prototype paints. The ability of the coatings to withstand the repeated cycling between -5 and +35 °C correlated well with the  $T_g$ s of the polymers. Those polymers which had the lowest  $T_g$ s, (MESQ(I)v2, v8 and v9) plasticised the paint film preventing the film from cracking and deteriorating during cycling. The antithesis was also demonstrated with the highest  $T_g$  polymers, all of which had 60 mol% iBoMA (3-5) (MESQ(I)25v4, v7 and v10) producing films whose performances were inferior to that of others with matching comonomers. The inclusion of the 3<sup>rd</sup> comonomer clearly helped reduce the  $T_g$  of the polymers and substantially improved the mechanical robustness of the second generation MESQ(I) coatings, compared with the previous version, MESQ(I)v25. From the presented data it can be concluded that 60 mol% iBoMA (3-5) over-balanced the mechanical properties of the polymers, resulting in coatings which proved brittle when subjected to semi rapid boot top cycling.

PAINT	CYCLE									
	3	4	5	6	7	8	9	10	11	12
<i>Pass Std</i>	5	5	5	5	5	5	5	5	5	5
<i>Fail Std</i>	4	3.5	3	3	3	3	3	3	3	3
MESQ(I)25v2	5	5	5	5	5	5	5	5	5	5
MESQ(I)25v3	5	5	5	5	5	5	5	5	5	5
MESQ(I)25v4	5	5	4.5	4.5	4	4	4	4	4	4
MESQ(I)25v5	5	5	5	5	5	5	5	5	5	5
MESQ(I)25v6	5	5	4.5	4.5	4.5	4.5	4.5	4.5	4.5	4
MESQ(I)25v7	4	4	4	4	4	4	3	3	3	3
MESQ(I)25v8	5	5	5	5	5	5	5	5	5	5
MESQ(I)25v9	5	5	5	5	5	5	5	5	5	5
MESQ(I)25v10	5	5	4	4	4	4	4	4	4	4

**Table 3:8: Semi rapid boot top data for paints, omitting the first 2 cycles as pass, fail and test coatings were all rated 5.**

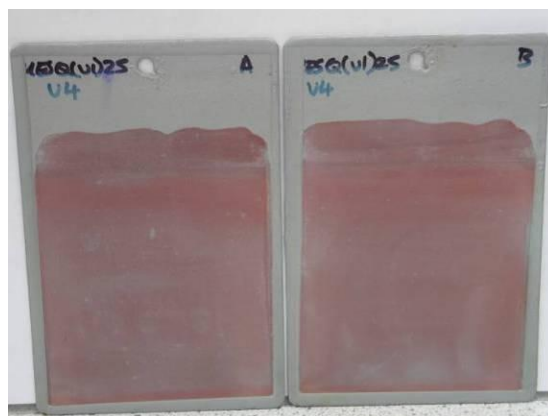


**Figure 3:19: MESQ(I)25v4 after 12 semi rapid cycles showing enhanced mechanical properties compared to the first generation coatings, which failed after 6 cycles.**

The clear polymers were also tested alongside the paints. These polymers were without the additional plasticisation imparted by the other raw materials in the paint formulation and hence failed earlier in their testing. It was hoped that this extreme test could help screen the polymers and offer some insight into the long term performance of the full formulated paints, **Table 3:9**. The polymers MESQ(I)25v4 and v7, the two highest predicted  $T_g$ s, cracked and disintegrated during the pre-immersion prior to the start of the cycling phase. These polymers were all formulated with the highest levels of iBoMA (**3-5**) and were the most brittle resulting in their premature failure. Polymers MESQ(I)25v8 and v9, the two lowest predicted  $T_g$ s, both sagged at the immersion line. Both these polymers were formulated with LMA (**3-8**) which had the lowest  $T_g$  of the three comonomers used resulting in its greater capacity to internally plasticise the polymers. The sagging was attributed to the overall  $T_g$ s of the polymers being substantially below 35 °C, the temperature of the immersion bath, allowing the plasticised polymer to flow causing sagging. From the presented data it can be concluded that LMA (**3-8**) would not be an appropriate comonomer for further polymer development as resultant polymers would have  $T_g$  which would be too low. Considering both the polymer and paint semi rapid boot top test results, the most promising polymers would be MESQ(I)25v3 and v6, which contained EHMA (**3-6**) and BMA (**3-7**) respectively at 37.5 mol%.

PAINT	CYCLE							
	1	2	3	4	5	6	7	8
MESQ(I)25v2	5*	5*	5*	5*	5*	5*	5*	5*
MESQ(I)25v3	5	5	5	5	5	5	5	5
MESQ(I)25v4	-	-	-	-	-	-	-	-
MESQ(I)25v5	5*	5*	5*	5*	5*	5*	5*	5*
MESQ(I)25v6	5	5	5	4.5	4.5	4	4	3
MESQ(I)25v7	-	-	-	-	-	-	-	-
MESQ(I)25v8	5*	5*	5*	5*	5*	5*	5*	5*
MESQ(I)25v9	5*	5*	5*	5*	5*	5*	5*	5*
MESQ(I)25v10	2	2	2	2	2	-	-	-

**Table 3:9: SRBT results for polymers, (-) - corresponds to complete failure of polymer by detached from the substrate, (\*) - corresponding to sagging at waterline.**

### 3.7.2 Polishing Rate Determination

Due to the poor performance of paints MESQ(I)25v2, v5 and v8 on semi rapid boot top cycling, especially their corresponding polymers, these coatings were removed from the polishing disks prior to testing due to expected cold flow, **Figure 3:20**. The number of replicates of each test coating was increased from two to six for the second generation of paints in an effort to increase the statistical confidence of the data.

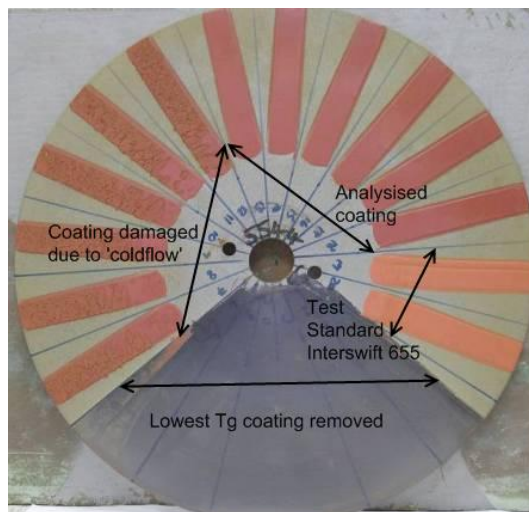


**Figure 3:20:** Post test LMA (3-8) paints polishing disk which has the six strips of MESQ(I)25v8, the softest coating, removed also displaying the effects of 'cold flow' on MESQ(I)25v9, the first 6 strips.

For the EHMA (3-6) coatings, **Figure 3:21**, only MESQ(I)25v3 showed evidence of polishing after the first 60 days of testing, although the depletion was less than that of the standard, Interswift 655. After 60 days the film depletion was not sustained and the film thickness began to increase, most likely due to ingress of water into the coating causing film swelling. A similar trend was also evident in the BMA (3-7) coatings, **Figure 3:22**, with MESQ(I)25v6 initially showing a film thickness loss which later began to swell. For the LMA (3-8) coatings, **Figure 3:23**, only MESQ(I)25v10 was analysable. No data was possible for MESQ(I)25v9 due to extensive cold flow, **Figure 3:20**. MESQ(I)25v10 also showed the initial polishing followed by swelling. Overall, none of the second generation coatings display the anticipated sustained film thickness loss/polishing behaviour. One reason for this maybe the rate of swelling being greater, or the same as the rate of polishing, resulting in an overall appearance of diminished or no polishing.

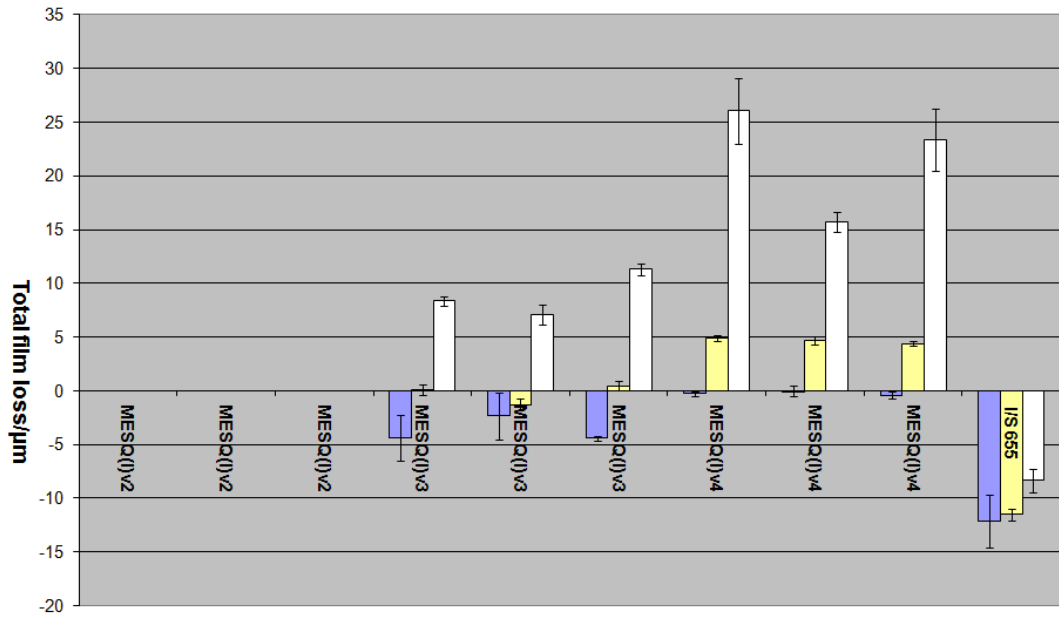


**Figure 3:21: Total film loss over 60 (blue), 90 (yellow) and 120 (white) days immersion of EHMA (3-6) containing coatings: MESQ(I)25v3 and v4**

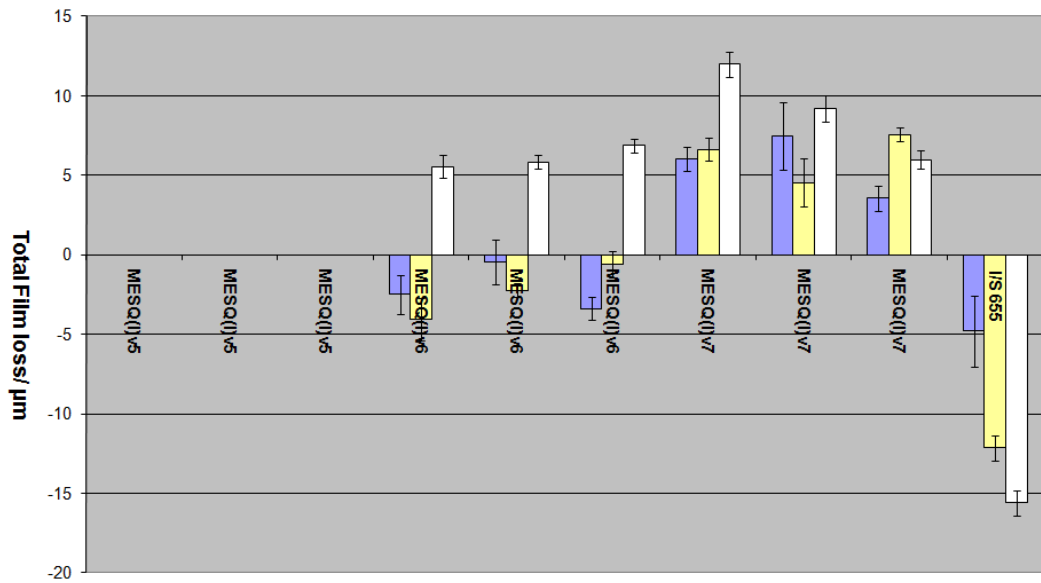


**Figure 3:22: Total film loss over 60 (blue), 90 (yellow) and 120 (white) days immersion of BMA (3-7) containing coatings: MESQ(I)25v6 and v7**

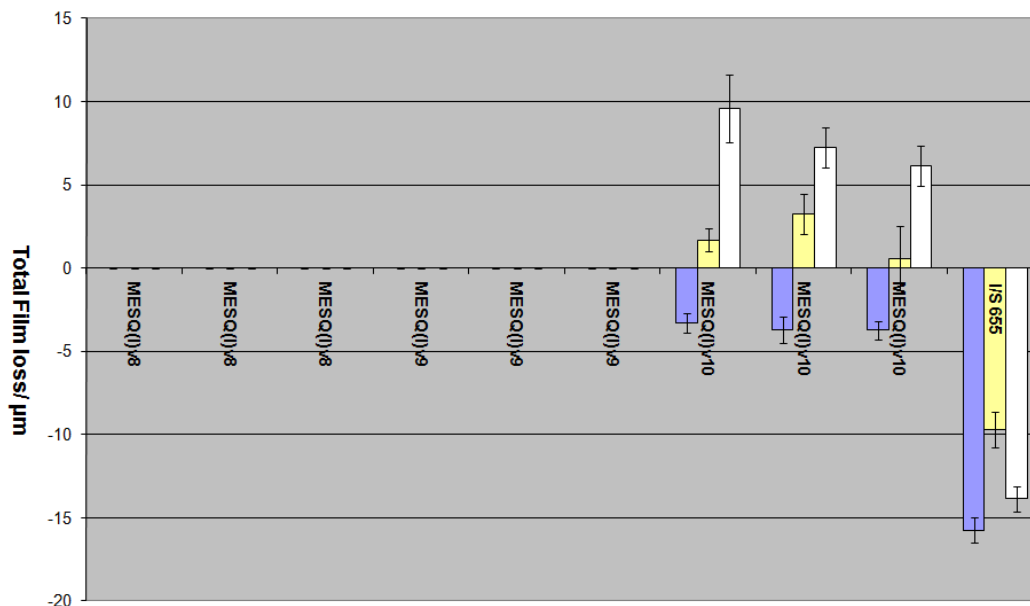


Figure 3:23: Total film loss over 60 (blue), 90 (yellow) and 120 (white) days immersion of LMA (3-8) containing coatings: MESQ(I)25v10

### 3.7.3 Antifouling Performance

#### 3.7.3.1 Clear Polymer Results

Antifouling boards were prepared as previously described. Of all the second generation clear polymers only two showed acceptable antifouling performance after 17 weeks immersion at Newton Ferrers. These polymers were coatings 2031 (**Figure 3:24**) and 2037 (**Figure 3:26**) which were MESQ(I)25v4 and v10 which contained the highest iBoMA (3-5) percentages for the EHMA (3-6) and LMA (3-8) coating series respectively. The data presented for the percentage coverage for hard-bodied animal fouling on the LMA (3-8) polymer board, **Figure 3:26**, showed particularly large error bars. These were a manifestation of non-uniform fouling growth, combined with the use of the Latin square arrangement on the antifouling boards, which required the six replicate squares of each test coating to be distributed around the board in different positions. When an intense and localised growth of fouling occurs in one region of the board, from one edge for example; the performance of those test squares nearest to the infestation would be significantly below that of their replicates in other regions of the board, which results in large error bars for the analysed data. Such intense and localised attacks are common for weed and hard-bodied animal fouling and hence diverse results are sometimes inevitable. However, the range in performance is averaged over the whole antifouling board to give a representative average performance for the test coating. For the BMA (3-7) coatings (**Figure 3:25**) the performances of all the coatings was inferior to the standard, Intersmooth 460.

By 24 weeks only MESQ(I)25v10, **Figure 3:27**, was still showing a differentiated performance from the other test polymers. The performance, however, was still inferior to that of the standard

coating. The standard coating was a fully formulated paint which contained additional boosting biocides, so it would be expected to outperform the clear polymers. The use of a fully formulated paint as a standard within this experiment was, perhaps, not appropriate and in future tests a clear standard was selected. Nevertheless, the antifouling performance of the unformulated MESQ(I)25v10 was remarkably good. Noteworthy also on the LMA (3-8) polymer board, **Figure 3:27**, was the presence of horizontal drip-like structures from coating 2035 (MESQ(I)25v8) which were manifestations of cold flow caused by the polymer having too low a  $T_g$ . The polymer was sufficiently plasticised and the shear forces of water moving across its surface were strong enough to cause the drip-like structures to form. MESQ(I)25v8 had the lowest percentage of iBoMA (3-5) in the LMA (3-8) series and the lowest predicted  $T_g$  of all the MESQ(I) polymers, hence would be the most susceptible to cold flow. The clear polymer boards containing the EHMA (3-6), BMA (3-7) and LMA (3-8) version polymers were removed from test after the 24 weeks inspection.

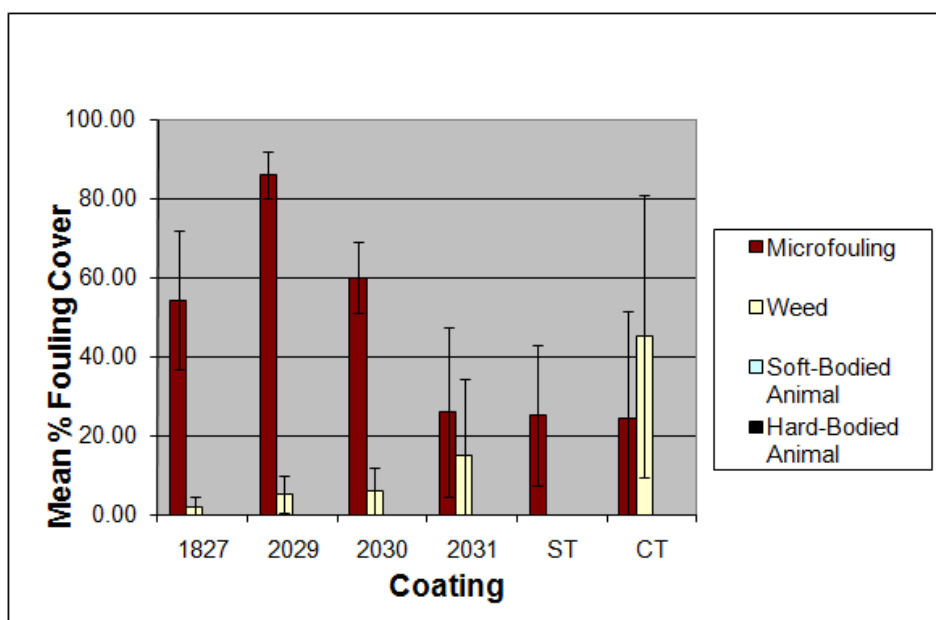


**Figure 3:24: EHMA containing polymers antifouling results. Polymer 1827 is MESQ(I)v25 and 2029, 2030 and 2031 are MESQ(I)25v2, 3 and 4 respectively after 17 weeks immersion**

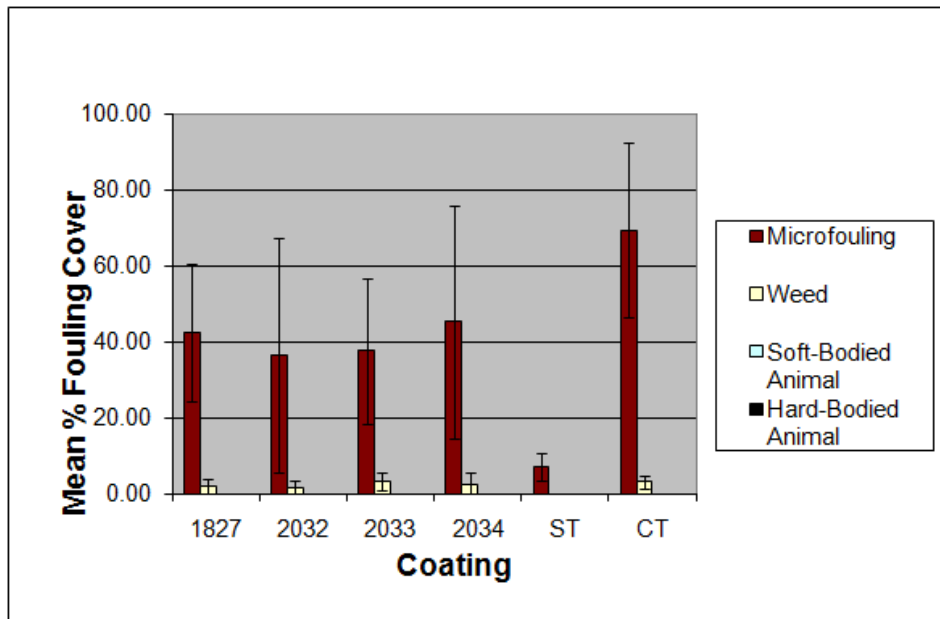


Figure 3:25: BMA containing polymers antifouling results. Polymer 1827 is MESQ(I)v25 and 2032, 2033 and 2034 are MESQ(I)25v5, 6 and 7 respectively after 17 weeks immersion

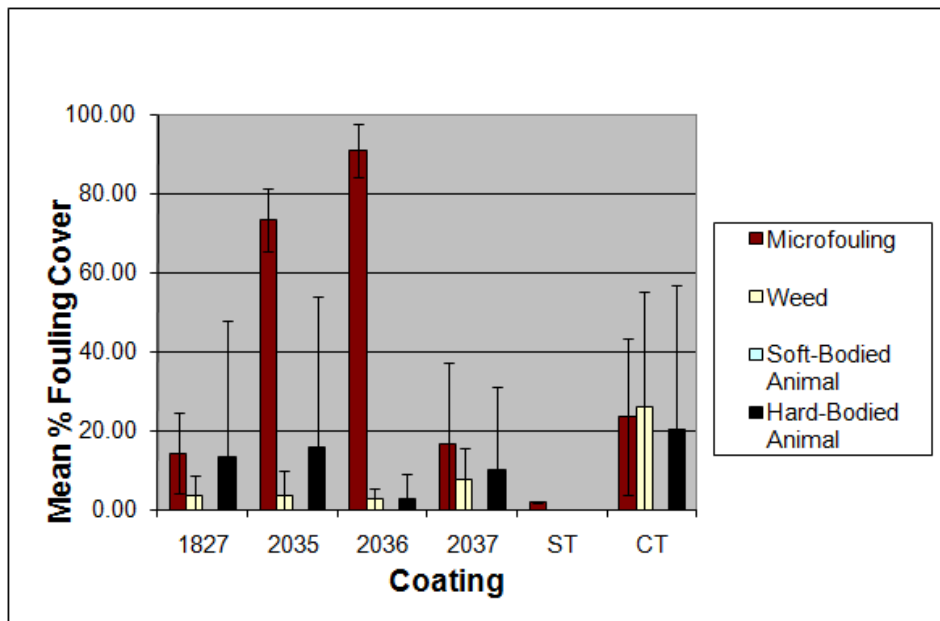


Figure 3:26: LMA containing polymers antifouling results. Polymer 1827 is MESQ(I)v25 and 2035, 2036 and 2037 are MESQ(I)25v8, 9 and 10 respectively after 17 weeks immersion

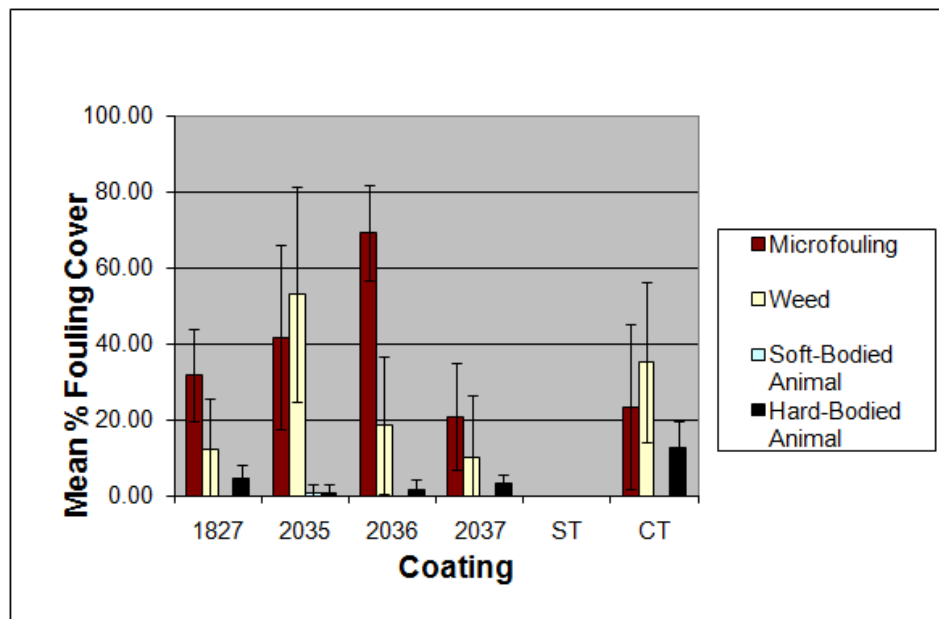


Figure 3:27: LMA containing polymers antifouling results. Polymer 1827 is MESQ(I)v25 and 2035, 2036 and 2037 are MESQ(I)25v8, 9 and 10 respectively after 24 weeks immersion

### 3.7.3.2 Paint Results

The performance of the test paints at 17 weeks was superior to that of the clear polymers due to the presence of additional biocides, **Figure 3:28** (EHMA paints), **Figure 3:29** (BMA paints) and **Figure 3:30** (LMA paints). However, it was still possible to discern the same underlying trend in performance as the clear polymers with paints 2022 (**Figure 3:28**) and especially 2028 (**Figure 3:30**), MESQ(I)25v4 and v10 respectively, showing the best antifouling activity. No results were generated at 24 weeks for the paints because it was anticipated that due to their elevated antifouling activity clearer differentiation in performance would become more established after a prolonged trial period.

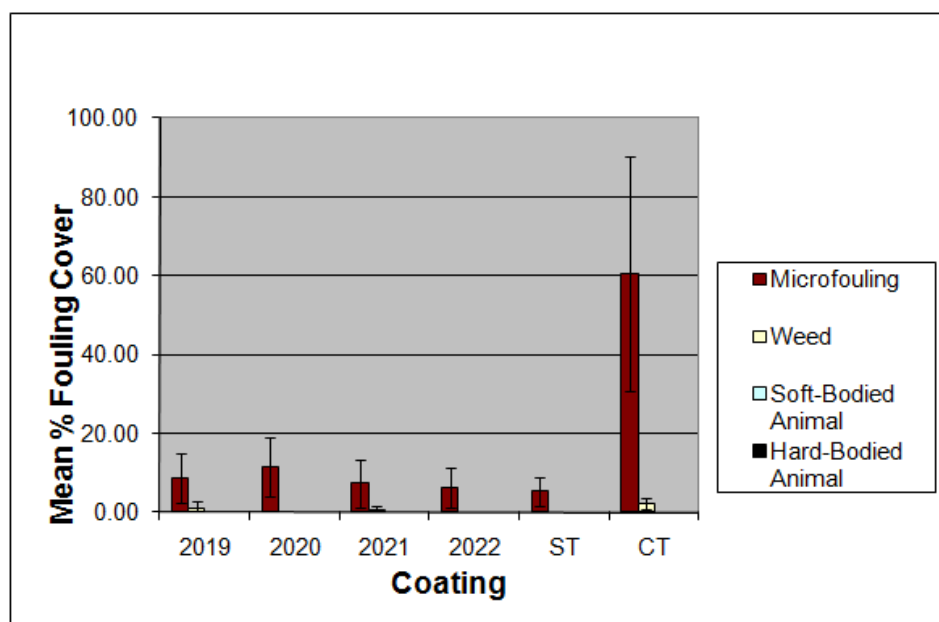
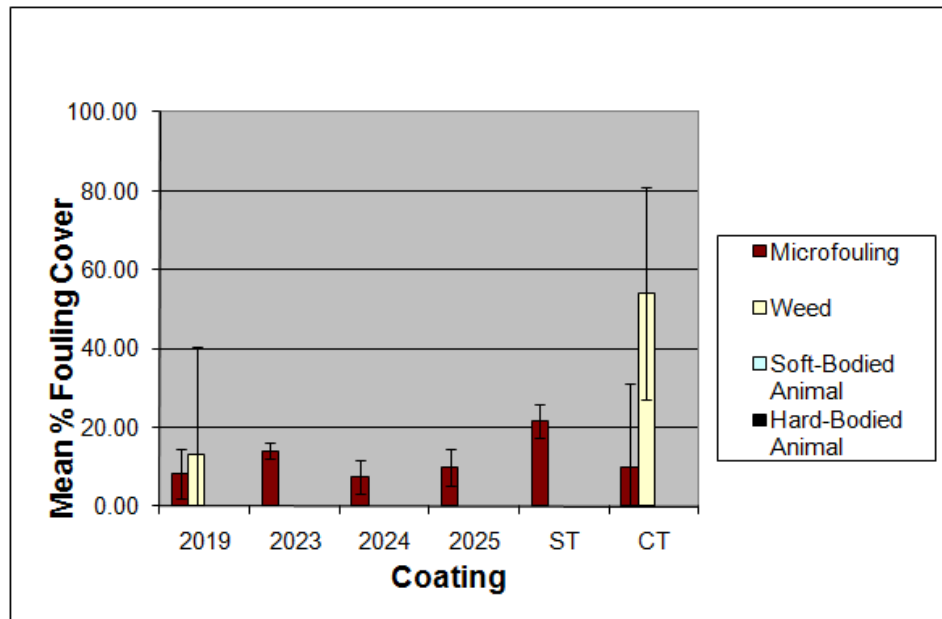
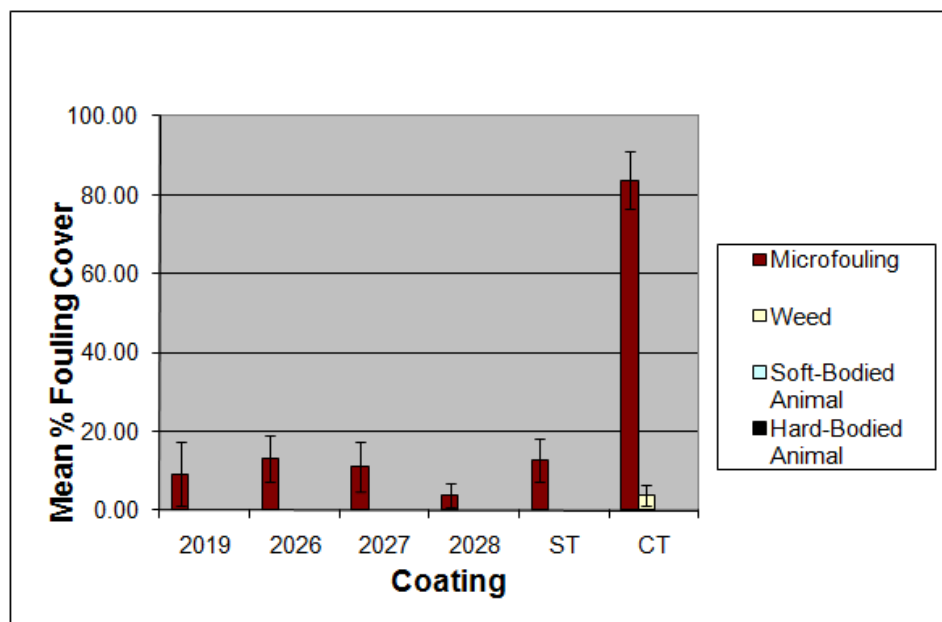


Figure 3:28: Test EHMA paints antifouling results. Paint 2019 is MESQ(I)v25 and 2020, 2021 and 2022 are MESQ(I)25v2, 3 and 4 respectively after 17 weeks immersion



**Figure 3:29: Test BMA paints antifouling results. Paint 2019 is MESQ(I)v25 and 2023, 2024 and 2025 are MESQ(I)25v5, 6 and 7 respectively after 17 weeks immersion**



**Figure 3:30: Test LMA paints antifouling results. Paint 2019 is MESQ(I)v25 and 2026, 2027 and 2028 are MESQ(I)25v8, 9 and 10 respectively after 17 weeks immersion**

The fouling season in the UK peaks between March and August (approx 28 weeks)<sup>177</sup>, outside this window the sea temperature is too low for sustained fouling growth. Therefore given that the clear polymer were able to survive to 24 weeks, it would be anticipated that the formulated paints with their additional boosting co-biocides would be able to survive well past the 30 week high fouling season and into the low season. Ordinarily panels which have survived a whole season are left immersed through the low season and first inspected prior to the start of the second season, the following spring. In case of the MESQ(I) second generation paints this inspection was after 53 weeks immersion. During this inspection it was discovered that the fouling growth, specifically the

microfouling on the panels was to such a large extent, that there was no clear differentiation in performance between any of the test paints, **Figure 3:31** (EHMA paints), **Figure 3:32** (BMA paints) and **Figure 3:33** (LMA paints). The incorporation of the quats, which have known antimicrobial properties, was envisioned to provide enhanced anti-microfouling performance. This was clearly demonstrated during the inspection at 17 weeks with all the test paints displaying less microfouling coverage than the control coating, **Figure 3:28** (EHMA paints), **Figure 3:29** (BMA paints) and **Figure 3:30** (LMA paints). Unfortunately this performance was not sustained and by 53 weeks no discernable anti-microfouling activity was demonstrated. This loss in performance was unexpected, but maybe attributed to the release rate of the quat decreasing to below a critical level, at which no antifouling effect was possible. After this inspection the panels were removed from test.

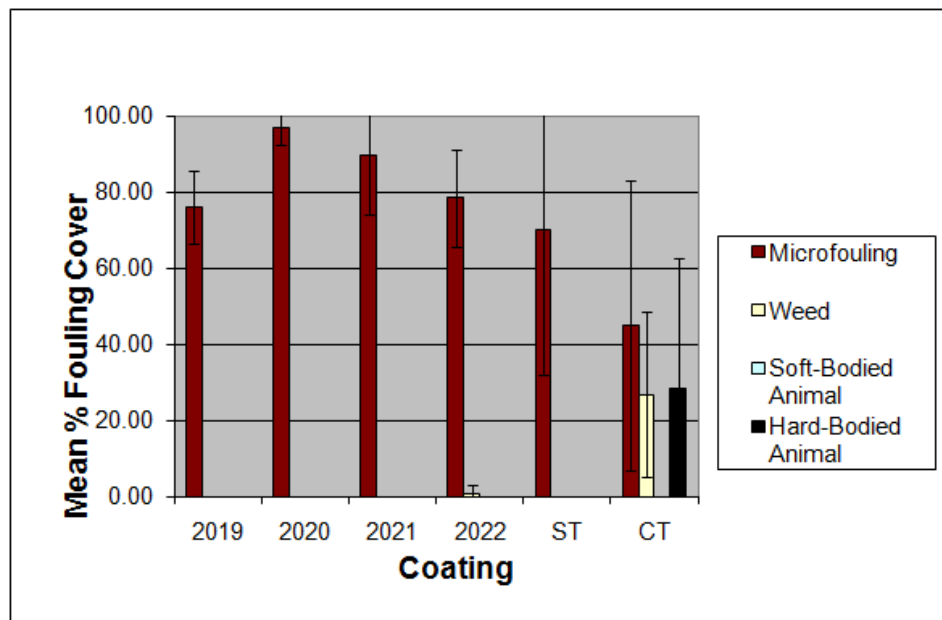


**Figure 3:31: Test EHMA paints antifouling results. Paint 2019 is MESQ(I)v25 and 2020, 2021 and 2022 are MESQ(I)25v2, 3 and 4 respectively after 53 weeks immersion.**

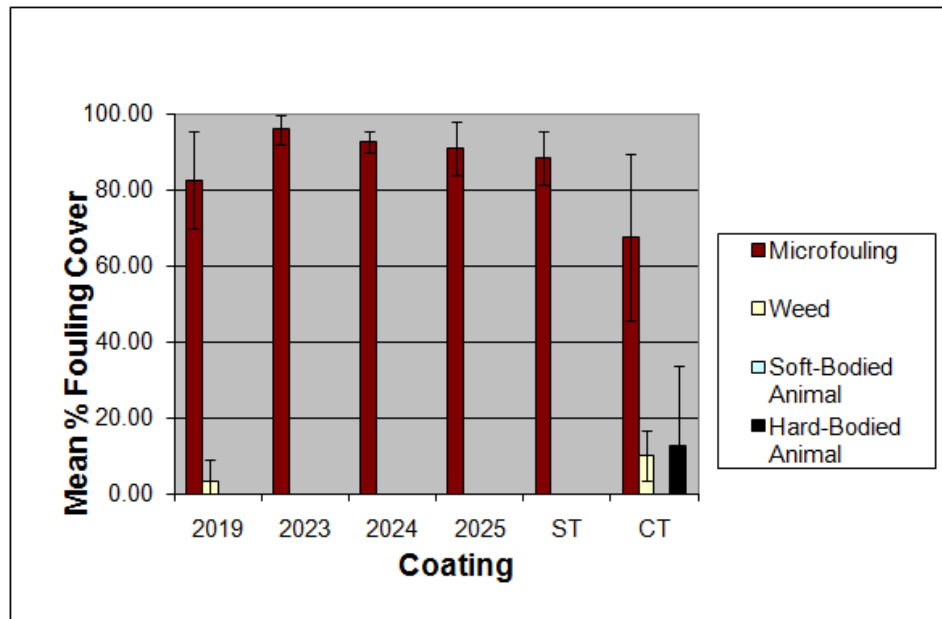


Figure 3:32: Test BMA paints antifouling results. Paint 2019 is MESQ(I)v25 and 2023, 2024 and 2025 are MESQ(I)25v5, 6 and 7 respectively after 53 weeks immersion.

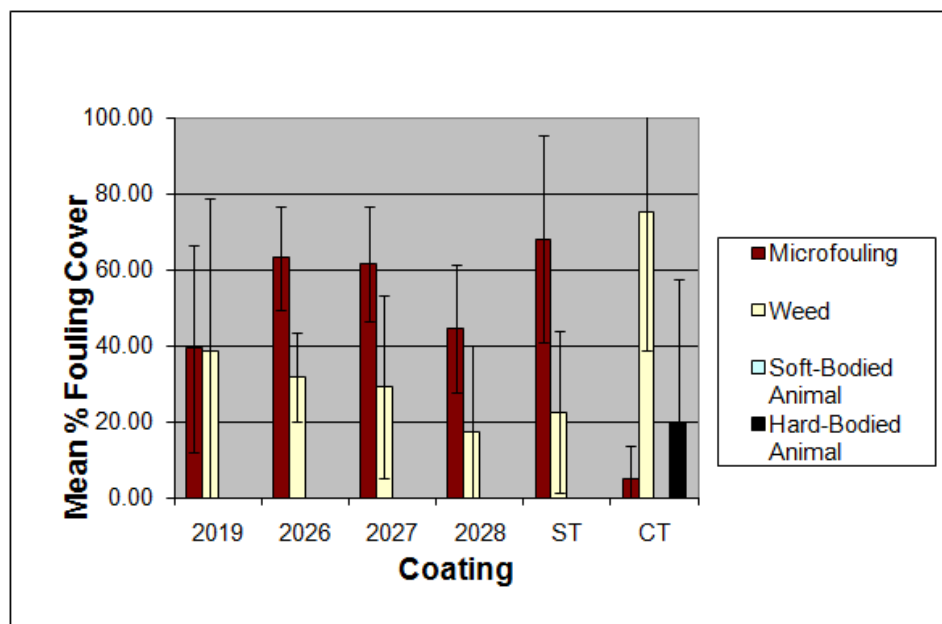
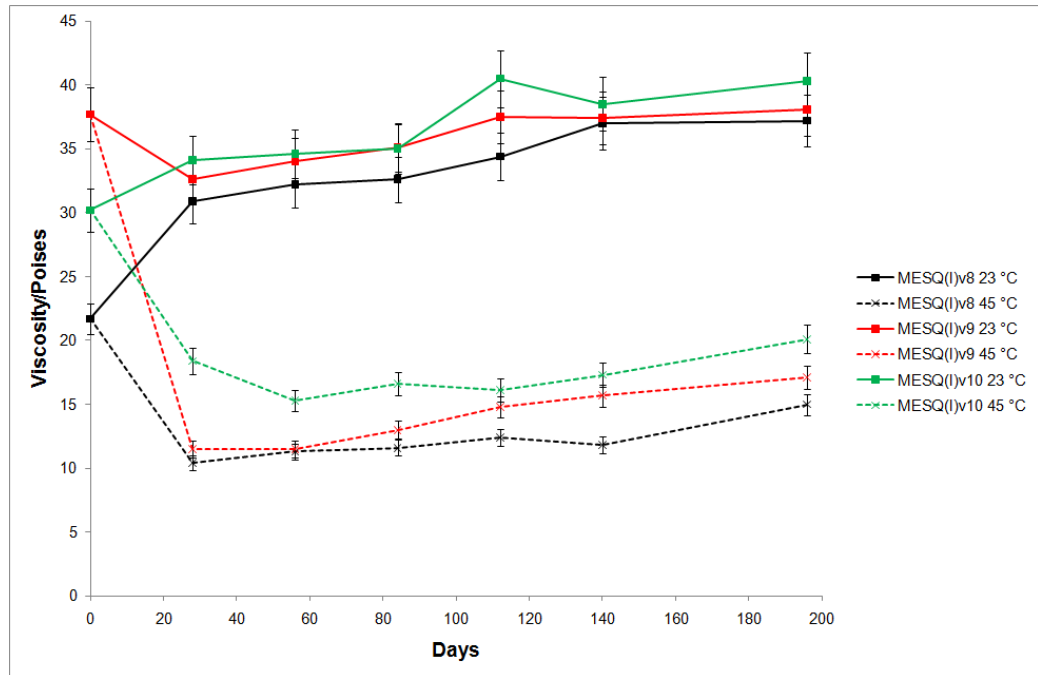


Figure 3:33: Test LMA paints antifouling results. Paint 2019 is MESQ(I)v25 and 2026, 2027 and 2028 are MESQ(I)25v8, 9 and 10 respectively after 53 weeks immersion.

### 3.7.4 Storage Stability

While on storage the new paints showed the same changes in viscosity and grind as demonstrated by the first generation of paints (see section 3.3.4, **Figure 3:15**), as exemplified by the LMA (3-8) containing coatings, **Figure 3:34**. This dramatic change in viscosity particularly at higher temperatures was very significant. This result highlighted that the paint formulations were unstable. This instability could be symptomatic of a chemical reaction causing degradation of the polymers. It was envisaged that degradation products could be interacting with other paint components, resulting in the growth of new particulates manifested by the increased grind.



**Figure 3:34:** Chart showing the temperature dependence of the change in viscosity of the LMA.

The new particulate material was manually extracted from the dried paint film, and divided using a scalpel, so that their cores could be analysed. Infrared (IR) microscopy analysis of the cores of the particles revealed that it was chemically distinct from the paint matrix, **Figure 3:35**. The spectra demonstrated that there were a number of differences between the paint matrix and that of the particulates, namely the changes in intensity of the transmitted IR energy at 1450 and 900-800  $\text{cm}^{-1}$ . These changes were indicative of a significant chemical change creating the particulate material.

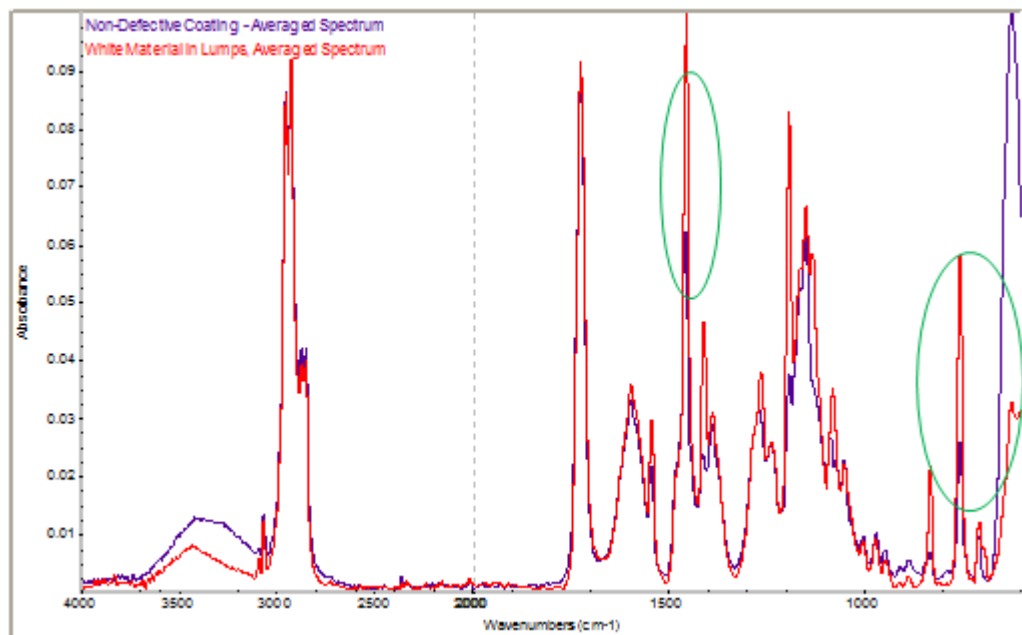


**Figure 3:35:** IR spectra of the new particulate material in the paint (red) and the spectra of the non defective coating (blue). Ovals indicate significant differences between the two IR spectra at 1450 and 900-800  $\text{cm}^{-1}$ .

Generation of the IR spectra of the particulates without interference from the paint matrix, was achieved by subtracting the spectra of the paint matrix from the spectra of the particulates. This calculated spectrum highlighted regions in which there were changes in intensity of the transmitted IR energy. Comparisons of the calculated spectrum with those of the raw materials present in the paint, suggested that the composition of the particulates was associated with copper pyrrhione (**1-2**). However, there were a number of differences between the two spectra, namely the difference in adsorbance ( $\sim 1150 - 1100 \text{ cm}^{-1}$ ) and small shifts in the wave numbers of others ( $\sim 1450 - 1400 \text{ cm}^{-1}$ ) which suggested the chemical nature of the particulates was chemically related to, but not identical to copper pyrrhione (**1-2**), **Figure 3:36**.

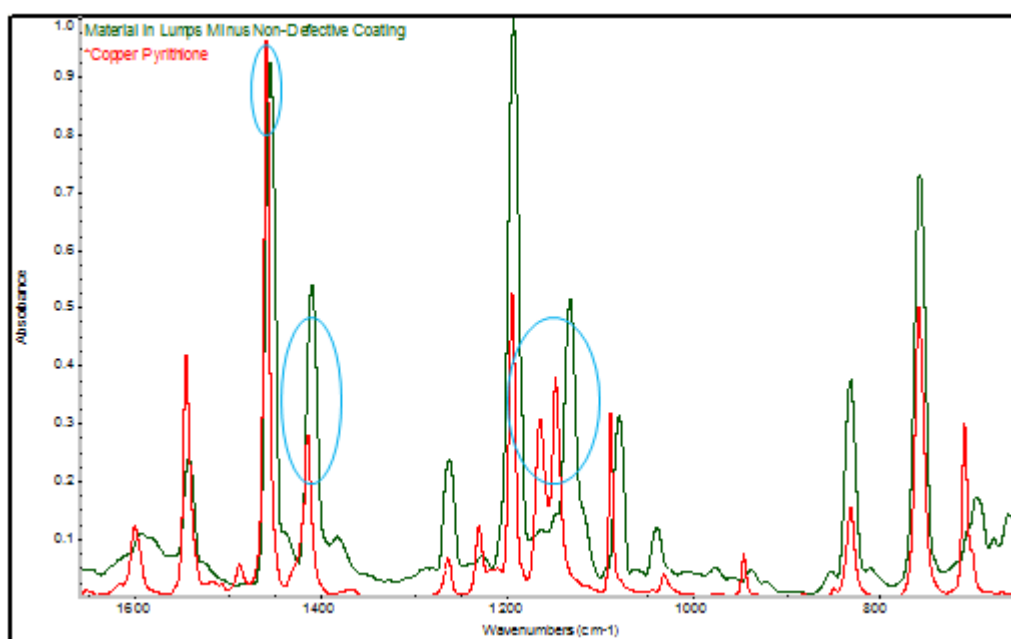


**Figure 3:36: Comparison between the calculated spectra of the 'lumps' (green) and that of copper pyrrhione (1-2) (red). Ovals indicate significant differences between the two IR spectra at  $1450-1400$  and  $1150-1100 \text{ cm}^{-1}$ .**

It was conceived that the middle ester functionality of the MES (**3-1**) maybe susceptible to a transesterification reaction with either water or alcoholic solvents, which could provide a potential mechanism for the storage instability, **Figure 3:37**.

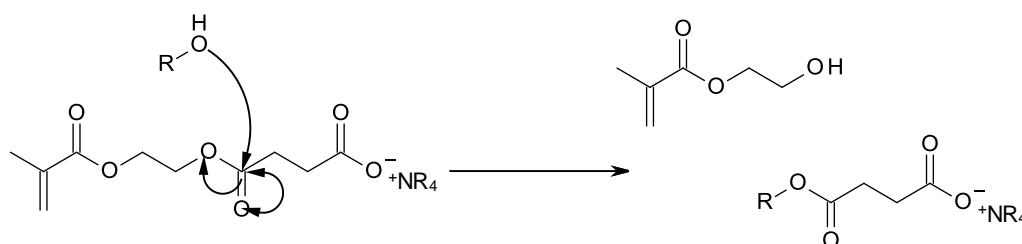


**Figure 3:37: Cleavage of MESQ through transesterification**

To evaluate whether transesterification of the ester linkage of MES (**3-1**) was the source of the storage instability, a freshly prepared MESQ(I) monomer (**3-3**) was placed on storage at 5, 23 and 45 °C in four different solvents and checked regularly by NMR. The four solvents were methanol, n-butanol, t-butanol and xylene, which varied the steric size of the nucleophilic alcohol with xylene as a non-nucleophilic control. Although the instability had been evident in the polymers, it was hoped that experimentation with the monomer would provide a simpler study and hence evidence for the likelihood of the transesterification reaction. It rapidly became apparent that all the alcoholic solvents resulted in the breakdown of MESQ(I) monomer (**3-3**) especially at 45 °C with the most aggressive being methanol and the least t-butanol conforming with the increase in steric hindrance from methanol to t-butanol. However, even the control, xylene, displayed significant degradation, **Figure 3:38**.

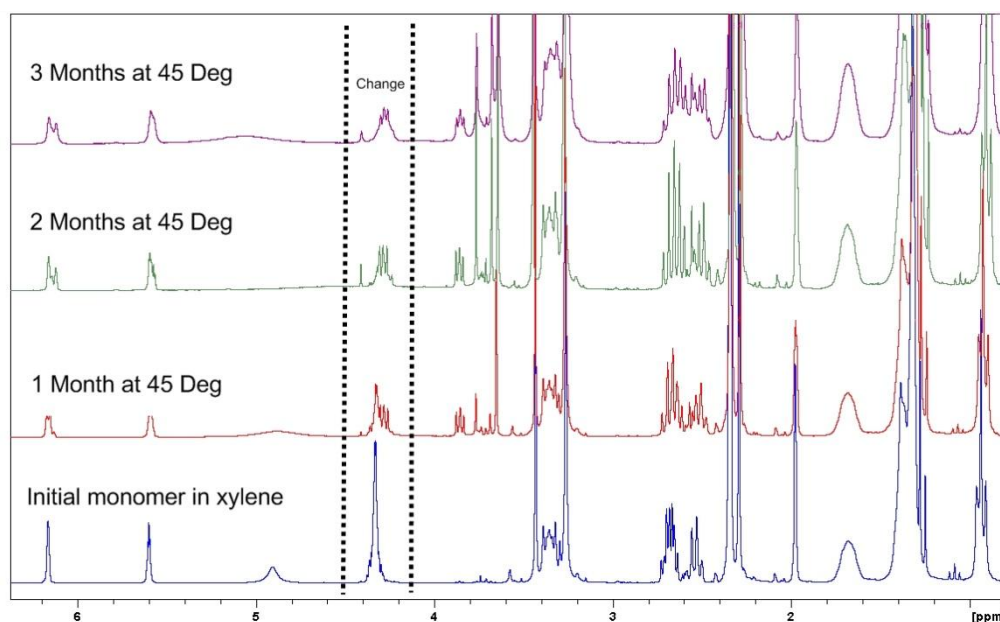


**Figure 3:38:**  $^1\text{H}$  NMR displaying the degradation of the MESQ(I) monomer (**3-3**) overtime

Given that the paints were all xylene only formulations, it is likely that this degradation is the cause of the instability. A re-evaluation of the preparation of the monomer highlighted that there was a percentage of residual methanol still present, which could not be removed, and was carried forward into the polymer preparation. This methanolic by-product, is believed to be the source of the degradation of the quat-monomer and the test paints.

### 3.8 Conclusions

The hydrophilic nature of MES (**3-1**) compared to other acid functionalized monomers might account for the poor mechanical performance of the first generation test polymers and paints manifested by cracking on immersion of the clear polymers, the poor semi-rapid performance of the paints and inconclusive polishing data. This increased hydrophilicity would be further

exacerbated during the sodium-monomer salt formation during the ion exchange reaction, resulting in polymers which would be susceptible to water ingress causing swelling of the polymers. This swelling would adversely affect the mechanical properties of the coatings and likely cause the film thickness increases during the polishing rates trials. It would also increase the internal film stresses resulting in the poor results observed during the semi rapid boot top testing. Conversely, large percentages of iBoMA (**3-5**) within the polymers would result in brittle polymers which would be susceptible to cracking. The increase in grind during storage further points to polymer instability.

The incorporation of a third co-monomer can clearly be seen to have improved the mechanical properties of the polymers, as demonstrated by the semi rapid boot-top cycling test after 12 cycles; where a number of coatings were still performing comparably with the pass standard, which was a two fold increase on the number of cycles from the first generation of polymers. However the persistent nature of the poor storage stability and subsequent discovery of its degradation mechanism generates significant concerns over the suitability of MES (**3-1**) as a framework monomer. Although the improvements in antifouling activity for the second generation of coatings was not as marked as for their mechanical properties, there was sufficient evidence to conclude that quat-polymers do possess sufficient antifouling properties. The poorly differentiated performance between the first and second generation coatings may, in part, be due to four months between initial manufacture of the polymers and subsequent application of the paint to the immersion boards. During this period the polymers were subjected to the transesterification reaction cleaving the quat containing functionality from the polymer and hence severely curtailing their antifouling performance.

There were a number of solutions to the storage stability issues of the MESQ polymers each with their own ease of implementation. Firstly, a more rigorous monomer purification step to remove the methanolic by-product might result in a more stable polymer. However given that the monomer preparation already extensively used evaporative distillation, it was likely that only a minimal benefit could be achieved by further heating. Additionally since the monomer instability was shown to be caused by alcoholic solvent, it was also likely that it could be caused by water. Therefore the paints were likely to be moisture sensitive which would require extensive formulation modifications, such as additional moisture scavengers, to regulate the instability. To do this would require prolonged product development and was beyond the scope of this thesis. A more succinct solution was to find an alternative framework acid functionalized monomer which did not have the problematic ester functionality. This is explored in Chapter 4 using the monomer, 2-acrylamido-2-methyl-1-propanesulfonic acid (AMPS, **3-2**).

## 4 Sequential Preparation of Monomer then Polymer 2

The previous elucidated work, whilst appearing to indicate that quats showed an enhanced antifouling effect, the ability to draw definitive conclusions was hampered due to a number of fundamental failings. First, the coatings produced via the post-quaternisation route were too soft to enable full evaluation, specifically via the polishing rate assay. Attempts to remedy this resulted in the alternative route to quat-polymers, synthesised by the sequential preparation of monomer then polymerisation using MES (**3-1**). Unfortunately the quat-monomers, MESQ(I) (**3-3**) and MESQ(II) (**3-4**), and their final polymers, were unstable because of the reaction of the central ester functionality of MES (**3-1**) with methanol produced as a by-product during the quaternisation of the MES monomer. Therefore the use of a new monomer in which the problematic ester-functionality was absent, such as AMPS (**3-2**), could produce quat-polymers which were significantly more stable enabling the suitability of quats as antifoulants to be conclusively determined.

The previously attempted routes to quat-polymers used a linear iterative polymer synthesis process to try to identify the ‘ideal’ polymer candidate. This required the synthesis of a small number of polymers which were anticipated to establish the boundary conditions of the polymer composition, from which a ‘trial and error’ iterative process of polymer synthesis would ultimately identify the ‘ideal’ candidate. Unfortunately the initial choice of framework polymer ultimately proved incorrect and the ‘trial and error’ process was never fully implemented. This iterative process while requiring a minimum initial experimentation could ultimately result in an excessive number of total polymers being synthesised, especially during the iterative phase. The success and swiftness of the whole process therefore ultimately depends upon the identification of the right initial boundary conditions. A more structured approach was employed with the AMPS (**3-2**) systems which used experimental design software. This software was ideally suited to devising experiments from which complex interactions of multiple components can be deconvoluted and modelled, i.e. such as the effect of three different monomers on the properties of polymers. This approach differed from that previously attempted as it required a greater amount of initial experimentation to define the boundary conditions, with the trade off that it enabled the effects of the different monomers to be modelled. This modelled system could then be used to predict subsequent likely ‘ideal’ candidate polymer compositions for testing. This approach was anticipated to reduce the total number of synthesised polymers with the additional benefit that the ‘ideal’ candidate could be more rapidly identified.

## 4.1 Monomer Synthesis

The quat-functionalized monomers were synthesised by quaternisation of AMPS (**3-2**) in an analogous reaction to that used to create MESQ(I) (**3-3**) and MESQ(II) (**3-4**). Similarly the resulting monomers were named AMPSQ(I) (**4-1**) and AMPSQ(II) (**4-2**) containing the biocidal didecyltrimethylammonium cation and non-biocidal trioctylmethylammonium cation respectively, **Figure 4:1**. The quat salts of AMPS were prepared via the synthesis of the correct quat methylcarbonate which was then reacted with AMPS (**3-2**) to create the final quaternised AMPS (**3-2**) species.

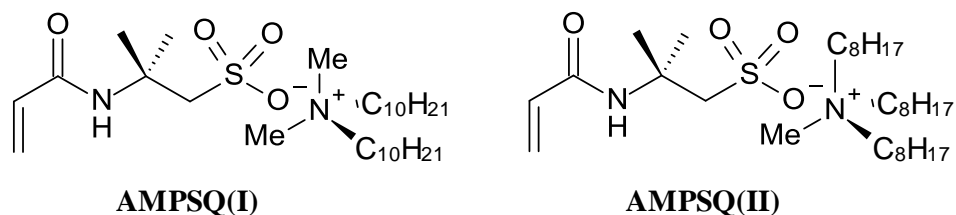
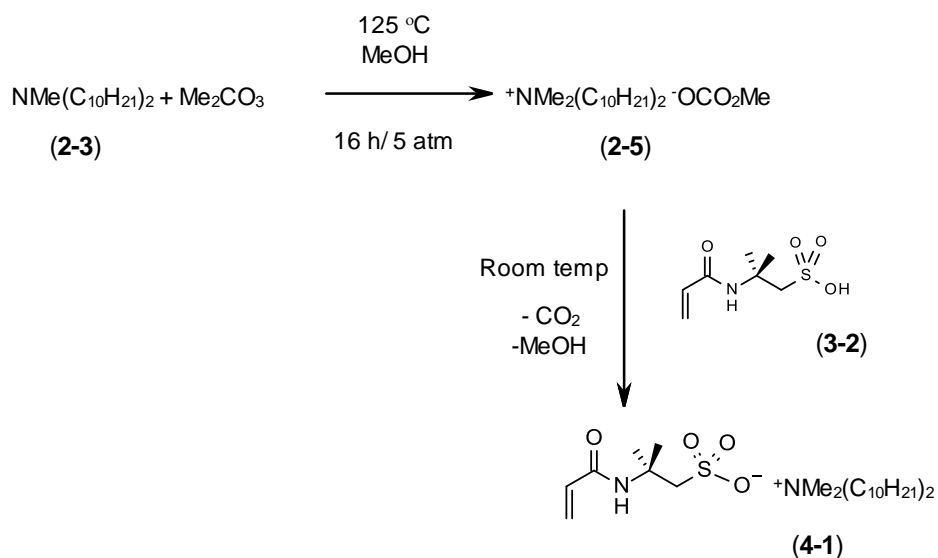


**Figure 4:1: Structures of biocidal AMPSQ(I) (4-1) and non-biocidal AMPSQ(II) (4-2) monomers**

Both didecyltrimethylammonium methylcarbonate (**2-5**) and trioctylmethylammonium methylcarbonate (**2-6**) were prepared as previously described without any alteration to the previously detailed methodology. AMPSQ(I) (**4-1**) and AMPSQ(II) (**4-2**) were synthesised by reaction of the quat methylcarbonates and AMPS (**3-2**) in methanol after 12 hours continuous stirring. The final quat-monomer was then isolated from the reaction liquor by evaporative distillation to remove the methanol, **Scheme 4:1**. Prior to further synthesis these compounds were dissolved in 200 g of the polymerisation solvent.



**Scheme 4:1: Two step synthetic sequence for the preparation of didecyltrimethylammonium quat-monomer-AMPSQ(I) (4-1)**

The success of the reaction was confirmed prior to the addition of 200 g of solvent for polymerisation. This was achieved firstly by observation of the evolution of carbon dioxide during synthesis and secondly, by  $^1\text{H}$  NMR post synthesis, which exhibited signals for both AMPS (**3-2**) and the relevant quat cation with the correct relative integrals. No signal was observed which for the methylcarbonate anion as the corresponding singlet was absent from the signal at  $\delta$  3.38 (m, 4H), post reaction. Of particular note was the change in shift of the methyl protons adjacent to the amide groups of AMPS (**3-2**),  $\delta$  1.37 (s, 6H), which changed their environments following the formation of the quat-monomer, AMPSQ(I), and the signals were now superimposed on the signal of the  $\beta$ -methylene protons of the quat alkyl chain forming a coincident signal,  $\delta$  1.65 (m, 10H). Also the integration per proton was the same for both the quat cation and AMPS (**3-2**) protons confirming a 1:1 reaction, **Figure 4:2**.

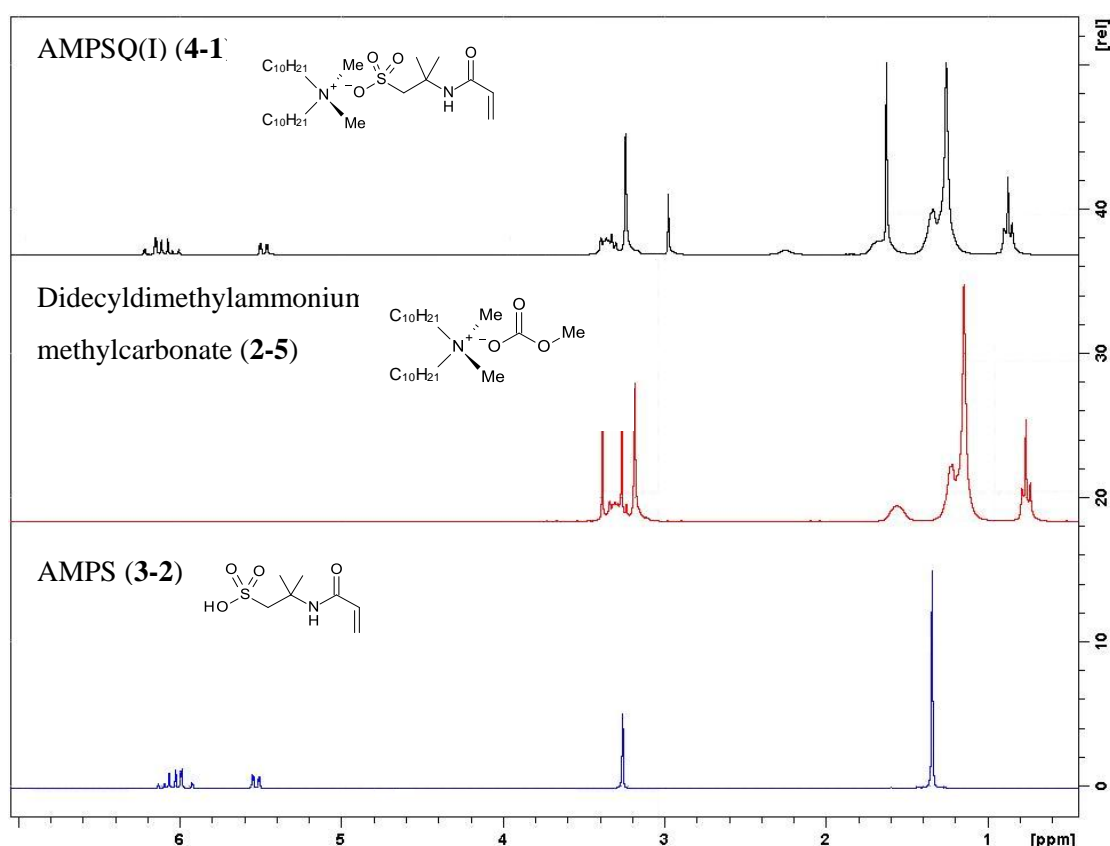


**Figure 4:2:** i)  $^1\text{H}$  NMR of final didecyldimethyl quat-monomer (black) (4-1) and its starting materials ii) didecyldimethyl quat-methylcarbonate (red) (2-5) and iii) AMPS acid (blue) (3-2)

## 4.2 Polymer Syntheses

The AMPSQ polymers contained three monomers for the reasons established in Chapter 3. The monomers were: a functional monomer which contained the quat moiety, a film forming monomer which created the polymer film and a third co-monomer to help modify the properties of the final polymer film. The functional monomer was AMPSQ(I) (**4-1**), the film forming monomer was isobornyl methacrylate (iBoMA, **3-5**) and the third co-monomer was butyl methacrylate (BMA, **3-**

7). AMPSQ(I) was presumed to be very hydrophilic with amide, sulphonate and quat functionalities within the monomer, conversely iBoMA and BMA tend towards hydrophobicity. Experimental design software package, Design Expert®, was used to create an initial set of 12 polymer formulations, including two replicates, which were distributed over an experimental design space, **Figure 4:3**. This design enabled first and second order interactions of the monomers to be identified. The initial polymer compositions were bounded such that the AMPSQ monomer was in the range 25 – 35 mol%, iBoMA (3-5) was 65 – 75 mol% and BMA (3-7) was 0 – 10 mol%, **Table 4:1**. These limits were created by drawing comparisons with monomer compositions established in similar SPC polymeric systems<sup>183, 184</sup>. The polymers were named AMPSQ(I)v1-12 for the biocidal didecyl-quat containing polymer. A non-biocidal matched polymer was also synthesised containing the non-biocidal AMPSQ(II) monomer (4-2) 28.3 mol%, iBoMA (3-5) 68.3 mol% and BMA (3-7) 6.4 mol%. This was named AMPSQ(II)v4, **Table 4:1**.

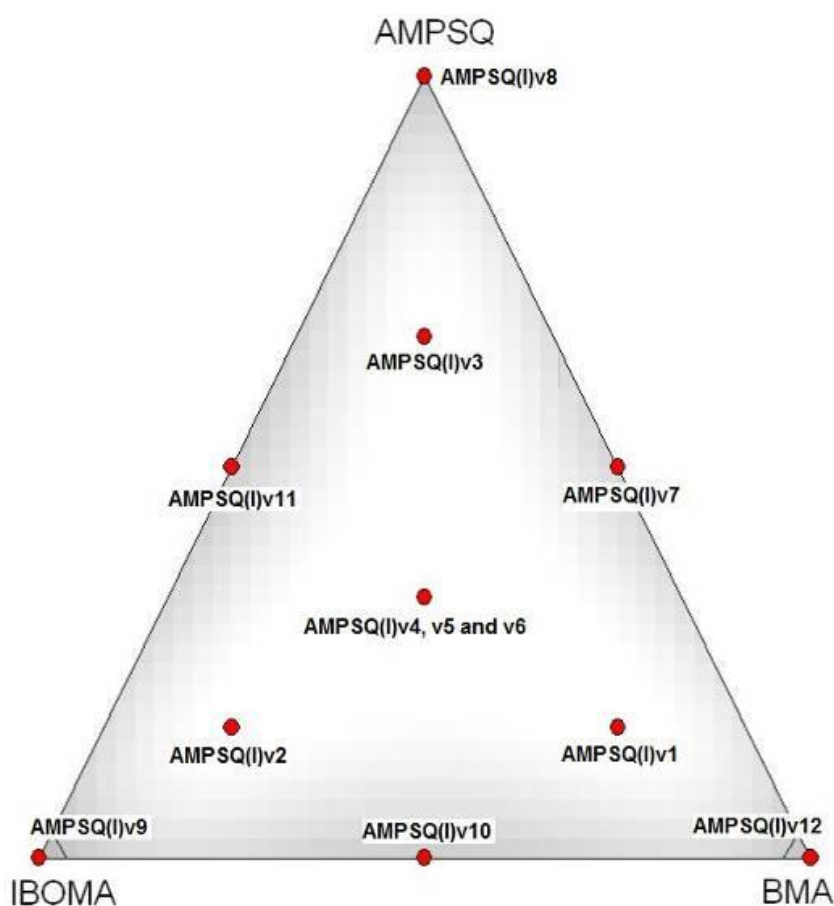


**Figure 4:3: Experimental design triangle of AMPSQ(I) polymers**

<i>Polymer Name</i>	<i>Monomer Composition (mol%)</i>			
	<i>AMPSQ(I)</i>	<i>AMPSQ(II)</i>	<i>iBoMA</i>	<i>BMA</i>
<i>AMPSQ(I)v1</i>	26.3	-	66.7	7.0
<i>AMPSQ(I)v2</i>	26.3	-	71.7	2.0
<i>AMPSQ(I)v3</i>	32.3	-	66.7	2.0
<i>AMPSQ(I)v4</i>	28.3	-	68.3	3.4
<i>AMPSQ(I)v5</i>	28.3	-	68.3	3.4
<i>AMPSQ(I)v6</i>	28.3	-	68.3	3.4
<i>AMPSQ(I)v7</i>	30.0	-	65.0	5.0
<i>AMPSQ(I)v8</i>	35.0	-	65.0	0.0
<i>AMPSQ(I)v9</i>	25.0	-	75.0	0.0
<i>AMPSQ(I)v10</i>	25.0	-	70.0	5.0
<i>AMPSQ(I)v11</i>	30.0	-	70.0	0.0
<i>AMPSQ(I)v12</i>	25.0	-	65.0	10.0
<i>AMPSQ(II)v4</i>	-	28.3	68.3	3.4

**Table 4:1: Table of AMPSQ Polymers and their monomer compositions**

The thirteen AMPSQ polymers were synthesised containing the monomer compositions as per **Table 4:1**. Those polymers containing AMPSQ(I) were biocidal with AMPSQ(II) polymers being the non-biocidal analogues. All the polymers were synthesised via the same free radical polymerisation reaction as elucidated in Chapter 3, with the minor modification being an alteration to the length of final boost from 30 to 120 mins. The polymerisation was performed at 85 °C with a 3.5 hour monomer feed upon completion of which the temperature was raised and maintained at 95 °C for a further 2 hours. At the start of the 2 hour period and again 1 hour later a 0.5 mol% initiator dissolved in 10 g of reaction solvent was added to the reaction. The final polymers were formulated to be 50 % solids in 3:1 xylene:butanol to create a simple polymeric solution, which could be incorporated in a prototype paint formulation. Each polymer was characterised in terms of <sup>1</sup>H NMR, **Figure 3:6**, viscosity, percentage non-volatile content (NVC), specific gravity (SG), total unreacted monomer molar percentage and unreacted monomer molar percentage, number average molecular weight ( $M_N$ ), weight average molecular weight ( $M_W$ ) and polymer polydispersity (data presented in the Experimental Chapter).

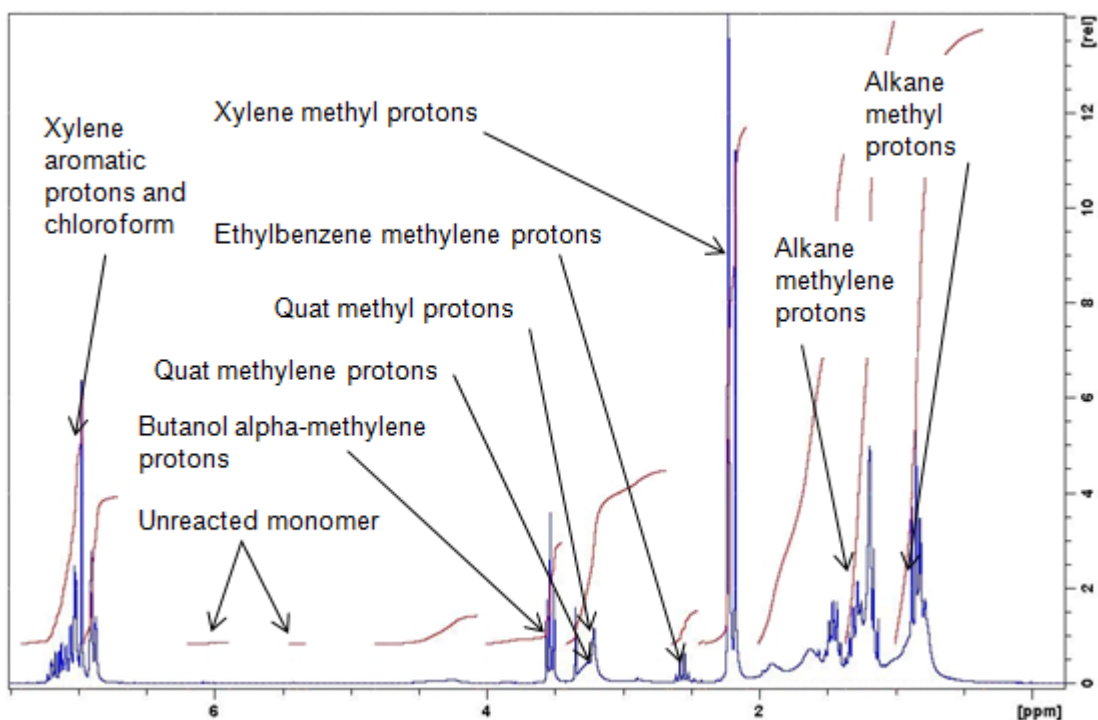


Figure 4:4: Example of  $^1\text{H}$  NMR of final quat-polymer solution in xylene:butanol 3:1, AMPSQ(I)v4

#### 4.2.1 Polymer Glass Transition Temperature Determination

Prior to the manufacture of the prototype paints the glass transition temperature ( $T_g$ ) of each polymer was determined in order to ensure that the subsequent coatings would be sufficiently mechanically robust to survive testing. The  $T_g$ s of the AMPSQ polymers as measured by DSC, **Table 4:2**, as per the method detailed in *Chapter 3, section 3.6*.

Polymer	Measured $T_g$ / °C
AMPSQ(I)v1	80
AMPSQ(I)v2	76
AMPSQ(I)v3	75
AMPSQ(I)v4	80
AMPSQ(I)v5	83
AMPSQ(I)v6	83
AMPSQ(I)v7	77
AMPSQ(I)v8	71
AMPSQ(I)v9	80
AMPSQ(I)v10	81
AMPSQ(I)v11	85
AMPSQ(I)v12	82
AMPSQ(II)v4	72

Table 4:2: Measured  $T_g$ s for the AMPSQ polymers

It was clear from these results that all the polymers had  $T_g$ s which were significantly above that of average seawater temperatures and therefore were all suitable for incorporation into the prototype paint formulation detailed in *Chapter 2, section 2.2*.

As the twelve AMPSQ(I) polymers only contained three monomers in varying proportions, only one of which had an unknown  $T_g$ , the  $T_g$ s of each of the twelve polymers were used to calculate the

unknown  $T_g$ , of the AMPSQ(I) (4-1) monomer via the modified Fox equation (see Chapter 3, section 3.5.1, Equation 3:2) and the published  $T_g$ s for the other component monomers<sup>180</sup>, Table 4:3.

Monomer	$T_g/K$
iBoMA (3-5)	383
BMA (3-7)	293

Table 4:3: Published  $T_g$  for co-monomers used in AMPSQ polymers<sup>180</sup>

The calculated  $T_g$  for the AMPSQ(I) homopolymer was 256.2 K. In order to validate this value the homopolymer was synthesised in an analogous method to that used to synthesise the twelve AMPSQ(I) polymers. The measured  $T_g$  for AMPSQ(I) homopolymer was 251.4 K. There was a good correlation between these two values especially considering the difficulties in correctly identifying the  $T_g$  for acrylic polymers when analysed by DSC, because the transitions can be diffuse due to their low change in energy at the transition temperature and the temperature range over which the transition occurs, circa 20 °C.

It was interesting that a minor alteration to the polymer, such as the substitution of the trioctyl-quat for a didecyl-quat, such as AMPSQ(I)v4 to AMPSQ(II)v4 suppressed the  $T_g$  of the polymer by 11.4 °C to 71.9 °C. This corresponded with the AMPSQ(II) homopolymer  $T_g$  being 34.7 K lower than that of the AMPSQ(I) homopolymer. The  $T_g$  reduction associated with the change in quat was anticipated, because the trioctyl-quat contained a greater proportion of alkyl groups, than the didecyl-quat and hence could internally plasticise the polymer to a greater extent.

#### 4.2.2 Polymer Free Surface Energy Determination

The hydrophobicities of the AMPSQ polymers have important consequences for the polishing characteristics of the prototype paints. The ability of the polymers to successfully react with the seawater is influenced by their hydrophilicity. Consequently the free surface energies of the polymer coatings were calculated in an attempt to quantify the hydrophobicity of the polymers. If the surface of the polymers were hydrophobic then the contact angle of a drop of water would be large, i.e. greater than 90 °, with corresponding low free surface energy. Conversely hydrophilicity would be indicated by smaller contact angles and higher surface energy.

Glass panels were coated with one of each of the AMPSQ polymers ensuring an unblemished surface and dried for 5 days in an environmental cabinet at 23 °C. The free surface energy of the coatings was determined by measurement of the angle subtended at the surface of the coating by droplets of either distilled water or diiodomethane, Figure 4:5. To ensure accuracy a Dataphysics GmbH OCA-35 automated instrument with SCA-20 software<sup>185</sup> was used to perform the contact angle measurements and calculation of the surface energy, using the Owens-Wendt-Rabel-Kaelble method, Table 4:4.

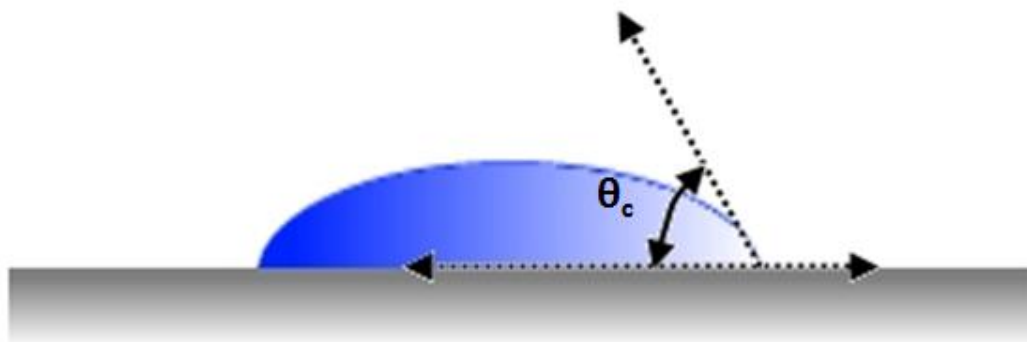


Figure 4:5: Schematic of a surface droplet and its contact angle

Polymer	AMPSQ (mol%)	Average Measured Surface Energy (mN/m)	Surface Energy Standard Deviation
AMPSQ(I)v1	26.3	38.51	0.78
AMPSQ(I)v2	26.3	41.45	0.28
AMPSQ(I)v3	32.3	41.16	0.69
AMPSQ(I)v4	28.3	41.12	0.65
AMPSQ(I)v5	28.3	39.52	0.26
AMPSQ(I)v6	28.3	38.69	0.65
AMPSQ(I)v7	30.0	42.75	0.55
AMPSQ(I)v8	35.0	40.43	0.32
AMPSQ(I)v9	25.0	42.34	0.21
AMPSQ(I)v10	25.0	40.57	1.23
AMPSQ(I)v11	30.0	41.87	0.90
AMPSQ(I)v12	25.0	38.21	0.24
AMPSQ(II)v4	28.3	38.76	0.52

Table 4:4: AMPSQ percentage and average surface energies (n = 6)

Under comparable test parameters published values for the free surface energy of hydrophobic (PTFE) and hydrophilic (Polyamide-6,6) polymers are of the order of 20.0<sup>186</sup> and 40.8<sup>187</sup> mN/m respectively. Therefore compared with these values the AMPSQ polymers were relatively hydrophilic, which was anticipated due to their sulphonate moieties. Unfortunately there appears to be no discernable correlation between the experimentally determined free surface energy (hydrophilicity) of the polymers and the proportion of the AMPSQ monomers within the polymers. There were a number of possible factor which could adversely affect the measurement of the surface free energy, especially by contact angle, which could account for the poor correlation. Contact angle measures have been shown to be sensitive to alterations in surface texture and roughness<sup>188, 189</sup>. Additionally it was possible that the droplets of the reagents (water and diiodomethane) used to determine the contact angle could interact with the coatings, especially water, changing the contact angle.

To further analyse trends in performance, a theoretical value for the hydrophilicity of each of the polymers was calculated. The calculation was based on the following assumptions:

1. The co-monomers used to synthesis the AMPSQ polymers were fully miscible
2. The hydrophilicity of the each co-monomer was additive

3. The hydrophilic contribution of each co-monomer to the final polymer's hydrophilicity was dependent upon that co-monomer's weight fraction, **Equation 4:1**.

The theoretical calculated hydrophilicity of the polymers used the log octanol-water partition coefficient ( $\log K_{ow}$ ) as a basis for hydrophilicity, which was derived using predictive algorithm ALOGPS from Virtual Computational Chemistry Laboratory<sup>190</sup> (VCCLAB), **Table 4:5**.

$$\log K_{ow,p} = \sum x_i \log K_{ow,i}$$

**Equation 4:1: Proposed equation to derive the theoretical hydrophilicity of a blended polymer ( $\log K_{ow,p}$ ), where  $x_i$  is the co-monomer's weight fraction within the polymer and ( $\log K_{ow,i}$ ) is the co-monomer's hydrophilicity**

Monomer	$\log K_{ow}$
AMPSQ	-0.97
iBOMA (3-5)	3.84
BMA (3-7)	2.50

**Table 4:5: Computationally derived  $\log K_{ow}$  of the co-monomers of the AMPSQ polymers**

The conclusions drawn from the theoretically derived value for the hydrophilicity of the AMPSQ(I) polymers, **Table 4:6**, were contradictory to those from the free surface energy measurements. The calculated  $\log K_{ow}$  values for the polymers were the same order of magnitude as hydrophobic molecular species and hence it appeared from this method that the polymers were hydrophobic. Given that 65 – 75 mol% of the constituent co-monomers within the polymers were relatively hydrophobic, it would appear logical that the polymers were classified as such. There was also no correlation between the theoretical values and the experimentally determined free surface energies, **Figure 4:6**. It was surprising that these two attempts to discriminate between the polymers, in terms of hydrophilicity, resulted in such starkly contrasting conclusions. Considering that the free surface energy measurements were experimentally determined and the validity of the theoretical method has yet to be established, it was deemed that the experimentally derived conclusion, namely that the polymers were hydrophilic, was more reliable.

Polymer	Derived ( $\log K_{ow,p}$ )
AMPSQ(I)v1	2.47
AMPSQ(I)v2	2.54
AMPSQ(I)v3	2.29
AMPSQ(I)v4	2.43
AMPSQ(I)v5	2.43
AMPSQ(I)v6	2.43
AMPSQ(I)v7	2.33
AMPSQ(I)v8	2.16
AMPSQ(I)v9	2.64
AMPSQ(I)v10	2.57
AMPSQ(I)v11	2.40
AMPSQ(I)v12	2.50

**Table 4:6: Theoretically derived  $\log K_{ow}$  for the AMPSQ(I) polymers**

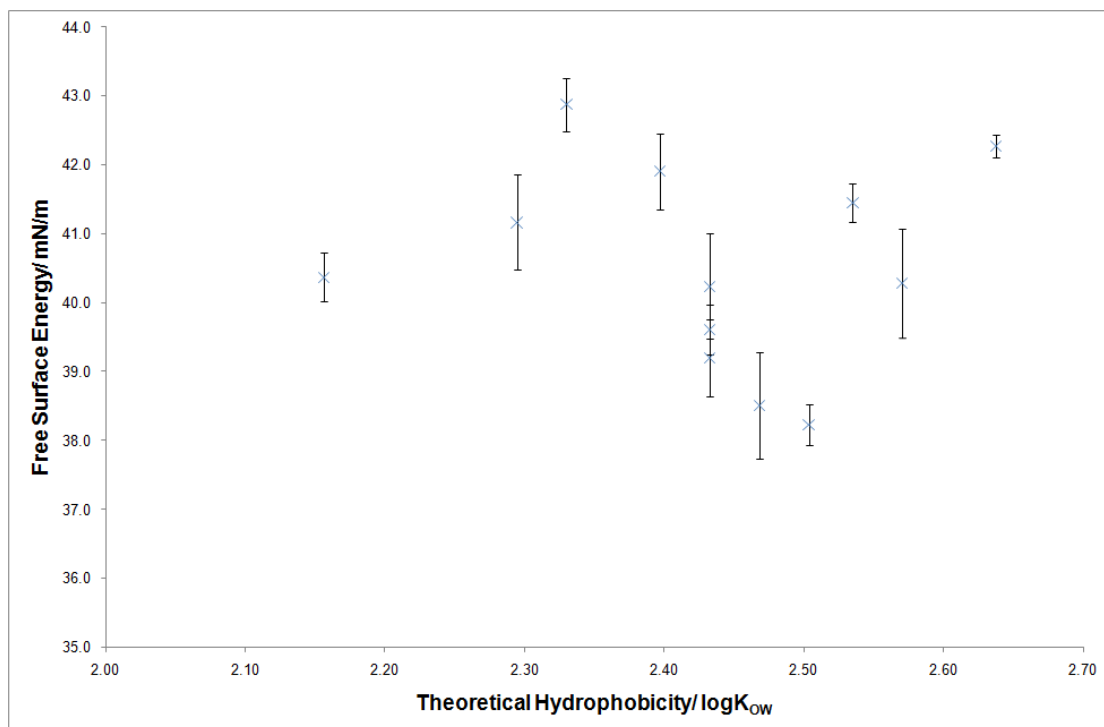


**Figure 4:6: Correlation between theoretical and experimental hydrophobicities of the AMPSQ(I) polymer**

### 4.3 Paint Formulation and Manufacture

Thirteen different paints, one per polymer, were prepared in an analogous fashion to those prepared to evaluate the experimental polymers in Chapters 2 and 3; i.e. systematic replacement of the binder of the prototype formulation with the synthesised polymers, ensuring that the test paints were equivalent in terms of volume solids and co-biocide content. These new test paints were named as per the test polymer used to prepare them.

The final paints were monitored for grind and viscosity (data presented in the Experimental Chapter).

### 4.4 Paint Testing

The coatings developed via this route were evaluated using the same test methods as previously used with the paints from previous chapters.

#### 4.4.1 Semi Rapid Boot-Top Cycling

The semi rapid boot-top cycling test was suspended after 12 cycles because sufficient differentiation between the coatings performance had been achieved, **Table 3:2**. At this stage only four coatings were rated 3 or more: AMPSQ(II)v4 and AMSQ(I)v1, v3 and v8, of which only AMPSQ(II)v4 and AMPSQ(I)v8 were still rated 5 (no visual deterioration).

The marked difference in performance between AMPSQ(II)v4 and the three replicate coatings AMPSQ(I)v4, v5 and v6 was consistent with the ability of the trioctyl-quat in AMPSQ(II)v4 to provide greater plasticisation than the didecyl-quat due to the additional alkyl chain of the quat. Increased internal plasticisation enhancing semi rapid performance also appeared consistent with the other successful coatings. AMPSQ(I)v8 and v3 which had the greatest mol% of AMPSQ(I) monomer (4-1) of all the polymer compositions (35 and 32.3 mol% respectively) and their corresponding performances were again consistent with the increasing internal plasticisation provided by the functional monomer. Furthermore the performance of AMPSQ(I)v9 was again consistent having the highest mol% of iBoMA (3-5) and lowest content of AMPSQ(I) (4-1) consequently failing after 7 cycles substantially earlier than all the other coatings.

PAINT	CYCLE											
	1	2	3	4	5	6	7	8	9	10	11	12
<i>Pass Std</i>	5	5	5	5	5	5	5	5	5	5	5	5
<i>Fail Std</i>	5	4	3	3	3	3	3	2	2	2	1	1
AMPSQ(I)v1	5	5	4	4	4	4	3	3	3	3	3	3
AMPSQ(I)v2	5	4	3	3	3	3	3	3	2	2	2	2
AMPSQ(I)v3	5	5	4	4	4	4	4	4	3	3	3	3
AMPSQ(I)v4	5	4	3	3	3	3	3	2	2	2	2	1
AMPSQ(I)v5	5	5	4	3	3	3	3	2	2	2	2	1
AMPSQ(I)v6	5	5	4	3	3	3	3	2	2	2	2	1
AMPSQ(I)v7	5	5	5	4	4	4	4	4	3	3	2	2
AMPSQ(I)v8	5	5	5	5	5	5	5	5	5	5	5	5
AMPSQ(I)v9	5	4	3	2	1	1	1	-	-	-	-	-
AMPSQ(I)v10	5	4	4	3	3	3	3	2	2	2	2	2
AMPSQ(I)v11	5	5	4	3	3	2	2	2	2	2	1	1
AMPSQ(I)v12	5	5	4	3	3	3	3	3	2	2	2	2
AMPSQ(II)v4	5	5	5	5	5	5	5	5	5	5	5	5

Table 4-7: Semi rapid boot-top results for AMPSQ coatings

#### 4.4.2 Polishing Rate Determination

It was anticipated that the polishing rate would be proportional to the percentage composition of the functional monomer in the polymer, AMPSQ(I) (4-1), because AMPSQ(I) participates in the ion exchange reaction that causes polishing. Therefore the daily polishing rate was calculated for different coatings which contained the AMPSQ(I) monomer (4-1) in varying proportions. The coatings were AMPSQ(I)v10, v3 and v8 which contained 25.0, 32.5 and 35.0 mol% of the AMPSQ(I) monomer (4-1) respectively, together with a polishing standard coating Interswift 655.

After eight days the polishing standard coating had the greatest polishing rate, 1.99  $\mu\text{m}/\text{day}$ , which was significantly faster than those for the AMPSQ(I) coatings, **Figure 4:7**. However the polishing rates of the AMPSQ(I) coatings were not consistent with the anticipated performance dictated by the polymer composition i.e. AMPSQ(I)v10, which contained the least functional monomer had the highest polishing rate, 0.96  $\mu\text{m}/\text{day}$ , which was faster than both AMPSQ(I)v3 and v8, both of which contained higher proportions of the functional monomer.

After 65 days the daily polishing rates for all the coatings were dramatically reduced to such an extent that the AMPSQ(I) coatings v3 and v8 displayed a significant rate of film thickness increase, manifested as negative polishing rates. The relative order of the polishing rates of the AMPSQ(I) coatings also changed compared to that established after eight days, which was now inversely proportional to the AMPSQ(I) monomer proportion. The same general trends were also evident after 130 days i.e. both AMPSQ(I)v3 and v8 showed a negative polishing rate but with lower magnitudes. AMPSQ(I)v10 displayed no change between 65 and 130 days having a daily polishing rate of zero. The large error bars of the standard coating at 130 days were a manifestation of some replicates of the coating displaying a rate of film thickness decrease, while others displayed a rate of film thickness increase (negative polishing rates), which resulted in a larger standard deviation than for the other coatings.

The film thickness increase of AMPSQ(I)v3 and v8 after 65 days was likely due to water adsorption into the coating film, resulting in swelling of the film. Swelling was likely to be controlled by the hydrophilicity of the coating which would primarily be associated with the percentage of AMPSQ(I) monomer (**4-1**) within the polymer, because this was the only hydrophilic monomer used. Consequently, there were a number of competing factors effecting the changes in film thickness. Namely changes in film thickness associated with the loss of solvent trapped within the dry paint film and the degree of water absorption and hydrophilicity of the coatings, which were both related to the proportion of the AMPSQ(I) monomer in the polymer. Therefore measurements of the polishing rate cannot be made, with confidence, without first deconvoluting the effect of the rate of swelling from the rate of polishing. It was assumed that the rate of solvent evaporation from the paint films was consistent between coatings due to their comparable paint formulations.

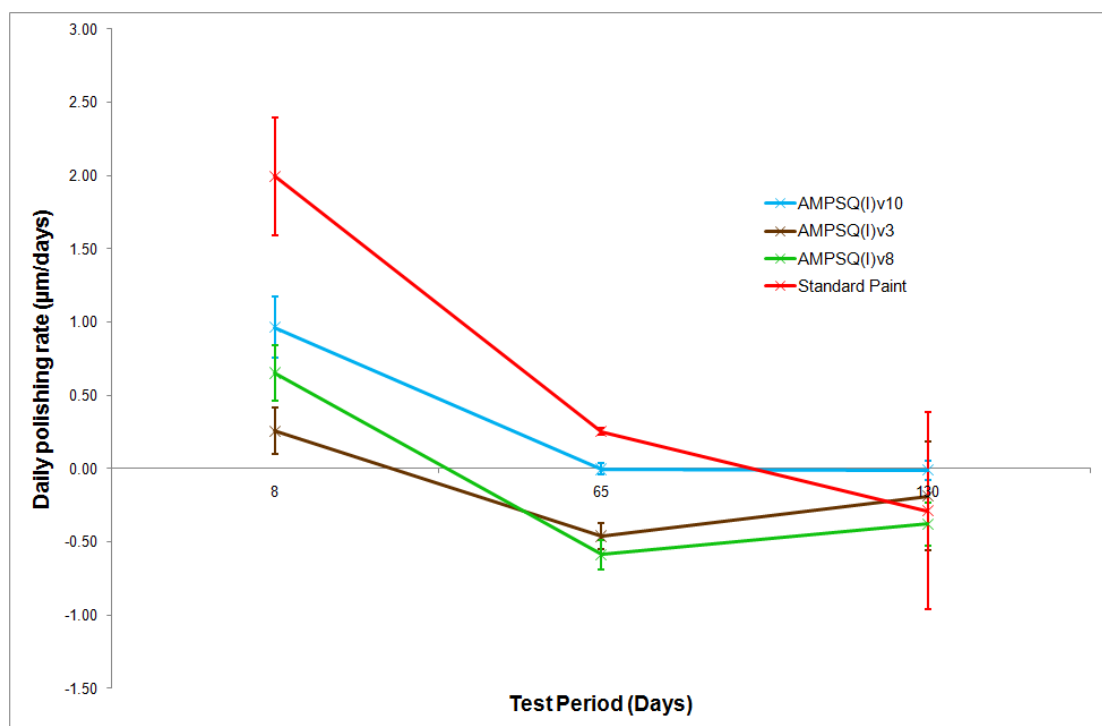


**Figure 4:7: Daily polishing rate of AMPSQ(I)v3, v8 and v10**

However, when the polishing rate data was analysed, taking into account film swelling there appeared to be a correlation with the percentage of AMPSQ(I) monomer. A number of factors needed to be considered to aid the understanding of the data. Firstly, a finite amount of water can be absorbed into the coating, after which the coating would become saturated and cannot absorb any more water. The degree of water adsorption was associated with the hydrophilicity of the polymer, which was related to the proportion of AMPSQ(I) monomer (4-1). Secondly the rate of polishing was also linked to the proportion of the hydrophilic monomer for the reasons stated above, and thirdly, the rate water of absorption was likely to be slower than the rate of polishing because the film was composed of predominately hydrophobic monomers, resulting in a latency to absorb water.

Therefore the experimental data for AMPSQ(I)v10 could be explained thus: AMPSQ(I)v10 which contained the least hydrophilic monomer, after eight days the rate of polishing was greater than the rate of swelling resulting in a net positive polishing rate. However by 65 days, and beyond, the rates of absorption and polishing have stabilised and were comparable resulting in a net negligible polishing rate. For AMPSQ(I)v8, which contained the most hydrophilic monomer, after eight days the polishing rate was faster than for AMPSQ(I)v10 but the swelling rate was also similarly enhanced, but not by the same extent. Therefore the net polishing rate was positive and appeared less than AMPSQ(I)v10 but faster than AMPSQ(I)v3, which had a smaller difference in rates hence the smaller net positive polishing rate. By 65 days the rates of swelling of both AMPSQ(I)v3 and v8 were greater than their polishing rates, resulting in net film thickness increases (negative

polishing rate). However by 130 days the rates of swelling reduced, probably due to the coating's saturation and hence there were apparent increases in the net polishing rate.

#### 4.4.2.1 Water Absorption

In an attempt to correlate the degree of water absorption and swelling of the AMSPQ(I) coatings 3 microscope slide per coating were coated with each of the AMPSQ(I)v1 – 12 and AMSQ(II)v4 paints. The paints were drawn down, using a 500  $\mu\text{m}$  application cube, to create a uniform dry film thickness. After 7 days drying at 23 °C in an environmental cabinet, the mass of dry paint was determined gravimetrically and its film thickness was measured by profilometry. The slides were then immersed in artificial seawater and the mass and film thickness was monitored twice over a 24 day period. Prior to monitoring the slides were dabbed dry with a cloth to remove surface water.

After 10 days immersion in the artificial seawater all the AMPSQ coatings displayed an increase in mass compared to that of the dry slide, **Table 4:8**. The increase in mass was attributed to absorption of water into the paint matrix, which was also corroborated by the increased film thickness. There appeared to be a good correlation between the change in paint film mass and the formulation of the AMPSQ polymer used as the binder within the paint. For example the paint/polymer which contained the highest amount of the hydrophilic AMPSQ(I) monomer (**4-1**) (AMPSQ(I)v8) displayed the greater increase in mass, while the coating with the greatest percentage of the hydrophobic monomer, iBoMA (**3-5**), had the lowest increase in mass. After 24 days immersion the difference between the recorded mass and the previously recorded mass after 10 days was all negative, i.e. the slides weighed less at 24 days. A positive change between measurements would have been indicative of the coatings continuing to absorb water. Therefore the negative change was taken as an indication that the paint films were now saturated.

The corresponding profilometry data all showed the expected increase in film thickness, however the data did not present the same trend, as was evident from the gravimetric data. Additionally there appeared to be no correlation between the increase in film thickness and increase in mass of the paint films. Interestingly the difference between the measured film thickness at 24 and 10 days displayed both positive and negative changes, which indicated that some films were increasing while others were decreasing. However, the gravimetric data demonstrated that between 24 and 10 days the coatings absorbed no further water. This therefore suggested there must be an additional mechanism/factor which affects the film thickness which was not accounted for by this rudimentary test. The ability for the binder of the paints to polish was not factored into this absorption test, because it was not obvious how to eliminate it without fundamentally altering the polymer/paint and hence influencing the integrity of the absorption test. The gravimetric data also did not account for the mass of any material which leached out of the coatings during immersion.

Another possibility was that there was latency in the thickening of the film post absorption of water, although the mechanism via which this could occur was not clear at this stage.

AMPSQ Coating	Average change in Mass (wt%)			Average change in Film Thickness ( $\mu\text{m}$ )		
	10 Days	24 Days	Difference between 24 and 10 days	10 Days	24 Days	Difference between 24 and 10 days
v1	3.56	3.54	-0.02	3.88	5.63	1.74
v2	3.59	3.42	-0.17	9.65	6.04	-3.61
v3	4.92	4.71	-0.20	13.16	14.22	1.06
v4	4.82	4.35	-0.47	11.38	13.20	1.82
v5	4.72	4.53	-0.19	10.08	12.16	2.09
v6	4.50	4.04	-0.47	8.17	11.71	3.54
v7	5.55	5.09	-0.46	11.28	10.33	-0.95
v8	6.31	5.96	-0.35	16.89	19.84	2.95
v9	2.91	2.81	-0.10	5.40	7.91	2.51
v10	3.40	3.18	-0.23	0.81	-0.57	-1.38
v11	5.08	4.25	-0.83	10.64	3.86	-6.78
v12	3.50	3.42	-0.07	11.70	11.25	-0.45
Q(II)v4	1.51	0.79	-0.72	5.46	4.47	-0.99

**Table 4:8: Gravimetric and Profilometry changes in AMPSQ coatings**

The ability of the painted slides to absorb water should be associated with the hydrophilicity of the coating. There was a range of chemicals with varying hydrophilicities which were incorporated into the paint formulation, not least being the AMPSQ polymeric binder. However only the polymeric binder was varied between each of the AMPSQ test paints, therefore it was anticipated that there should be a correlation between the hydrophilicity of the polymer and the gravimetric and profilometry data. Unfortunately there was no correlation between either the gravimetric and profilometry data when compared to the measured surface free energy of the coatings. However, when the gravimetric data was compared to the theoretically derived hydrophilicity of the coatings, there was a good correlation with an  $R^2$  greater than 0.9, **Figure 4:8**. A correlation between hydrophilicity and mass of water absorbed would be expected and in line with theory, i.e. the greater the degree the coating interacts with the water the more water that would be absorbed. Unfortunately there further work would be required to explore this apparent correlation.

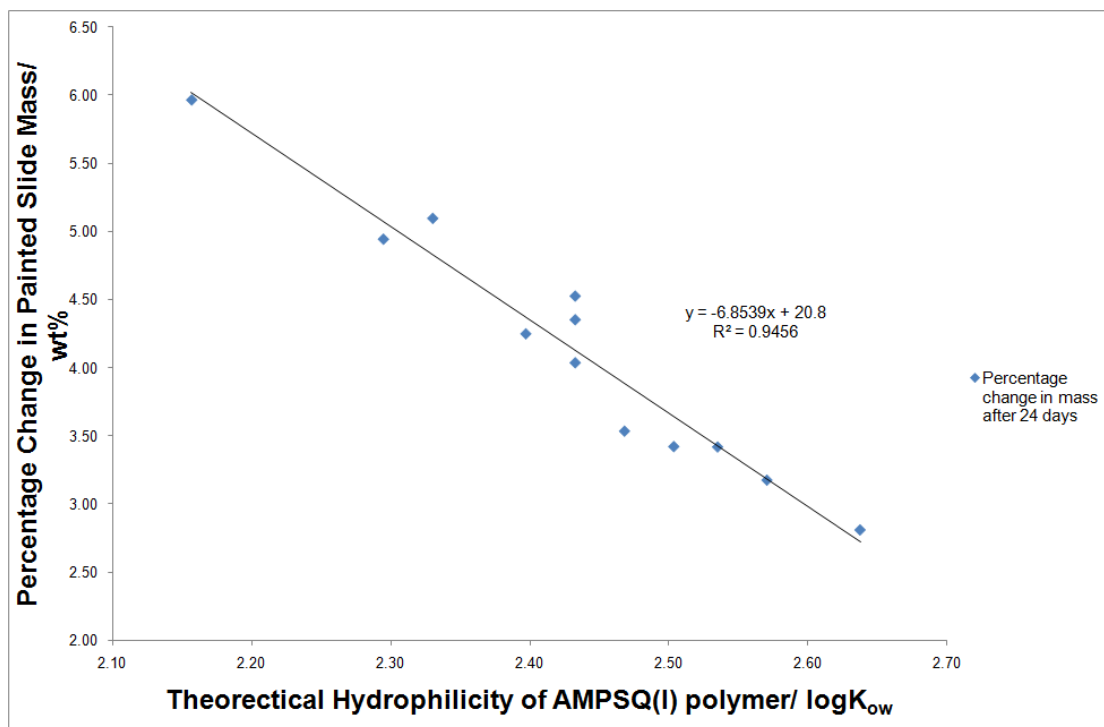
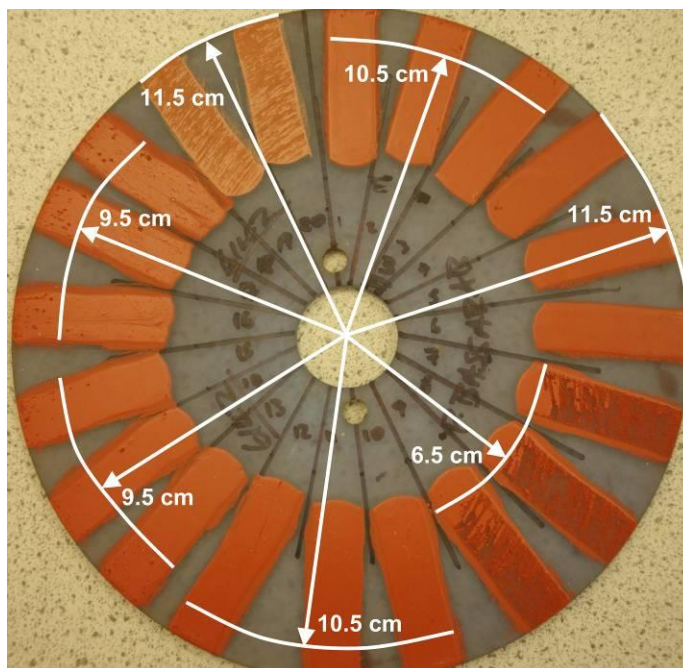


Figure 4:8: Correlation between changes in mass and hydrophilicity of AMPSQ(I) coatings

#### 4.4.2.2 Speed Threshold of Coating Defects

Following visual inspection of the polishing disks the degree of surface deformation which occurred during the polishing rate testing was not consistent across all the AMPSQ(I) paints. Some coatings were deformed to such an extent that no polishing data could be obtained, while for other coatings there was no deformation apparent, **Figure 4:9**. Since the polishing disks were of a known diameter and spun at a known constant rate, 750 rpm, the radius from the central axis of rotation to the surface deformation was used to calculate the speed threshold above which deformation occurred, **Table 4:9**. The calculated speeds were constrained because of the dimensions of the polishing disks. No results were possible past the radius of the disk giving an upper limit for speed, so coatings which displayed no apparent deformation were ascribed a speed of 32.3 Km/h, which corresponded with the speed of the edge of the polishing disk. Likewise it was not possible discern speed threshold below 14.1 Km/h because the coating strips did not extend to the centre of the disk.



**Figure 4:9: Picture of a polishing disk with varying surface deformations and their distances from the centre of the disk**

<i>Paint</i>	<i>Speed threshold (Km/h)</i>
AMPSQ(I)v1	29.5
AMPSQ(I)v2	32.3
AMPSQ(I)v3	18.2
AMPSQ(I)v4	26.7
AMPSQ(I)v5	26.7
AMPSQ(I)v6	26.7
AMPSQ(I)v7	16.8
AMPSQ(I)v8	15.4
AMPSQ(I)v9	32.3
AMPSQ(I)v10	32.3
AMPSQ(I)v11	26.7
AMPSQ(I)v12	28.1

**Table 4:9: Speed limit above which the test paints displayed surface defects**

The deformation of the paints was presumed to be caused by the coatings not being sufficiently robust to withstand the hydrodynamical shear during testing. Therefore it was likely that factors which affected the ‘hardness’ of the paints would influence the speed threshold. Although the determination of the speed threshold for the paints was crude, with the distances from the centre measured to the nearest 0.5 cm, there appeared to be apparent correlations with the theoretical  $T_g$ , percentage of AMPSQ(I) monomer (4-1) and the theoretical hydrophilicity of the polymers as well as the percentage change in mass of the paint films during immersion (water absorption), **Figure 4:10** and **Figure 4:11..** The degree of correlation ranged from  $R^2 = 0.76$  to 0.88, with the best correlation being with the theoretical hydrophilicity of the polymers. Again the validity of this correlation was uncertain but given this was second occurrence of a correlation for the theoretical hydrophilicities with a property derived from a physical characteristic of the paints, it seemed to suggest that there was some degree of validity in attempting correlations with a set of calculated

hydrophilicities. There was no correlation between the surface free energy of the polymers and the speed threshold of the corresponding paints.

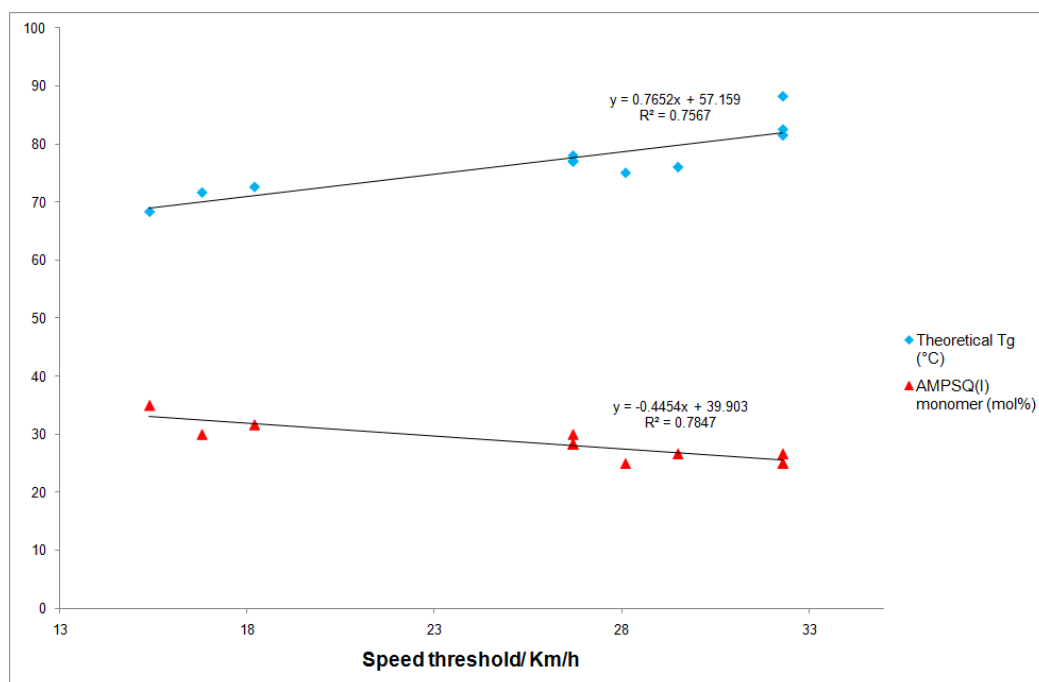


**Figure 4:10: Apparent correlation between the speed threshold of the AMPSQ(I) paints and the theoretical T<sub>g</sub> and percentage of AMPSQ(I) monomer**

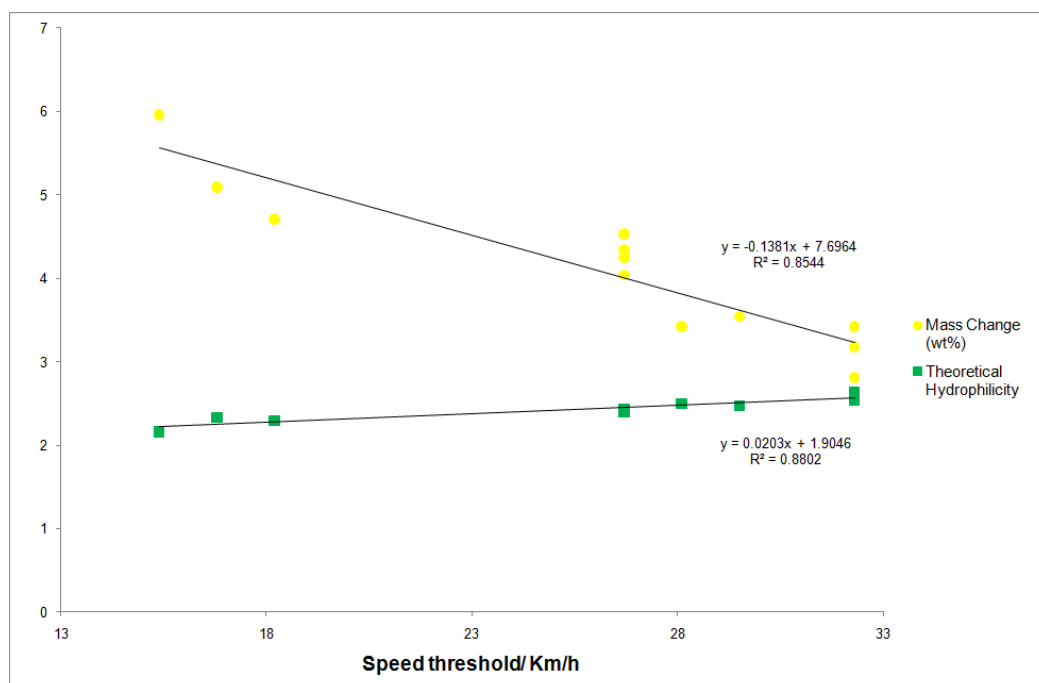


**Figure 4:11: Apparent correlation between the speed threshold of the AMPSQ(I) paints and the percentage mass of water absorbed and theoretical hydrophilicity**

### 4.4.3 Antifouling Performance

Analogous to the antifouling testing performed with the MESQ coatings (*see Chapter 3, section 3.4.3 and 3.7.4*), 6×6 Latin square antifouling boards were prepared with the AMPSQ coatings and immersed at Newton Ferrers. Clear coatings of the AMPSQ polymers were also tested in the analogous fashion but with the inclusion of a non-biocidal clear standard coating, AMPSQ(II)v4. Again, it was anticipated that the performance of these clears was unlikely to be as sustained as that for the formulated paints, but the clears would give an early indication of the underlying antifouling performance of the polymers and aid in differentiating the paint's properties.

#### 4.4.3.1 Clear Polymer Results

To assess whether the release of quats from antifouling coatings needed to be controlled, an additional clear coating was also included. This coating was based on the clear non-biocidal standard but with biocidal alkylbenzyltrimethylammonium (alkylbenzyl-quat) chloride mixed into the coating. The additional biocide was added such that in the dry modified AMPSQ(II)v4 polymer film the weight percentage of the biocide was matched to that of the biocide, didecyl-quat, in AMPSQ(I)v4. Ideally the same biocide would have been used to enable a direct comparison between polymers, but no suitable source of didecyltrimethylammonium halide was available at that time, therefore alkylbenzyl-quat was used as a surrogate.

The modified AMPSQ(II)v4 was anticipated to function through the same polishing mechanism as the other AMPSQ(I) coatings, releasing the quat through an ion exchange reaction, but in this case the non-biocidal trioctyl-quat. However, this coating would crucially synergistically release the biocidal alkylbenzyl-quat. The release of the alkylbenzyl-quat would be through simple dissolution of the biocide entrained within the polymer matrix, not an ion exchange reaction. Therefore the antifouling performance of the modified AMPSQ(II)v4 would only be as sustained as the release of the alkylbenzyl-quat.

In general after 8 weeks immersion all the AMPSQ(I) coatings were displaying better antifouling performance than that of the standard coating, AMPSQ(II)v4, **Figure 4:12**, **Figure 4:13**, **Figure 4:14** and **Figure 4:15**. This enhanced performance validated the previous assumption that the trioctyl-quat was less efficacious than the didecyl-quat. A number of coatings performance's were noteworthy at this early stage; AMPSQ(I)v3 and v8 (2666 and 2671 respectively, **Figure 4:12** and **Figure 4:14**) and the modified AMPSQ(II)v4 (2717), **Figure 4:13**.

The enhanced performance of these coatings conforms to the anticipated efficacy of the polymers. Both AMPSQ(I)v8 and v3 have the highest proportions of the biocidal monomer within their polymer compositions and hence would be expected to display an enhanced performance. The

enhanced performance displayed by the modified AMPSQ(II)v4 (2717) polymer, which had the same weight percentage of biocide as AMPSQ(I)v4, v5 and v6 (2667, 2668, 2669 respectively; all three replicates of the same polymer composition), **Figure 4:13**, possibly had two reasons: Namely the antifouling efficacy of the alkylbenzyl-quat was significantly greater than that of the didecyl-quat or the release rate of the alkylbenzyl-quat, which was not chemically bound into the polymer was faster than that of the didecyl-quat. In the latter case, the enhanced performance was unlikely to be sustained because the elevated release rate would quickly deplete the amount of alkylbenzyl-dimethylammonium halide within the polymer, curtailing the coatings performance. This was confirmed when the coatings were assessed after 14 weeks immersion. The performance of the modified AMPSQ(II)v4 had deteriorated to such an extent that it was now comparable to the unmodified non-biocidal AMPSQ(II)v4, **Figure 4:16**. This dramatic change in activity was akin to the performance that would be associated with a free association biocide, i.e. one that has a biocide physically dispersed within the coating matrix. For such a system the release profile of the biocide would be logarithmic (*see Chapter 1, section 1.1.4, Figure 1:4*). Conversely the enhanced performance of the other coatings, especially AMPSQ(I)v3 and v8, was maintained further suggesting that the early enhanced performance of the modified AMPSQ(II)v4 was due to an excessive release rate. This starkly demonstrated the need to control the release rate of quats in order to prolong their antifouling activity.

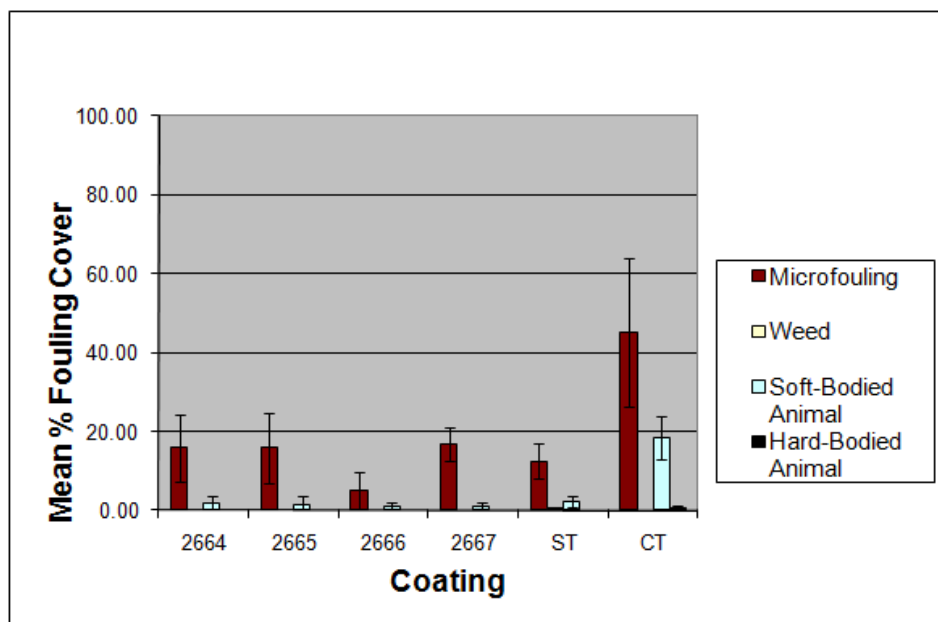


**Figure 4:12: Test Polymers antifouling results. Biocidal polymers 2664, 2665, 2666 and 2667 are AMPSQ(I)v1, v2, v3 and v4 respectively. Standard (ST) is non-biocidal polymers AMPSQ(II)v4 after 8 weeks immersion**

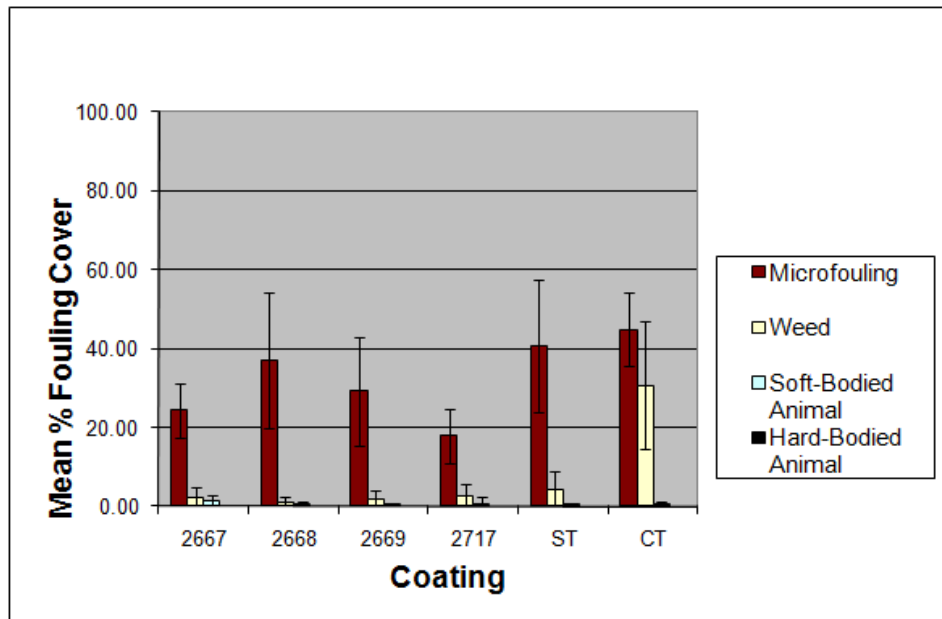


**Figure 4:13: Test Polymers antifouling results. Biocidal polymers 2667, 2668, 2669 and 2717 are AMPSQ(I)v4, v5, v6 and modified AMPSQ(II)V4 respectively. Standard (ST) is non-biocidal polymer AMPSQ(II)v4 after 8 weeks immersion**

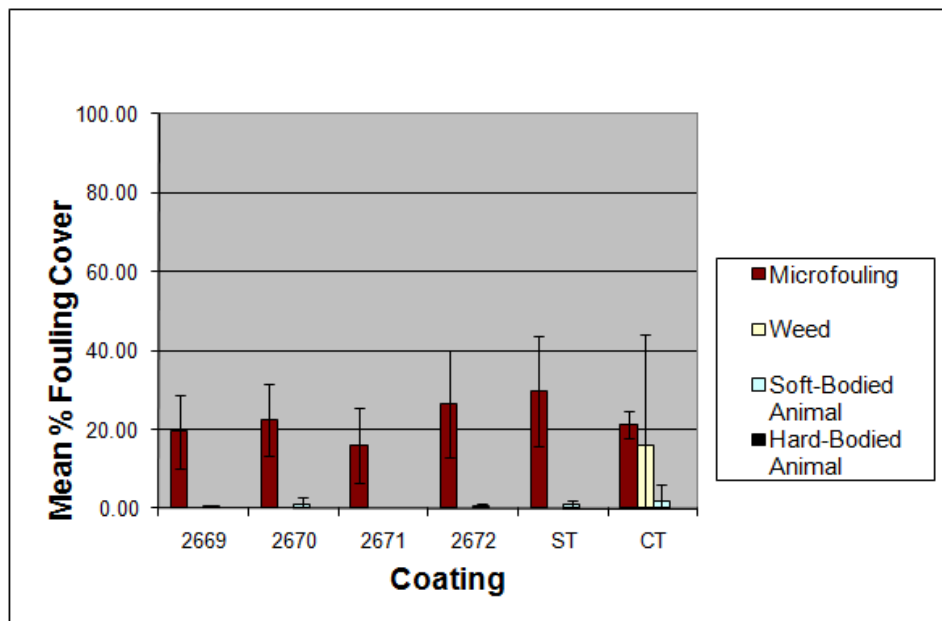


**Figure 4:14: Test Polymers antifouling results. Biocidal polymers 2669, 2670, 2671 and 2672 are AMPSQ(I)v6, v7, v8 and v9 respectively. Standard (ST) is non-biocidal polymer AMPSQ(II)v4 after 8 weeks immersion**

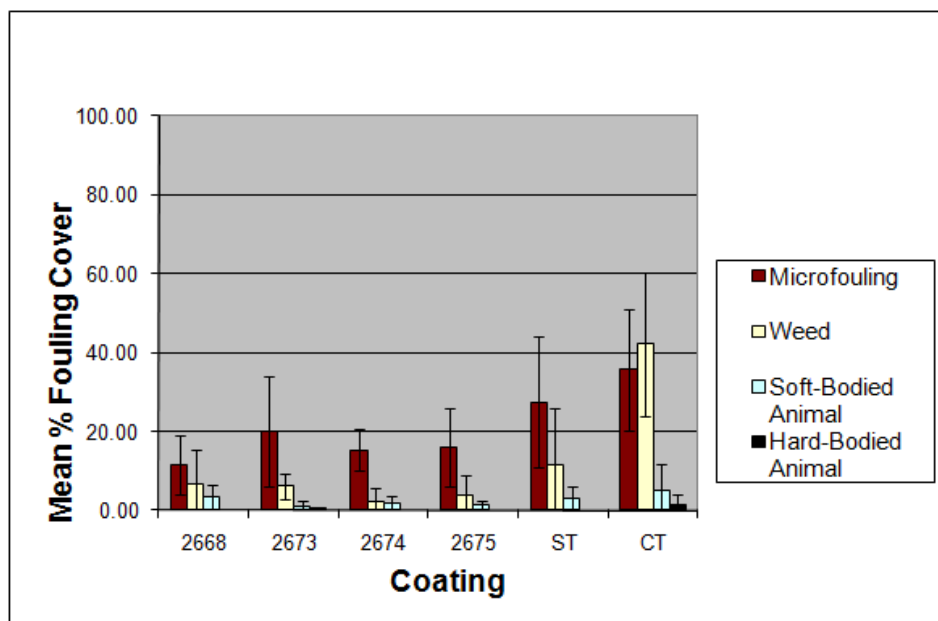


**Figure 4:15: Test Polymers antifouling results. Biocidal polymers 2668, 2673, 2674 and 2675 are AMPSQ(I)v5, v10, v11 and v12 respectively. Standard (ST) is non-biocidal polymer AMPSQ(II)v4 after 8 weeks immersion**

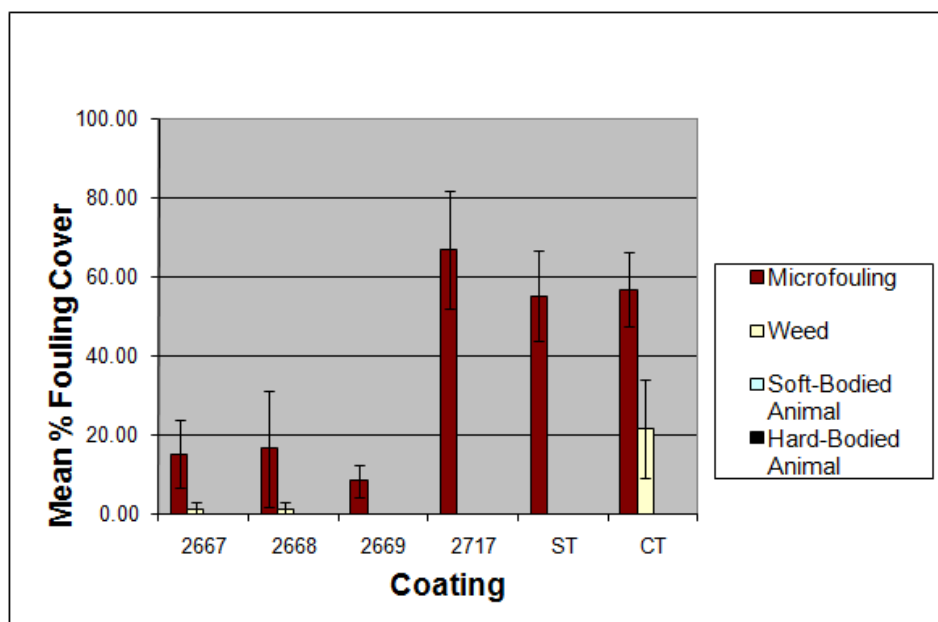


**Figure 4:16: Test Polymers antifouling results. Biocidal polymers 2667, 2668, 2669 and 2717 are AMPSQ(I)v4, v5, v6 and modified AMPSQ(II)V4 respectively. Standard (ST) is non-biocidal polymer AMPSQ(II)v4 after 14 weeks immersion**

In general after 14 weeks immersion the AMPSQ(I) polymer coatings were all displaying better performance than the standard, AMPSQ(II)v4. Of particular note were AMPSQ(I)v8, v7, v3 (2670, 2669 and 2666 respectively, **Figure 4:17** and **Figure 4:18**) and the triplicate coatings AMPSQ(I)v4, v5 and v6 (2667, 2668 and 2669 respectively, **Figure 4:16**). These coatings all contained greater than 28 mol% AMPSQ(I) monomer (4-1). The only other which contained greater than this level of monomer was AMPSQ(I)v11 (2674), **Figure 4:19**. Although this coating displayed good resistance to microfouling (red bar) there was an appreciable surface coverage of

weed fouling (yellow bar), which was absent from the polymers tested alongside it AMPSQ(I)v5, v10 and v12 (2668, 2673 and 2675 respectively) and in particular the non-biocidal standard. This was therefore taken as a sign that the performance of AMPSQ(I)v11 had diminished. This polymer had a significantly greater proportion of iBoMA (3-5), 30 mol%, compared to the other polymers with the greater than 28 mol% AMPSQ(I) (4-1). The hydrophobicity of iBoMA (3-5) might be such that after the ion exchange reaction to release the quat, the resultant sodium salt of the acid functional polymer was not sufficiently hydrophilic to be removed from the surface of the coating, which would negatively impact on the antifouling performance of the coating.

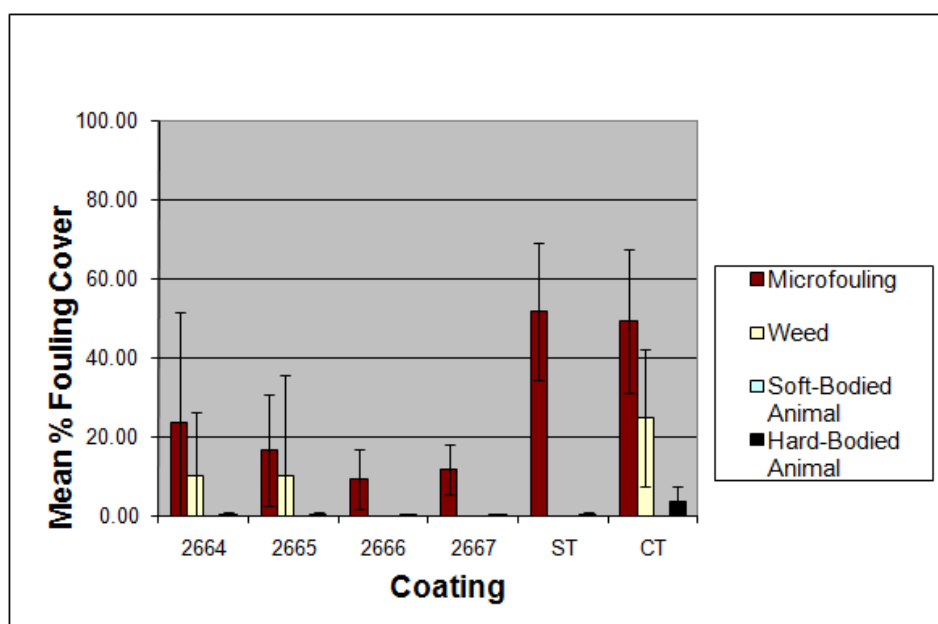


**Figure 4:17: Test Polymers antifouling results. Biocidal polymers 2664, 2665, 2666 and 2667 are AMPSQ(I)v1, v2, v3 and v4 respectively. Standard (ST) is non-biocidal polymer AMPSQ(II)v4 after 14 weeks immersion**

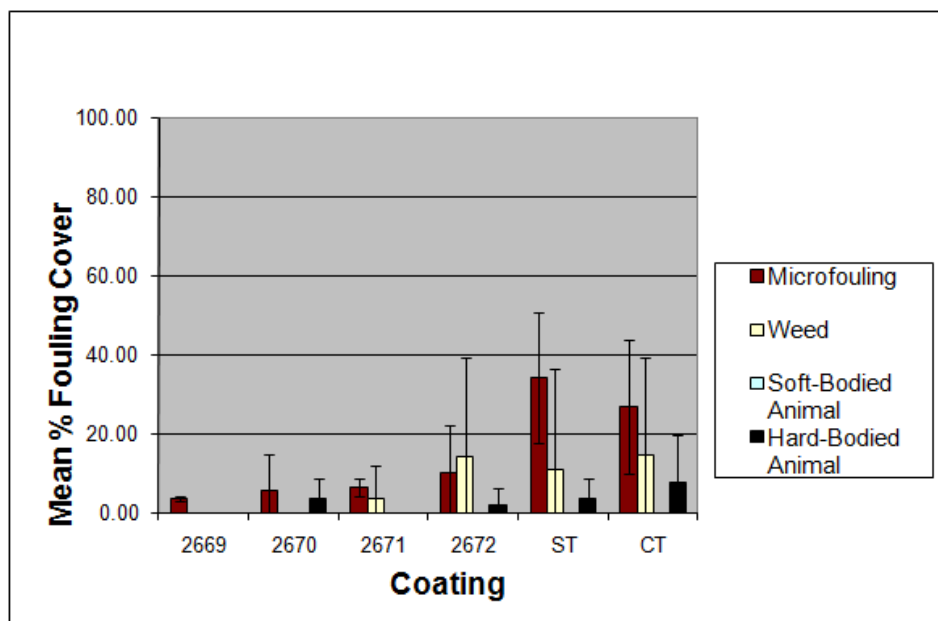


Figure 4:18: Test Polymers antifouling results. Biocidal polymers 2669, 2670, 2671 and 2672 are AMPSQ(I)v6, v7, v8 and v9 respectively. Standard (ST) is non-biocidal polymer AMPSQ(II)v4 after 14 weeks immersion

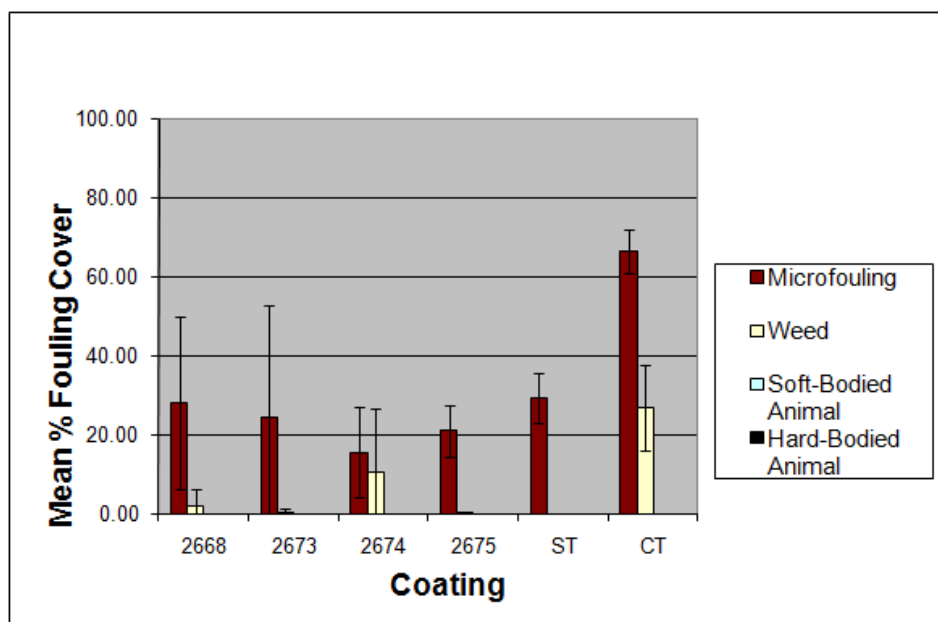


Figure 4:19: Test Polymers antifouling results. Biocidal polymers 2668, 2673, 2674 and 2675 are AMPSQ(I)v5, v10, v11 and v12 respectively. Standard (ST) is non-biocidal polymer AMPSQ(II)v4 after 14 weeks immersion

When the polymer coatings were re-examined after 17 weeks immersion there was no longer any differentiated performance between the AMPSQ(I) coatings and that of the non-biocidal standard. Therefore the panels were removed from test.

#### 4.4.3.2 Paint Results

Conversely after 14 weeks immersion the test paints AMPSQ(I)v1 and v2 (2652 and 2653 respectively) had an average smaller percentage coverage of microfouling (red bar) than either

AMPSQ(I)v3, v4 or the standard Intersmooth 460 (a commercial product), **Figure 4:20**. The poorest performing coating was AMPSQ(I)v3 (2654) which was only marginally poorer than the standard. From **Figure 4:21** both AMPSQ(I)v6 and v7 (2657 and 2658 respectively) were performing better than the standard and the poorest performing coating, AMPSQ(I)v8 (2659) which was still comparable with the standard, Intersmooth 460. A similar trend was also evident from **Figure 4:22**, where all the AMPSQ coatings had on average less coverage of microfouling than the standard. The performance of the test paints seemed counter intuitive compared to that exhibited by the clear coatings, particularly AMPSQ(I)v8 and v3 (2659 and 2654 respectively), whose performance seemed to be below that of the other coatings. However, definitive conclusions could not be drawn at this early stage because of overlapping error bars. **Figure 4:23** displayed the antifouling data for the triplicate coatings AMPSQ(I)v4, v5 and v6 (2655, 2656 and 2657) and the analogous non-biocidal AMPSQ(II)v4 (2676). At 14 weeks immersion there did not appear to be any differentiation between these coatings. This poorly differentiated performance was not unexpected at this early stage because the quats only represent 15 wt% of the paint's dry film and hence the difference in antifouling activity was likely to be masked by other components in the antifouling formulation, especially the additional biocides.

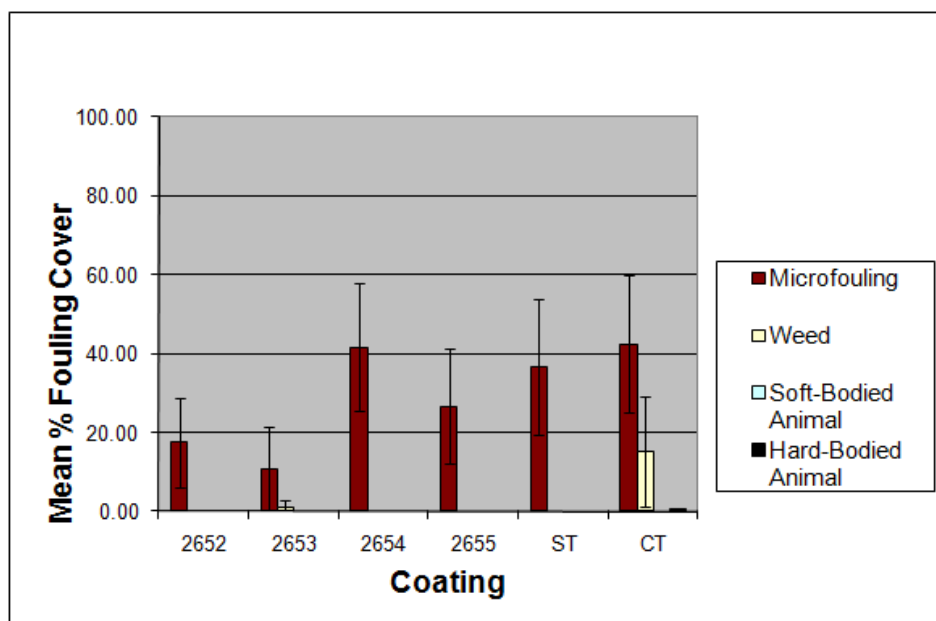


**Figure 4:20: Test Paints antifouling results. Biocidal paints 2652, 2653, 2654 and 2655 are AMPSQ(I)v1, v2, v3 and v4 respectively. Standard (ST) is Intersmooth 460 after 14 weeks immersion**

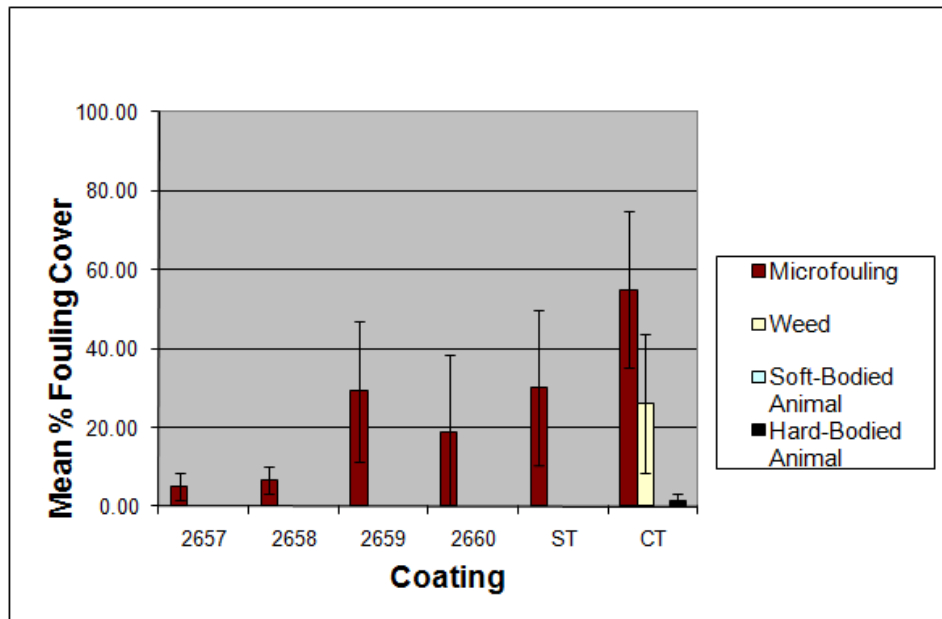


Figure 4:21: Test Paints antifouling results. Biocidal paints 2657, 2658, 2659 and 2660 are AMPSQ(I)v6, v7, v8 and v9 respectively. Standard (ST) is Intersmooth 460 after 14 weeks immersion

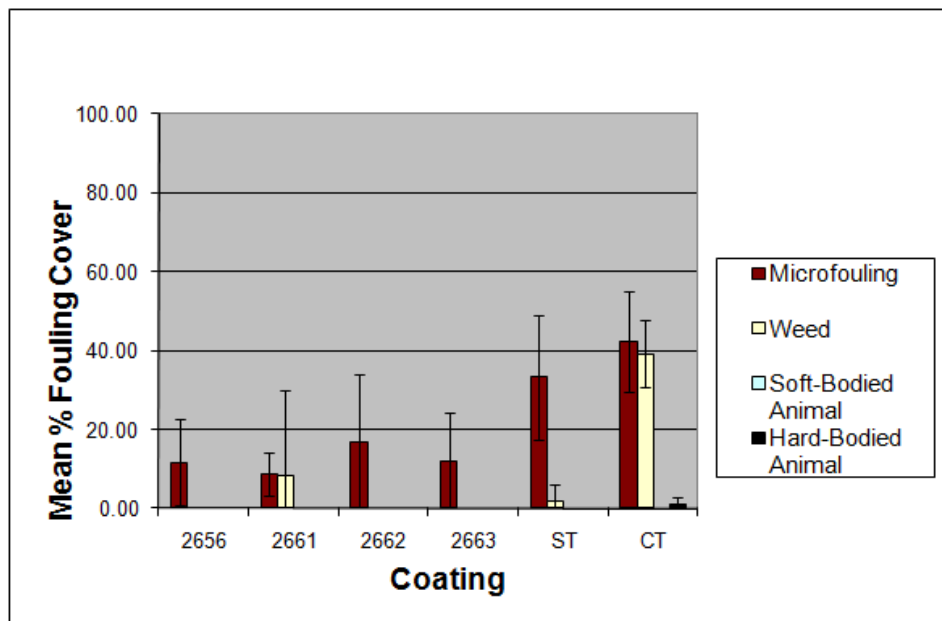
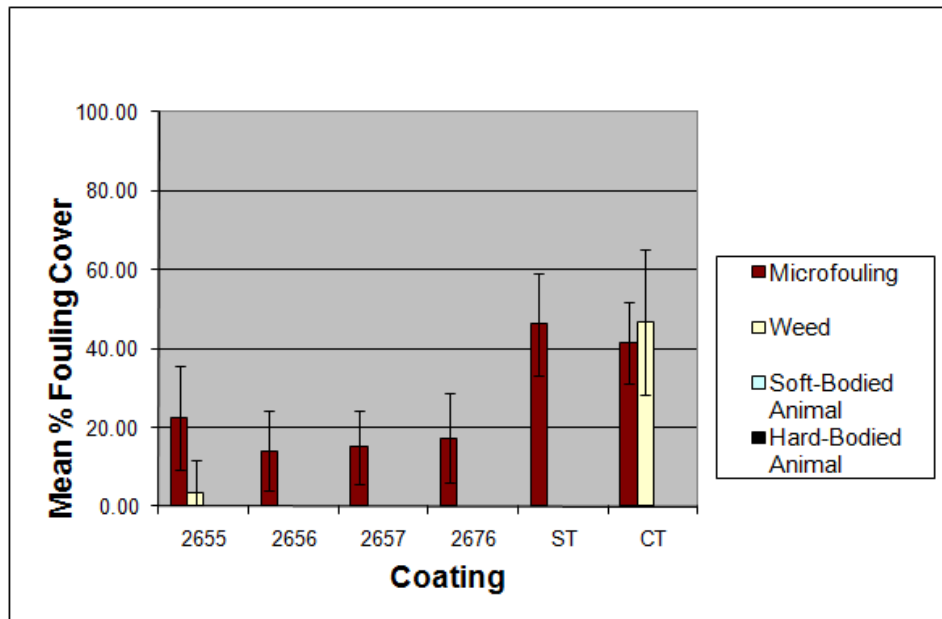


Figure 4:22: Test Paints antifouling results. Biocidal paints 2656, 2661, 2662 and 2663 are AMPSQ(I)v5, v10, v11 and v12 respectively. Standard (ST) is Intersmooth 460 after 14 weeks immersion



**Figure 4:23: Test Paints antifouling results. Biocidal paints 2655, 2656 and 2657 are AMPSQ(I)v4, v5 and v6 respectively. Non-biocidal paint 2676 is AMPSQ(II)V4. Standard (ST) is Intersmooth 460 after 14 weeks immersion**

After 59 weeks immersion, **Figure 4:24, Figure 4:25, Figure 4:26 and Figure 4:27**, the enhanced performance of the both the AMPSQ(I) and AMPSQ(II) coatings became more established, especially AMPSQ(I)v1-7 (2642 to 2658 inclusive) and AMPSQ(II)v4 (2676) which were all performing better than Intersmooth 460, the standard. The remaining coatings had, in general, less microfouling than the standard but their enhanced performance was not as pronounced due to the poor separation of the 95 % confidence error bars with those of the standard. Although analysis of individual antifouling panels demonstrated the performance of the AMPSQ systems ranged from better than, to comparable to, the standard, there was no clear differentiation between individual AMPSQ coatings.

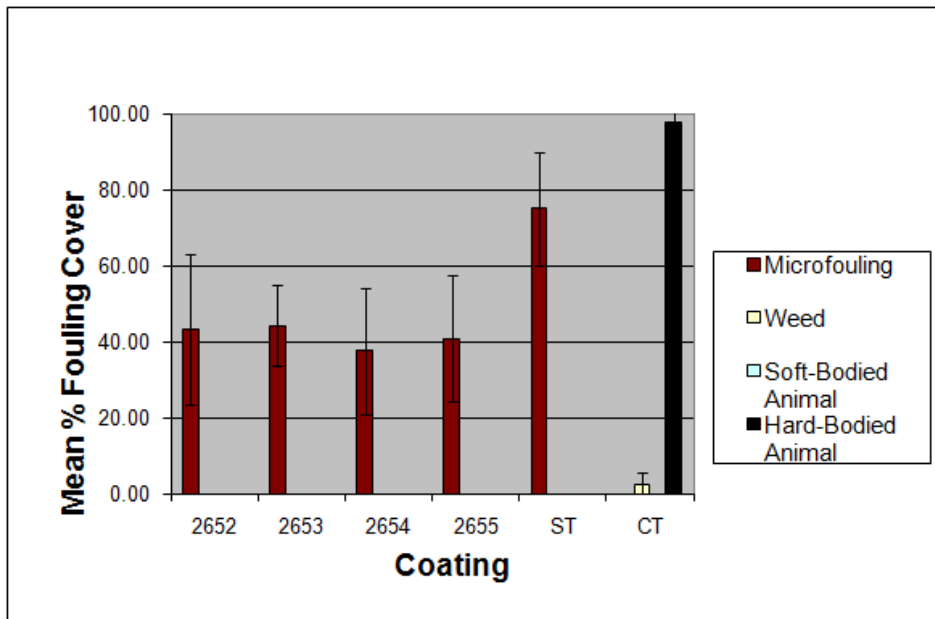


Figure 4:24: Test Paints antifouling results. Biocidal paints 2652, 2653, 2654 and 2655 are AMPSQ(I)v1, v2, v3 and v4 respectively. Standard (ST) is Intersmooth 460 after 59 weeks immersion

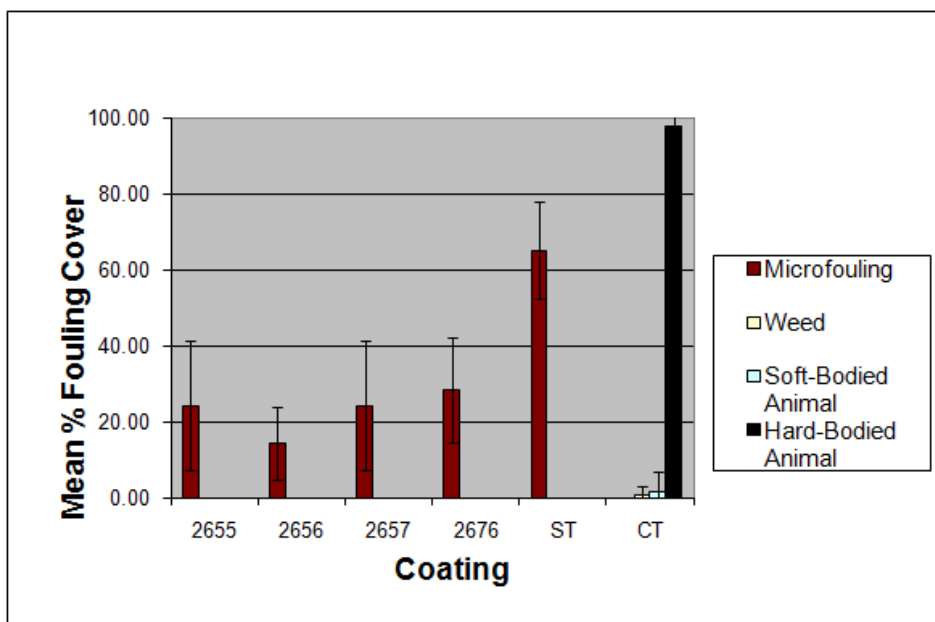


Figure 4:25: Test Paints antifouling results. Biocidal paints 2655, 2656 and 2657 are AMPSQ(I)v4, v5 and v6 respectively. Non-biocidal paint 2676 is AMPSQ(II)V4. Standard (ST) is Intersmooth 460 after 59 weeks immersion

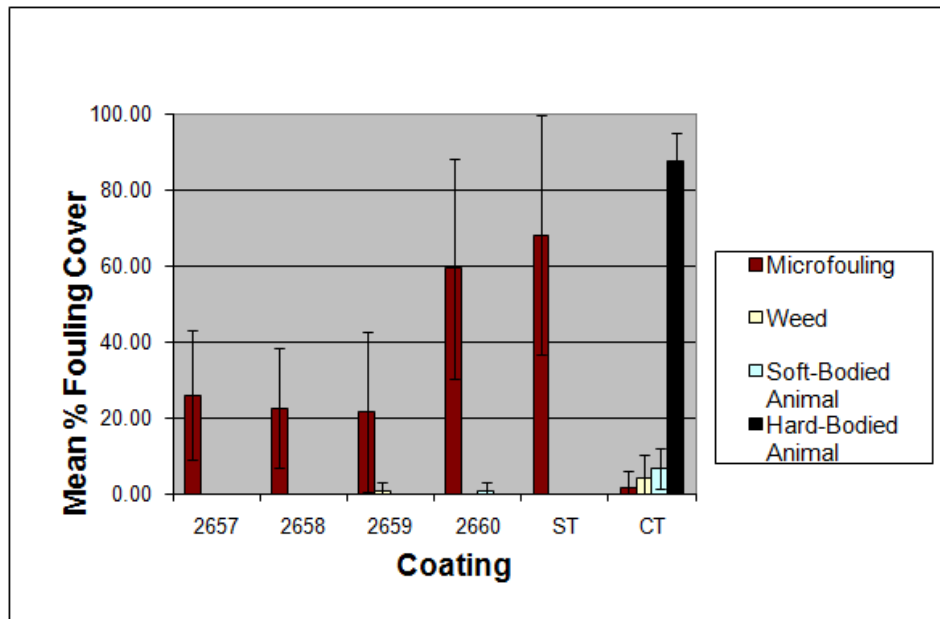


Figure 4:26: Test Paints antifouling results. Biocidal paints 2657, 2658, 2659 and 2660 are AMPSQ(I)v6, v7, v8 and v9 respectively. Standard (ST) is Intersmooth 460 after 59 weeks immersion

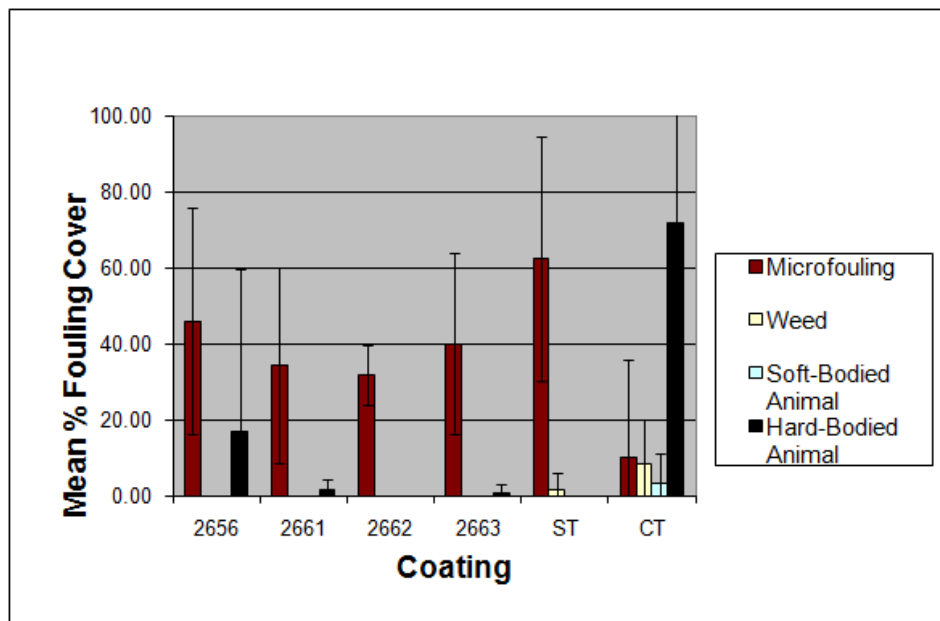


Figure 4:27: Test Paints antifouling results. Biocidal paints 2656, 2661, 2662 and 2663 are AMPSQ(I)v5, v10, v11 and v12 respectively. Standard (ST) is Intersmooth 460 after 59 weeks immersion

#### 4.4.3.3 Statistical Analysis of Antifouling data

In an effort to identify the most suitable candidate coating(s) for future development the antifouling data was analysed using a statistical software package, SPSS version 8. The above antifouling data, as currently analysed, was categorised depending upon the percentage area coverage of the four generic fouling classifications (slime, weed, soft-bodied animal and hard-bodied animal fouling) which was too fragmented to enable the assessment of which coating was ‘the best overall antifouling’ via a statistical software package. Therefore the antifouling data for each fouling classification was amalgamated to give a single fouling ranking (hydrodynamical rating, *H*) for

each of the 36 individual coatings squares on each antifouling board. Each of the four fouling classifications was ascribed a drag factor ( $d$ ) based on that fouling type's friction drag, i.e. slime with lowest drag coefficient had the smallest drag factor, and conversely, hard-bodied animal fouling with the highest drag coefficient had the biggest drag factor<sup>191, 192</sup>. The hydrodynamical rating was calculated, **Equation 4:2**, and the polymer and paints was analysed by a generalised linear model using a Tweedie distribution with a logarithmic transformation. This model tested the hydrodynamical rating with coating, immersion period, antifouling board number, board row and board column. The coatings were ranked by a simple contrast test with a sequential Bonferroni adjustment for  $p$  values for multiple comparisons. A contrast between the AMPSQ test coatings and either the standards or control is statistically significant if the  $p$  values is  $\leq 0.05$ .

$$H = \sum d_i c_i$$

**Equation 4:2: Hydrodynamical rating, where H is the hydrodynamical rating,  $d_i$  the fouling drag factor and  $c_i$  the fouling type's percentage coverage of the test square.**

The statistical analysis of the antifouling performance of the AMPSQ(I) polymers compared with the standard polymer (non-biocidal AMPSQ(II)v4), **Table 4:10**, identified that after 8 weeks immersion only AMPSQ(I)v1, v2, v3, v11, v12 and the modified AMPSQ(II)v4 were statistically better. This result for the modified AMPSQ(II)v4 again suggested the additional quat-biocide mixed into the AMPSQ(II)v4 polymer was having a significant antifouling effect. At this early stage it was unanticipated that only a minor selection of the biocidal AMPSQ(I) polymers would outperform the non-biocidal polymer. There was also no correlation between the proportion of the biocidal monomer within polymers and their antifouling performance as would have been expected. This poorly differentiated performance was attributed to that fact that after only 8 weeks immersion there was not sufficient time immersed to adequately test the polymer. This presumption was supported after 14 weeks immersions when only AMPSQ(I)v1 and v9 were not performing statistically better than the AMPSQ(II)v4 polymer. Interestingly, the antifouling performance of the modified AMPSQ(II)v4 polymer, after 14 weeks, was no longer statistically differentiated from the non-biocidal AMPSQ(II)v4. This added further weight to the highlighted conjecture that the additional biocidal quat in the modified AMPSQ(II)v4 had been released at such an excessive release rate that by 14 weeks there was insufficient biocide being released to provide adequate antifouling protection. After 14 weeks immersion there appeared to be a general correlation between the percentage of the AMPSQ(I) monomer (**4-1**) within the polymers and their antifouling performance. This was because all the polymers, which were statistically better than the non-biocidal AMPSQ(II)v4 standard contained 28.3 mol% or greater AMPSQ(I) monomer (**4-1**). Only the control coating, Primocon (non-biocidal primer), was statistically inferior to AMPSQ(II)v4. This suggested that AMPSQ(II)v4 was actually displaying a limited antifouling

performance. It was unclear whether this was due to the trioctyl-quat generating a weak biocidal effect, which could explain the poorly differentiated performance of the AMPSQ(I) polymers after 8 weeks, or due to a physical mechanism, such as polishing, which the AMPSQ(II)v4 polymer would also be able to achieve, but at a different rate effecting the antifouling performance.

Rank vs. AMPSQ(II)v4	Coating	8 weeks		14 weeks		
		Contrast Estimate	Bonferroni Significance (p)	Coating	Contrast Estimate	Bonferroni Significance (p)
1	AMPSQ(I)v3	-5.49	0	AMPSQ(I)v6	-8.89	0
2	AMPSQ(I)v11	-3.46	0.001	AMPSQ(I)v3	-8.26	0
3	modified Q(II)v4	-3.34	0.002	AMPSQ(I)v8	-8.00	0
4	AMPSQ(I)v12	-3.31	0.002	AMPSQ(I)v4	-7.39	0
5	AMPSQ(I)v2	-2.83	0.039	AMPSQ(I)v7	-6.00	0
6	AMPSQ(I)v1	-2.75	0.047	AMPSQ(I)v10	-5.68	0.001
7	AMPSQ(I)v8	-2.64	0.085	AMPSQ(I)v5	-5.58	0
8	AMPSQ(I)v4	-2.47	0.019	AMPSQ(I)v12	-5.56	0.002
9	AMPSQ(I)v10	-2.35	0.085	AMPSQ(I)v2	-4.74	0.017
10	AMPSQ(I)v5	-1.68	0.186	AMPSQ(I)v11	-4.41	0.039
11	AMPSQ(I)v6	-1.65	0.186	AMPSQ(I)v9	-3.66	0.124
12	AMPSQ(I)v7	-0.08	1	AMPSQ(I)v1	-3.49	0.124
13	AMPSQ(I)v9	0.86	1	modified Q(II)v4	3.30	0.244
14	Control	9.59	0	Control	7.90	0

**Table 4:10: Antifouling performance of AMPSQ(I) polymers ranked statistically against the non-biocidal AMPSQ(II)v4 polymer. Yellow and green indicates statistically superior and inferior antifouling performance respectively**

The comparative performance of the AMPSQ paints against the standard coating, Intersmooth 460 (current commercial product), was superior even after a short immersion period of only 14 weeks, **Table 4:11**. At the 14 weeks immersion assessment all the AMPSQ paints were either outperforming or displaying comparable performance to Intersmooth 460. In fact the only coatings not statistically outperforming the standard were AMPSQ(I)v4, v8 and v3, which was unexpected, as the AMPSQ(I)v3 and v8 contained the highest proportions of the biocidal monomer. However, after 59 weeks immersion the top performing paint was AMPSQ(I)v8. A similar trend of increasing performance with prolonged immersion periods was also evident from the clear polymeric coating and presumed to be associated with the release rate of the biocidal quat. The only coating which was statistically inferior to the standard was, as anticipated, the non-biocidal control, Primocon.

Rank vs. standard coating	Coating	14 weeks		59 weeks		
		Contrast Estimate	Bonferroni Significance	Coating	Contrast Estimate	Bonferroni Significance
1	AMPSQ(I)v7	-5.83	0	AMPSQ(I)v8	-9.23	0
2	AMPSQ(I)v6	-5.50	0	AMPSQ(I)v7	-9.08	0
3	AMPSQ(I)v5	-5.05	0	AMPSQ(I)v6	-8.37	0
4	AMPSQ(I)v12	-5.02	0	AMPSQ(I)v11	-7.66	0
5	AMPSQ(I)v2	-4.62	0	AMPSQ(II)v4	-7.29	0
6	AMPSQ(II)v4	-4.48	0	AMPSQ(I)v4	-7.14	0
7	AMPSQ(I)v11	-4.11	0.002	AMPSQ(I)v3	-6.6	0
8	AMPSQ(I)v10	-3.62	0.016	AMPSQ(I)v5	-6.55	0
9	AMPSQ(I)v1	-3.40	0.036	AMPSQ(I)v10	-5.6	0.006
10	AMPSQ(I)v9	-3.28	0.045	AMPSQ(I)v1	-5.57	0.006
11	AMPSQ(I)v4	-2.14	0.163	AMPSQ(I)v2	-5.44	0.006
12	AMPSQ(I)v8	-0.93	0.66	AMPSQ(I)v12	-5.39	0.006
13	AMPSQ(I)v3	2.13	0.66	AMPSQ(I)v9	-1	0.661
14	Control	10.24	0	Control	82.05	0

**Table 4:11: Antifouling performance of AMPSQ(I) paints ranked statistically against the standard product paint (Intersmooth 460). Yellow and green indicates statistically superior and inferior antifouling performance respectively**

Unfortunately statistical comparisons between the biocidal AMPSQ(I) paints and the non-biocidal AMPSQ(II)v4 paint, **Table 4:12**, were not as favourable as the comparable comparison between the clear polymeric systems, **Table 4:10**. Consistently the only paints which were performing statistically inferior to AMPSQ(II)v4 were the current commercial products, Intersmooth 460 and Primocon. It was believed that this poorly differentiated performance between the AMPSQ paints was due to the additional biocide present within the prototype paint formulation, which masked the antifouling efficacy of the biocidal didecyl-quat compared to the non-biocidal trioctyl-quat that was established from the clear polymeric coatings.

Rank vs. AMPSQ(II)v4	Coating	14 weeks		59 weeks		
		Contrast Estimate	Bonferroni Significance	Coating	Contrast Estimate	Bonferroni Significance
1	AMPSQ(I)v7	-1.36	1	AMPSQ(I)v8	-1.94	1
2	AMPSQ(I)v6	-1.03	1	AMPSQ(I)v7	-1.8	1
3	AMPSQ(I)v5	-0.58	1	AMPSQ(I)v6	-1.08	1
4	AMPSQ(I)v12	-0.55	1	AMPSQ(I)v11	-0.38	1
5	AMPSQ(I)v2	-0.15	1	AMPSQ(I)v4	0.15	1
6	AMPSQ(I)v11	0.36	1	AMPSQ(I)v3	0.69	1
7	AMPSQ(I)v10	0.85	1	AMPSQ(I)v5	0.73	1
8	AMPSQ(I)v1	1.08	1	AMPSQ(I)v10	1.69	1
9	AMPSQ(I)v9	1.20	1	AMPSQ(I)v1	1.71	1
10	AMPSQ(I)v4	2.33	0.349	AMPSQ(I)v2	1.85	1
11	AMPSQ(I)v8	3.54	0.379	AMPSQ(I)v12	1.9	1
12	Int 460	4.48	0	AMPSQ(I)v9	6.28	0.114
13	AMPSQ(I)v3	6.61	0.035	Int 460	7.29	0
14	Control	14.72	0	Control	89.34	0

**Table 4:12: Antifouling performance of AMPSQ(I) paints ranked statistically against the non-biocidal AMPSQ(II)v4 paint. Green indicates statistically inferior antifouling performance.**

In general, it was concluded from the polymer coatings that the release rate of the quat-biocides needed to be controlled in order to sustain their antifouling action, and the incorporation of a biocidal quat into the polymer architecture was a suitable mechanism to achieve controlled release

of the biocide. It was also concluded that the anticipated enhanced performance with increased AMPSQ(I) (4-1) mol% was not borne out by the antifouling data from the test paints. Neither was the anticipated difference in efficacy between the biocidal and non-biocidal quats from the same data set which was obvious from the clear coatings. These results, however, clearly demonstrated that even after over a year's immersion, the experimental systems based on quat-biocides were suitable for use as antifoulants, displaying greater efficacy than the current commercial product used as the standard. However, a year's immersion was not sufficient to adequately differentiate between different AMPSQ prototype paints.

#### 4.4.4 Storage Stability

A representative set of the AMPSQ paints were placed on test. These were specifically chosen to include the non-biocidal AMSQ(II)v4 and those AMPSQ(I) paints which spanned the broadest compositional range: AMPSQ(I)v4, v8, v9 and v12. AMPSQ(I)v6 was also included because it was a replicate of the polymer composition used in AMPSQ(I)v4.

As clearly demonstrated from **Figure 4:28** all the paints were stable on storage at both 23 and 45 °C. None of the paints displayed the dramatic temperature dependent changes in viscosity of the previous coating systems (see *Chapter 3 section 3.3.4, Figure 3:15 and section 3.7.4, Figure 3:33*). Only AMPSQ(I)v4 showed any change in viscosity changing by 0.91 poise between the initial and final measurements. This small change was within error and not significant and this paint was deemed to be stable, especially considering the replicate formulation AMPSQ(I)v6 displayed no change. The difference between AMPSQ(I)v4 and v6 was however significant. The reason(s) for the difference was not obvious at this stage as neither coating had been treated significantly different since manufacture. Therefore it seemed likely that the difference was due to variations during the synthesis and preparation of the polymers and paints, although the exact source of variation was not apparent.

Substitution of the didecyl-quat of AMPSQ(I)v4 or v6 for the trioctyl-quat of AMPSQ(II)v4 reduced the viscosity of the paint, however the magnitude of the viscosity reduction was not clear especially given the variation in the viscosity demonstrated by the two replicates AMSQ(I)v4 and v6. This reduction in viscosity appeared consistent with theory because the trioctyl-quat of AMPSQ(II)v4 had a greater proportion of alkyl residues than the didecyl-quat of AMPSQ(I)v4 and hence would be better solvated by the non-polar solvent of the paint formulation, xylene, resulting in the lower viscosity.

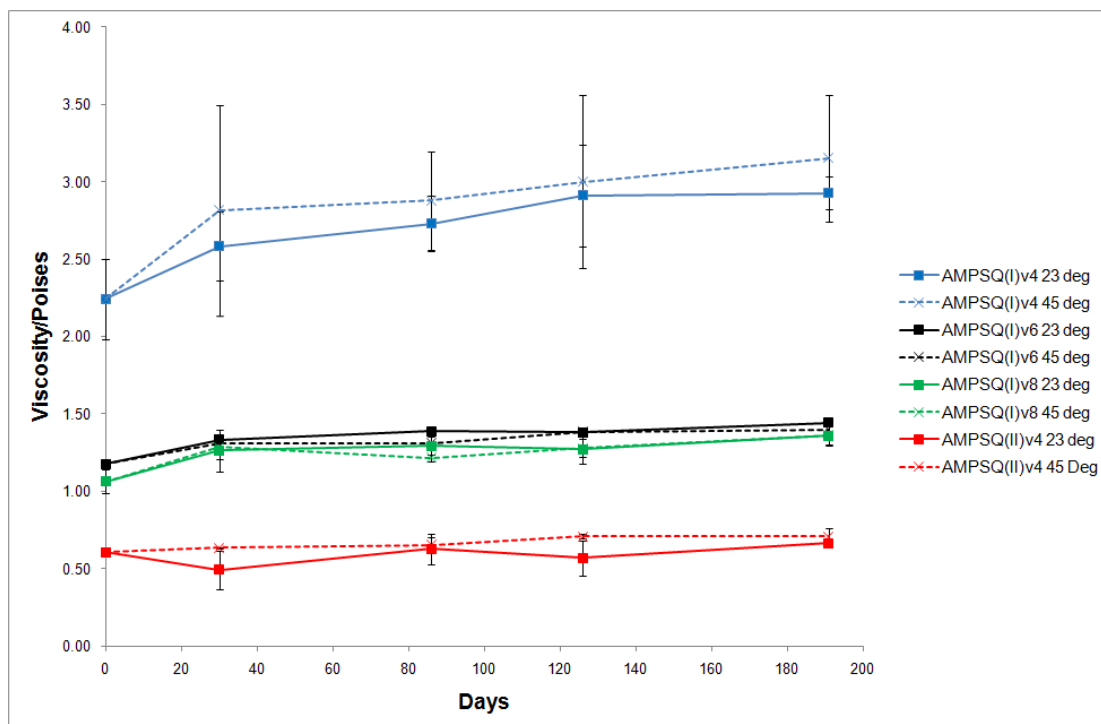


**Figure 4:28: Viscosity measurements of various AMPSQ paints**

## 4.5 Conclusions

The use of AMPS (3-2) has finally provided a suitable polymeric system to enable the efficacy of quat-biocides to be evaluated. The developed coatings have demonstrated sufficient potential throughout the testing that they would be suitable for future commercial development. Using these polymers it was clear that quats provided an enhanced antifouling activity over and above of that of current commercial product, together with the need for their release to be controlled to sustain their activity. It is somewhat surprising that even after 59 weeks testing there was no difference between paints formulated with the biocidal and non-biocidal quats. It is anticipated that given sufficient time the difference would become apparent. The demonstrated antifouling activity was to such an extent that the testing of the coatings has been extended to more challenging environments, such as Singapore and scaled up for test patching on vessels. A selection of the AMPSQ coatings are currently on a vessel moored in Hartlepool, UK but no further antifouling data is available at this time, **Figure 4:29**.



**Figure 4:29: Photographs of the stern (right) and bow (left) starboard sections of the test patching vessel. Yellow circles indicate AMPSQ coating test patches**

The 'ideal' polymer candidate for future development would be the one which can provide the established antifouling activity with good semi rapid boot top testing performance with a consistent polishing rate. Although the potential for good semi rapid performance has been displayed by a number of systems, this is not matched by their polishing rates. Indeed only limited proof of polishing has been displayed so far not withstanding the range in ability of the coatings to full survive the test without surface defects and the speed thresholds associated with them. At present there appears to be a trade-off between the properties required to provide both good semi rapid and polishing performance which will require further experimentation with the AMPSQ polymeric system to find the 'ideal' candidate polymer. An additional difficulty is that the ability of the AMPSQ systems to polish seems intricately linked with the potential of the coatings to absorb water. Therefore it seems unlikely that for the AMPSQ coatings the polishing rate can adequately be determined with the current polishing rate test protocol. A modification such as ensuring that the coatings are fully saturated prior to testing would negate the problems associated with interpreting the results and trying to deconvolute the polishing rate from the water uptake.

The key requirement of the AMPSQ coatings is that they react with seawater through the ion exchange reaction to cause the polishing of the coating with the synergistic release the quat-biocides. Therefore an additional test to measuring the polishing rate would be to monitor the release rate of the quat-biocides through a leach rate testing, the development and implementation of which are the subjects of Chapters 5 and 6.

## 5 Analytical Method Development

The fundamental principle of biocidal antifouling coatings is that they release one or more biologically active agents, biocides, which prohibit the growth of fouling. Therefore a thorough understanding of their release rates (leach rates), of these biocides is vital from both development and regulatory perspectives. Currently this is achieved by regular quantification of the amount of biocide released which is repeated for extended periods of time, up to years. This therefore, necessitates that suitable analytical procedures be established for each target biocide.

As antifouling coatings are, in essence, the vector for the delivery of their biocides, the coatings performance/working lifetime is dependent upon the flux of these biocides being above a minimum critical level required to deter fouling. Once the flux of biocide is below this critical level the antifouling coating no longer provides fouling protection. The development of new antifouling requires the successful blending of key ingredients of the paint formulation to optimise the release rate of these biocides maximising the coatings lifetime. The determination of this requires the extensive use of suitable analytical procedures.

Additionally the quantification of biocides and calculation of their release rates is also an important tool for the antifouling regulatory authorities. Since the 1990s and the TBT ban the regulatory authorities have become more proactive in their attempts to safeguard the environment with legislation such as Registration, Evaluation and Authorisation of Chemicals<sup>193</sup> (REACH), Biocidal Products Directive<sup>37</sup> (BPD) and Water Framework Directive<sup>194</sup> (WFD). Under such legislature the authorities can stipulate maximum environmental levels and even release rates of the biological agents of concern, and this has had a direct influence on the antifouling industry.

To date, there are two core test methods designed to measure the release rate of biocides from antifouling coatings which aim to simulate either a stationary<sup>195</sup> or a moving vessel<sup>196</sup>. These methods can be further divided depending upon the specific biocide being quantified. Currently there are internationally accepted methods for the key biocides used in the antifouling industry such as copper oxide<sup>196</sup>, zinc/copper pyrithione<sup>164</sup> (**1-1** and **1-2**), and seanine-211<sup>164</sup> (**1-3**). These methods stipulate the correct analytical protocol for each biocide including instrumentation, procedures and limits of detection/quantification, frequently in the low parts per billion (ppb) region. For a new biocide to be fully commercialised as an antifoulant it requires the creation of an analytical protocol to facilitate the development of the coating and to aid its registration with the authorities. Currently there is no such method for quats, specifically didecyldimethylammonium (**2-1**) and alkylbenzyltrimethylammonium halides (**1-21**).

To establish a new analytical method will require the successful resolution of several key requirements:

- Sampling protocol (including investigating the necessity of sample pre-treatment)
- The most suitable analytical instrument and detector
- Optimisation of all the operating conditions

The identification of the most appropriate detection method and instrumentation is the first major step in method development. To a large extent these are dictated by constraints imposed by both the analyte and its sample matrices. For example analytes without chromophores will be unsuitable for detection by UV spectroscopy and samples in aqueous matrices represent significant problems for analysis by GC without sample pre-treatment.

For this particular application (measurement of quats from antifouling coatings), the sample matrix will be seawater and the biocidal analytes, either alkylbenzyltrimethylammonium halide (benzylquat, **1-1**) or didecyltrimethylammonium halide (didecylquat, **2-1**). The major constituent of the benzylquat homologs is the C<sub>12</sub> species<sup>61</sup> and as such this will be used as a surrogate for this group of quats. The non-biocidal quat, trioctyltrimethylammonium halide (trioctylquat, **2-2**), will also be included because it was used as the experimental control for the evaluation of the efficacy of the biocidal didecyl-quats (**2-1**) during immersion testing. Consequently, the release rate of the non-biocidal quats may also need to be measured. Although there are published methods for the quantification of quats<sup>113, 130, 134</sup>, to the best of my knowledge, none are specific for seawater samples. However, it is clear that both gas chromatography (GC)<sup>126, 127</sup> and liquid chromatography (LC)<sup>159, 161</sup> have been successfully used for the quantification of quats.

## 5.1 Initial Instrumentation Evaluation

Initial evaluation of LC systems with various detectors concluded that the analytes in acetonitrile (ACN) could be analysed to a limit of detection of *circa*. 10 parts per million (ppm), depending upon the detector. Of the detectors used, UV and evaporative light scattering (ELS), only ELS could detect all the analytes. Unfortunately their limits of detection were not sufficient, especially for samples in organic solvent (e.g. ACN). A pre-concentration step in the order of 1000s prior to analysis, would be required to achieve the targeted low ppb level detection limits, and hence comparable with similar release rate methods. The practicability of achieving concentrations in the order of 1000s was not explored at this stage in favour of finding a more sensitive detection method.

Direct analysis of quats was not possible by GC because the analytes were ionic and hence not sufficiently volatile to enable GC analysis. However, it was possible to analyse quats by

converting them to tertiary amines, which have substantially shorter retention times. This was achieved through a semi-pyrolytic method involving the injection of the quats into the injection port held at high temperatures, *circa.* 350 °C, which caused the quat to breakdown forming a tertiary amine through a Hofmann elimination reaction (*see Chapter 1, section 1.2.3, Figure 1:31*). Unfortunately, GC analysis using either flame ionisation or nitrogen-phosphorous detectors offered no advantages over the previously discussed LC systems in terms of detection limit.

However, analysis by GC mass spectroscopy (MS) was far more successful<sup>197</sup>. The MS detector while offering the capability to detect all the analytes also substantially improved the limits of detection, *circa* 100 ppb. However, when considering that this was achieved with non-aqueous samples, the detection limit was still poor because the anticipated samples from the leach rate experiment are likely to be below this level, estimated from comparable tests. Injection of aqueous samples, especially seawater, into GCs is extremely problematic. For example a 1 µl injection of aqueous sample into an injection port at 350 °C (to allow GC analysis) with a column head pressure of 14 psi would generate 1450 µl of water vapour; substantially greater than the volume of a standard liner (~990 µl)<sup>198</sup>. This vapour could also condense in “cold” regions of the injection port, only to be vaporised again once the oven cycle had warmed these “cold” areas. This would leads to broad, tailing contamination peaks. The residual salts from the seawater would also cause selectivity problems in subsequent analysis.

The aqueous nature of the prospective samples and the problems associated with their analysis combined with the greater sensitivity of the MS detector indicated that liquid chromatography with mass spectroscopy (LC-MS) would be the most appropriate instrumentation and detector for the quats. The use of a pre-concentration step would enable the required low ppb detection limits to be achieved. A simple laboratory technique frequently used to achieve this is solid phase extraction (SPE).

## 5.2 LC-MS Method Development

### 5.2.1 Mass Spectrometer Tuning and Ion Identification

A 10 ppm methanolic solution of benzyl-quat (**1-21**) was directly infused into the MS to facilitate the tuning of the instrumentation. Several settings such as electrospray ion source temperature, sheath and sweep gases were adjusted manually through an iterative process to increase the sensitivity of the MS to the quat. Once finished, the automatic optimisation function of the MS software (LCQ Tune) was performed to complete the optimisation of the MS. The final settings were: electrospray ion source 280 °C; sheath gas flow rate 25 (arbitrary units); sweep gas 12 (arbitrary units); ionisation spray voltage 4.00 kV; capillary voltage 4.0 V and tube lens offset 5.0 V. These setting were then used in all future experimentation.

Following the preparation of a 10 ppm stock solution of each analyte and their direct infusion into the MS, the mass ions and their fragmentation ions were determined, **Table 5.1**:

<i>Compound</i>	<i>Mass Ion (amu)</i>	<i>Major Fragmentation Ion (amu)</i>
<i>dodecylbenzyltrimethylammonium cation</i>	304.0	212.4
<i>didecyltrimethylammonium cation</i>	326.2	186.4
<i>trioctyltrimethylammonium cation</i>	368.4	256.5

**Table 5.1: Quats' mass ions and major fragmentation ions**

The major fragmentation ions of the quats were formed by the fragmentation of the molecular ion upon entering the MS resulting in the loss of a smaller “stable” molecule. For the benzyl-quat cation the fragmentation ion was formed by the loss of a toluene molecule from the molecular cation, creating an unsaturated dodecyltrimethyliminium ion (**5-1**), **Figure 5.1**. This was presumably achieved by the cleavage of the N<sup>+</sup>-benzyl nitrogen-carbon bond resulting in a benzyl cation, which then abstracted hydrogen from the alkyl residue in the alpha position from the nitrogen centre, forming the iminium ion. The fragmentation ion formed from the didecyl-quat cation was a decyltrimethylammonium ion (**5-2**) formed by the elimination of a decene molecule from the original cation forming a tertiary amine which was then protonated, **Figure 5.1**. This presumably occurred through β – elimination at the N<sup>+</sup>-decyl nitrogen-carbon bond forming the decene molecule and the tertiary amine, which was subsequently protonated. The same pattern was also evident for trioctyl-quat cation with the overall process resulting in the loss of an octene molecule forming a dioctyltrimethylammonium ion (**5-3**), **Figure 5.1**.

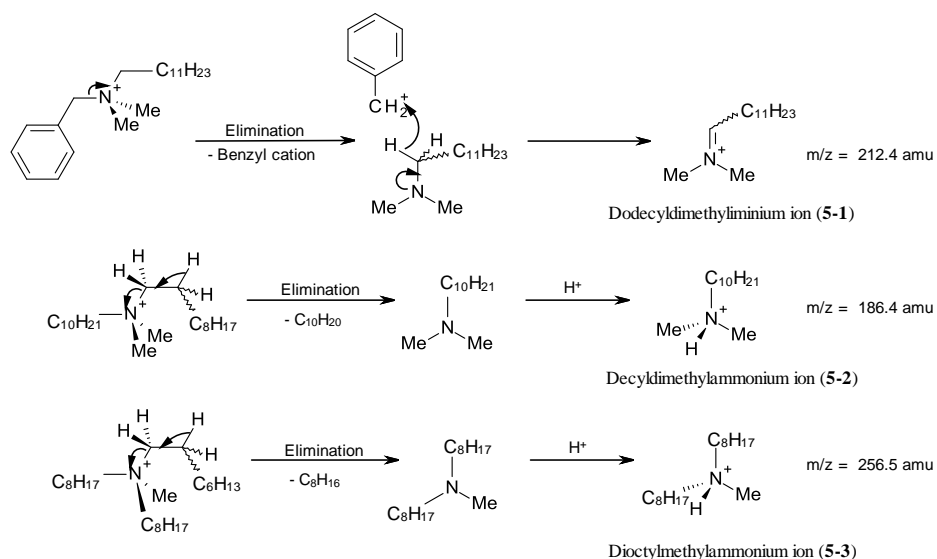


**Figure 5.1: Potential routes to formation the major fragmentation ions of the quats**

## 5.2.2 Liquid Chromatography Set up

Following a review of the scientific literature concerning the chromatography of quats (*see Chapter 1, section 1.2.3*) a couple of observations were drawn:

1. There was no consistently used LC column. The majority of recent publications have favoured 'C<sub>18</sub> coated' columns while for earlier publications a 'CN coated' column was preferred.
2. There was an overwhelming uses of buffered eluents with organic solvents. Generally methanol or ACN were used in combination with an aqueous eluent containing ammonium salts at low pH.

The reasons for the uses of acidified buffered eluents were not obvious when considering the analytes themselves, as they were not pH sensitive. It has been proposed that the use of the acidic conditions was to limit unfavourable interactions between the analytes and silanol groups present in the stationary phase of the LC column<sup>139</sup>. These silanol groups were naturally present in the column stationary phase due to incomplete coating of the base silica used to hold the stationary phase. The uses of buffered eluents with ammonium salts reduced these unfavourable interactions further. Bluhm *et al*<sup>139</sup> observed the addition of ammonium salts in the eluent improved the peak shape of the quat analytes by reducing peak tailing, a visual manifestation of these unfavourable interactions. Bluhm *et al* also noted that the shorter the alkyl residue on the ammonium salt the more pronounced the reduction in tailing of the target analyte. It was postulated that this was due to the greater penetrative power of the smaller ammonium salts into the organic stationary phase of the LC column and subsequent enhanced shielding of the analytes from the silanol groups<sup>139</sup>.

A range of different manufacturers' C<sub>18</sub> and CN stationary phase LC columns were initially selected to be evaluated. These were (*manufacturer*):

1. Gemini C<sub>18</sub> 3 μm 2.0 × 50.0 mm (*Phenomenex*)
2. Ultracarb C<sub>8</sub> 5 μm 3.2 × 75.0 mm (*Phenomenex*)
3. Xterra C<sub>18</sub> MS column 2.5 μm 4.6 × 50.0 mm (*Waters*)
4. Luna CN 5 μm 2.0 × 50.0 mm (*Phenomenex*)
5. Supelcosil CN 3 μm 4.6 × 75.0 mm (*Sigma Aldrich*)

The C<sub>18</sub> and CN stationary phases interact differently with the analytes. The C<sub>18</sub> interactions were predominately via hydrophobic interactions between the long alkyl groups of both the stationary phase and the quats. Given that there was a range of alkyl chain lengths, C<sub>8</sub>-C<sub>12</sub>, in the analytes as well as the number of alkyl chains, 1-3, theoretically the C<sub>18</sub> stationary phase would be a suitable choice to obtain chromatographic separation of quats. If the interaction with the C<sub>18</sub> phase was too strong, the C<sub>8</sub> phase could provide an alternative weaker version. The CN stationary phase interactions could conceivably be twofold. The primary interaction would be through the lone-pair electrons of the nitrogen atom in the CN group interacting through an electrostatic interaction with the cationic analytes. This interaction was then further tempered by the varying hydrophobic

interaction of the analytes' alkyl residues with that of the columns, providing the chromatographic separation.

The initial organic solvent was selected as ACN with 1 % acetic acid. ACN was chosen in preference to methanol because of its better health and safety profile; likewise acetic acid was chosen in preference to formic acid as it was less corrosive. The aqueous eluent contained ammonium acetate at various concentrations acidified to pH 3.6 with acetic acid. The initial concentrations of the ammonium acetate were 200, 100 and 50 mM.

Following an iterative process the following optimal LC conditions were obtained: Xterra C<sub>18</sub> MS column 2.5  $\mu\text{m}$   $\times$  4.6  $\times$  50.0 mm; eluent 90(A):10(B), where (A) was ACN acidified with 1% acetic acid and (B) was aqueous 50 mM ammonium acetate solution acidified to pH 3.6 with acetic acid; the flow rate was 400  $\mu\text{Lmin}^{-1}$ . The Xterra column was chosen in preference to the other columns due to its better overall chromatography i.e. good peak shape for all the analytes at lower flow rates. Other columns provided good chromatography for one or other analyte but required higher flow rates, which were unsuitable for use with the MS detector. A concentration of 50mM ammonium acetate was chosen in preference to the other concentrations, as this gave a lower background ion concentration maximising the sensitivity of the MS detector.

In order to assess the working range of the MS detector a set of calibration standards were analysed with the method outlined above. Methanolic standard solutions of benzyl-quat (**1-21**) were prepared in 'A' grade volumetric glassware in the range 50 to 1000 ppb and analysed, **Figure 5:2**.

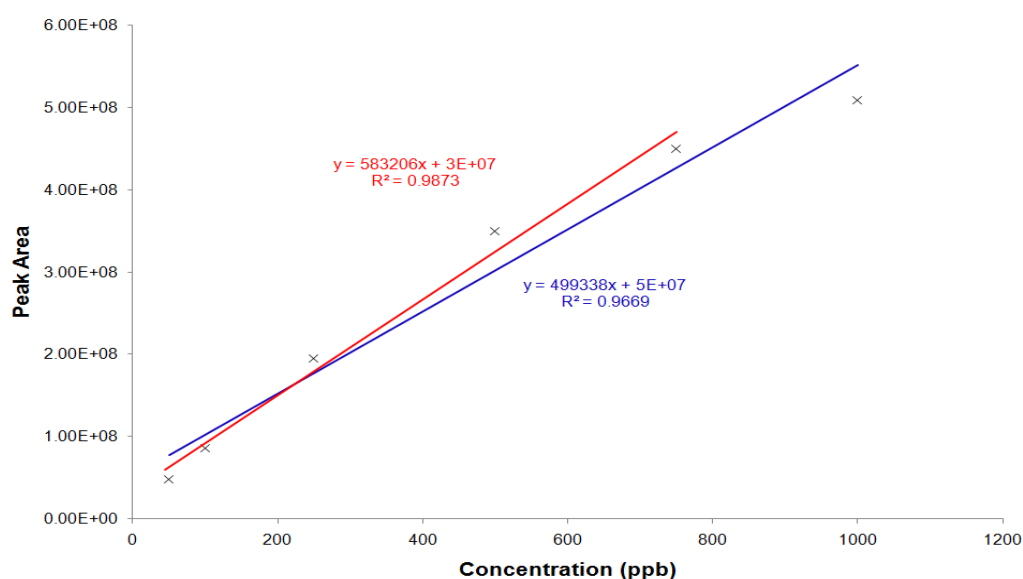


**Figure 5:2: Initial calibration plot: 50-1000ppb benzyl-quat (1-21)**

The produced calibration plot showed a linearity of  $R^2 = 0.9669$ ,  $n = 6$  (blue trendline). This demonstrated that there was a good correlation between the concentration of the sample and the peak area. However, on closer inspection of the plot it was clear that the high concentration standards, particularly 1000 ppb, deviated significantly from the 'best' trendline. This could be due to the higher concentration samples overloading the detector and hence outside of its linear working range, or be due to a poorly created calibration set. To clearly identify the source of error the same 500 ppb standard was injected six times, varying the injection volume, such that a comparable calibration range would be created with operator error minimised. Again this produced a linearity of  $R^2 = 0.9669$ ,  $n = 6$ , but with the 1000 ppb standard removed the linearity increases to  $R^2 = 0.9873$  (red), **Figure 5:2**. This suggested that the source of error was not operator dependent, but due to a non-linear response of the detector at the top end of the calibration. To further improve the calibration, an internal standard was included which would reduce errors in the calibration which were associated with the injector of the LC. *Tetra n-butylammonium nitrate* (**5-4**), **Figure 5:3**, was found to be a suitable compound as its retention time (1.38 mins) was found to be sufficiently different to that of benzyl-quat (**1-21**) (1.93 mins), **Figure 5:4**. Its mass ion was confirmed to have a  $m/z$  of 242.5 amu and a major fragmentation ion at a  $m/z$  of 186.4 amu.

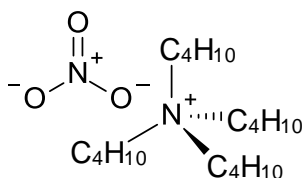


**Figure 5:3: Structure of internal standard compound - tetra n-butylammonium nitrate (5-4)**

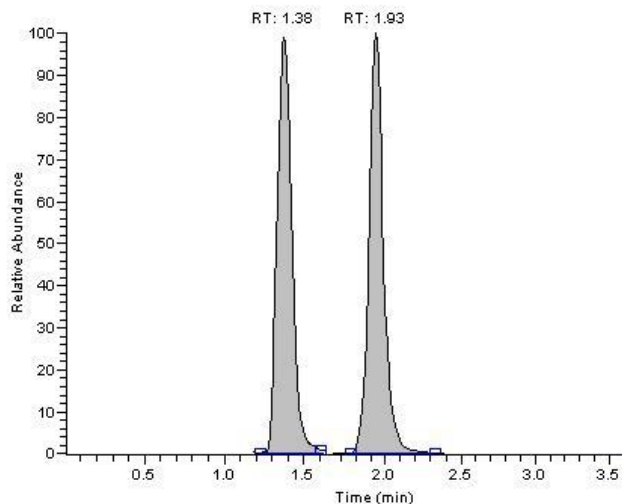


**Figure 5:4: Chromatogram of tetra-butylammonium nitrate (5-4) (1.38 mins) and benzyl-quat (1-21) (1.93mins)**

Prior to attempting a calibration range spanning the lower ppb concentration range, the settings of the injector and MS were scrutinised to increase the reproducibility of the method by minimising the relative standard deviations (RSDs) associated with this vital component of the LC system.

This was achieved by determining which detection settings, either single ion monitoring (SIM) or the fragmentation ion ( $MS^2$ ) combined with either a full or partial injection loop was the most reproducible. This was achieved by calculating the RSDs for the peak areas of five repeat injections of the same sample, 500 ppb, associated with each setting. Benzyl-quat (**1-21**) and *tetra* n-butylammonium nitrate (**5-4**) were used as the test compounds, **Table 5:2**.

		<i>tetra</i> n-butylammonium nitrate (Internal Standard)	dodecylbenzyltrimethylammonium chloride
<b>Full Loop</b>	<b>SIM</b>	1.58	1.67
	<b><math>MS^2</math></b>	3.03	1.77
<b>Partial Loop</b>	<b>SIM</b>	1.10	2.52
	<b><math>MS^2</math></b>	5.04	1.78

**Table 5:2: RSDs calculated detection settings from five repeat injections of 500 ppb sample**

From the data it was clear that greater reproducibility could be achieved for analysis of the internal standard compound, *tetra* n-butylammonium nitrate (**5-4**), via SIM as for both injection modes the associated RSDs were significantly lower than for  $MS^2$ . The distinction was less clear for benzyl-quat (**1-21**).  $MS^2$  was selected because, on balance, it had lower and more consistent RSDs. Therefore to increase the overall reproducibility of the method *tetra* n-butylammonium nitrate was henceforth detected via SIM ( $m/z = 242.2$  amu) and benzyl-quat (**1-21**) was detected by  $MS^2$  ( $m/z = 212.1$  amu). Previously both compounds were detected by SIM. The full injection loop setting limited the injection volume to a maximum of 20  $\mu$ l. This injection volume was sufficient for samples that contain high concentrations of the analytes, however samples which contain low ppb amounts would require a larger injection volume. To determine the most appropriate injection volume for low ppb samples 10 and 100 ppb methanolic solutions of benzyl-quat (**1-21**) were each repeatedly injected (five repeats) whilst varying the injection volumes, and the RSDs were calculated for the associated peak area ratio to the internal standard (**5-4**), **Table 5:3**.

<b>Injection Volume</b>		<b>1 <math>\mu</math>l</b>	<b>2 <math>\mu</math>l</b>	<b>5 <math>\mu</math>l</b>	<b>10 <math>\mu</math>l</b>	<b>20 <math>\mu</math>l</b>	<b>50 <math>\mu</math>l</b>
<b>10 ppb injection</b>	<b>Average Area Ratio</b>	$5.41 \times 10^{-3}$	$4.60 \times 10^{-3}$	$5.43 \times 10^{-3}$	$7.02 \times 10^{-3}$	$10.00 \times 10^{-3}$	$11.00 \times 10^{-3}$
	<b>RSD</b>	23.46	39.77	13.69	7.96	8.54	1.52
<b>100 ppb injection</b>	<b>Average Area Ratio</b>	$3.12 \times 10^{-3}$	$3.27 \times 10^{-3}$	$4.45 \times 10^{-3}$	$5.35 \times 10^{-3}$	$6.35 \times 10^{-3}$	$6.57 \times 10^{-3}$
	<b>RSD</b>	8.61	11.48	3.39	2.43	1.58	4.51

**Table 5:3: 10 and 100 ppb injection data**

From the above data for the 10 ppb samples it was clear that increasing the injection volume dramatically reduced the RSDs, improving the reproducibility with the lowest RSD occurring for 50  $\mu$ l. The same general trend could also be seen for the data for the higher concentration 100 ppb samples, although the trend was not as pronounced. Therefore for a calibration spanning the lower ppb concentration range the injection volume was chosen to be 50  $\mu$ l.

To determine whether a calibration range spanning the lower ppb range of concentrations was possible a new calibration range was created, 5 to 100 ppb,  $n = 6$  which included the internal standard at 50 ppb, **Figure 5:5**. The linearity was greatly improved,  $R^2 = 0.9961$  which corresponded to an error of 0.4 % and therefore suitable for an ‘approved’ analytical method.

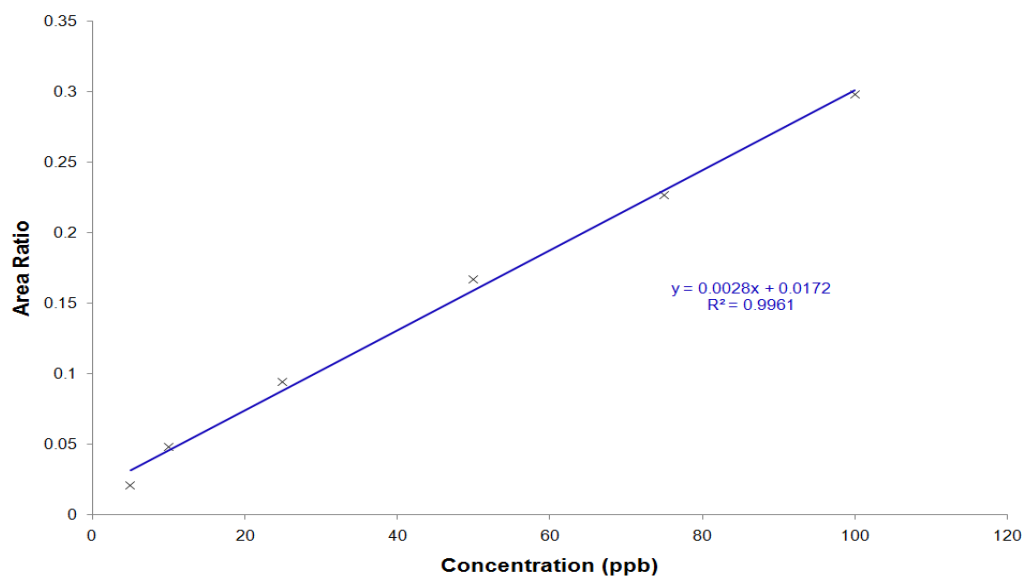


**Figure 5:5: Calibration plot: 5-100 ppb benzyl-quat (1-21) using internal standard (5-4)**

The current developed method would be suitable for the analysis of benzyl-quat (**1-21**) samples in organic solvent matrices. Unfortunately the LC-MS system was not compatible with samples/eluents which contained non-volatile salts, such as sodium chloride and consequently the anticipated samples were problematic. Therefore a pre-treatment step was required to remove the salt so that this method could be used to quantify quats in seawater. Solid phase extraction (SPE) was selected in an attempt to achieve this.

### 5.3 Solid Phase Extraction Development

SPE is a basic chromatographic technique which utilises phase separation between a suitable sorbent (stationary phase) and an elution solvent (mobile phase). The development of the SPE procedure for the benzyl-quat (**1-21**) was attempted prior to establishing the LC-MS methods for the other analytes, (didecyl-(**2-1**) and trioctyl-quats (**2-2**)). The ideal SPE procedure would elute the analyte directly into a 2 ml autosampler vial ready for LC-MS analysis. A rudimentary fractionation collection experiment was performed to determine whether the first 2 ml or a subsequent 2 ml elution aliquot contained the analyte. The initial eluent and stationary phase of the SPE process were based on the corresponding conditions in the LC-MS procedure, i.e.  $C_{18}$  stationary phase and ACN with 1 % acetic acid. Analysis of these 2 ml extracts and comparison with the original aqueous stock solution produced unpredicted results. There was a greater amount of the analyte present in the majority of each individual extracts, than was present in the original

aqueous sample, and significantly the cumulative total of the peak areas of the analyte in organic solvent was an order of magnitude greater than in the initial aqueous sample, **Table 5:4**.

<i>Sample</i>	<i>Peak Area (<math>\times 10^6</math>)</i>
<i>Extract 1</i>	1
<i>Extract 2</i>	13
<i>Extract 3</i>	51
<i>Extract 4</i>	106
<i>Extract 5</i>	121
<i>Extract 6</i>	100
<i>Extract 7</i>	89
<i>Blank</i>	4
<i>Aqueous Stock Solution</i>	57

**Table 5:4: SPE  
extractions**

extracts was not possible and therefore the development of the SPE was based on qualitative comparisons between the extracts and ‘blank’ samples.

The major difference between the 2 ml aliquots and the aqueous sample was the sample matrix. The different responsiveness of the analytes in different matrices has a major implication for the overall SPE-LC-MS method. If there is a different response from the analytes in different matrices it would require the matrix of both the extracted samples and the calibration standards be of the same composition. In short, the elution eluent used for the SPE process must be the solvent used to make up the calibration standard. Hence until the elution eluent was finalised, direct quantification of the SPE

The first stage of the development of the SPE protocol required the identification of the correct stationary phase of the SPE cartridges. To facilitate this, eight different phases along with twelve eluents were screened for their ability to retain and then release the analytes. The test phases covered a broad range from hydrophobic and hydrophilic, C<sub>18</sub> and CN, to cation exchange and polymeric phases. A stock solution containing the benzyl-quat (**1-21**) was prepared using distilled water as a surrogate for the seawater in an attempt to simplify the preliminary SPE development work. Following the screening process only four phase types were successful, which were substantially different in their chemical nature. The successful phases were CN, weak cation exchange (WCX) and two polymeric phases, styrene-divinylbenzene (SBL-B) and Strata-X, **Table 5:5**. The successful eluents were all composed of acidified acetonitrile, **Table 5:5**. Surprisingly, given the surfactant-like nature of the analytes it was discovered that pure organic solvents gave no elution from the sorbents.

Phase	Eluents											
	Water	ACN	MeOH	Water + 5% Acid	ACN + 1% Acid	ACN + 5% Acid	50:50 Water: ACN	90:10 Water: ACN	50mM Amm. Acetate	90:10 ACN 5% Acid: Water	90:10 ACN: Water 5% Acid	90:10 ACN 5% Acid: Water 5% Acid
C18 U	*	*	*	*	*	*	*	*	*	*	*	*
C18 E	*	*	*	*	*	*	*	*	*	*	*	*
C8	*	*	*	*	*	*	*	*	*	*	*	*
CN	*	*	*	*	*	✓	*	*	*	✓	(✓) poor recovery	✓
WCX	*	*	*	*	*	✓	*	*	*	✓	(✓) poor recovery	✓
X-CW	*	*	*	*	*	*	*	*	*	*	*	*
Strata-X	*	*	*	*	✓	✓	*	*	*	✓	(✓) poor recovery	✓
SBL-B	*	*	*	*	*	✓	*	*	*	✓	(✓) poor recovery	✓

**Table 5:5: SPE eluent and stationary phase search; (✓) – analyte successfully recovered, (\*) – no analyte recovered**

The four successful phases were further evaluated with a more extensive ranged of acidified acetonitrile eluents, and the peak areas for the benzyl-quat (**1-21**) in the first and each subsequent aliquot recorded, **Table 5:6**, **Table 5:7** and **Table 5:8**.

Sorbant	Extraction Aliquot (Peak Area)				
	1	2	3	4	5
CN	1.09×10 <sup>+8</sup>	2.41×10 <sup>+7</sup>	1.66×10 <sup>+8</sup>	-	-
WCX	1.13×10 <sup>+8</sup>	1.68×10 <sup>+7</sup>	1.15×10 <sup>+6</sup>	-	-
X	1.05×10 <sup>+8</sup>	6.83×10 <sup>+6</sup>	-	-	-
SDB-L	1.13×10 <sup>+8</sup>	5.99×10 <sup>+6</sup>	-	-	-

**Table 5:6: Elution eluent 90:10 ACN 5 % acetic acid:water 0 % acetic acid**

Sorbant	Extraction Aliquot (Peak Area)				
	1	2	3	4	5
CN	1.15×10 <sup>+8</sup>	1.65×10 <sup>+7</sup>	-	-	-
WCX	1.13×10 <sup>+8</sup>	6.91×10 <sup>+6</sup>	-	-	-
X	1.25×10 <sup>+8</sup>	5.22×10 <sup>+6</sup>	-	-	-
SDB-L	1.37×10 <sup>+8</sup>	2.15×10 <sup>+6</sup>	-	-	-

**Table 5:7: Elution eluent 90:10 ACN 5 % acetic acid:water 5 % acetic acid**

Sorbant	Extraction Aliquot (Peak Area)		
	1	2	3
CN	1.25×10 <sup>+8</sup>	3.62×10 <sup>+6</sup>	-
WCX	1.17×10 <sup>+8</sup>	3.62×10 <sup>+6</sup>	-
X	1.27×10 <sup>+8</sup>	5.05×10 <sup>+6</sup>	-
SDB-L	1.13×10 <sup>+8</sup>	3.82×10 <sup>+6</sup>	-

**Table 5:8: Elution eluent 90:10 ACN 10 % acetic acid:water 10 % acetic acid**

Appraisal of the above eluents and stationary phase data highlighted a trend; the more acidic the eluent the greater the recovery of the quat together with Strata-X being the best phase. Evident also was that it was not possible to extract all the quat in one 2 ml aliquot, because after repeat aliquot extractions there were still significant quantities of analyte being eluted. Since the proposed LC-MS method required the use of an internal standard, this necessitated that the internal standard was also added to the SPE extracts post extraction to enable them to be analysed. It is crucial that the final volume of the SPE extract is known, so the internal standard concentration was at the correct

level. Therefore the SPE process was modified. A 10 ml aliquot of stock solution was loaded onto the SPE cartridge and subjected to the SPE protocol. The extract was then transferred to a 10 ml volumetric flask and the appropriate volume of internal standard added and the flask made up to the mark. This ensured that the concentration of the analyte was the same as the initial sample, to allow direct measure of the efficiency of the SPE process.

A similar screening method to the one used to identify the correct stationary phase and eluent was then used to identify the correct bed volume of the SPE cartridges given the 10 ml samples size. This was identified to be 200 mg.

A rudimentary SPE recovery test comparing quat samples in seawater and distilled water matrices highlighted the need for a wash step to be included in the SPE protocol, due to the presence of a fine precipitate in the recovered extracts from the seawater samples, which was absent in the distilled water samples. Evaluation of different eluents for the wash step found that both distilled water and acidified distilled water performed adequately. Crucially they were both incapable of eluting the analyte from the cartridge. Given the previously established requirement for acidified eluents to elute the quats, acidified distilled water was preferred as the wash step because it prevented any sudden changes in pH during the SPE procedure. The optimal SPE protocol as determined at this stage was, **Table 5:9**:

<b>Conditioning:</b>	i) 5 ml acetonitrile ii) 10 ml distilled water
<b>Load Sample:</b>	10 ml sample at constant rate of 20 ml min <sup>-1</sup>
<b>Wash:</b>	10 ml distilled water with 10% acetic acid
<b>Elution:</b>	8.5 ml of 90(A):10(B); A is acetonitrile acidified with 10% acetic acid, B is distilled water with 10 % acetic acid
<b>Post Step:</b>	Transfer to 10 ml volumetric flask; add internal standard and made up to 10 ml with SPE eluent solution

**Table 5:9: SPE protocol**

This SPE protocol was then tested for robustness for both distilled water and seawater matrices samples by repeating the procedure 5 times at 2 different benzyl-quat (**1-21**) concentrations, 5 and 50 ppb, **Table 5:10**.

<b>Repeat</b>	<b>Distilled Water</b>		<b>Seawater</b>	
	<b>5 ppb</b>	<b>50 ppb</b>	<b>5 ppb</b>	<b>50 ppb</b>
<b>1</b>	3.15	46.08	4.78	41.22
<b>2</b>	2.89	41.46	3.15	41.78
<b>3</b>	1.75	48.76	2.30	36.31
<b>4</b>	3.16	46.63	1.62	31.33
<b>5</b>	-	41.87	1.52	32.08
<b>Average</b>	2.74	44.96	2.67	36.54
<b>RSD</b>	24.45	7.05	50.38	13.44

**Table 5:10: Recovery results from initial attempts to improve SPE process**

The results in **Table 5:10** demonstrated that the SPE protocol appeared adequate for distilled water matrix samples at both concentrations. At the higher benzyl-quat (1-21) concentration the mean recovery was 44.96 ppb which represented approximately 90 % recovery for the SPE process. The relative standard deviation of 7 % demonstrated that the method was reproducible. At the lower concentration the results were not as successful with the average recovery just 2.7 ppb for a 5 ppb sample, which was a 54 % recovery with the corresponding RSD for the process also higher. However, taking into consideration that 5 ppb was the lowest standard of the calibration, it was anticipated that there would be an increased RSD at the lower end of the calibration. Therefore the statistics for distilled water matrix samples were deemed to be adequate. (The 5<sup>th</sup> repetition of the 5 ppb distilled water sample had a significantly higher recovery than the remaining 4 aliquots. The 10 ml flask used to make this sample had previously been used for the 100 ppb standard; as a consequence this result was omitted from the table). When compared, the statistics for the distilled water and seawater samples were not favourable; the RSDs for both test concentrations in seawater were approximately double the comparable RSDs for the distilled water samples. The average recoveries were also significantly lower.

Initial efforts to rectify this disparity in results involved increasing the wash step from 10 to 20 ml in an attempt to ensure that there were no compounds, particularly salts, co-eluting with the quats from the artificial seawater which were absent in the distilled water. Unfortunately this proved unsuccessful, **Table 5:11**, but for subsequent SPE testing the larger volume wash step was retained.

Repeat	5 ppb		50 ppb	
	Same Flask	Different Flasks	Same Flask	Different Flasks
1	2.48	2.48	49.24	49.24
2	3.55	3.43	53.72	51.52
3	2.04	5.56	45.37	45.33
4	1.16	6.82	37.75	46.27
5	0.62	5.41	33.02	52.15
Average	1.97	4.74	43.82	48.90
RSD	43.02	37.00	19.20	6.24

**Table 5:11: Recovery results from initial attempts to improve seawater SPE process**

Analysis of the SPE results in **Table 5:11** showed that the SPE method appeared reproducible from different flasks as the average recoveries and RSDs were acceptable at both concentrations. However when taking repeat aliquots from the same flask there was a significant deterioration in the recovery with repetition, as exemplified by the 50 ppb seawater samples changing by 17 ppb over the five aliquots. The major difference between these replicates was the time between the sample stock solution being made and the time when the five aliquots were extracted. Therefore the deterioration was time dependent rather than replicate dependent. When this was considered together with the surfactant nature of the analytes, the deterioration was likely to be due to loss of the analytes to the surface of the glassware. This was confirmed by a slight modification to the

SPE process. Two 50 ppb seawater samples were made up in 10 ml volumetric flasks and their contents subjected to the established SPE protocol with a 20 ml wash step. However, for one sample, prior to the addition of the 8.5 ml of eluent to the SPE cartridge, this eluent aliquot was first swirled around the inside of the 10 ml flask and then inserted directly into the cartridge from the flask. The SPE method was then followed without further alteration. The results demonstrated an increased level of recovery for the washed flask sample (45 ppb) compared to the unwashed glass (41 ppb), this highlighted that the losses observed were due to the adsorption of the analyte to the surface of the glassware. It was likely that the adsorption was due to the interaction between the positively charged cation of the quats and exposed silanol groups of the glass.

### 5.3.1 Surface Adsorption Test

In order to find a replacement surface to glassware and eliminate the adsorption of the analyte, several alternatives to standard borosilicate glassware were evaluated. The alternatives were three different types of plasticware (polypropylene (PP), polymethylpentene (PMP) and a perfluoroalkoxyl copolymer (PFA)) together with two borosilicate glassware treated with two different surface silanising agents (Siliconize L-25 and Sigmacote SL-2) and a standard borosilicate as a control. All were 100 ml volumetric flasks to ensure a comparable surface area for adsorption. Equivalent plastics from two different manufactures (Kartell and Nalgene) were included to compare different suppliers.

The test protocol was: 50 000 ppb benzyl-quat (**1-21**) seawater solution was made in each 100 ml flask and left for 30 mins to fully saturate the surface. The flasks were then emptied and thoroughly rinsed three times with deionized water to ensure that any benzyl-quat (**1-21**) transferred in solution, rather than surface contamination, would be insignificant. An 8.75 ml aliquot of the SPE eluent was then placed into each 100 ml flask and swirled round to fully desorb any analyte. This liquor was then transferred to a 10 ml volumetric flask, internal standard added, made up to the mark and analysed. Following a rinse with water an additional 8.75 ml aliquot of SPE eluent was added to the 100 ml flask and the process repeated to determine if all the quat was removed in the first wash, **Table 5:12**.

<i>Volumetric Flask</i>	<i>First Solvent Wash (ppb)</i>	<i>Second Solvent Wash (ppb)</i>
<i>Nalgene (PP)</i>	282	23
<i>Nalgene (PMP)</i>	401	53
<i>Kartell (PMP)</i>	397	21
<i>Siliconize L-25</i>	451	112
<i>Sigmacote SL-2</i>	528	138
<i>Perfluoroalkoxyl polymer</i>	208	6
<i>Control (Untreated borosilicate)</i>	344	119

**Table 5:12: Recovered benzyl-quat (1-21) from volumetric flasks made of different materials**

The results clearly demonstrated that there was a significant level of adsorption to all surfaces, including the silanised glassware and the fluoro-plastic, which retained the least. Washing the flasks with the SPE eluent clearly desorbed the quat from the surface of the flasks as the recovery in the second wash was significantly reduced in all cases. These results demonstrated that a thorough cleaning protocol was required to ensure that there was no significant build up of residue of the analyte at the surface of the flasks. Evaluation of each surface against the control (untreated borosilicate glassware) draws unfavourable conclusions. All the surfaces except Nalgene (PP) and PFA polymer adsorbed more quat than untreated glassware. In short, these attempts to reduce the adsorption of the quat onto the flasks actually exacerbated the problem. The results of the second wash were more discriminating between the surfaces. All the glassware flasks (control, Siliconize L-25 and Sigmacote SL-2) retained a comparable level of quat from the first extraction, and hence, silanisation of the glassware surface had no benefit when trying to prevent quat adsorption. The results also suggested that the adsorption of the quats to the surface of the plasticware was not as strong as to glassware because the amount of quat present in the second wash from all the plasticware surfaces was an order of magnitude lower than from the control. However none of the surfaces completely prevented the adsorption of the quat and consequently, if these surfaces were to be used to attempt to quantify the release of the quats, the results obtained would be lower than the actual levels due to the losses from adhesion to the glassware during the experiment.

No quat was detected in the aqueous rinsing between the first and second solvent washes, signifying that the quat remained strongly adsorbed to the surfaces in aqueous solutions. This indicated that the analytes can easily withstand transference from aqueous solution to solution if not removed as all the second solvent washes contained quat. This result posed a question: *would aqueous samples made up in glassware pre-saturated with the analyte be stable, or would the analyte become desorbed from the glassware increasing the concentration in the sample flask?* To evaluate this two 100 ml volumetric flasks and the additional glassware which came into contact with the analyte were first ensured to be pristine by soaking overnight in a solution of a non-cationic cleaning detergent, Decon 90. Following this all the glassware was thoroughly rinsed three times with water to remove the cleaning agent and then soaked in a 50 000 ppb solution of the benzyl-quat (**1-21**) in artificial seawater and left overnight to ensure that the surfaces were fully saturated with quat. Following a thorough rinsing, benzyl-quat (**1-21**) seawater samples at the two concentrations, 5 and 50 ppb, were prepared in the pre-treated flasks and five repeat aliquots from each sample were subject to the SPE protocol, **Table 5:13**.

Repeat	5 ppb Same Flask	50 ppb Same Flask
1	2.84	56.10
2	3.27	58.05
3	3.65	52.92
4	3.11	53.69
5	3.25	50.83
Average	3.22	54.32
RSD	10.49	5.18

**Table 5:13: Results for the recovery of benzyl-quat (1-21) with glassware pre-soaked with benzyl-quat (1-21)**

The results in **Table 5:13**, clearly demonstrated that the benzyl-quat (**1-21**) did not appreciably desorb from pre-treated glassware and the samples were stable in the working concentrations.

## 5.4 LC-MS Development for Other Quats

The above LC-MS method was then used to create a calibration plot of 5 - 100 ppb for both the didecyl-(**2-1**) and trioctyl-quats (**2-2**) analytes. The resulting plot was comparable in terms of linearity to that calculated for the benzyl-quat, **Figure 5:6**.

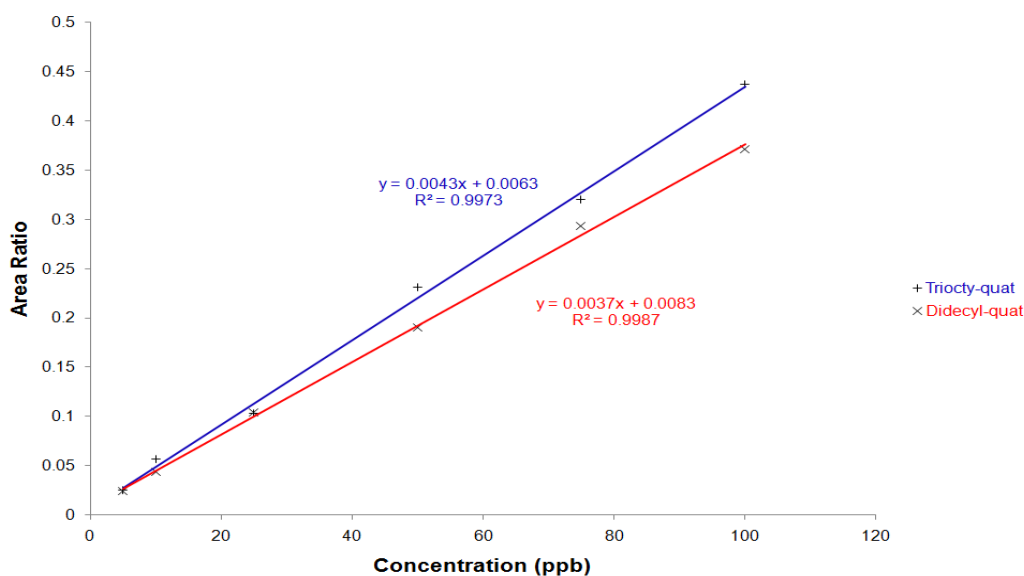


**Figure 5:6: Amalgamated calibration plot: 5-100 ppb trioctyl-(2-2) and didecyl-quat (2-1) with Internal Standard (5-4)**

The same recovery process of repeated aliquot SPE, as outlined above, was used with the analyte and the quat used to saturate the glassware replaced with didecyl-quat (**2-1**), **Table 5:14**.

Repeat	5ppb		50ppb	
	Same Flask	Different Flasks	Same Flask	Different Flasks
1	5.84	5.84	50.22	50.22
2	6.82	2.90	42.52	45.55
3	5.65	3.33	43.84	56.67
4	6.27	6.30	44.00	40.64
5	8.01	4.21	45.75	43.61
Average	6.52	4.52	45.27	47.34
RSD	8.46	33.28	7.17	13.24

**Table 5:14: Results for the recovery of didecyl-quat (2-1) with glassware pre-soaked with didecyl-quat (2-1)**

The results in **Table 5:14** demonstrated the applicability of pre-saturating the glassware with a strong solution of the target quat analyte. The averaged recoveries from the same flasks at both concentrations were 130 % (5 ppb) and 92 % (50 ppb), which suggested that the samples were stable in solution. Given that the SPE process was a manual operation and when the issues of sample stability were considered, recoveries above 90% represent a significant accomplishment. The results from the different flasks demonstrated that the manual SPE process was reproducible. The RSD for the 50 ppb samples from different flask was 7.2 % while it was higher for the 5 ppb sample at 33.3 %. It was anticipated that the RSD would be higher for the lower concentration sample, as this is close to the limit of linearity of the calibration range.

The retention times of analytes were 2.68 mins, trioctyl-quat (**2-2**), and 2.87 mins for didecyl-quat (**2-1**), both of which were longer than those for the internal standard (**5-4**) and the benzyl-quat (**1-21**). Consequently there was scope to reduce the number of analytical methods by combining two analytes into one method. Unfortunately because of the similarity in retention times between the didecyl-(**2-1**) and trioctyl-quats (**2-2**) these compounds required separate methods. While the two analytes had separate ions and fragmentation ions which presented no problem for the MS detector, the difficulty was the small difference in retention time between the analytes and the limitations of the MS software in switching rapidly between SIM and MS<sup>2</sup> for different analytes. Therefore didecyl-(**2-1**) and benzyl-quats (**1-21**) were combined into a new method. The MS was re-configured to detect both analytes at their prospective retention times, and one set of calibrants was prepared, which contained both analytes at the 0.1-100 ppb concentration range, **Figure 5:7**.

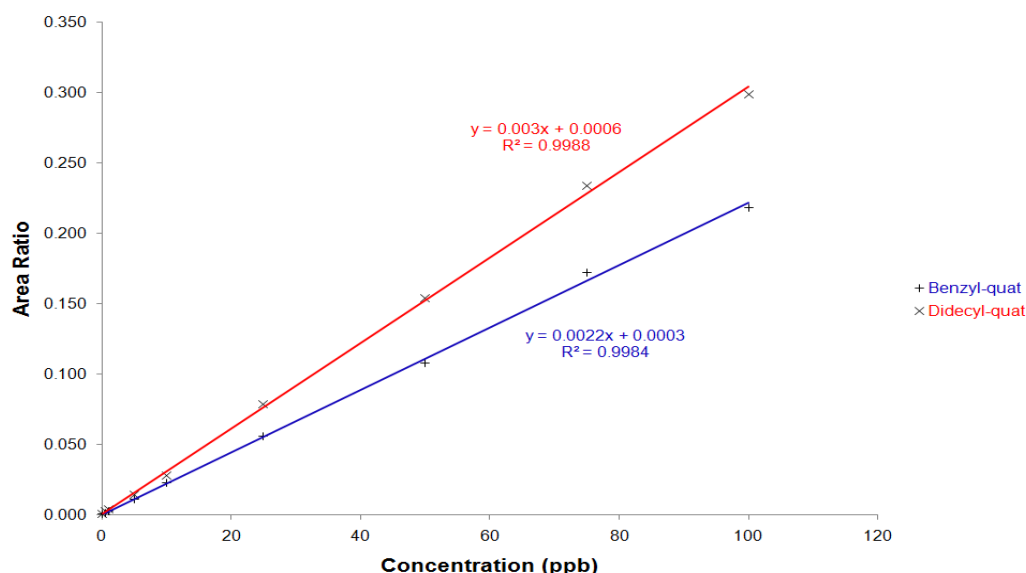


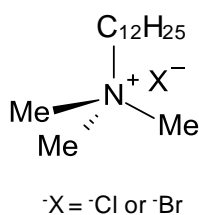
**Figure 5:7: Calibration plot: dual quat method**

Using this dual method and the method established for the trioctyl-quat (2-2) the limits of detection (LOD) and quantification (LOQ) for the analytes were determined, **Table 5:15**. The LOQ was calculated based on  $\times 10$  the standard deviation of a blank and the LOD was  $\times 3$  the same standard deviation; both values were found to be in the part per trillion (ppt) range.

Analyte	Limit of Detection (ppt)	Limit of Quantification (ppt)
benzyl-quat	146	487
didecyl-quat	151	503
trioctyl-quat	30	97

**Table 5:15: Calculated limits of the developed analytical methods**

At this stage it was decided to identify which quat should be used as the pre-saturation quat for the glassware. Should unexpectedly high recoveries be obtained while using the same quat for the pre-saturation and analyte the immediate suspicion would be that the quat had desorbed from the glassware compromising the validity of the results. Therefore an alternative quat was sought which was used solely to pre-saturate the surface of the glassware. Dodecyltrimethylammonium halide (pre-saturation-quat) (5-5) was a quat which was structurally similar to the target analyte quat and hence would be expected to exhibit similar chemical properties, **Figure 5:8**.



**Dodecyltrimethylammonium Halide**

**Figure 5:8: Structure of dodecyltrimethylammonium halide (5-5)**

This quat was used to replace the target analyte quats in the dual method as the soak solution and the stability of solutions of the analytes in glassware pre-treated with dodecyltrimethylammonium halide (5-5) was determined by repeat SPE, **Table 5:16**.

Repeat	benzyl-quat				didecyl-quat			
	5 ppb		50 ppb		5 ppb		50 ppb	
	Same Flask	Different Flasks	Same Flask	Different Flask	Same Flask	Different Flask	Same Flask	Different Flask
1	6.72	6.72	64.97	64.97	5.92	5.92	46.79	46.79
2	6.50	5.78	58.18	44.61	5.99	5.74	38.51	46.83
3	6.75	6.19	55.80	44.40	5.64	4.75	37.19	48.10
4	6.00	6.50	56.59	49.10	5.24	5.48	38.13	46.31
5	5.92	7.63	51.02	52.13	3.86	5.48	33.50	49.80
<b>Average</b>	6.38	6.57	57.31	51.04	5.33	5.48	38.62	47.57
<b>RSD</b>	5.36	10.75	8.81	16.53	5.94	8.16	13.36	2.97

**Table 5:16: Repeat SPE results with glassware soaked with pre-saturation-quat.**

The results in **Table 5:16** demonstrated the validity of using dodecyltrimethylammonium halide (5-5) as the pre-saturation-quat. For both analytes, and at both concentrations, the average recoveries from the five replicates were, in general, above 92 % of the original sample concentration and therefore this method will be used for the future analysis of both analytes. The variation in the percentage recoveries, 76 - 130 %, when considering the SPE-LC-MS protocol as a whole, was acceptable because there was a large manual component to this protocol. The manual component comprised a number of key procedures which are integral to the robustness of the protocol which could not be optimised further. Hence there was a significant portion of the error/variance in the method which was operator dependent. A number of steps were taken to minimise these errors, such as limiting the vacuum on the SPE pump, ensuring a consistent flow rate through the SPE cartridge, as well as the use of auto-pipettors for the manipulation of specific volumes of liquids. However, no suitable auto-pipetter was available for the addition of the 10 ml of quat containing seawater onto the SPE cartridge. This was achieved through multiple additions of 5 ml, which represented a possible cause for the variation in the final analysed sample, because this directly influenced the amount of quat which passed through the whole SPE protocol. Deficiencies in the volume loaded onto the SPE cartridge (i.e. less than the prescribed 10 ml) would result in corresponding lower quantified samples.

An additional difficulty being that it was not possible to totally eliminate the use of glassware and plasticware from the protocol, both of which have been shown to adsorb the analytes which adversely affects the results. The validity of the use of the pre-saturation-quat to regulate the adsorption of the quats onto the surface of glassware was only applicable to aqueous solutions of quats, and not applicable to organic solvent quat solutions, because organic solvents were shown to desorb quats from the surface. Therefore the organic solvents would also desorb the pre-saturation-

quat as well. At the same time the calibrants and samples in auto-sampler vials were shown to be unstable, presumably due to slower rates of adsorption to the surface of the glassware. However, from the previous calibration plots the samples were sufficiently stable to enable calibrations with excellent linearity over the 50 – 100 000 ppt concentration range,  $R^2 = 0.9988$  and  $0.9984$  for benzyl- and didecyl-quat respectively. In an attempt to minimise losses of the quat samples to the surface of the auto-sampler vials, silanised vials were used exclusively throughout this thesis.

There were also limitations associated with the LC-MS setup which would also affect the reproducibility of the combined protocol. The MS used as part of the LC-MS in this thesis was an ion trap MS which was particularly well suited for qualitative analysis, or structural identification of analytes, but not quantification for which a triple quadrupole MS was most suited<sup>199</sup>. This was because the ion trap MS was capable of ‘trapping’ and isolating ions within the ‘ion trap’ of the MS through a combination of the quadrupole lenses and the oscillating voltage. Ions are then ejected and analysed, on demand, by altering the oscillating voltage. The limitation of this setup was that the ‘ion trap’ can only contain a limited number of ions (i.e. it has a more limited dynamic range) which is problematic for trace analysis in dirty matrices (quats in seawater) as the trap becomes filled with both trace analyte ions (very small number) and matrix ions (large number).

A more suitable MS setup would be a triple quadrupole MS which has a better dynamic range and sensitivity as, uniquely, this MS is capable of performing multiple reaction monitoring (MRM) because its quadrupoles are separately tuneable. The first quadrupole is set to isolate the parent ion, which when passed into the second quadrupole (collision chamber), is shattered into characteristic fragments. These fragment ions are then isolated in the third quadrupole. The ratio of fragment ions to parent ion is reproducible and characteristic for each analyte, ensuring a greater level of precision enabling more consistent quantification.

## 5.5 Development of Leaching Protocol

The developed leaching protocol was based on a modified Ketchum Bubbler method<sup>195</sup>. This test method was designed to simulate and then enable the prediction of the leaching of copper compounds from antifouling coatings on vessels during stationary periods. As such, it used panels coated with the test antifouling coating which were used as mimics for whole vessels. These panels were prepared in triplicate and fully immersed in a storage tank containing seawater, which mimics the stationary vessels in a harbour for example, during which period the biocide/analyte was continually released from the coating. In order to measure the leach rate, panels were removed from the storage tank after a known period of time and placed into beakers containing fresh ‘clean’ seawater. The panels were then left immersed in these beakers for a predetermined time interval after which they were removed and replaced in the storage tank. The ‘exposed’ seawater in the

beakers was then sampled and analysed for its biocide content which, combined with the time interval the panels were immersed in the beakers was used to calculate the release rate at that specific point of time. Repeated point measurements were then made over the period of time the panels were on test immersed in the storage tank and used to construct the leach rate profile. Therefore in order to utilise this established test protocol for the quats, a number of key factors needed to be evaluated and modified to ensure the suitability of this method for the new analytes. These included:

- 1) The current embodiment of the leaching protocol required that the pre-saturation-quat procedure was suitable for larger volume glassware.
- 2) To perform the whole SPE-LC-MS analytical procedure on each panel/beaker one at a time was likely to result in large variations in the time between the removal of the panels from the beakers at the end of the release rate test and the sampling of the final beaker of the set. This variation could be reduced by loading the samples onto SPE cartridges one at a time and then eluting then all at once. Therefore it needed to be determined whether the analytes were stable stored on the SPE cartridges.
- 3) The current testing regime used 1.5 l of seawater for each panel, which were coated with 100 cm<sup>3</sup> of test antifouling coating. That these volume and surface area were suitable for the quat leaching needed to be ascertained.

The suitability of the pre-saturation-quat (5-5) protocol was evaluated by first ensuring that two 2 l beakers were thoroughly cleaned using the non-cationic detergent, Decon 90, then one beaker was treated with the pre-saturation-quat (5-5) protocol. 1.5 l of seawater solution containing both didecyl- and benzyl-quat analytes at 20 ppb was made up in both beakers and monitored for the concentration of both quats with time and the results compared, **Table 5:17**.

	<i>Time/hrs</i>	<i>0.5</i>	<i>1.5</i>	<i>2</i>	<i>4</i>	<i>5</i>	<i>6</i>	<i>24+</i>
<i>Pre-saturation-quat</i>	<i>benzyl-quat</i>	22.00	19.76	20.09	22.40	22.28	20.49	20.34
	<i>didecyl-quat</i>	23.50	22.37	21.52	23.20	25.22	26.58	21.76
<i>Untreated Beaker</i>	<i>benzyl-quat</i>	22.00	20.36	21.13	18.03	20.84	19.93	16.63
	<i>didecyl-quat</i>	16.60	18.91	18.41	15.83	17.05	16.73	11.85

**Table 5:17: Measured concentrations of both benzyl- and didecyl-quat in treated and untreated 2 l beakers**

The results in **Table 5:17** showed that quat solutions were stable in a beaker treated with the pre-saturation-quat protocol. There was only limited change in the concentration of both analytes over a 24 hr period. After 25 hrs the concentrations of didecyl- and benzyl-quats in the beaker treated with the pre-saturation-quat (5-5) were 21.76 and 20.34 ppb respectively, which were both significantly higher than the results from the untreated beaker (11.85 and 16.63 ppb). It is also clear from the stability data that the didecyl-quat was the least stable in solution.

The stability of the analytes once loaded onto an SPE cartridge was checked by loading four groups of four SPE cartridges with 10 ml samples from the same seawater containing both analytes at 50 ppb. One group of cartridges was then eluted and the concentration of both analytes established. This process was repeated with each of the remaining three groups of cartridges after 3, 7 and 10 days storage in a refrigerator at 5 °C, **Figure 5:9**.

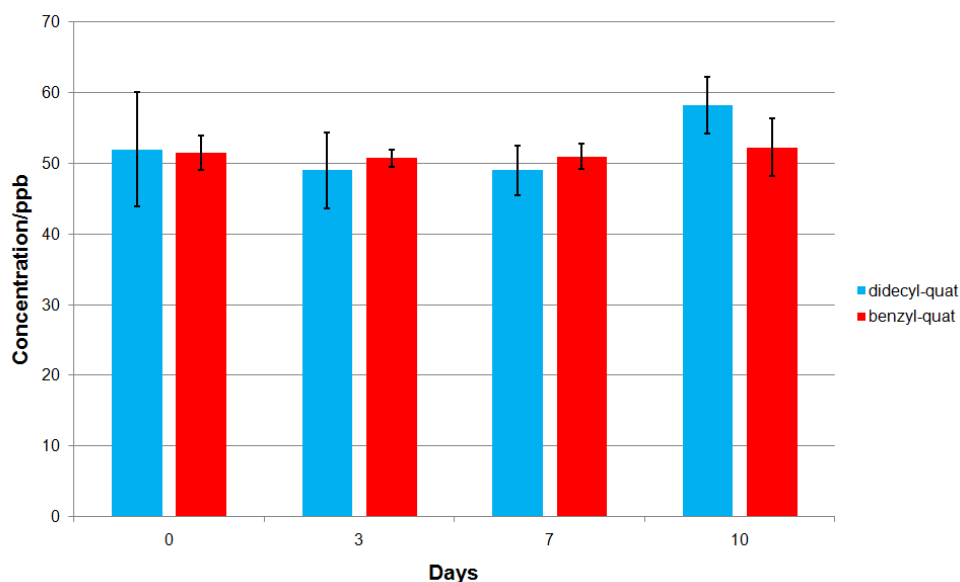


**Figure 5:9: Average recoveries from 'loaded' SPE cartridges stored for 3, 7 and 10 days. Error bars are 95 % confidence limits.**

As can be seen from **Figure 5:9** the average recovered amount of both analytes was, within experimental error, consistently 50 ppb over the 10 day storage period which demonstrated that quats 'loaded' onto SPE cartridges were stable and do not degrade. Therefore storage of 'loaded' SPE cartridges will not result in the loss of the quat analytes which enables elution of the analyte on a different day to which they were obtained.

A mock leaching test was then performed to enable final tuning of the leaching protocol for the quats, based on the modified Ketchum Bubbler method. This test monitored four panels over a 23 day trial period. The panels were coated with 100 cm<sup>3</sup> of the test formulation which were: a didecyl-quat polymer, a trioctyl-quat polymer, a polymeric coating containing 'free' benzyl-quat and a didecyl-quat paint. The didecyl- and trioctyl-quat polymers were anticipated to display controlled release properties, while the polymeric coating containing 'free' benzyl-quat was expected to display a classic logarithmic profile characteristic of uncontrolled release. A quat containing paint formulation was also included to enable the difference in polymer and paint formulation release rates to be established. These panels then followed the leaching protocol established in modified Ketchum Bubbler method which used 1.5 l of seawater in the glass beakers. **Figure 5:10** shows the results after 23 days.

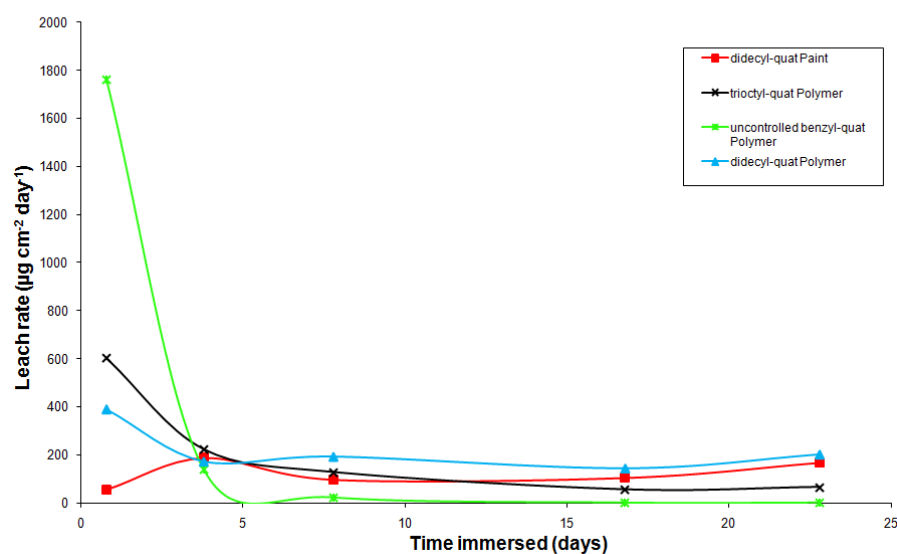


**Figure 5:10: Trial leach rate profiles for didecyl-, trioctyl- and benzyl-quat polymers together with a didecyl-quat paint formulation**

The above figure demonstrated that both the didecyl- and trioctyl-quat polymers displayed the anticipated controlled release of the quats as after 100 hrs immersion as the release rate of the analytes appears to be constant with time. Clear also was that the polymer containing the ‘free’ benzyl-quat displayed a significantly different release profile to the other coatings. The profile was logarithmic in shape as would be anticipated for a biocide which was not controlled in its release<sup>24</sup>. The didecyl-quat paint displayed a lower initial release rate than its corresponding polymeric coating, which was also anticipated, because in the paint formulation the didecyl-quat polymer is only approximately 15 wt% of the dry film volume of the paint, compared to 100 wt% for the polymeric coating.

Although this initial trial clearly demonstrated the suitability of the established method, the amount of analytes released and quantified in the glass beakers was well outside the established calibration range, i.e. the samples contained up to 4000 ppb of analyte for 15 mins leaching in the clean seawater, which was outside of the established 0.05 – 100 ppb calibration range. Since the quantified amounts were well outside the established calibration range the reliability of the results was in question because the samples concentrations were outside of the established linear range of the detector. Therefore in an effort to rectify this issue the leaching panels and the coated area of the test formulations were reduced in size so that the test formulation were now 25 cm<sup>3</sup> together while reducing the volume of the seawater used in the glass beakers to 400 ml. These new parameters will be used, together with those established earlier, for a more rigorous leaching trial of the quat containing coatings which will be the subject of Chapter 6

## 6 Quat Leaching Experiment

As elucidated earlier, the determination of the release rate of biocides from antifouling coatings is dually important both from regulatory and developmental perspectives. Release rate methods are required by regulatory authorities in some countries as part of a risk assessment for determining the suitability of antifouling products for use in the marine environment. However, release rate methods are primarily utilized by antifouling coating manufacturers to aid their product development. The determination of the release rate of the biocide from the coating is a vital part of product development as once the release rate of a biocide from a particular coating formulation is determined; the effects from both formulation changes and polymer architecture developments become apparent. Determination of these relationship enables the longevity of the biocide to be maximised ensuring the antifouling coating provides the longest protection possible for that system.

Until now analysis of the release rates of quat-biocides has not been attempted due to the lack of a suitable analytical protocol for the quantification of the quat-biocides (*see Chapter 5, section 5.5*). A further research question to investigate was whether the alterations to quat-polymer architecture would affect the release rate of quat-biocides. To address both issues four different didecyl-quat containing coatings were developed and the didecyl-quat release rate for each coating types was measured.

### 6.1 Coating Development

#### 6.1.1 AMPSQ(I)v10 Paint

The paint was manufactured as described previously (*see Chapter 2, section 2.3; Chapter 3, section 3.3 and Chapter 4, section 4.3*) i.e. by the creation of uniform dispersions of the raw materials in the binder using high speed dispersion (HSD). The previously described prototype paint formulation was used without modification along with the same AMPSQ(I)v10 polymer as described in Chapter 4. The final paint was monitored for grind and viscosity (data presented in the Experimental section).

#### 6.1.2 AMPSQ(I)v10 Polymer

The AMPSQ(I)v10 polymer as previously developed and tested in Chapter 4 was modified by the addition of a plasticiser to improve the mechanical properties of the clear coatings to prevent cracking during the leaching experiment. The plasticiser was the same compound (Jayflex DINP - an aromatic dicarboxylate) added at the same ratio to AMPSQ(I)v10 polymer as was used in the AMPSQ(I)v10 paint formulation (*see Chapter 2, section 2.3 and Chapter 4, section 4.4*).

### 6.1.3 Free Association Didecyl-Quat Paint

In the initial development of the leaching protocol a rudimentary coating in which benzyl-quat was physically dispersed within the AMPSQ(II)v4 polymer was used to identify what likely ‘uncontrolled release’ rates of quats would be because this paint formulation would represent a free association of the quats within the AMPSQ(II)v4 polymer matrix. This coating was not suitable for this more rigorous leach rate experiment because released quat (benzyl-quat) was different to that being released from the other coatings in the leach rate experiment (didecyl-quat). The use of two different quats would not enable the leach rates from different coatings to be directly compared due to different solubility of the quats. To remove this variance, a new coating was developed. At the same time the polymer into which the quat was freely associated was also changed. Previously it had been the non-biocidal AMPSQ(II)v4 polymer. However, this polymer was expected to perform in an analogous fashion to the AMPSQ(I)v10 polymer, i.e. releasing the tethered trioctyl-quat (**2-2**) through the same cation exchange reaction with seawater. As the AMPSQ(II)v4 polymer relied on the cation exchange suggested that it was not the best choice for a control matrix. Therefore an alternative polymer which did not release quat, but still performed a similar polishing reaction was sort. Such a polymer already existed within International Paint polymer library, and this polymer underwent the same exchange mechanism but importantly the exchange was between the **anion** of the polymer and the **anions** present within seawater, **Figure 6:1**. Crucially this polymer did not release quats and therefore was considered to be a better control matrix than AMPSQ(II)v4.

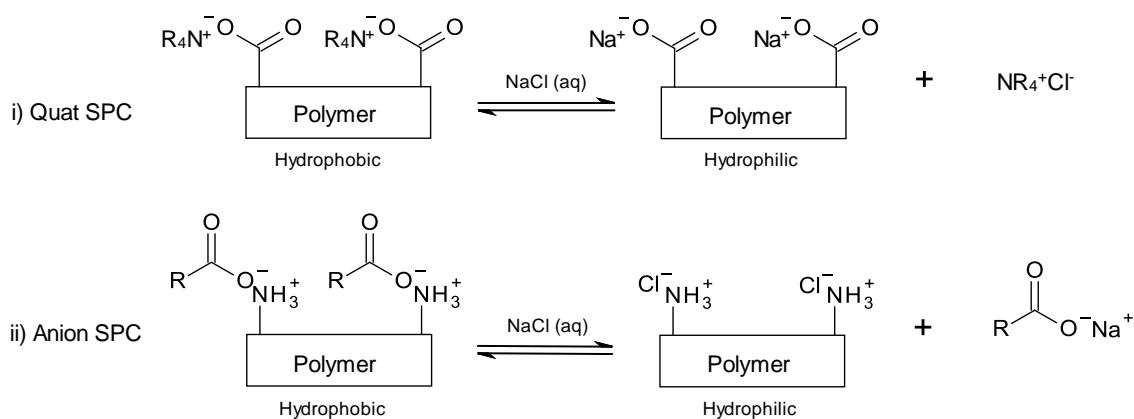


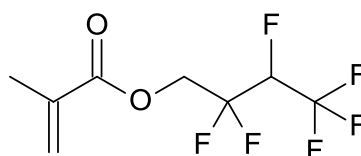
**Figure 6:1: Example of mediated ion exchange reaction of different SPCs systems i) quat SPC and ii) anion SPC**

Therefore an additional prototype paint was prepared in an analogous fashion to those prepared to evaluate the experimental polymers of Chapter 2, 3 and 4; i.e. systematic replacement of the binder of the prototype formulation with the new anion-SPC polymer, ensuring that the test paint was equivalent in terms of volume solids and co-biocide content to the others in the leaching experiment. Furthermore this paint was also formulated to contain the same wt% of didecyl-quat

(2-1) as contained within the other coatings to guarantee a comparable leach rate test. The final paint's grind and viscosity was also checked (data presented in the Experimental Chapter).

#### 6.1.4 AMPSQ(I)v10 FB Paint

The ability of the AMPSQ polymers to interact with seawater, which have been shown to be strongly influenced the hydrophilicity of the polymer (*see Chapter 4, section 4.4.2.1*) was likely to have an effect on the release rate of the didecyl-quat (2-1). The release rate of the quat-biocide was proposed to be controlled by the polishing rate of the polymer, which is ultimately affected by the rate of the cation exchange reaction and dissolution rate of the hydrophilic sodium salt of the acid functionalized polymer. Consequently an additional AMPSQ polymer was prepared which was a minor modification of the AMPSQ(I)v10 polymer, in that the entire BMA (3-7) component was replaced with a fluorinated structural analogue, 2, 2, 3, 4, 4, 4 – Hexafluorobutyl methacrylate (HFBMA, 6-1), **Figure 6:2**, which was predicted to be significantly less hydrophilic.



2, 2, 3, 4, 4, 4 – Hexafluorobutyl  
methacrylate

**Figure 6:2: Structure of 2, 2, 3, 4, 4, 4 – Hexafluorobutyl methacrylate (6-1)**

The new polymer was synthesised via the same free radical polymerisation reaction as elucidated in Chapter 4. The monomer feed composition was 28.3 mol% AMPSQ(I) (4-1), 68.3 mol% iBoMA (3-5) and 3.4 mol% HFBMA (6-1). The polymerisation was performed at 85 °C with a 3.5 hour monomer feed upon completion of which the temperature was raised and maintained at 95 °C for a further 2 hours. At the start of the 2 hour period and again 1 hour later a 0.5 mol% initiator was added to the reaction. The final polymers were formulated to be 50% solids in 3:1 xylene:butanol to create a simple polymeric solution which could be incorporated into a prototype paint formulation. The polymer was characterised in terms of <sup>1</sup>H NMR, viscosity, percentage non-volatile content (NVC), specific gravity (SG), total unreacted monomer molar percentage and unreacted monomer molar percentage, number average molecular weight ( $M_N$ ), weight average molecular weight ( $M_W$ ) and polymer polydispersity (data presented in the Experimental Chapter).

A final paint was prepared from this fluorinated version of AMPSQ(I)v10 as previously described in terms of prototype paint formulation and HSD method without modification as described in Chapter 4. The final paint was monitored for grind and viscosity (data presented in the Experimental section).

## 6.2 Leaching Panel Preparation

Three polycarbonate panels (11.0 x 6.5 cm) were prepared for each of the above four test coatings. After the mass of the panels had been determined a 25 cm<sup>3</sup> area was masked off and the subsequent area lightly abraded. Two coats of one of the four test coatings was applied to the masked area of three of the panels, monitoring the mass of wet paint applied each time to maintain a consistent mass of paint on each of the three panels. After the panels had dried for 7 days at ambient temperature and the removal of the masking the final mass of paint applied to panel was determined, **Figure 6:3** and **Table 6:1**.



**Figure 6:3: Photograph of four types of final leaching panel**

<i>Panel</i>	<i>Final Panel Mass/ g</i>	<i>Initial Panel Mass/ g</i>	<i>Mass of Applied Paint/ g</i>
<i>Free Association 1</i>	17.79	17.23	0.56
<i>Free Association 2</i>	17.30	16.77	0.53
<i>Free Association 3</i>	17.52	16.92	0.60
<i>AMPSQ(I)v10 FB 1</i>	17.75	17.23	0.52
<i>AMPSQ(I)v10 FB 2</i>	17.37	16.90	0.47
<i>AMPSQ(I)v10 FB 3</i>	17.30	16.77	0.53
<i>AMPSQ(I)v10 1</i>	17.90	17.26	0.64
<i>AMPSQ(I)v10 2</i>	17.44	16.76	0.68
<i>AMPSQ(I)v10 3</i>	17.59	16.86	0.73
<i>AMPSQ(I)v10 polymer 1</i>	17.87	17.20	0.67
<i>AMPSQ(I)v10 polymer 2</i>	17.76	17.17	0.59
<i>AMPSQ(I)v10 polymer 3</i>	17.84	17.19	0.65

**Table 6:1: Final dried paint mass on each leaching panel**

## 6.3 Leaching Experiment

The prepared leaching panels were then subjected to the quat leaching protocol as described in Chapter 5. The panels were fully immersed in artificial seawater in a storage tank, **Figure 6:4**, such that they were allowed to continually leach, noting the date and time of immersion. The artificial seawater in the storage tank was continually passed through both activated carbon and cation exchange resin filters to ensure that the concentration of didecyl-quat (**2-1**) within the storage tank was kept to a minimum.



**Figure 6:4: Photograph of leaching storage tank**

The three leach panels of one coating were then removed from the storage tank and immersed into separate glass beakers containing 400 ml of pristine artificial seawater which had been previously been filtered to remove particles greater than 0.45  $\mu\text{m}$  diameter. N.B. the glass beakers had previously been pre-treated using the pre-saturation-quat (5-5) protocol as described in Chapter 5. The panels were left immersed in the glass beakers for a known period of time, during which time the artificial seawater was agitated by a continual stream of bubbles to ensure homogeneity, **Figure 6:5**, and then the panels were returned to the storage tank.



**Figure 6:5: Photograph of a leach rate experiment using bubble agitation**

An aliquot of seawater from each beaker was then subjected to the developed quat SPE protocol (see Chapter 5) and analysed in duplicate by the developed LC-MS method<sup>200</sup>, such that six injections of sample were performed per coating type and the sample concentrations determined.

After a period of time the determined sample concentrations, sampling time in the glass beakers and time since immersion in the storage tank were then used to follow the leaching characteristics of each of the coating types.

## 6.4 Leach Rate Results

Leach data was successfully collected for the four test coatings to enable analysis and directly compared. Direct comparisons were possible because the test paints all contained the didecyl-quat (**2-1**) analyte to a similar concentration and the panels were coated with comparable masses of test paints with equivalent surface areas. There were a number of fundamental questions regarding quat containing antifouling paints and their associated release rates which were answered through the leach rate experiment:

- Does the formulation of the AMPSQ(I)v10 polymer into a paint affect the release rate of the didecyl-quats?
- Can the release rate of the didecyl-quat be controlled?
- Does polymer composition affect the release rate of didecyl-quat?

The characterised release rates for the AMPSQ(I)v10 polymer and paints, **Figure 6:6**, demonstrated that the polymeric coatings released the didecyl-quat (**2-1**) both faster and at higher concentrations than the analogous paint formulation. This was anticipated as the didecyl-quat (**2-1**) corresponded to 28.8 wt% of the dry polymer but only 4.8 wt% of the dry paint - the polymer contained 6 times more quat than the paint so it should be anticipated that the polymer would release a greater quantity of the quat compared to the paint. Additionally the proportion of the surface of the paint occupied by the AMPSQ(I)v10 polymer in the paint formulation would be less than the 100 % coverage for the pure polymer.

For the first 28 days of the test both coatings displayed decreasing release rates which was unanticipated as the release rate was expected to be constant over time (i.e. zero order with respect to time). The zero order release rate was an expected outcome of a cation exchange release mechanism. However after 30 days and until the end of the test, both coatings then appeared to display the expected zero order release rate. The difference between the pre- and post 28 days was assumed to be associated with the absorption of water by the coatings over the initial 28 day period and then subsequently the fully hydrated coatings operated under zero order kinetic release of the didecyl-quat. Previous work within this thesis (*see Chapter 4, section 4.4.2.1*) had already established that the AMPSQ coatings were still mechanically affected by water absorption up to a period of 24 days, and their visual appearance was seen to alter over this period, as clear colourless coatings were seen to go cloudy.

In the ASTM for leaching of organic biocides from antifouling coatings<sup>164</sup> it is stipulated that, a coating can be considered to be releasing the biocide in a “pseudo-steady state” if:

“For a period of at least 24 days and containing 4 or more data points in which the arithmetic mean of the release rate values for each set of triplicate test panels at each data point differs from the weighted mean release value over the calculated period by no more than 15%”.

For both the polymer and paints the calculated weighted mean release rates between 28 and 71 days were 8.9 and 1.9  $\mu\text{gcm}^{-1}\text{day}^{-1}$  which was within 15 % of their respective arithmetic mean release rates, with the proviso that only 3 measurements were taken during this period. Due to instrument failure, more leach rate measurements could not be taken to comply with this ASTM protocol. However it can be concluded that both the polymer and paint test coatings demonstrated a pseudo-steady state release rate which is characteristic of self polishing co-polymer technologies.

Using the calculated steady state release rates and the amount of quat-biocide remaining within the coatings the time to depletion of the biocide was determined. The amount of biocide released was estimated from the area under the release rate profiles by division of the area into trapezoids and summation of their respective area. Based on these rudimentary calculations the time to depletion of the remaining didecyl-quat (**2-1**), assuming pseudo-steady state release was 210 and  $556 \pm 20\%$  days for the paint and polymer respectively.

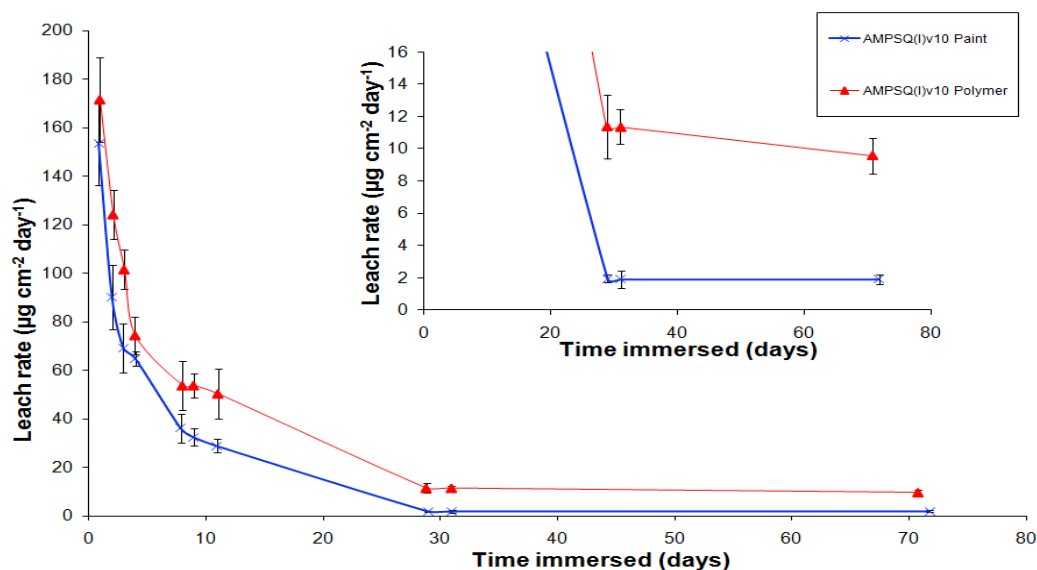


**Figure 6:6: Leach rate profiles for AMPSQ(I)v10 polymer (red) and AMPSQ(I)v10 paint (blue), inlay is a blown up view of the same chart**

Comparisons between the release rate profile of the free association didecyl-quat paint and that for AMPSQ(I)v10 paint demonstrated that the release rate profiles were markedly different, **Figure 6:7**. Additionally comparisons between the two quat containing coatings and an analogous free association paint containing an alternative organic biocide, seanine-211 (**1-3**) clearly demonstrated that the release rates from both quat coatings was excessive. This result while unanticipated for the AMPSQ(I)v10 paint, which contained the quat chemically bond to the binder of the paints, was

expected for the free association didecyl-quat paint because surfactants, such as the didecyl-quat (**2-1**), have substantially higher aqueous solubility than seanine-211 (**1-3**). The leach rate profile for the free associations coatings (with its high initial release rate which dramatically decreases with time in an apparent logarithmic manner) was characteristic of a free associated biocidal paint (see Chapter 1, section 1.1.4, **Figure 1:4**). It had been expected that for the free association paint the initial excessive release rate would quickly decrease and, in a short period of time, have become lower than that of the analogous paint which contained the didecyl-quat (**2-1**) chemically bound to the binder. This crossover in release rate would have been indicative of controlled release, as had been demonstrated during the initial testing of the quat leaching protocol (see Chapter 5, section 5.5, **Figure 5:10**). However, there was no experimental evidence which demonstrated this crucial cross over, so it cannot be said with certainty that the AMPSQ polymer provides a controlled release effect. In addition, from calculation it can be shown that more didecyl-quat (**2-1**) was released from the AMPSQ(I)v10 paint (23 mg) than from the free association didecyl-quat paint (12 mg). Given that the AMPSQ(I)v10 paint and its corresponding polymer have previously been shown to produce a zero order release rate, after 28 days, **Figure 6:6**, which in itself was a sign of controlled release, these results were unexpected. Two possible reasons for the discrepancy were:

- 1) The release rate of the free association didecyl-quat paint was such that for the period between initial immersion and first leach rate measurement (0.76 days) the crossover was not observed
- 2) The matrix paint used for the free association paint dramatically altered the apparent release rate of the quat.

The most likely reason appears to be the paint matrix because the required release rate for the free association paint to achieve at least parity with the amount of didecyl-quat (**2-1**) release from the AMPSQ(I)v10 paint was in the order of  $315 \mu\text{gcm}^{-2}\text{day}^{-1}$  which seemed unrealistic, especially considering that the paint matrix had been altered.

As described earlier, in the initial experiment testing the leaching protocol that demonstrated controlled release (see Chapter 5, section 5.5, **Figure 5:10**) was achieved by comparisons between different quat's release rates i.e. the equivalent previously used free association paint which contained AMPSQ(II)v4 (the non-biocidal trioctyl-quat (**2-2**) polymer) as the binder and benzyl-quat (**1-21**) freely dispersed within it. During the more rigorous leaching experiments conducted within this chapter it was decided to restrict the target analytes to one specific quat, didecyl-quat (**2-1**) The replacement paint binder utilized an analogous **anion** exchange reaction to achieve a similar polishing mechanism to the AMPSQ paints. Consequently it was simultaneously releasing the chemically bound anions of the polymer used in the binder at the same time as the dispersed quat-cations were released. It can therefore be suggested that leachate seawater containing both the

release anions and quat-cations would be akin to chromatographic ion-pair solutions and consequently any didecyl-quat (**2-1**) as part of an ion-pair would exhibit substantially different chromatography to that established during the method development of the leaching protocol. The established chromatographic separation was developed using both the charge and the organic nature of the didecyl-quat to achieve separation from the seawater and as such would be sensitive to alterations to either of these properties, such as in an ion-pair. Alternatively the matrix of the free-association coating might result in non-similar dissolution properties.

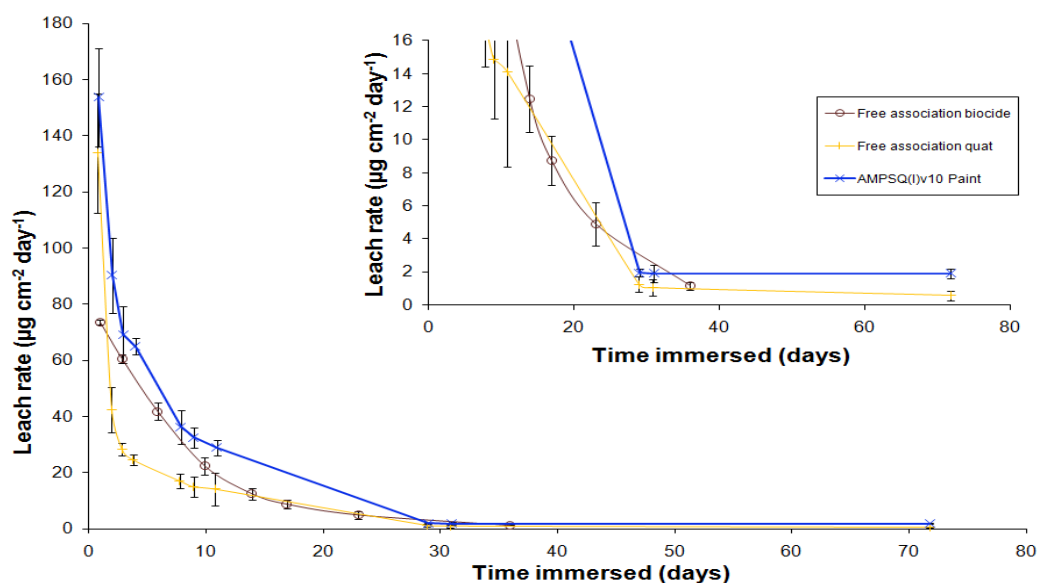


**Figure 6:7: Leach rate profiles for AMPSQ(I)v10 paint (blue), free association didecyl-quat paint (yellow) and an alternative free association biocide paint (brown), inset is a blown up view of the same chart**

Comparisons between the leach rates for AMPSQ(I)v10 FB paint (fluoro-monomer containing system) and AMPSQ(I)v10 paint appeared not to demonstrate any substantial difference because of overlapping error bars, **Figure 6:8**. However, when the amount of didecyl-quat (**2-1**) release was estimated using the previously described method the results demonstrated that fluorinated version of the matching systems had released the least 19 mg compared to 23 mg for AMPSQ(I)v10 paint, the non-fluorinated system. This was consistent with our predictions because the fluorinated system was anticipated to be more hydrophobic than the non-fluorinated coatings and hence its interaction with seawater would have been less resulting in a lower amount of didecyl-quat (**2-1**) release. Similar with the non-fluorinated paint (AMPSQ(I)v10 paint) the fluorinated AMPSQ(I)v10 FB paint also demonstrated pseudo-steady state release between 28 and 71 days with its calculated weighted mean release rate being  $0.7 \mu\text{gcm}^{-1}\text{day}^{-1}$  which was within 15 % of their respective arithmetic mean release rates. This steady state release rate was also below the comparable rate for the non-fluorinated analogous system, AMPSQ(I)v10 paint ( $1.9 \mu\text{gcm}^{-1}\text{day}^{-1}$ ). This suggested that the incorporation of even a small amount of a hydrophobic monomer into the AMPSQ polymer architecture can have an effect on the release rate of the didecyl-quat (**2-1**) biocide.

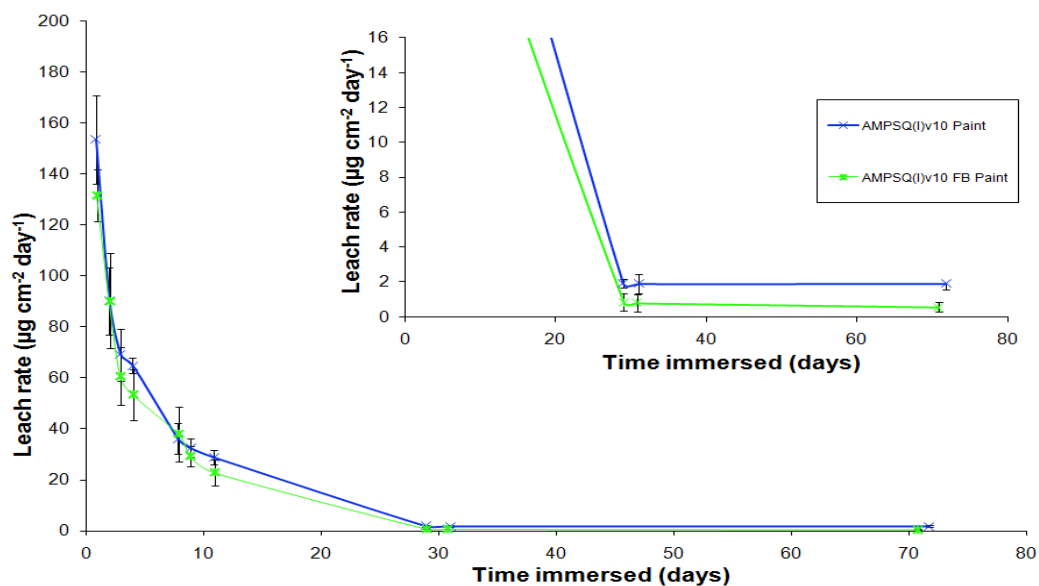


**Figure 6:8:** Leach rate profiles for AMPSQ(I)v10 paint (blue) and AMPSQ(I)v10 FB paint (fluorinated monomer, green), inset is a blown up view of the same chart

## 6.5 Conclusions

From this work it was clear that the new quat leaching protocol developed within this thesis was sufficiently robust to enable the release rates of various quat containing coatings to be analysed for the first time. The results of the leaching experiment have demonstrated that the anticipated zero order controlled release of the quat-biocides would be possible and that the method of chemically binding them into the binder of an antifouling paint formulation through an electrovalent bond was viable. There was even limited evidence which suggested that the release rate of the didecyl-quat (2-1) could be altered by variations to the hydrophilicity of the polymer architecture. However further work with a more extensive range of polymer formulations would be required to determine with confidence whether the polymer architecture does predictably alter the release rate.

## 7 Conclusions

From the experimental work undertaken within Chapter 2 it can be concluded that quat methylcarbonates are a good synthetic reagent to enable the addition of quat-moieties to acid functional organic compounds. Additionally the incorporation of quat-moieties into a pre-existing polymer substantially alters its mechanical properties, in particular resulting in ‘soft’ coatings. There were a number of critical issues associated with the quat-polymers synthesised via the post-quaternisation route which meant that this route could not be fully evaluated, namely the incorporation of the quats into the pre-existing polymer resulted in soft coatings. This softness was attributed to being a manifestation of the quats, which internally plasticised the coatings with their long alkyl-chains. Another major flaw of this route was the acid functionality of the framework polymer could not be fully quaternised. This resulted in a latent instability in the paint formulation which was ultimately exposed during the storage trials. The resolution of this issue was to use an alternative route to quat-polymers; namely the sequential preparation of the quat-monomer then polymer.

The initial attempt to produce quat-polymers via the sequential preparation of the quat-monomer then polymerisation used MES (**3-1**) as the framework to create the quat-monomer, which was the focus of Chapter 3. A consequence of using MES (**3-1**), which was highly hydrophilic due to its ester-, and acid-functionalities, was hydrophobic monomers were required to modify the hydrophilicity of the quat-polymers. IBoMA (**3-5**) was the initial choice, but this resulted in brittle polymeric films with poor mechanical properties. Therefore a third comonomer was incorporated into the polymer composition to modify the mechanical properties of the polymer film. Unfortunately this work ultimately proved unsuccessful because the MES (**3-1**) framework monomer was not stable in the presence of alcoholic solvents, which was manifested as changes in grind and viscosity of the paints while on storage. The source of the instability was a transesterification reaction between MES (**3-1**) and methanol produced as a by-product during the quaternisation reaction of MES (**3-1**). The solution to the stability issues of the MESQ polymer was to use an alternative framework monomer which did not have the problematic ester functionality. This was explored in Chapter 4 using the monomer, 2-acrylamido-2-methyl-1-propanesulfonic acid (AMPS, **3-2**).

The use of AMPS (**3-2**) finally provided a suitable polymeric system to enable the efficacy of quat-biocides to be evaluated. From the work in Chapter 4, a number of conclusions regarding the potential use of quats as antifoulants could be drawn:

First, didecyl-quats have been confirmed as suitable antifouling agents. However, to gain the maximum longevity of action for these compounds, they cannot be simply dispersed within the

paint. This thesis has shown how the antifouling performance of such coatings deteriorates unacceptably rapidly. Therefore to enable these biocides to be fully utilized commercially they require a mechanism to control their release. Such a mechanism has been developed within this thesis based on tethering the quat-cation of the biocides into the polymeric binder of the antifouling paint by a Coulombic attraction. These novel polymers use the sulphonate functionality of AMPS (3-2) derived moieties to chemically bind the quat-cation into the polymer which, in addition, have been demonstrated to be able to be formulated into a prototype antifouling paint formulation using industry standard components and methods. The most effective AMPSQ based coatings have demonstrated a clear and statistical enhancement in antifouling performance over and above of that of a current fully formulated commercial product, Intersmooth 460, over a period of 1 year testing. These coatings have demonstrated sufficient potential for this new technology to be considered a potential future commercial candidate, warranting more extensive testing to determine the optimum paint formulation to maximise the efficacy of the quat-biocides.

Second, this work has suggested that there is a correlation between a number of physical properties of the coatings and the theoretical hydrophilicity of these polymer systems. While definitive conclusions cannot be drawn due to the limited range in polymer compositions assayed, the apparent correlation warrants further experimentation to determine whether this correlation holds true for more generally polymer composites or only specifically for the AMPSQ coatings.

A major element of this thesis was to develop an analytical method to enable the quantification of quats in seawater and determination of the leach rate of the quats from the antifouling coatings, which was the focus of Chapter 5 (Method Development) and Chapter 6 (Leach Rate Measurement). From this work it was clear that the new quat leaching protocol developed within this thesis was sufficiently robust to enable the release rates of various quat containing coatings to be characterised for the first time. The results of the leaching experiment have demonstrated that the anticipated zero order controlled release of the quat-biocides would be possible and that the mechanism of ionic tethering of the quats into the binder is an effective solution to prolonging the effective release of the quats and hence extending the performance of quat containing antifouling coatings. As part of this work the leach rate of two analogous polymeric compositions were directly compared. The polymers either contained BMA (3-7) or a fluorinated structural analogue HFBMA (6-1). From this work there appeared to be limited evidence which suggested that the release rate of the didecyl-quat (2-1) could be altered by variations to the polymer architecture i.e. the fluorinated species released less quat. However, further work with a more extensive range of polymer formulations would be required to determine with confidence whether the polymer architecture altered the release rate, which would be part of further work and beyond the scope of this thesis.



## 8 Future Work

The work presented within this thesis can be used as the basis for a number of future research topics. Firstly polymeric systems using AMPS have been shown to be stable within an antifouling paint formulation and as such could be used as a vehicle to assess the efficacy of different quats. This work has been partly undertaken during the research for this thesis specifically the use of trioctyl-quats as a non-biocidal control for the biocidal didecyl-quats. It has been clearly demonstrated that inclusion of either didecyl- or trioctyl-quats can significantly alter the fundamental properties of the antifouling coatings, i.e. the non biocidal AMPSQ(II)v4 had better performance on mechanical property testing than the biocidal AMPSQ(I)v4. These quats were identified from other end-uses where they have demonstrated good antimicrobial efficacies such as in hospital sterilisation and pesticides in agriculture, but until this work, little data existed on their use in marine antifouling coatings due to issues of controlling their release. The AMPSQ coating systems, developed as part of this work can act as the basis of future work aimed at examining the antifouling efficacy of a wider range of quats with the ultimate aim of identifying the most effective for use as marine antifoulants.

Further research can also be directed towards developing the AMPSQ polymeric architecture rather than the quat moiety. The issue of water absorption and consequently determination of predictable and controlled film loss requires further experimentation. Within this body of work it has already been established that fluoro-monomers are compatible with the elucidated synthetic method and monomers and it can be anticipated that the incorporation of alternative hydrophobic monomers, such as fluoro-methacrylates/acrylates, into the polymer architecture might prevent the ingress of water.

From the current experimental work there appears to be a correlation between a polymer's propensity to absorb water and the polymer's constituent monomer's water-octanol partition coefficient. However, the data set over which this correlation was identified was too small to draw definitive conclusions. Further work is required in order to extend the range and types of polymers and to determine whether water-octanol partition coefficients can be used more generally to predict the water absorption characteristics of polymers.

The developed leach rate protocol could also be used with a broader range of polymer compositions to explore, in greater detail, the effect of polymer architecture on the release rate of a specific quats, as has initially been explored within this thesis. Alternatively, the variation in leach rate of different quats from the same polymer composition might also be the focus of future work. A particular area of research which remains unresolved is the issue of the uncontrolled release paint (free association didecyl-quat paint) releasing the quat more slowly than the controlled release

formulation (AMPSQ(I)v10 paint). This could be explored by repeating the undertaken leaching experiment but replacing the binder of the uncontrolled paint with an AMPSQ polymer to enable a more comparable test.

Finally from a commercial development approach the next steps would be the optimisation of the antifouling paint formulation. The current prototype paint formulation while enabling the potential of the quats to be evaluated will require extensive testing and re-formulation to ensure that the final paint fulfils all requirements of a prospective commercial product. This will require further optimisation of the formulation to enhance the application properties, drying characteristic and more rigorous testing through a series of fitness for purpose tests. A key aspect of this fitness for purpose assessment will be more extensive antifouling testing both statically and as test patches on a broader range of vessels. This work is currently underway because the technology has shown such early promise. As these polymer systems have demonstrated antimicrobial activity it is possible that they could have other commercial applications over and above their use as marine antifoulants. For example it might be possible to incorporate these polymers into domestic decorative coatings or specialist industrial coatings to enable targeted microbial control.

## **9 Appendix 1: Scientific Publication Detailing Analytical Method for the Quantification of Quaternary Ammonium Compounds in Seawater.**





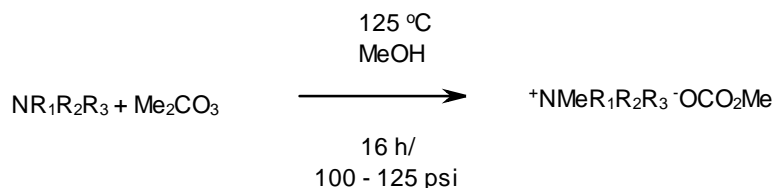






# 10 Experimental

## 10.1 Monomer Precursor Syntheses:



Where:

a)  $\text{R}_1 = \text{Me}$  and  $\text{R}_2, \text{R}_3 = \text{C}_{10}\text{H}_{21}$  [Didecylmethylamine]

b)  $\text{R}_1, \text{R}_2$  and  $\text{R}_3 = \text{C}_8\text{H}_{17}$  [Trioctylamine]

### 10.1.1 Didecyldimethylammonium methylcarbonate

Didecylmethylamine (141.0 g, 0.4524 moles), dimethyl carbonate (DMC) (300 g, 3.3296 moles) and methanol (200 g), were placed in a stainless steel, high pressure reaction vessel. The sealed vessel was heated to 125 °C during which 100-125 psi pressure developed, the reaction was allowed to remain under these conditions for 16 h and the pressure released at room temperature. The cooled solution was gravity filtered and the excess solvent was removed *in vacuo*. Any residual DMC was removed by the addition of methanol (~150 g as an azeotrope) and further evaporative distillation. The viscous amber liquid was submitted for <sup>1</sup>H and <sup>13</sup>C NMR and used without further purification.

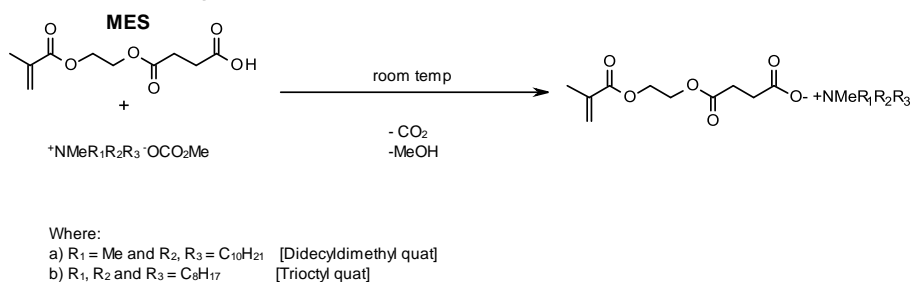
Didecyldimethylammonium methylcarbonate: (Quantitative yield) <sup>1</sup>H NMR (CDCl<sub>3</sub>) δ: 3.30 (N<sup>+</sup>-CH<sub>2</sub>-CH<sub>2</sub> and -O-C(=O)-OCH<sub>3</sub>: m, 7H), 3.20 (N<sup>+</sup>-CH<sub>3</sub>: s, 6H), 1.58 (N<sup>+</sup>-CH<sub>2</sub>-CH<sub>2</sub>-CH<sub>2</sub>: m, 4H), 1.20 (-CH<sub>2</sub>-CH<sub>2</sub>-CH<sub>2</sub>: m, 28H), 0.8 (-CH<sub>2</sub>-CH<sub>2</sub>-CH<sub>3</sub>: t, 6H); <sup>13</sup>C NMR (CDCl<sub>3</sub>) δ: 157.2 (-O-C(=O)-OMe, s), 62.4 (2 × N<sup>+</sup>-CH<sub>2</sub>-CH<sub>2</sub>-, s), 51.0 (-O-C(=O)-OCH<sub>3</sub>, s), 49.5 (2 × N<sup>+</sup>-CH<sub>3</sub>, s), 30.7 (2 × -CH<sub>2</sub>-CH<sub>2</sub>-CH<sub>3</sub>, s), 28.3 (4 × -CH<sub>2</sub>-CH<sub>2</sub>-CH<sub>2</sub>-, m), 28.1 (4 × -CH<sub>2</sub>-CH<sub>2</sub>-CH<sub>2</sub>-, m), 25.2 (2 × N<sup>+</sup>-CH<sub>2</sub>-CH<sub>2</sub>-CH<sub>2</sub>-, s), 21.6 (2 × N<sup>+</sup>-CH<sub>2</sub>-CH<sub>2</sub>-CH<sub>2</sub> and 2 × -CH<sub>2</sub>-CH<sub>2</sub>-CH<sub>3</sub>, m), 12.9 (2 × -CH<sub>2</sub>-CH<sub>2</sub>-CH<sub>3</sub>, s); IR: ν<sub>C-H</sub> 2926.9, 2856.9, ν<sub>C=O, methylcarbonate</sub> 1665.2 cm<sup>-1</sup>

### 10.1.2 Trioctylmethylammonium methylcarbonate

Trioctylamine (160.0 g, 0.4524 moles), dimethyl carbonate (DMC) (300 g, 3.3296 moles) and methanol (200 g), were placed in a stainless steel, high pressure reaction vessel. The sealed vessel was heated to 125 °C during which 100-125 psi pressure developed, the reaction was allowed to remain under these conditions for 16 h and the pressure released at room temperature. The cooled solution was gravity filtered and the excess solvent was removed *in vacuo*. Any residual DMC was removed by the addition of methanol (~150 g as an azeotrope) and further evaporative distillation. The viscous amber liquid was submitted for <sup>1</sup>H and <sup>13</sup>C NMR and used without further purification.

Triocylmethylammonium methylcarbonate: (Quantitative yield)  $^1\text{H}$  NMR ( $\text{CDCl}_3$ )  $\delta$ : 3.30 ( $\text{N}^+\text{-CH}_2\text{-CH}_2$  and  $-\text{O-C(=O)-OCH}_3$ : m, 9H), 3.20 ( $\text{N}^+\text{-CH}_3$ : s, 3H), 1.58 ( $\text{N}^+\text{-CH}_2\text{-CH}_2\text{-CH}_2$ : m, 6H), 1.20 ( $-\text{CH}_2\text{-CH}_2\text{-CH}_2$ : m, 36H), 0.8 ( $-\text{CH}_2\text{-CH}_2\text{-CH}_3$ : t, 9H);  $^{13}\text{C}$  NMR ( $\text{CDCl}_3$ )  $\delta$ : 158.4 ( $-\text{O-C(=O)-OMe}$ , s), 61.1 ( $3 \times \text{N}^+\text{-CH}_2\text{-CH}_2$ -, s), 52.1 ( $-\text{O-C(=O)-OCH}_3$ , s), 49.7 ( $\text{N}^+\text{-CH}_3$ , s), 31.5 ( $3 \times \text{-CH}_2\text{-CH}_2\text{-CH}_3$ , s), 29.0 ( $6 \times \text{-CH}_2\text{-CH}_2\text{-CH}_2$ -, m), 28.9 ( $6 \times \text{-CH}_2\text{-CH}_2\text{-CH}_2$ -, m), 26.1 ( $3 \times \text{N}^+\text{-CH}_2\text{-CH}_2\text{-CH}_2$ -, s), 22.4 ( $3 \times \text{N}^+\text{-CH}_2\text{-CH}_2\text{-CH}_2$  and  $3 \times \text{-CH}_2\text{-CH}_2\text{-CH}_3$ , m), 13.9 ( $3 \times \text{-CH}_2\text{-CH}_2\text{-CH}_3$ , s); IR:  $\nu_{\text{C-H}}$  2926.9, 2856.9,  $\nu_{\text{C=O, methylcarbonate}}$  1665.2  $\text{cm}^{-1}$

## 10.2 Monomer Syntheses:



### 10.2.1 Didecyldimethylammonium salt of MES (MESQ(I))

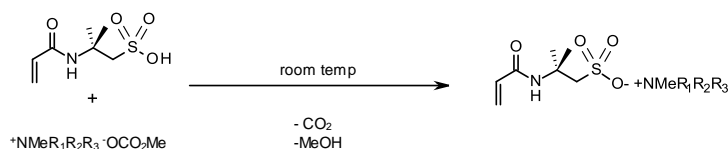
Didecyldimethylammonium methylcarbonate (183.0g, 0.4557 moles) was dissolved in xylene (100 g) and placed in a 2 L three-necked round bottom flask. To this stirring solution was added drop wise, MES (101.8 g, 0.4420 moles) in xylene (100 g). Gas ( $\text{CO}_2$ ) evolution was observed as the acid reacted. The reaction mixture was stirred at room temperature overnight. The resulting viscous amber liquid was submitted for  $^1\text{H}$  and  $^{13}\text{C}$  NMR and used without further purification.

Didecyldimethylammonium salt of MES (MESQ(I)): (Quantitative yield)  $^1\text{H}$  NMR ( $\text{CDCl}_3$ )  $\delta$ : 7.4-6.9 (Ar-H, m), 6.15 ( $\text{H}_2\text{C}=\text{C}(\text{Me})$ -, s, 1H), 5.59 ( $\text{H}_2\text{C}=\text{C}(\text{Me})$ -, s, 1H), 4.30 ( $-\text{O-CH}_2\text{-CH}_2\text{-O-}$ , dt, 4H), 3.30 ( $\text{N}^+\text{-CH}_2\text{-CH}_2$ -, m, 4H), 3.25 ( $\text{N}^+\text{-CH}_3$ , s, 6H), 2.68 ( $\text{O-C(=O)-CH}_2\text{-CH}_2\text{-O-C(=O)-}$ , m, 2H), 2.50 ( $\text{O-C(=O)-CH}_2\text{-CH}_2\text{-O-C(=O)-}$ , m, 2H), 1.75 ( $\text{H}_2\text{C}=\text{C}(\text{CH}_3)\text{-C(=O)-}$ , s, 3H), 1.50 ( $\text{N}^+\text{-CH}_2\text{-CH}_2$ -, m, 4H), 1.07 ( $-\text{CH}_2\text{-CH}_2\text{-CH}_2$ -, m, 28H), 0.7 ( $-\text{CH}_2\text{-CH}_2\text{-CH}_3$ , t, 6H);  $^{13}\text{C}$  NMR ( $\text{CDCl}_3$ )  $\delta$ : 176.0 ( $-\text{C(=O)-O}^-$ , s), 173.1 ( $\text{CH}_2\text{-O-C(=O)-CH}_2$ -, s), 166.8 ( $\text{CH}_2=\text{C}(\text{Me})\text{-C(=O)-O}$ -, s), 137.5-125.7 (Ar-H, m), 125.6 ( $\text{H}_2\text{C}=\text{C}(\text{Me})$ -, s), 63.2 ( $2 \times \text{N}^+\text{-CH}_2\text{-CH}_2$ -, s), 61.9 ( $-\text{O-CH}_2\text{-CH}_2\text{-O-}$ , s), 61.4 ( $-\text{O-CH}_2\text{-CH}_2\text{-O-}$ , s), 49.0 ( $2 \times \text{N}^+\text{-CH}_3$ , s), 32.8 ( $\text{O-C(=O)-CH}_2\text{-CH}_2\text{-O-C(=O)-}$ , s), 31.4 ( $-\text{CH}_2\text{-CH}_2\text{-CH}_2$ -, s), 31.0 ( $\text{O-C(=O)-CH}_2\text{-CH}_2\text{-O-C(=O)-}$ , s), 28.9 - 25.9 ( $-\text{CH}_2\text{-CH}_2\text{-CH}_2$ -, m), 22.2 ( $2 \times \text{N}^+\text{-CH}_2\text{-CH}_2$ -, s), 17.8 ( $\text{CH}_2=\text{C}(\text{CH}_3)\text{-C(=O)-O}$ -, s), 13.6 ( $2 \times \text{-CH}_2\text{-CH}_2\text{-CH}_3$ , s).

## 10.2.2 Trioctylmethylammonium salt of MES (MESQ(II))

Trioctylmethylammonium (200.77g, 0.4524 moles) was dissolved in xylene (100 g) and placed in a 2 L three-necked round bottom flask. To this stirring solution was added drop wise, MES (98.9 g, 0.4298 moles) in xylene (100 g). Gas (CO<sub>2</sub>) evolution was observed as the acid reacted. The reaction mixture was stirred at room temperature overnight. The resulting viscous amber liquid was submitted for <sup>1</sup>H and <sup>13</sup>C NMR and used without further purification.

Trioctylmethylammonium salt of MES (MESQ(II)): (Quantitative yield) (Quantitative yield) <sup>1</sup>H NMR (CDCl<sub>3</sub>) δ: 7.4-6.9 (Ar-H, m), 6.15 (H<sub>2</sub>C=C(Me)-, s, 1H), 5.59 (H<sub>2</sub>C=C(Me)-, s, 1H), 4.30 (-O-CH<sub>2</sub>-CH<sub>2</sub>-O-, dt, 4H), 3.30 (N<sup>+</sup>-CH<sub>2</sub>-CH<sub>2</sub>-, m, 6H), 3.25 (N<sup>+</sup>-CH<sub>3</sub>, s, 3H), 2.68 (O-C(=O)-CH<sub>2</sub>-CH<sub>2</sub>-O-C(=O)-, m, 2H), 2.50 (O-C(=O)-CH<sub>2</sub>-CH<sub>2</sub>-O-C(=O)-, m, 2H), 1.75 (H<sub>2</sub>C=C(CH<sub>3</sub>)-C(=O)-, s, 3H), 1.50 (N<sup>+</sup>-CH<sub>2</sub>-CH<sub>2</sub>-, m, 6H), 1.07 (-CH<sub>2</sub>-CH<sub>2</sub>-CH<sub>2</sub>-, m, 30H), 0.7 (-CH<sub>2</sub>-CH<sub>2</sub>-CH<sub>3</sub>, t, 9H); <sup>13</sup>C NMR (CDCl<sub>3</sub>) δ: 176.0 (-C(=O)-O-, s), 173.1 (CH<sub>2</sub>-O-C(=O)-CH<sub>2</sub>-, s), 166.8 (CH<sub>2</sub>=C(Me)-C(=O)-O-, s), 137.5-125.7 (Ar-H, m), 125.6 (H<sub>2</sub>C=C(Me)-, s), 61.9 (-O-CH<sub>2</sub>-CH<sub>2</sub>-O-, s), 61.4 (-O-CH<sub>2</sub>-CH<sub>2</sub>-O-, s), 61.1 (3 × N<sup>+</sup>-CH<sub>2</sub>-CH<sub>2</sub>-, s), 49.7 (N<sup>+</sup>-CH<sub>3</sub>, s), 32.8 (O-C(=O)-CH<sub>2</sub>-CH<sub>2</sub>-O-C(=O)-, s), 31.4 (-CH<sub>2</sub>-CH<sub>2</sub>-CH<sub>2</sub>-, s), 31.0 (O-C(=O)-CH<sub>2</sub>-CH<sub>2</sub>-O-C(=O)-, s), 28.9 - 25.9 (-CH<sub>2</sub>-CH<sub>2</sub>-CH<sub>2</sub>-, m), 25.7 (3 × N<sup>+</sup>-CH<sub>2</sub>-CH<sub>2</sub>-CH<sub>2</sub>-, s), 17.8 (CH<sub>2</sub>=C(CH<sub>3</sub>)-C(=O)-O-, s), 13.9 (3 × -CH<sub>2</sub>-CH<sub>2</sub>-CH<sub>3</sub>, s).



Where:

- a) R<sub>1</sub> = Me and R<sub>2</sub>, R<sub>3</sub> = C<sub>10</sub>H<sub>21</sub> [Didecyldimethyl quat]  
 b) R<sub>1</sub>, R<sub>2</sub> and R<sub>3</sub> = C<sub>8</sub>H<sub>17</sub> [Trioctyl quat]

## 10.2.3 Didecyldimethylammonium salt of AMPS (AMPSQ(I))

Didecyldimethylammonium methylcarbonate (183.0g, 0.4557 moles) was dissolved in methanol (200 g) and placed in a 2 L three-necked round bottom flask. To this stirring solution was slowly added solid AMPS (91.0 g, 0.4391 moles). Gas (CO<sub>2</sub>) evolution was observed as the acid reacted. The reaction mixture was stirred at room temperature overnight. The solution was gravity filtered and the excess solvent was removed *in vacuo*. The resulting viscous amber liquid was submitted for <sup>1</sup>H and <sup>13</sup>C NMR and used without further purification.

Didecyldimethylammonium salt of AMPS (AMPSQ(I)): (Quantitative yield) <sup>1</sup>H NMR (CDCl<sub>3</sub>) δ 8.12 (-C(=O)-NH-, b, 1H) 5.85 and 5.80 (*trans* CH<sub>2</sub>=CH-C(=O)-, m, 2H), 5.25 (*cis* CH<sub>2</sub>=CH-C(=O)-, dd, 1H, <sup>2</sup>J<sub>HH</sub> 2.21 Hz; <sup>3</sup>J<sub>HH</sub> 9.64 Hz), 3.15 (N<sup>+</sup>-CH<sub>2</sub>-CH<sub>2</sub>-, m, 4H), 3.05 (N<sup>+</sup>-CH<sub>3</sub>, s, 6H),

2.25 (-NH-C(Me)<sub>2</sub>-CH<sub>2</sub>-S(=O)<sub>2</sub>-), s, 2H), 1.5 - 1.4 (N<sup>+</sup>-CH<sub>2</sub>-CH<sub>2</sub>- and -NH-C(CH<sub>3</sub>)<sub>2</sub>-CH<sub>2</sub>-S(=O)<sub>2</sub>- , m, 10H), 1.13 (-CH<sub>2</sub>-CH<sub>2</sub>-CH<sub>2</sub>-, m, 28H), 0.75 (-CH<sub>2</sub>-CH<sub>2</sub>-CH<sub>3</sub>, t, 6H); <sup>13</sup>C NMR (CDCl<sub>3</sub>) δ 164.8 (CH<sub>2</sub>=CH-C(=O)-, s), 133.1 (CH<sub>2</sub>=CH-C(=O)-, s), 124.2 (CH<sub>2</sub>=CH-C(=O)-, s), 63.8 (2 × N<sup>+</sup>-CH<sub>2</sub>-CH<sub>2</sub>-, s), 61.1 (-C(Me)<sub>2</sub>-CH<sub>2</sub>-S(=O)<sub>2</sub>-O<sup>-</sup>, s), 52.2 (-NH-C(Me)<sub>2</sub>-CH<sub>2</sub>-, s), 51.1 (2 × N<sup>+</sup>-CH<sub>3</sub>, s), 31.8 (2 × -CH<sub>2</sub>-CH<sub>2</sub>-CH<sub>3</sub>, s), 29.4 - 29.1 (-CH<sub>2</sub>-CH<sub>2</sub>-CH<sub>2</sub>-, m), 26.2 (-NH-C(CH<sub>3</sub>)<sub>2</sub>-CH<sub>2</sub>-, s), 22.6 (2 × N<sup>+</sup>-CH<sub>2</sub>-CH<sub>2</sub>- and 2 × -CH<sub>2</sub>-CH<sub>2</sub>-CH<sub>3</sub>, m), 14.0 (2 × -CH<sub>2</sub>-CH<sub>2</sub>-CH<sub>3</sub>, s); IR: ν<sub>N-H, amide</sub> 3447.9, ν<sub>C-H</sub> 2926.9, 2856.9, ν<sub>C=O, amide</sub> 1668.3, 1547.9, ν<sub>S(=O)<sub>2</sub>-O</sub>, 1377.0, 1181.9 cm<sup>-1</sup>

## 10.2.4 Trioctylmethylammonium salt of AMPS (AMPSQ(II))

Trioctylmethylammonium (200.77g, 0.4524 moles) was dissolved in methanol (200 g) and placed in a 2 L three-necked round bottom flask. To this stirring solution was slowly added solid AMPS (91.0 g, 0.4391 moles). Gas (CO<sub>2</sub>) evolution was observed as the acid reacted. The reaction mixture was stirred at room temperature overnight. The solution was gravity filtered and the excess solvent was removed *in vacuo*. The resulting viscous amber liquid was submitted for <sup>1</sup>H and <sup>13</sup>C NMR and used without further purification.

Trioctylmethylammonium salt of AMPS (AMPSQ(II)): (Quantitative yield) <sup>1</sup>H NMR (CDCl<sub>3</sub>) δ 8.12 (-C(=O)-NH-, b, 1H) 5.85 and 5.80 (*trans* CH<sub>2</sub>=CH-C(=O)-, m, 2H), 5.25 (*cis* CH<sub>2</sub>=CH-C(=O)-, dd, 1H, <sup>2</sup>J<sub>HH</sub> 2.21 Hz; <sup>3</sup>J<sub>HH</sub> 9.64 Hz), 3.15 (N<sup>+</sup>-CH<sub>2</sub>-CH<sub>2</sub>-, m, 6H), 3.05 (N<sup>+</sup>-CH<sub>3</sub>, s, 3H), 2.25 (-NH-C(Me)<sub>2</sub>-CH<sub>2</sub>-S(=O)<sub>2</sub>-), s, 2H), 1.5 - 1.4 (N<sup>+</sup>-CH<sub>2</sub>-CH<sub>2</sub>- and -NH-C(CH<sub>3</sub>)<sub>2</sub>-CH<sub>2</sub>-S(=O)<sub>2</sub>- , m, 12H), 1.13 (-CH<sub>2</sub>-CH<sub>2</sub>-CH<sub>2</sub>-, m, 30H), 0.75 (-CH<sub>2</sub>-CH<sub>2</sub>-CH<sub>3</sub>, t, 9H); <sup>13</sup>C NMR (CDCl<sub>3</sub>) δ 164.8 (CH<sub>2</sub>=CH-C(=O)-, s), 133.1 (CH<sub>2</sub>=CH-C(=O)-, s), 124.2 (CH<sub>2</sub>=CH-C(=O)-, s), 63.8 (3 × N<sup>+</sup>-CH<sub>2</sub>-CH<sub>2</sub>-, s), 61.1 (-C(Me)<sub>2</sub>-CH<sub>2</sub>-S(=O)<sub>2</sub>-O<sup>-</sup>, s), 52.2 (-NH-C(Me)<sub>2</sub>-CH<sub>2</sub>-, s), 51.1 (N<sup>+</sup>-CH<sub>3</sub>, s), 31.8 (3 × -CH<sub>2</sub>-CH<sub>2</sub>-CH<sub>3</sub>, s), 29.4 - 29.1 (-CH<sub>2</sub>-CH<sub>2</sub>-CH<sub>2</sub>-, m), 26.2 (-NH-C(CH<sub>3</sub>)<sub>2</sub>-CH<sub>2</sub>-, s), 22.6 (3 × N<sup>+</sup>-CH<sub>2</sub>-CH<sub>2</sub>- and 3 × -CH<sub>2</sub>-CH<sub>2</sub>-CH<sub>3</sub>, m), 14.0 (3 × -CH<sub>2</sub>-CH<sub>2</sub>-CH<sub>3</sub>, s); IR: ν<sub>N-H, amide</sub> 3447.9, ν<sub>C-H</sub> 2926.9, 2856.9, ν<sub>C=O, amide</sub> 1668.3, 1547.9, ν<sub>S(=O)<sub>2</sub>-O</sub>, 1377.0, 1181.9 cm<sup>-1</sup>

## 10.3 Polymer Syntheses:

### 10.3.1 Development of RC957Q polymer preparation

Data for Figure 2:7, is detailed in Table 10:1

Time/ hrs	Reaction Completion/ %	Temperature/ °C
2.5	78	25
4.5	86	73
5.5	88	73
19.5	91	73
25.5	93	95

Table 10:1: Percentage completion of quaternisation of RC957 polymer

### 10.3.2 RC957Q(I)

RC957 polymer solution (470.4 g) was added drop wise over 1 hr to mechanically stirred didecyldimethylammonium methylcarbonate (230.4 g, 0.5746 moles). Gas (CO<sub>2</sub>) evolution was observed as the acid reacted. The reaction was maintained at 100 °C for 24 hours. Following this the acid value of the resulting polymer was checked and ensured to be 7 % of the original acid value of RC957. The resulting viscous amber liquid was submitted for <sup>1</sup>H NMR and used without further purification.

<sup>1</sup>H NMR (CDCl<sub>3</sub>) δ: 7.3 – 6.8 (Ar-H, m), 3.6 (HO-CH<sub>2</sub>-CH<sub>2</sub>-, t), 3.5 – 3.2 (N<sup>+</sup>-CH<sub>2</sub>-CH<sub>2</sub>- and N<sup>+</sup>-CH<sub>3</sub>, m), 2.5 (Ar-CH<sub>2</sub>-CH<sub>3</sub>, dd), 2.2 (Ar-CH<sub>3</sub>, m), 1.5 – 1.2 (CH<sub>3</sub>-CH<sub>2</sub>-, m), 1.0 – 0.75 (CH<sub>3</sub>-CH<sub>2</sub>-, m)

### 10.3.3 RC957Q(II)

The above experimental method was altered as follows:

RC957 polymer solution (470.4 g);

Triocylmethylammonium methylcarbonate (246.5 g, 0.5746 moles)

<sup>1</sup>H NMR: same as RC957Q(I)

The above polymers was characterised in terms of viscosity, percentage non-volatile content (NVC), specific gravity (SG), number average molecular weight (M<sub>N</sub>), weight average molecular weight (M<sub>w</sub>) and polymer polydispersity, data presented in Table 10:2 and Table 10:3. The GPC data was collected using an HP 1100 liquid chromatography system with differential refractive index detector using the following conditions: 2 × Polymer Labs PLgel columns of Minimix- C pore size ( 5 μm 250 × 4.6 mm); eluent was 0.2 % Lithium nitrate/THF at a flow rate of 0.3 ml/min; column oven set at 40 °C; RI Detector's internal temperature set at 35 °C with an injection volume of 20 μl. Standards: Polystyrene covering a molecular weight range ≥ 0.5M; (n = 11).

Polymer	NVC/ %	S.G/gcm <sup>-3</sup>		Viscosity/ Poise
		Polymer Solution	Solid Resin	
RC957Q(I)	55	0.9264	0.9987	3.86
RC957Q(II)	54	0.9252	0.9993	2.65

Table 10:2: QA data of RC957 polymers

Polymer	Average M <sub>N</sub>	Average M <sub>w</sub>	Polydispersity
RC957Q(I)	4867	12194	2.51
RC957Q(II)	4953	12659	2.56

Table 10:3: GPC data of RC957 polymers

### 10.3.4 MESQ(I)v25

To a polymerisation reaction vessel containing mechanically stirred xylene at 85<sup>0</sup>C (335g) was added drop wise, a solution of monomers consisting of: MESQ(I) 245.3 g, 0.4420 moles and iBoMA (294.8 g, 1.3260 moles) in xylene (200 g), and AMBN initiator (3.41 g, 0.0177 moles). The monomer feed was added using a Watson-Marlow peristaltic pump at a rate such that complete addition took 3.5 h. On completion the temperature was increased to 95 <sup>0</sup>C. Once the temperature reached 95 <sup>0</sup>C a boost amount of AMBN was added (1.70 g, 0.0088 moles) and the reaction was maintained at this temperature for a further 30 mins. The resulting viscous amber liquid was submitted for <sup>1</sup>H NMR and used without further purification.

### 10.3.5 MESQ(I)v30

The above experimental method was altered as follows:

MESQ(I) - 245.3g, 0.4420 moles (30 mol%)

iBoMA - 229.3 g, 1.0313 moles (70 mol%)

Solvent - 479 g (279 in reactor)

Initial AMBN - 2.83 g, 0.0147 moles

Boost AMBN - 1.42 g, 0.0074 moles

### 10.3.6 MESQ(II)v25

To a polymerisation reaction vessel containing mechanically stirred xylene at 85<sup>0</sup>C (356g) was added drop wise, a solution of monomers consisting of: MESQ(II) (265.1 g, 0.4434 moles) and iBoMA (295.7 g, 1.3302 moles) in xylene (200 g), and AMBN initiator (3.41 g, 0.0177 moles). The monomer feed was added using a Watson-Marlow peristaltic pump at a rate such that complete addition took 3.5 h. On completion the temperature was increased to 95 <sup>0</sup>C. Once the temperature reached 95 <sup>0</sup>C a boost amount of AMBN was added (1.70 g, 0.0088 moles) and the reaction was maintained at this temperature for a further 30 mins. The resulting viscous amber liquid was submitted for <sup>1</sup>H NMR and used without further purification.

### 10.3.7 MESQ(II)v30

The above experimental method was altered as follows:

MESQ(II) - 265.1 g, 0.4434 moles (30 mol%)

iBoMA - 230.0 g, 1.0346 moles (70 mol%)

Solvent - 500g (300 in reactor)

Initial AMBM - 2.84 g, 0.0148 moles

Boost AMBN - 1.42 g, 0.0074 moles

Each of the above polymers was characterised in terms of  $^1\text{H}$  NMR, viscosity, percentage non-volatile content (NVC), specific gravity (SG), total unreacted monomer molar percentage and unreacted monomer molar percentage, number average molecular weight ( $M_N$ ), weight average molecular weight ( $M_W$ ) and polymer polydispersity, data presented in **Table 10:4** and **Table 10:5**. GPC data collected using the method previously stated.

All polymers has very similar  $^1\text{H}$  NMR, ( $\text{CDCl}_3$ )  $\delta$ : 7.3 – 6.8 (Ar- $\underline{H}$ , m), 3.4 ( $\text{N}^+$ - $\underline{\text{CH}_2}$ - $\text{CH}_2^-$ , m), 3.2 ( $\text{N}^+$ - $\underline{\text{CH}_3}$ , s), 2.5 (Ar- $\underline{\text{CH}_2}$ - $\text{CH}_3$ , dd), 2.2 (Ar- $\underline{\text{CH}_3}$ , m), 1.5 – 1.2 ( $\text{CH}_3$ - $\underline{\text{CH}_2^-}$ , m), 1.0 – 0.75 ( $\underline{\text{CH}_2^-}$ - $\text{CH}_2^-$ , m)

Polymer	NVC/ %	S.G/gcm <sup>-3</sup>		Viscosity/ Poise	Unreacted Monomer mol%		
		Polymer Solution	Solid Resin		MESQ(I or II)	iBoMA	TOTAL
MESQ(I)v25	51	0.9470	1.0419	40.2	9.1	9.1	9.1
MESQ(I)v30	50	0.9450	1.0413	20.0	9.0	8.4	8.8
MESQ(II)v25	48	0.9420	1.0425	6.2	9.6	10.7	10.2
MESQ(II)v30	50	0.9380	1.0245	11.8	12.0	12.1	12.1

Table 10:4: QA data of MESQ(I)v25 and 30 and MESQ(II)v25 and 30 polymers

Polymer	Average $M_N$	Average $M_W$	Polydispersity
MESQ(I)v25	10372	22637	2.18
MESQ(I)v30	9259	18872	2.04
MESQ(II)v25	10062	23326	2.32
MESQ(II)v30	9057	19838	2.19

Table 10:5: GPC data of MESQ(I)v25 and 30 and MESQ(II)v25 and 30 polymers

### 10.3.8 Preparation of polymer MESQ(I)25v2-10

The above experimental conditions were altered as follows, **Table 10:6**.

Polymer	Reactor Xylene (g)	Monomer Xylene (g)	Monomer Composition			Initial AMBN (g)	Boost AMBN (g)
			MESQ(I) (mol%)	iBoMA (mol%)	Other (mol%)		
v2	320.0	200.0	25	15	60 EHMA	3.40	1.70
v3	329.0	200.0	25	37.5	37.5 EHMA	3.40	1.70
v4	339.0	200.0	25	60	15 EHMA	3.40	1.70
v5	260.0	200.0	25	15	60 BMA	3.40	1.70
v6	292.0	200.0	25	37.5	37.5 BMA	3.40	1.70
v7	324.0	200.0	25	60	15 BMA	3.40	1.70
v8	379.0	200.0	25	15	60 LMA	3.40	1.70
v9	366.0	200.0	25	37.5	37.5 LMA	3.40	1.70
v10	353.0	200.0	25	60	15 LMA	3.40	1.70

Table 10:6: Altered synthetic factors for the manufacture of MESQ(I)25v2-10

Each of the above polymers was characterised in terms of  $^1\text{H}$  NMR, viscosity, percentage non-volatile content (NVC), specific gravity (SG), total unreacted monomer molar percentage and unreacted monomer molar percentage, number average molecular weight ( $M_N$ ), weight average molecular weight ( $M_W$ ) and polymer polydispersity, data presented in **Table 10:7** and **Table 10:8**. GPC data collected using the method previously stated.

All polymers has very similar  $^1\text{H}$  NMR, ( $\text{CDCl}_3$ )  $\delta$ : 7.3 – 6.8 (Ar- $\underline{H}$ , m), 3.4 ( $\text{N}^+$ - $\underline{\text{CH}_2}$ - $\text{CH}_2^-$ , m), 3.2 ( $\text{N}^+$ - $\underline{\text{CH}_3}$ , s), 2.5 (Ar- $\underline{\text{CH}_2}$ - $\text{CH}_3$ , dd), 2.2 (Ar- $\underline{\text{CH}_3}$ , m), 1.5 – 1.2 ( $\text{CH}_3$ - $\underline{\text{CH}_2^-}$ , m), 1.0 – 0.75 ( $\underline{\text{CH}_3}$ - $\text{CH}_2^-$ , m)

Polymer	NVC/ %	S.G/ $\text{gcm}^{-3}$		Viscosity/ Poise	Unreacted Monomer %			
		Polymer Solution	Solid Resin		MESQ(I)	iBoMA	Other	TOTAL
MESQ(I)25v2	48	0.9310	1.0149	9.16	6.8	7.6	6.1	6.5
MESQ(I)25v3	48	0.9400	1.0374	9.68	8.1	8.6	8.1	8.3
MESQ(I)25v4	48	0.9410	1.0400	12.84	6.3	9.0	8.4	8.2
MESQ(I)25v5	48	0.9350	1.0248	13.40	6.3	8.6	6.0	6.5
MESQ(I)25v6	48	0.9370	1.0299	11.44	5.9	8.6	6.6	7.2
MESQ(I)25v7	50	0.9450	1.0413	21.24	6.0	8.2	8.0	7.4
MESQ(I)25v8	49	0.9210	0.9875	7.32	5.2	8.7	6.5	6.5
MESQ(I)25v9	49	0.9270	1.0017	13.24	6.0	7.2	6.3	6.6
MESQ(I)25v10	49	0.9380	1.0283	12.28	6.4	8.0	8.5	7.7

**Table 10:7: Second Generation MESQ Polymer QA**

Polymer	Average $M_N$	Average $M_W$	Polydispersity
MESQ(I)25v2	11586	27303	2.36
MESQ(I)25v3	11067	24563	2.22
MESQ(I)25v4	11412	24418	2.14
MESQ(I)25v5	9697	19629	2.02
MESQ(I)25v6	10458	22396	2.14
MESQ(I)25v7	9867	20725	2.10
MESQ(I)25v8	15605	37545	2.41
MESQ(I)25v9	12857	30709	2.39
MESQ(I)25v10	10770	24630	2.29

**Table 10:8: GPC data for Second Generation MESQ Polymers**

### 10.3.9 Preparation of AMPSQ polymer

The following polymers were prepared using an experimental design developed experimental design software; Design – Expert 7 version 7.1.6 (2008), available from Stat-Ease, Inc, Minneapolis, USA.

To a polymerisation reaction vessel containing mechanically stirred xylene:butanol (3:1) at  $85^\circ\text{C}$  (307 g) was added drop wise, a solution of monomers consisting of: AMPSQ(I) (229.6 g, 0.4433 moles), iBoMA (254.0 g, 1.1424 moles) and BMA (17.0 g, 0.1194 moles) in xylene:butanol (3:1) (200 g), and AMBN initiator (3.28 g, 0.0171 moles). The monomer feed was added using a Watson-Marlow peristaltic pump at a rate such that complete addition took 3.5 h. On completion

the temperature was increased to 95 °C. Once the temperature reached 95 °C a boost amount of AMBN was added (1.64 g, 0.0088 moles) and the reaction was maintained at this temperature for a further 60 mins after which an additional boost of AMBN was added (1.64 g, 0.0088 moles) and the reaction maintained at this temperature for a further 60 mins. The resulting viscous amber liquid was submitted for <sup>1</sup>H NMR and used without further purification.

The above experimental conditions were altered as follows, **Table 10:9**.

Polymer	Reactor Solvent (g)	Monomer Solvent (g)	Monomer Composition			Initial AMBN (g)	2 × Boost AMBN (g)
			AMPSQ (I or II) (mol%)	iBoMA (mol%)	Other (mol%)		
AMPSQ(I)v2	314.0	200.0	26.0	72.0	2.0	3.28	1.64
AMPSQ(I)v3	245.0	200.0	32.0	67.0	3.0	2.66	1.33
AMPSQ(I)v4	284.0	200.0	28.0	68.0	4.0	3.04	1.52
AMPSQ(I)v5	284.0	200.0	28.0	68.0	4.0	3.04	1.52
AMPSQ(I)v6	284.0	200.0	28.0	68.0	4.0	3.04	1.52
AMPSQ(I)v7	259.0	200.0	30.0	65.0	5.0	2.84	1.42
AMPSQ(I)v8	217.0	200.0	35.0	65.0	-	2.44	1.22
AMPSQ(I)v9	332.0	200.0	25.0	75.0	-	3.41	1.70
AMPSQ(I)v10	325.0	200.0	25.0	70.0	5.0	3.41	1.70
AMPSQ(I)v11	265.0	200.0	30.0	70.0	-	2.85	1.42
AMPSQ(I)v12	317.0	200.0	25.0	65.0	10.0	3.41	1.70
AMPSQ(II)v4	284.0	200.0	28.0	68.0	4.0	3.04	1.52
AMPSQ(I)v10 FB	334.0	200.0	25.0	70.0	5.0	3.41	1.70

**Table 10:9: Altered synthetic factors for the manufacture of remaining AMPSQ polymer**

Each of the above polymers was characterised in terms of <sup>1</sup>H NMR, viscosity, percentage non-volatile content (NVC), specific gravity (SG), total unreacted monomer molar percentage and unreacted monomer molar percentage, number average molecular weight (M<sub>N</sub>), weight average molecular weight (M<sub>w</sub>) and polymer polydispersity, data presented in **Table 10:10** and **Table 10:11**. GPC data collected using the method previously stated.

All polymers has very similar <sup>1</sup>H NMR, (CDCl<sub>3</sub>) δ: 7.3 – 6.8 (Ar-H, m), 3.6 (HO-CH<sub>2</sub>-CH<sub>2</sub>-, t), 3.5 – 3.2 (N<sup>+</sup>-CH<sub>2</sub>-CH<sub>2</sub>- and N<sup>+</sup>-CH<sub>3</sub>, m), 2.5 (Ar-CH<sub>2</sub>-CH<sub>3</sub>, dd), 2.2 (Ar-CH<sub>3</sub>, m), 1.5 – 1.2 (CH<sub>3</sub>-CH<sub>2</sub>-, m), 1.0 – 0.75 (CH<sub>3</sub>-CH<sub>2</sub>-, m)

Polymer	NVC/ %	S.G/gcm <sup>-3</sup>		Viscosity/ Poise	Unreacted Monomer mol%		
		Polymer Solution	Solid Resin		AMPSQ(I or II)	iBoMA	TOTAL
AMPSQ(I)v1	53	1.0139	0.9380	7.23	3.3	0.95	1.39
AMPSQ(I)v2	52	1.0286	0.9430	9.28	4.3	1.05	1.65
AMPSQ(I)v3	52	1.0195	0.9390	9.41	3.3	0.83	1.48
AMPSQ(I)v4	51	1.0231	0.9390	8.00	3.4	0.92	1.44
AMPSQ(I)v5	52	1.0309	0.9360	8.24	3.9	0.93	1.33
AMPSQ(I)v6	51	1.0497	0.9420	8.75	3.1	0.84	1.46
AMPSQ(I)v7	50	1.0521	0.9410	9.45	4.1	0.77	1.49
AMPSQ(I)v8	51	1.0257	0.9320	9.43	4.1	0.78	1.68
AMPSQ(I)v9	51	1.0497	0.9420	8.54	4.2	1.05	1.73
AMPSQ(I)v10	51	1.0521	0.943	8.85	2.6	0.79	1.18
AMPSQ(I)v11	51	1.0424	0.939	7.43	4.7	0.92	1.63
AMPSQ(I)v12	51	1.0473	0.941	8.17	4.3	0.92	1.67
AMPSQ(II)v4	54	1.0170	0.9333	4.44	6.1	0.40	1.99
AMPSQ(I)v10 FB	52	1.0526	0.9452	7.52	10.4	1.90	4.06

**Table 10:10: QA data of AMPSQ polymers**

<i>Polymer</i>	<i>Average <math>M_N</math></i>	<i>Average <math>M_W</math></i>	<i>Polydispersity</i>
<i>AMPSQ(I)v1</i>	6988	17681	2.53
<i>AMPSQ(I)v2</i>	7144	18445	2.58
<i>AMPSQ(I)v3</i>	6240	14767	2.37
<i>AMPSQ(I)v4</i>	6887	16656	2.42
<i>AMPSQ(I)v5</i>	6553	17189	2.62
<i>AMPSQ(I)v6</i>	6762	16852	2.49
<i>AMPSQ(I)v7</i>	6675	15764	2.36
<i>AMPSQ(I)v8</i>	5601	12613	2.25
<i>AMPSQ(I)v9</i>	7275	19068	2.62
<i>AMPSQ(I)v10</i>	7321	19468	2.66
<i>AMPSQ(I)v11</i>	6213	15034	2.42
<i>AMPSQ(I)v12</i>	7380	19342	2.62
<i>AMPSQ(II)v4</i>	6470	16028	2.48
<i>AMPSQ(I)v10 FB</i>	7329	20447	2.79

**Table 10:11: GPC data of AMPSQ polymers**

## 10.4 Paint Manufacture

A 650 ml prototype paint formulation was used for all the paints created for testing during this thesis. This formulation was created using specialist paint formulation software which ensured the paints have the same volatile organic content (VOC) and that they contain the same volume of test polymer in the dry paint film, **Table 10:12**. Consequently, all the paints contain the same mass of each raw material except the test polymer and solvent. These are reciprocally adjusted to account for changes in the non-volatile content of the polymers ensuring consistency between the test paints.

<i>Raw Material</i>	<i>Dry Film Volume %</i>
<i>Test Polymer</i>	<b>44.7</b>
<i>Copper Oxide</i>	<b>26.6</b>
<i>Copper Pyrithione</i>	<b>13.3</b>
<i>Rheology Modifier</i>	<b>1.5</b>
<i>Pigmentation</i>	<b>5.1</b>
<i>Plasticiser</i>	<b>8.8</b>

**Table 10:12: Standard Prototype Paint Formulation**

### 10.4.1 RC957Q(I) Paint

RC957Q(I) (200.0 g), pigment (88.6 g) and rheology modifier (28.5 g) were added together and mixed with high speed dispersion (HSD) 2000 rpm for 10 minutes. Copper oxide (557.2 g) and copper pyrithione (83.6 g) were then added to the mixture and at HSD 3000 rpm for 30 minutes. The particles size was checked to be less than 60  $\mu\text{m}$  using a grind gauge (see Grind Determination below). RC957Q(I) (147.9 g), and xylene (74.6 g) were then added to the mixture and at HSD 2000 rpm for 10 minutes. Finally the paint was filtered through a mesh filter, pore size 125  $\mu\text{m}$ . The final paint was tested for grind and viscosity, **Table 10:13**.

#### 10.4.2 RC957Q(II) Paint

RC957Q(II) (200.0 g), pigment (88.6 g) and rheology modifier (28.5 g) were added together and mixed with high speed dispersion (HSD) 2000 rpm for 10 minutes. Copper oxide (557.2 g) and copper pyrithione (83.6 g) were then added to the mixture and at HSD 3000 rpm for 30 minutes. The particles size was checked to be less than 60  $\mu\text{m}$  using a grind gauge (see Grind Determination below). RC957Q(II) (145.5 g), and xylene (75.8 g) were then added to the mixture and at HSD 2000 rpm for 10 minutes. Finally the paint was filtered through a mesh filter, pore size 125  $\mu\text{m}$ . The final paint was tested for grind and viscosity, **Table 10:13**.

#### 10.4.3 RC957 Acid Paint

RC957 (200.0 g), pigment (88.6 g) and rheology modifier (28.5 g) were added together and mixed with high speed dispersion (HSD) 2000 rpm for 10 minutes. Seanine-211 (253.4 g) was then added to the mixture and at HSD 3000 rpm for 30 minutes. The particles size was checked to be less than 60  $\mu\text{m}$  using a grind gauge (see Grind Determination below). RC957 (110.7 g), and xylene (80.1 g) were then added to the mixture and at HSD 2000 rpm for 10 minutes. Finally the paint was filtered through a mesh filter, pore size 125  $\mu\text{m}$ . The final paint was tested for grind and viscosity, **Table 10:13**.

	<i>RC957Q(I)</i>	<i>RC957Q(II)</i>	<i>RC957 (acid)</i>
<i>Grind/<math>\mu\text{m}</math></i>	40	40	40
<i>Viscosity/ Poise</i>	1.0	0.63	6.0

**Table 10:13: Physical properties of RC957 paints**

#### 10.4.4 First and Second Generation MESQ Paints

MESQ(VI) (200.0 g), pigment (80.2 g) and rheology modifier (25.7 g) were added together and mixed with high speed dispersion (HSD) 2000 rpm for 10 minutes. Copper oxide (504.5 g) and copper pyrithione (75.7 g) were then added to the mixture and at HSD 3000 rpm for 30 minutes. The particles size was checked to be less than 60  $\mu\text{m}$  using a grind gauge (see Grind Determination below). MESQ(VI) (98.5 g), xylene (146.4 g) and plasticiser (25.7 g) were then added to the mixture and at HSD 2000 rpm for 10 minutes. Finally the paint was filtered through a mesh filter, pore size 125  $\mu\text{m}$ . The final paint was tested for grind and viscosity, **Table 10:14**.

	<i>MESQ(I)v25</i>	<i>MESQ(I)v30</i>	<i>MESQ(II)v25</i>	<i>MESQ(II)v30</i>
<i>Grind/<math>\mu\text{m}</math></i>	40	40	40	40
<i>Viscosity/ Poise</i>	53.7	24.4	14.1	20.5

**Table 10:14: Physical properties of MESQ paints**

The above experimental conditions were altered as follows for the remaining MESQ polymers. The total mass of the polymer required for the formulation was added in two aliquots during the manufacture process. The first is 200.0 g and the second is the remaining mass of required to ensure a consistent volume of test polymer in the dry paint film, **Table 10:15**. The final paint was tested for grind and viscosity, **Table 10:14**.

<i>Test Paint</i>	<i>Mass of Polymer/g</i>	<i>Mass of Solvent/g</i>
<i>MESQ(I)v30</i>	94.1	120.9
<i>MESQ(II)v25</i>	106.7	108.5
<i>MESQ(II)v30</i>	89.4	123.3
<i>MESQ(I)25v2</i>	98.6	112.7
<i>MESQ(I)25v3</i>	105.2	109.2
<i>MESQ(I)25v4</i>	106.0	108.9
<i>MESQ(I)25v5</i>	101.5	111.2
<i>MESQ(I)25v6</i>	103.0	110.4
<i>MESQ(I)25v7</i>	94.1	120.9
<i>MESQ(I)25v8</i>	84.6	122.8
<i>MESQ(I)25v9</i>	88.7	120.7
<i>MESQ(I)25v10</i>	96.4	116.8

**Table 10:15: Altered mass of polymer and solvent for the manufacture of MESQ paint**

	<i>MESQ (I) 25v2</i>	<i>MESQ (I) 25v3</i>	<i>MESQ (I) 25v4</i>	<i>MESQ (I) 25v5</i>	<i>MESQ (I) 25v6</i>	<i>MESQ (I) 25v7</i>	<i>MESQ (I) 25v8</i>	<i>MESQ (I) 25v9</i>	<i>MESQ (I) 25v10</i>
<i>Grind/μm</i>	40	40	40	40	40	40	40	40	40
<i>Viscosity/Poise</i>	42.1	36.8	31.7	35.0	39.8	63.7	21.7	37.4	30.2

**Table 10:16: Physical properties of Second Generation MESQ paints**

#### 10.4.5 AMPSQ Paints

AMPSQ(I)v1 (200.0 g), pigment (80.2 g) and rheology modifier (25.7 g) were added together and mixed with high speed dispersion (HSD) 2000 rpm for 10 minutes. Copper oxide (504.5 g) and copper pyrithione (75.7 g) were then added to the mixture and at HSD 3000 rpm for 30 minutes. The particles size was checked to be less than 60 μm using a grind gauge (see Grind Determination below). AMPSQ(I)v1 (72.5 g), xylene (139.0 g) and plasticiser (27.0 g) were then added to the mixture and at HSD 2000 rpm for 10 minutes. Finally the paint was filtered through a mesh filter, pore size 125 μm. The final paint was tested for grind and viscosity, **Table 10:18**.

The above experimental conditions were altered as follows for the remaining AMPSQ polymers. The total mass of the polymer required for the formulation was added in two aliquots during the manufacture process. The first is 200.0 g and the second is the remaining mass of required to ensure a consistent volume of test polymer in the dry paint film, **Table 10:17**. The final paint was tested for grind and viscosity, **Table 10:18**.

Test Paint	Mass of Polymer/g	Mass of Solvent/g
AMPSQ(I)v2	81.8	131.7
AMPSQ(I)v3	79.3	132.9
AMPSQ(I)v4	85.8	126.9
AMPSQ(I)v5	80.0	131.4
AMPSQ(I)v6	90.7	123.3
AMPSQ(I)v7	97.2	117.0
AMPSQ(I)v8	84.1	126.6
AMPSQ(I)v9	90.7	123.3
AMPSQ(I)v10	91.4	122.9
AMPSQ(I)v11	88.7	124.3
AMPSQ(I)v12	90.0	123.6
AMPSQ(II)v4	66.0	143.7
AMPSQ(I)v10 FB	101.8	133.2

Table 10:17: Altered mass of polymer and solvent for the manufacture of AMPSQ paint

	v1	v2	v3	v4	v5	v6	v7	v8	v9	v10	v11	v12	Q(II) v4	v10 FB
Grind/ $\mu$ m	40	40	40	40	40	40	40	40	40	40	40	40	40	40
Viscosity/ Poise	2.02	2.27	2.26	2.24	1.61	1.18	1.27	1.06	1.24	1.08	0.96	1.17	0.61	1.45

Table 10:18: Physical properties of Second Generation AMPSQ paints

## 10.5 Test Methodology/Procedure

### 10.5.1 NMR Experiments

NMR analysis of samples was performed on a Bruker Avance equipped with a 250 MHz Oxford magnet and a 5 mm dual resonance probe. Spectra were recorded at  $25.0 \pm 0.5$  °C and processed using Topspin 2.1 software.

### 10.5.2 Specific Gravity Determination – Pressure Cup method

The weight of the empty cup was recorded (to at least two decimal places) -  $M_1$ . The cup was then nearly filled with the test liquid and closed by fitting and locking the pressure release cap. The test liquid was then compressed to a final volume of 100 ml by turning the pressure-application handle clockwise which inserted a piston into the cup. During this process, a small amount of excess liquid was forced out between the cup and the pressure-release cap. Following cleaning and drying to remove this extraneous liquid, the weight of the filled cup was recorded -  $M_2$ .

The density of the paint was then calculated as follows:

$$\frac{(M_2 - M_1)}{100} \text{ (grams/ml)}$$

$M_1$  - mass of empty pressure cup/grams;  $M_2$  - mass of pressure cup containing fully compressed sample/grams.

The measured densities were that of the experimental polymer solutions which represent the combined density of the solid polymer resin and that of the co-solvents. If the non-volatile content (NVC) of the polymer solution is known, the specific density of the polymer resin can be calculated. The experimental solid polymer density was calculated as follows:

$$\frac{M_2 - M_1 - D_s(100 - \text{NVC})}{\text{NVC}} \text{ (grams/ml)}$$

$M_1$  - mass of empty pressure cup (grams);  $M_2$  - mass of pressure cup containing fully compressed sample (grams);  $D_s$  - density of co-solvents (grams/ml) and NVC - non-volatile content of polymer solution (%).

### 10.5.3 Non-volatile Content Determination

Aluminium dishes (60 mm diameter x 20 mm deep) were labelled and prepared in triplicate. A partially unfolded paper clip was placed into each dish and the assembly weighed on an analytical top-pan balance (weight recorded to 4 decimal places) –  $W_1$ . An aliquot of liquid test sample (0.5-1.0 g) was then inserted into the dish assembly and their combined weight recorded –  $W_2$ . This was repeated in triplicate for each liquid sample. The dishes were then placed in a calibrated convection oven, set at  $105 \pm 2^\circ\text{C}$  for 1 hour. After this period the dishes were then removed from the oven and allowed to cool for 30 minutes prior the final weight being recorded –  $W_3$ . The percentage non-volatile content is calculated by:

$$\frac{W_3 - W_1}{W_2 - W_1} \times 100 \text{ (\%)}$$

$W_1$  – weight of empty dish and paper clip;  $W_2$  – weight of liquid sample and dish with paper clip;  $W_3$  – weight of dry sample and dish with paper clip. The final percentage non-volatile content is the mean of the triplicate results.

### 10.5.4 Viscosity Measurements

A Brookfield CAP 1000 cone and plate viscometer was used to determine the viscosity of liquid samples. The thermostat of the viscometer's integral hotplate was set at  $(25.0 \pm 0.2^\circ\text{C})$  to ensure consistency and the appropriate cone was installed. Directly below the cone on the hotplate a 'drawing-pin head' sized aliquot of liquid test sample was placed. The cone was then immersed into the liquid sample and left for 10 seconds for temperature equilibration prior to the rotation of the cone. The cone is automatically rotated, stopping once the resistance to the rotation was constant. This final reading is recorded as the viscosity. This process was repeated in triplicate for each liquid sample and the mean value quoted as the final viscosity.

### 10.5.5 Grind Determination

The grind gauge was placed on a horizontal, flat, non-slip surface. Sufficient liquid paint was poured into the deep end of the gauge channel(s) so that it slightly overflows. The scraper was then drawn down the channel(s) at a uniform rate along the gauge, from the deep end of the channel to a point beyond zero depth. Sufficient downward pressure was applied to the scraper to spread the paint filling the channel(s) and to remove any surplus. The complete drawdown took no more than 1-2 seconds. Within 5 seconds of completion, the gauge was examined from the side, against good lighting, and viewing at an angle of 20 - 30 ° to the plane of the gauge surface. The point(s) in the channel(s) were observed where the test material shows a definite speckled appearance. This point was estimated to the nearest 5 µm for the 100 µm gauge and recorded. This value was quoted as the grind.

### **10.5.6 Differential Scanning Calorimetry**

Experimental solid polymer resin samples were obtained by placing aliquots of the experimental polymer solution in a temperature controlled oven at  $105 \pm 2$  °C for 1 hour solvent. 10-20 mg of this dried polymer resin was placed into small sealable aluminium crucibles and the sample weight recorded.

A Netzsch DSC 200 F3 Maia differential scanning calorimeter (DSC) programmed through the Proteus operational software was used to determine the glass transition temperature of the polymer samples using the following programme:

Samples were heated from to +150.0 °C at 25 °C/min to ensure that all the solvent had been removed from the polymer resin. Following cooling to -80.0 °C, the programme was repeated on the same sample recording the energy required to achieve changes in the temperature of the sample. The glass transition temperature was determined as the point of inflection of any stepwise transition present in a trace of energy per mass of sample against temperature.

### **10.5.7 Semi Rapid Boot-top Cycling**

Steel panels (102 × 152 × 0.8 mm) were degreased with solvent; dried and then primed with anticorrosive paint (Primocon). Following 24 hours curing at ambient laboratory temperature, the test coatings were applied to the panels using a drawdown application bar which ensured a uniform 500 µm film thickness and dried for a further 48 hours under ambient conditions. Panels were also prepared coated with 'pass' and 'fail' standard products (Pass – Intersmooth 460; Fail – Interspeed 340). All the panels, standards and test coatings, were pre-immersed prior to testing by fully submerging the panels in a seawater bath at 25 °C for 7 days. Once removed from the pre-immersion bath the panels were immediately transferred to a second seawater bath maintained at 35 °C with sufficient seawater to half immerse the test panels and subjected to a 48 hour testing

rotation. One rotation consisted of a 24 hour period during which the panels were half immersion in seawater at 35 °C after which they were immediately transferred to a temperature controlled environmental cabinet programmed for 12 hours at -5 °C followed by 12 hours at 10 ± 1 °C. After this 48 hour period the panels were inspected at ambient conditions and assessed as to the deterioration of the integrity of the coatings film. A 5 point rating system was used to assess the film integrity:

- 5 No cracking
- 4 Hairline cracking just visible to the naked eye
- 3 Cracking clearly visible
- 2+1 Progressively worse levels of cracking
- 0 Gross cracking over the whole film

Panel assessment ratings were compared against the rating of the pass and fail standards to gauge the performance of the test coatings. The 35/-5 °C cycling was continued until sufficient differentiation between the test coatings became apparent.

### 10.5.8 Polishing Rate

Perspex discs were prepared in triplicate (one disc for each immersion period 60, 90 or 120 days) by abrasion of the surface and washing with both water and then solvent to remove surface contamination. After drying at ambient laboratory conditions the coatings were applied using a cube applicator in straight stripes starting close to the centre of the disc emanating outward. This process is repeated rotating the disc after each strip until the disc is fully coated, *circa* 16 strips, **Figure 10:1**.

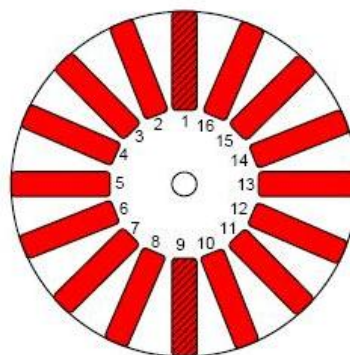


**Figure 10:1: Diagram of a prepared disc**

Each test coating, including a standard control paint (Interswift 655), applied to the discs had a minimum of 2 stripes positioned diametrically opposite to each other to reduce experimental error. Following the coatings application, the discs were dried for a minimum of 10 days at ambient laboratory temperature. The thickness of each strip was then measured at 2, 5 and 7 cm from the

edge of the disc using laser profilometry. The distance 2, 5 and 7 cm represent speeds of 18.5, 14.2 and 11.4 knots respectively.

The prepared discs were attached to a rotor-shaft and immersed in seawater at  $25 \pm 2^\circ\text{C}$  and spun at 700 rpm for 60, 90 and 120 days. On completion of the predetermined immersion period the discs were removed and dry for a minimum of 10 days at ambient laboratory temperature following which period the film thickness of the coatings were re-measured. The absolute loss of film thickness was determined as the difference between the initial film thickness and the film thickness after immersion, **Figure 10:2**. The polishing rate of the coatings, under the specified conditions of temperature and rotation speed, was calculated by the difference between the initial film thickness and the thickness after immersion, divided by the immersion period (in days). The result is multiplied by 30 to give the final polishing rate in the units of microns/month. The performance of each test coating is compared to that of the standards.

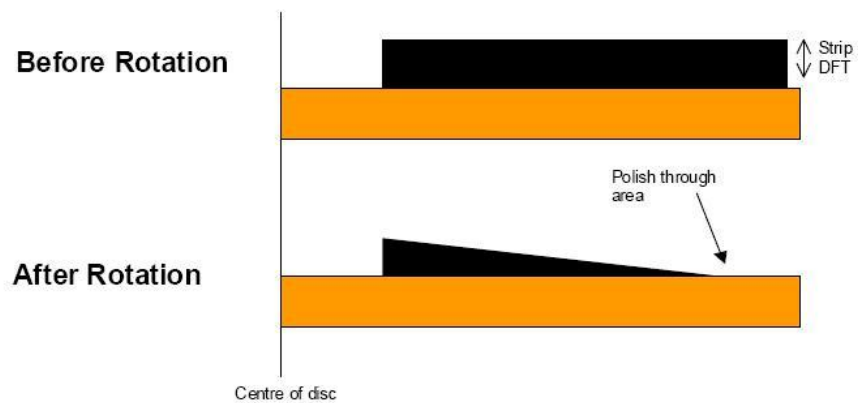


**Figure 10:2: Profile of coatings before and after testing, displaying variations in film thickness with angular velocity**

1<sup>st</sup> Generation MESQ polishing data for **Figure 3:8**

Paint	60				DAYS IMMERSION				60			
	Initial thickness / $\mu\text{m}$	Final thickness / $\mu\text{m}$	$\Delta$ thickness strip 1 / $\mu\text{m}$	Av.30 days	Initial thickness / $\mu\text{m}$	Final thickness / $\mu\text{m}$	$\Delta$ thickness strip 2 / $\mu\text{m}$	Av.30 days	Initial thickness / $\mu\text{m}$	Final thickness / $\mu\text{m}$	$\Delta$ thickness strip 3 / $\mu\text{m}$	Av.30 days
<b>MESQ(III) 30%</b>	52.53	58.48	5.95	2.98	52.86	69.91	17.05	8.53	76.22	63.89	-12.33	-6.17
<b>MESQ(III) 30%</b>	101.17	105.97	4.80	2.40	53.08	51.49	-1.59	-0.79	73.46	59.98	-13.48	-6.74
<b>MESQ(III) 25%</b>	54.27	54.05	-0.22	-0.11	53.71	53.28	-0.43	-0.22	53.51	63.68	10.17	5.09
<b>MESQ(III) 25%</b>	47.01	54.14	7.13	3.57	55.55	52.46	-3.09	-1.55	58.94	44.93	-14.01	-7.01
<b>MESQ(VI) 25%</b>	54.72	52.85	-1.87	-0.93	48.68	49.80	1.12	0.56	66.72	59.38	-7.34	-3.67
<b>MESQ(VI) 25%</b>	50.75	52.89	2.14	1.07	55.29	55.62	0.33	0.16	65.65	60.52	-5.13	-2.57
<b>MESQ(VI) 30%</b>	37.34	50.46	13.12	6.56	51.25	51.56	0.31	0.16	59.03	53.08	-5.95	-2.98
<b>MESQ(VI) 30%</b>	46.06	51.72	5.66	2.83	54.19	54.80	0.61	0.31	49.35	50.14	0.79	0.40
<b>MESQ(VI) 25%</b>	46.88	53.25	6.37	3.19	47.99	49.20	1.21	0.61	53.42	52.31	-1.11	-0.56
<b>MESQ(VI) 25%</b>	48.86	50.33	1.47	0.73	50.41	50.73	0.32	0.16	61.93	61.40	-0.53	-0.27
<b>I/S 655</b>	56.87	51.25	-5.62	-2.81	56.79	46.39	-10.40	-5.20	55.19	46.93	-8.26	-4.13
<b>I/S 655</b>	74.56	65.62	-8.94	-4.47	59.86	50.13	-9.73	-4.87	60.27	54.64	-5.63	-2.82

**Table 10:19: 60 days polishing data for 1<sup>st</sup> Generation MESQ paints**

1<sup>st</sup> Generation MESQ polishing data for **Figure 3:8**

Paint	90				DAYS IMMERSION				90			
	Initial thickness / $\mu\text{m}$	Final thickness / $\mu\text{m}$	$\Delta$ thickness strip 1 / $\mu\text{m}$	Av.30 days	Initial thickness / $\mu\text{m}$	Final thickness / $\mu\text{m}$	$\Delta$ thickness strip 2 / $\mu\text{m}$	Av.30 days	Initial thickness / $\mu\text{m}$	Final thickness / $\mu\text{m}$	$\Delta$ thickness strip 3 / $\mu\text{m}$	Av.30 days
<i>MESQ(III) 30%</i>	57.28	52.27	-5.01	-1.67	50.99	52.81	1.82	0.61	53.04	49.09	-3.95	-1.32
<i>MESQ(III) 30%</i>	56.18	54.26	-1.92	-0.64	52.45	49.27	-3.18	-1.06	57.89	53.19	-4.70	-1.57
<i>MESQ(III) 25%</i>	54.31	57.03	2.72	0.91	55.35	56.47	1.12	0.37	54.06	54.99	0.93	0.31
<i>MESQ(III) 25%</i>	53.53	54.25	0.72	0.24	51.49	54.77	3.28	1.09	50.54	54.24	3.70	1.23
<i>MESQ(VI) 25%</i>	49.18	45.85	-3.33	-1.11	52.45	53.45	1.00	0.33	82.76	82.94	0.18	0.06
<i>MESQ(VI) 25%</i>	49.83	52.66	2.83	0.94	50.94	53.69	2.75	0.92	54.27	58.69	4.42	1.47
<i>MESQ(VI) 30%</i>	52.90	54.76	1.86	0.62	48.42	47.11	-1.31	-0.44	50.69	49.65	-1.04	-0.35
<i>MESQ(VI) 30%</i>	49.70	50.90	1.20	0.40	50.31	50.21	-0.10	-0.03	54.41	49.67	-4.74	-1.58
<i>MESQ(VI) 25%</i>	46.81	46.50	-0.31	-0.10	51.97	51.69	-0.28	-0.09	51.33	50.91	-0.42	-0.14
<i>MESQ(VI) 25%</i>	50.44	53.94	3.50	1.17	48.60	50.33	1.73	0.58	50.58	52.39	1.81	0.60
<i>I/S 655</i>	55.14	47.24	-7.90	-2.63	57.50	46.41	-11.09	-3.70	75.68	58.84	-16.84	-5.61
<i>I/S 655</i>	58.28	50.06	-8.22	-2.74	64.35	49.79	-14.56	-4.85	60.69	54.02	-6.67	-2.22

**Table 10:20: 90 days polishing data for 1<sup>st</sup> Generation MESQ paints**

1<sup>st</sup> Generation MESQ polishing data for **Figure 3:8**

Paint	120				DAYS IMMERSION				120			
	Initial thickness / $\mu\text{m}$	Final thickness / $\mu\text{m}$	$\Delta$ thickness strip 1 / $\mu\text{m}$	Av.30 days	Initial thickness / $\mu\text{m}$	Final thickness / $\mu\text{m}$	$\Delta$ thickness strip 2 / $\mu\text{m}$	Av.30 days	Initial thickness / $\mu\text{m}$	Final thickness / $\mu\text{m}$	$\Delta$ thickness strip 3 / $\mu\text{m}$	Av.30 days
<i>MESQ(III) 30%</i>	53.34	51.57	-1.77	-0.44	62.82	57.31	-5.51	-1.38	70.54	69.57	-0.97	-0.24
<i>MESQ(III) 30%</i>	55.14	54.31	-0.83	-0.21	54.02	56.55	2.53	0.63	55.47	55.44	-0.03	-0.01
<i>MESQ(III) 25%</i>	56.28	60.51	4.23	1.06	52.52	57.03	4.51	1.13	62.24	63.49	1.25	0.31
<i>MESQ(III) 25%</i>	51.54	55.07	3.53	0.88	50.82	53.22	2.40	0.60	55.82	56.14	0.32	0.08
<i>MESQ(VI) 25%</i>	49.71	51.00	1.29	0.32	54.04	55.16	1.12	0.28	64.22	58.34	-5.88	-1.47
<i>MESQ(VI) 25%</i>	51.31	54.64	3.33	0.83	55.37	54.69	-0.68	-0.17	55.09	55.70	0.61	0.15
<i>MESQ(VI) 30%</i>	52.48	53.37	0.89	0.22	50.62	52.96	2.34	0.59	50.25	50.18	-0.07	-0.02
<i>MESQ(VI) 30%</i>	53.79	52.02	-1.77	-0.44	51.36	51.08	-0.28	-0.07	54.50	53.63	-0.87	-0.22
<i>MESQ(VI) 25%</i>	47.71	49.30	1.59	0.40	53.74	53.90	0.16	0.04	54.34	54.95	0.61	0.15
<i>MESQ(VI) 25%</i>	48.07	53.05	4.98	1.25	50.95	51.27	0.32	0.08	49.59	47.18	-2.41	-0.60
<i>I/S 655</i>	58.47	48.64	-9.83	-2.46	54.39	45.56	-8.83	-2.21	71.77	52.57	-19.20	-4.80
<i>I/S 655</i>	58.93	48.89	-10.04	-2.51	54.85	45.36	-9.49	-2.37	56.66	49.00	-7.66	-1.92

**Table 10:21: 120 days polishing data for 1<sup>st</sup> Generation MESQ paints**

2<sup>nd</sup> Generation MESQ polishing data for **Figure 3:21**

<b>60 DAYS IMMERSION</b>												
<i>Paint</i>	<i>Initial thickness /<math>\mu</math>m</i>	<i>Final thickness /<math>\mu</math>m</i>	<i><math>\Delta</math> thickness strip 1 /<math>\mu</math>m</i>	<i>Av.30 days</i>	<i>Initial thickness /<math>\mu</math>m</i>	<i>Final thickness /<math>\mu</math>m</i>	<i><math>\Delta</math> thickness strip 2 /<math>\mu</math>m</i>	<i>Av.30 days</i>	<i>Initial thickness /<math>\mu</math>m</i>	<i>Final thickness /<math>\mu</math>m</i>	<i><math>\Delta</math> thickness strip 3 /<math>\mu</math>m</i>	<i>Av.30 days</i>
<i>MESQ(VI)v3</i>	Coldflow	Coldflow	-	-	127.20	125.70	-1.50	-0.75	127.50	126.70	-0.80	-0.40
<i>MESQ(VI)v3</i>	Coldflow	Coldflow	-	-	134.00	130.80	-3.20	-1.60	141.80	129.70	-12.10	-6.05
<i>MESQ(VI)v3</i>	Coldflow	Coldflow	-	-	131.40	127.00	-4.40	-2.20	138.00	129.10	-8.90	-4.45
<i>MESQ(VI)v3</i>	Coldflow	Coldflow	-	-	122.50	125.00	2.50	1.25	120.30	121.80	1.50	0.75
<i>MESQ(VI)v3</i>	Coldflow	Coldflow	-	-	136.00	130.70	-5.30	-2.65	131.50	127.10	-4.40	-2.20
<i>MESQ(VI)v3</i>	Coldflow	Coldflow	-	-	131.20	127.10	-4.10	-2.05	133.50	129.60	-3.90	-1.95
<i>MESQ(VI)v4</i>	132.70	132.00	-0.70	-0.35	133.30	133.40	0.10	0.05	129.80	128.90	-0.90	-0.45
<i>MESQ(VI)v4</i>	126.30	125.50	-0.80	-0.40	124.30	124.30	0.00	0.00	122.10	122.70	0.60	0.30
<i>MESQ(VI)v4</i>	133.80	133.60	-0.20	-0.10	131.30	132.30	1.00	0.50	128.70	129.40	0.70	0.35
<i>MESQ(VI)v4</i>	134.20	133.50	-0.70	-0.35	129.80	130.70	0.90	0.45	127.80	125.80	-2.00	-1.00
<i>MESQ(VI)v4</i>	135.40	133.80	-1.60	-0.80	134.70	134.90	0.20	0.10	135.00	134.30	-0.70	-0.35
<i>MESQ(VI)v4</i>	128.30	128.10	-0.20	-0.10	119.90	120.80	0.90	0.45	118.10	117.10	-1.00	-0.50
<i>I/S 655</i>	144.70	136.80	-7.90	-3.95	152.60	129.40	-23.20	-11.60	160.30	146.90	-13.40	-6.70
<i>I/S 655</i>	97.30	86.90	-10.40	-5.20	93.30	81.90	-11.40	-5.70	93.90	87.50	-6.40	-3.20

**Table 10:22: 60 days polishing data for 2<sup>nd</sup> Generation MESQ paints**

2<sup>nd</sup> Generation MESQ polishing data for **Figure 3:21**

Paint	90				DAYS IMMERSION				90			
	Initial thickness / $\mu\text{m}$	Final thickness / $\mu\text{m}$	$\Delta$ thickness strip 1 / $\mu\text{m}$	Av.30 days	Initial thickness / $\mu\text{m}$	Final thickness / $\mu\text{m}$	$\Delta$ thickness strip 2 / $\mu\text{m}$	Av.30 days	Initial thickness / $\mu\text{m}$	Final thickness / $\mu\text{m}$	$\Delta$ thickness strip 3 / $\mu\text{m}$	Av.30 days
MESQ(VI)v3	Coldflow	Coldflow	-	-	129.60	130.00	0.40	0.13	131.10	130.40	-0.70	-0.23
MESQ(VI)v3	Coldflow	Coldflow	-	-	137.30	138.90	1.60	0.53	141.00	139.90	-1.10	-0.37
MESQ(VI)v3	Coldflow	Coldflow	-	-	127.30	126.00	-1.30	-0.43	131.10	131.40	0.30	0.10
MESQ(VI)v3	Coldflow	Coldflow	-	-	122.60	121.70	-0.90	-0.30	127.10	123.90	-3.20	-1.07
MESQ(VI)v3	Coldflow	Coldflow	-	-	128.40	129.40	1.00	0.33	126.60	126.80	0.20	0.07
MESQ(VI)v3	Coldflow	Coldflow	-	-	122.40	123.90	1.50	0.50	128.90	128.10	-0.80	-0.27
MESQ(VI)v4	126.80	132.20	5.40	1.80	127.00	132.40	5.40	1.80	125.40	129.10	3.70	1.23
MESQ(VI)v4	126.50	131.40	4.90	1.63	130.70	135.80	5.10	1.70	130.20	134.90	4.70	1.57
MESQ(VI)v4	129.90	136.20	6.30	2.10	134.30	138.90	4.60	1.53	142.80	147.90	5.10	1.70
MESQ(VI)v4	128.30	133.20	4.90	1.63	127.30	131.00	3.70	1.23	130.60	134.20	3.60	1.20
MESQ(VI)v4	132.90	137.70	4.80	1.60	133.00	137.90	4.90	1.63	131.60	135.70	4.10	1.37
MESQ(VI)v4	133.70	138.20	4.50	1.50	130.20	133.60	3.40	1.13	128.40	133.00	4.60	1.53
I/S 655	148.00	136.80	-11.20	-3.73	144.50	133.70	-10.80	-3.60	142.00	130.60	-11.40	-3.80
I/S 655	140.10	127.20	-12.90	-4.30	135.10	125.60	-9.50	-3.17	142.90	129.50	-13.40	-4.47

Table 10:23: 90 days polishing data for 2<sup>nd</sup> Generation MESQ paints

2<sup>nd</sup> Generation MESQ polishing data for **Figure 3:21**

Paint	120				DAYS IMMERSION				120			
	Initial thickness / $\mu\text{m}$	Final thickness / $\mu\text{m}$	$\Delta$ thickness strip 1/ $\mu\text{m}$	Av.30 days	Initial thickness / $\mu\text{m}$	Final thickness / $\mu\text{m}$	$\Delta$ thickness strip 2/ $\mu\text{m}$	Av.30 days	Initial thickness / $\mu\text{m}$	Final thickness / $\mu\text{m}$	$\Delta$ thickness strip 3/ $\mu\text{m}$	Av.30 days
MESQ(VI)v3	Coldflow	Coldflow	-	-	128.8	138.1	9.3	2.33	130.7	138.8	8.1	2.03
MESQ(VI)v3	Coldflow	Coldflow	-	-	136.6	145.7	9.1	2.28	144.3	151.3	7	1.75
MESQ(VI)v3	Coldflow	Coldflow	-	-	132.8	141.8	9	2.25	132	137.5	5.5	1.38
MESQ(VI)v3	Coldflow	Coldflow	-	-	127.2	136.4	9.2	2.3	121.2	125.9	4.7	1.18
MESQ(VI)v3	Coldflow	Coldflow	-	-	127.4	140.3	12.9	3.23	127.8	139.1	11.3	2.83
MESQ(VI)v3	Coldflow	Coldflow	-	-	128.4	139.8	11.4	2.85	129.7	139.4	9.7	2.43
MESQ(VI)v4	131.7	156.2	24.5	6.13	131	165.5	34.5	8.63	127.4	146.8	19.4	4.85
MESQ(VI)v4	128.5	158.7	30.2	7.55	131.9	164.1	32.2	8.05	142.2	157.9	15.7	3.93
MESQ(VI)v4	126.8	144.2	17.4	4.35	128.3	146.2	17.9	4.47	132.2	148.2	16	4
MESQ(VI)v4	130.1	147.3	17.2	4.3	129.2	142.4	13.2	3.3	124.8	137.5	12.7	3.18
MESQ(VI)v4	127.1	156.9	29.8	7.45	126.2	147.1	20.9	5.23	125	137.9	12.9	3.23
MESQ(VI)v4	128.2	160.7	32.5	8.13	129.7	153.9	24.2	6.05	136.9	156.6	19.7	4.93
I/S 655	134	124.2	-9.8	-2.45	132.1	123	-9.1	-2.28	129.5	119.3	-10.2	-2.55
I/S 655	110	105	-5	-1.25	128	123.1	-4.9	-1.23	130.6	119.6	-11	-2.75

Table 10:24: 120 days polishing data for 2<sup>nd</sup> Generation MESQ paints

2<sup>nd</sup> Generation MESQ polishing data for **Figure 3:22**

Paint	60				DAYS IMMERSION				60			
	Initial thickness / $\mu\text{m}$	Final thickness / $\mu\text{m}$	$\Delta$ thickness strip 1/ $\mu\text{m}$	Av.30 days	Initial thickness / $\mu\text{m}$	Final thickness / $\mu\text{m}$	$\Delta$ thickness strip 2/ $\mu\text{m}$	Av.30 days	Initial thickness / $\mu\text{m}$	Final thickness / $\mu\text{m}$	$\Delta$ thickness strip 3/ $\mu\text{m}$	Av.30 days
MESQ(VI)v6	125.50	126.70	1.20	0.60	131.30	129.30	-2.00	-1.00	131.30	129.30	-2.00	-1.00
MESQ(VI)v6	128.80	120.60	-8.20	-4.10	130.00	128.00	-2.00	-1.00	130.00	128.00	-2.00	-1.00
MESQ(VI)v6	126.90	130.00	3.10	1.55	130.80	128.50	-2.30	-1.15	130.80	128.50	-2.30	-1.15
MESQ(VI)v6	130.20	134.90	4.70	2.35	133.60	130.70	-2.90	-1.45	133.60	130.70	-2.90	-1.45
MESQ(VI)v6	133.90	132.40	-1.50	-0.75	131.40	126.90	-4.50	-2.25	131.40	126.90	-4.50	-2.25
MESQ(VI)v6	137.80	137.00	-0.80	-0.40	136.50	132.00	-4.50	-2.25	136.50	132.00	-4.50	-2.25
MESQ(VI)v7	127.20	132.50	5.30	2.65	126.80	130.70	3.90	1.95	126.80	130.70	3.90	1.95
MESQ(VI)v7	129.60	137.90	8.30	4.15	126.00	133.40	7.40	3.70	126.00	133.40	7.40	3.70
MESQ(VI)v7	127.80	136.50	8.70	4.35	126.20	134.00	7.80	3.90	126.20	134.00	7.80	3.90
MESQ(VI)v7	121.90	138.10	16.20	8.10	129.80	132.00	2.20	1.10	129.80	132.00	2.20	1.10
MESQ(VI)v7	126.10	127.30	1.20	0.60	129.90	133.70	3.80	1.90	129.90	133.70	3.80	1.90
MESQ(VI)v7	130.30	131.60	1.30	0.65	128.70	134.30	5.60	2.80	128.70	134.30	5.60	2.80
I/S 655	136.00	134.50	-1.50	-0.75	143.20	132.90	-10.30	-5.15	143.20	132.90	-10.30	-5.15
I/S 655	135.40	127.00	-8.40	-4.20	134.30	135.20	0.90	0.45	134.30	135.20	0.90	0.45

Table 10:25: 60 days polishing data for 2<sup>nd</sup> Generation MESQ paints

2<sup>nd</sup> Generation MESQ polishing data for **Figure 3:22**

Paint	90				DAYS IMMERSION				90			
	Initial thickness / $\mu\text{m}$	Final thickness / $\mu\text{m}$	$\Delta$ thickness strip 1 / $\mu\text{m}$	Av.30 days	Initial thickness / $\mu\text{m}$	Final thickness / $\mu\text{m}$	$\Delta$ thickness strip 2 / $\mu\text{m}$	Av.30 days	Initial thickness / $\mu\text{m}$	Final thickness / $\mu\text{m}$	$\Delta$ thickness strip 3 / $\mu\text{m}$	Av.30 days
MESQ(VI)v6	132.60	122.50	-10.10	-3.37	132.40	129.70	-2.70	-0.90	131.50	126.20	-5.30	-1.77
MESQ(VI)v6	130.40	129.50	-0.90	-0.30	132.50	129.40	-3.10	-1.03	138.40	136.20	-2.20	-0.73
MESQ(VI)v6	132.30	129.50	-2.80	-0.93	133.50	130.90	-2.60	-0.87	140.90	139.90	-1.00	-0.33
MESQ(VI)v6	133.10	132.00	-1.10	-0.37	133.30	131.00	-2.30	-0.77	136.90	133.40	-3.50	-1.17
MESQ(VI)v6	135.50	133.30	-2.20	-0.73	131.20	130.30	-0.90	-0.30	130.70	134.10	3.40	1.13
MESQ(VI)v6	135.60	134.20	-1.40	-0.47	129.70	128.80	-0.90	-0.30	132.10	130.50	-1.60	-0.53
MESQ(VI)v7	129.00	134.50	5.50	1.83	129.80	136.10	6.30	2.10	126.50	131.30	4.80	1.60
MESQ(VI)v7	127.70	137.60	9.90	3.30	130.00	136.30	6.30	2.10	140.00	147.00	7.00	2.33
MESQ(VI)v7	130.30	136.00	5.70	1.90	139.50	136.90	-2.60	-0.87	142.70	147.80	5.10	1.70
MESQ(VI)v7	128.70	136.90	8.20	2.73	126.80	133.00	6.20	2.07	129.20	133.90	4.70	1.57
MESQ(VI)v7	127.20	135.10	7.90	2.63	128.30	136.40	8.10	2.70	137.50	145.20	7.70	2.57
MESQ(VI)v7	126.30	135.20	8.90	2.97	132.20	139.10	6.90	2.30	139.20	145.10	5.90	1.97
I/S 655	111.60	100.10	-11.50	-3.83	108.50	96.80	-11.70	-3.90	108.80	97.60	-11.20	-3.73
I/S 655	128.00	112.00	-16.00	-5.33	119.20	107.20	-12.00	-4.00	120.10	109.70	-10.40	-3.47

Table 10:26: 90 days polishing data for 2<sup>nd</sup> Generation MESQ paints

2<sup>nd</sup> Generation MESQ polishing data for **Figure 3:22**

Paint	120				DAYS IMMERSION				120			
	Initial thickness / $\mu\text{m}$	Final thickness / $\mu\text{m}$	$\Delta$ thickness strip 1/ $\mu\text{m}$	Av.30 days	Initial thickness / $\mu\text{m}$	Final thickness / $\mu\text{m}$	$\Delta$ thickness strip 2/ $\mu\text{m}$	Av.30 days	Initial thickness / $\mu\text{m}$	Final thickness / $\mu\text{m}$	$\Delta$ thickness strip 3/ $\mu\text{m}$	Av.30 days
MESQ(VI)v6	Coldflow	Coldflow	-	-	123.80	130.40	6.60	1.65	120.80	124.30	3.50	0.88
MESQ(VI)v6	Coldflow	Coldflow	-	-	129.80	137.20	7.40	1.85	130.30	135.00	4.70	1.18
MESQ(VI)v6	Coldflow	Coldflow	-	-	133.20	140.40	7.20	1.80	143.50	148.60	5.10	1.28
MESQ(VI)v6	Coldflow	Coldflow	-	-	131.70	136.50	4.80	1.20	137.70	144.00	6.30	1.58
MESQ(VI)v6	Coldflow	Coldflow	-	-	130.50	136.10	5.60	1.40	131.90	138.30	6.40	1.60
MESQ(VI)v6	Coldflow	Coldflow	-	-	131.80	139.80	8.00	2.00	137.70	145.20	7.50	1.88
MESQ(VI)v7	130.80	143.90	13.10	3.28	131.80	142.10	10.30	2.58	140.00	150.00	10.00	2.50
MESQ(VI)v7	133.00	148.10	15.10	3.78	134.90	146.00	11.10	2.78	139.70	152.00	12.30	3.08
MESQ(VI)v7	129.80	141.80	12.00	3.00	131.40	141.60	10.20	2.55	138.60	147.80	9.20	2.30
MESQ(VI)v7	135.70	141.60	5.90	1.48	132.30	141.50	9.20	2.30	141.80	150.40	8.60	2.15
MESQ(VI)v7	131.40	138.80	7.40	1.85	132.20	139.00	6.80	1.70	131.90	137.60	5.70	1.43
MESQ(VI)v7	131.00	138.30	7.30	1.83	132.70	137.50	4.80	1.20	135.40	139.30	3.90	0.98
I/S 655	124.00	107.10	-16.90	-4.23	125.70	109.50	-16.20	-4.05	128.40	113.80	-14.60	-3.65
I/S 655	127.60	112.00	-15.60	-3.90	125.70	107.90	-17.80	-4.45	136.20	123.70	-12.50	-3.13

**Table 10:27: 120 days polishing data for 2<sup>nd</sup> Generation MESQ paints**

2<sup>nd</sup> Generation MESQ polishing data for **Figure 3:23**

60 DAYS IMMERSION												
Paint	Initial thickness / $\mu\text{m}$	Final thickness/ $\mu\text{m}$	$\Delta$ thickness strip 1/ $\mu\text{m}$	Av.30 days	Initial thickness / $\mu\text{m}$	Final thickness/ $\mu\text{m}$	$\Delta$ thickness strip 2/ $\mu\text{m}$	Av.30 days	Initial thickness / $\mu\text{m}$	Final thickness/ $\mu\text{m}$	$\Delta$ thickness strip 3/ $\mu\text{m}$	Av.30 days
MESQ(VI)v10	131.40	130.00	-1.40	-0.70	129.20	124.90	-4.30	-2.15	121.50	117.20	-4.30	-2.15
MESQ(VI)v10	126.90	125.20	-1.70	-0.85	129.40	126.00	-3.40	-1.70	131.40	126.60	-4.80	-2.40
MESQ(VI)v10	133.20	131.50	-1.70	-0.85	130.50	126.50	-4.00	-2.00	137.10	130.10	-7.00	-3.50
MESQ(VI)v10	133.40	131.70	-1.70	-0.85	131.70	128.50	-3.20	-1.60	132.20	127.60	-4.60	-2.30
MESQ(VI)v10	132.50	129.90	-2.60	-1.30	131.10	126.90	-4.20	-2.10	139.60	133.70	-5.90	-2.95
MESQ(VI)v10	129.00	126.20	-2.80	-1.40	127.30	125.00	-2.30	-1.15	131.50	126.90	-4.60	-2.30
I/S 655	143.80	125.70	-18.10	-9.05	141.10	126.70	-14.40	-7.20	138.20	123.50	-14.70	-7.35
I/S 655	143.60	125.70	-17.90	-8.95	137.60	123.80	-13.80	-6.90	146.70	131.20	-15.50	-7.75

Table 10:28: 60 days polishing data for 2<sup>nd</sup> Generation MESQ paints

2<sup>nd</sup> Generation MESQ polishing data for **Figure 3:23**

90 DAYS IMMERSION												
Paint	Initial thickness / $\mu\text{m}$	Final thickness/ $\mu\text{m}$	$\Delta$ thickness strip 1/ $\mu\text{m}$	Av.30 days	Initial thickness / $\mu\text{m}$	Final thickness/ $\mu\text{m}$	$\Delta$ thickness strip 2/ $\mu\text{m}$	Av.30 days	Initial thickness / $\mu\text{m}$	Final thickness/ $\mu\text{m}$	$\Delta$ thickness strip 3/ $\mu\text{m}$	Av.30 days
MESQ(VI)v10	134.60	134.80	0.20	0.07	130.70	133.10	2.40	0.80	131.90	132.30	0.40	0.13
MESQ(VI)v10	131.80	136.60	4.80	1.60	136.00	137.70	1.70	0.57	141.20	141.90	0.70	0.23
MESQ(VI)v10	132.10	136.70	4.60	1.53	134.40	135.90	1.50	0.50	140.30	139.60	-0.70	-0.23
MESQ(VI)v10	124.60	131.30	6.70	2.23	127.40	133.50	6.10	2.03	133.00	134.50	1.50	0.50
MESQ(VI)v10	131.40	136.10	4.70	1.57	132.90	135.60	2.70	0.90	143.60	135.00	-8.60	-2.87
MESQ(VI)v10	132.60	135.10	2.50	0.83	133.60	133.50	-0.10	-0.03	128.20	130.60	2.40	0.80
I/S 655	142.80	130.10	-12.70	-4.23	143.30	133.10	-10.20	-3.40	138.40	130.00	-8.40	-2.80
I/S 655	144.40	135.70	-8.70	-2.90	143.60	131.30	-12.30	-4.10	155.60	149.80	-5.80	-1.93

Table 10:29: 90 days polishing data for 2<sup>nd</sup> Generation MESQ paints

2<sup>nd</sup> Generation MESQ polishing data for **Figure 3:23**

Paint	120				DAYS IMMERSION				120			
	Initial thickness / $\mu\text{m}$	Final thickness / $\mu\text{m}$	$\Delta$ thickness strip 1 / $\mu\text{m}$	Av.30 days	Initial thickness / $\mu\text{m}$	Final thickness / $\mu\text{m}$	$\Delta$ thickness strip 2 / $\mu\text{m}$	Av.30 days	Initial thickness / $\mu\text{m}$	Final thickness / $\mu\text{m}$	$\Delta$ thickness strip 3 / $\mu\text{m}$	Av.30 days
MESQ(VI)v10	132.70	151.20	18.50	4.63	136.80	143.90	7.10	1.78	137.10	142.70	5.60	1.40
MESQ(VI)v10	132.30	144.60	12.30	3.08	133.60	140.90	7.30	1.83	140.90	147.70	6.80	1.70
MESQ(VI)v10	129.80	141.20	11.40	2.85	131.60	140.70	9.10	2.28	140.30	147.30	7.00	1.75
MESQ(VI)v10	137.10	145.50	8.40	2.10	134.90	139.00	4.10	1.03	137.30	140.80	3.50	0.88
MESQ(VI)v10	134.20	143.30	9.10	2.28	134.10	138.00	3.90	0.98	133.90	138.00	4.10	1.03
MESQ(VI)v10	131.40	141.90	10.50	2.63	132.10	137.50	5.40	1.35	131.80	135.50	3.70	0.92
I/S 655	136.60	121.90	-14.70	-3.68	135.10	121.00	-14.10	-3.53	133.40	122.40	-11.00	-2.75
I/S 655	136.00	120.80	-15.20	-3.80	133.90	118.00	-15.90	-3.98	142.40	130.20	-12.20	-3.05

**Table 10:30: 120 days polishing data for 2<sup>nd</sup> Generation MESQ paints**

AMPSQ polishing data for **Figure 4:7**

<b>8 DAYS IMMERSION</b>								
<i>Paint</i>	<i>Initial thickness /<math>\mu\text{m}</math></i>	<i>Final thickness /<math>\mu\text{m}</math></i>	<i><math>\Delta</math> thickness strip 1 /<math>\mu\text{m}</math></i>	<i>Av. daily /<math>\mu\text{mday}^{-1}</math></i>	<i>Initial thickness /<math>\mu\text{m}</math></i>	<i>Final thickness /<math>\mu\text{m}</math></i>	<i><math>\Delta</math> thickness strip 2 /<math>\mu\text{m}</math></i>	<i>Av. daily /<math>\mu\text{mday}^{-1}</math></i>
<i>AMPSQ(I)v3</i>	218.06	215.54	2.52	0.62	202.25	201.98	0.28	0.03
<i>AMPSQ(I)v3</i>	196.615	194.204	2.41	0.30	206.723	203.743	2.98	0.37
<i>AMPSQ(I)v8</i>	170.32	166.77	3.55	0.44	170.63	165.74	4.90	0.61
<i>AMPSQ(I)v8</i>	172.94	166.61	6.33	0.79	191.73	184.93	6.79	0.85
<i>AMPSQ(I)v10</i>	198.08	191.76	6.32	0.79	188.45	180.39	8.06	1.01
<i>AMPSQ(I)v10</i>	186.13	179.79	6.33	0.79	184.97	177.10	7.87	0.98
<i>AMPSQ(I)v8</i>	165.522	163.606	1.92	0.24	183.104	176.275	6.83	0.85
<i>AMPSQ(I)v8</i>	185.352	180.262	5.09	0.64	187.019	180.657	6.36	0.80
<i>AMPSQ(I)v10</i>	222.019	211.84	10.18	1.27	202.729	195.859	6.87	0.86
<i>AMPSQ(I)v10</i>	194.107	184.243	9.86	1.23	188.699	182.532	6.17	0.77
<i>I/S 655</i>	233.63	219.58	14.06	0.03	240.096	220.459	19.64	2.45
<i>I/S 655</i>	245.48	230.93	14.55	1.82	241.553	226.012	15.54	1.94

**Table 10:31: 8 days polishing data for AMPSQ paints**

AMPSQ polishing data for **Figure 4:7**

65 DAYS IMMERSION								
<i>Paint</i>	<i>Initial thickness /<math>\mu\text{m}</math></i>	<i>Final thickness /<math>\mu\text{m}</math></i>	<i><math>\Delta</math> thickness strip 1 /<math>\mu\text{m}</math></i>	<i>Av. daily /<math>\mu\text{mday}^{-1}</math></i>	<i>Initial thickness /<math>\mu\text{m}</math></i>	<i>Final thickness /<math>\mu\text{m}</math></i>	<i><math>\Delta</math> thickness strip 2 /<math>\mu\text{m}</math></i>	<i>Av. daily /<math>\mu\text{mday}^{-1}</math></i>
<i>AMPSQ(I)v3</i>	192.381	228.061	-35.68	-0.55	211.855	241.843	-29.99	-0.46
<i>AMPSQ(I)v3</i>	196.147	222.055	-25.91	-0.40	204.817	232.956	-28.14	-0.43
<i>AMPSQ(I)v8</i>	172.037	208.666	-36.63	-0.56	173.676	201.535	-27.86	-0.43
<i>AMPSQ(I)v8</i>	183.911	225.863	-41.95	-0.65	175.924	206.188	-30.26	-0.47
<i>AMPSQ(I)v10</i>	182.799	184.072	-1.27	-0.02	188.26	190.118	-1.86	-0.03
<i>AMPSQ(I)v10</i>	196.165	198.082	-1.92	-0.03	192.197	194.555	-2.36	-0.04
<i>AMPSQ(I)v8</i>	178.305	220.859	-42.55	-0.65	195.609	240.709	-45.10	-0.69
<i>AMPSQ(I)v8</i>	173.739	211.425	-37.69	-0.58	178.796	218.04	-39.24	-0.60
<i>AMPSQ(I)v10</i>	199.383	195.593	3.79	0.06	184.658	184.711	-0.05	0.00
<i>AMPSQ(I)v10</i>	193.049	190.823	2.23	0.03	190.482	192.155	-1.67	-0.03
<i>I/S 655</i>	221.007	205.266	15.74	0.24	234.506	215.791	18.72	0.29
<i>I/S 655</i>	228.853	209.092	19.76	0.30	237.213	225.517	11.70	0.18

**Table 10:32: 65 days polishing data for AMPSQ paints**

AMPSQ polishing data for **Figure 4:7**

<b>130 DAYS IMMERSION</b>								
<i>Paint</i>	<i>Initial thickness /<math>\mu\text{m}</math></i>	<i>Final thickness /<math>\mu\text{m}</math></i>	<i><math>\Delta</math> thickness strip 1 /<math>\mu\text{m}</math></i>	<i>Av. daily /<math>\mu\text{mday}^{-1}</math></i>	<i>Initial thickness /<math>\mu\text{m}</math></i>	<i>Final thickness /<math>\mu\text{m}</math></i>	<i><math>\Delta</math> thickness strip 2 /<math>\mu\text{m}</math></i>	<i>Av. daily /<math>\mu\text{mday}^{-1}</math></i>
<i>AMPSQ(I)v3</i>	201.61	246.75	-45.13	-0.34	206.91	258.11	-51.20	-0.39
<i>AMPSQ(I)v8</i>	171.72	239.54	-67.81	-0.52	156.91	214.24	-57.33	-0.44
<i>AMPSQ(I)v8</i>	179.14	245.75	-66.61	-0.51	163.09	-	-	-
<i>AMPSQ(I)v10</i>	194.08	202.69	-8.61	-0.07	177.10	186.62	-9.53	-0.07
<i>AMPSQ(I)v10</i>	201.35	208.51	-7.15	-0.05	184.02	191.96	-7.93	-0.06
<i>AMPSQ(I)v8</i>	181.49	183.89	-2.40	-0.02	183.32	233.19	-49.87	-0.41
<i>AMPSQ(I)v8</i>	172.65	209.56	-36.91	-0.30	178.54	218.40	-39.86	-0.33
<i>AMPSQ(I)v10</i>	217.84	187.31	30.52	0.25	210.65	182.89	27.76	0.23
<i>AMPSQ(I)v10</i>	177.33	189.28	-11.95	-0.10	172.02	197.18	-25.16	-0.21
<i>I/S 655</i>	255.53	241.18	14.36	0.11	174.39	233.13	-58.74	-0.48
<i>I/S 655</i>	243.87	244.09	-0.22	0.00	157.96	252.83	-94.88	-0.78

**Table 10:33: 130 days polishing data for AMPSQ paints**

### **10.5.9 Storage Stability**

Aliquots of the test paints were transferred to 250 ml paint tins, in duplicate, directly following the paints manufacture. These tins were sealed and placed in temperature controlled cabinets set at  $23 \pm 2$  °C and  $45 \pm 2$  °C for a period of up to 6 months. The paints were assessed on a monthly basis over the 6 month period for changes in viscosity and grind. Prior to each assessment the paint was thoroughly mixed to reincorporate any pigment settlement. For commercial reason the limitations of the test are:

- i 6 month test period - Commercial products are limited to shelf life of 6 months
- ii 45 °C - Representative of storage conditions encountered in tropical/equatorial regions

RC957 storage data for **Figure 2:15**

Days	Acid						RC957Q(I)						Standard Paint					
	5 °C		23 °C		45 °C		5 °C		23 °C		45 °C		5 °C		23 °C		45 °C	
	Visc./ Poises	Grind/ µm																
0	5.76		5.76		5.76		1.05		1.05		1.05		3.71		3.71		3.71	
	5.54	40	5.54	40	5.54	40	1.15	50	1.15	50	1.15	50	3.87	40	3.87	40	3.87	40
	6.61		6.61		6.61		0.93		0.93		0.93		3.91		3.91		3.91	
30	6.79		6.54		6.62		1.10		1.15		3.13		4.48		3.90		4.63	
	8.64	40	7.55	40	7.18	40	1.20	40	1.16	50	2.52	100	5.80	40	3.77	40	4.51	45
	6.59		6.62		6.59		1.13		1.17		2.74		4.29		4.95		4.84	
60	6.52		5.52		5.72		0.96		1.20				4.19		3.64		3.79	
	6.93	40	6.26	40	6.07	40	0.92	40	1.17	45	Gel	Gel	3.94	50	3.63	50	3.75	50
	6.35		6.65		5.84		1.02		1.14				4.59		3.82		3.96	
112	6.96		5.82		5.22		1.11		1.28				4.33		3.48		4.32	
	6.77	40	5.92	40	5.78	40	1.10	50	1.18	50	Gel	Gel	4.20	50	3.71	50	4.23	50
	7.18		5.65		5.53		1.13		1.31				4.75		3.47		4.86	
245	7.25		5.62		5.53		1.35		2.67				5.20		4.02		4.85	
	6.68	50	6.07	50	5.50	40	1.34	60	2.60	60	-	-	5.00	60	4.61	60	5.02	60
	6.80		5.69		5.11		1.41		2.57				5.25		4.32		4.87	

**Table 10:34: Storage data for RC957 paints**

1<sup>st</sup> Generation MESQ coatings storage data for **Figure 3:15**

Days	MESQ(I)v25				MESQ(I)v30				MESQ(II)v25				MESQ(II)v30			
	23 °C		45 °C		23 °C		45 °C		23 °C		45 °C		23 °C		45 °C	
	Visc./ Poises	Grind/ µm														
0	53.7	40	53.7	40	24.4	40	24.4	40	20.5	40	20.5	40	14.1	40	14.1	40
28	42.2	40	34.2	40	27.1	40	24.0	40	14.9	40	11.3	40	13.5	40	10.6	40
56	45.1	40	29.6	40	29.4	40	11.9	40	16.6	40	12.1	40	15.2	40	11.6	40
84	45.4	40	31.5	40	26.9	40	11.3	40	15.5	40	10.6	40	14.3	40	10.0	40
112	44.1	40	33.7	40	28.2	40	12.0	100	16.0	40	10.5	100	15.0	40	10.2	40
140	45.4	40	36.4	45	29.6	40	13.6	100	16.0	40	11.6	100	14.6	40	10.8	40
196	45.7	40	42.6	50	29.9	40	20.1	-	15.9	40	14.0	-	15.6	40	11.9	45

Table 10:35: Storage data for 1<sup>st</sup> Generation MESQ paints

2<sup>nd</sup> Generation MESQ coatings storage data **Figure 3:34**

Days	MESQ(I)v2		MESQ(I)v3		MESQ(I)v4		MESQ(I)v5		MESQ(I)v6		MESQ(I)v7		MESQ(I)v8		MESQ(I)v9		MESQ(I)v10	
	Visc./ Poise s	Grind/ µm	Visc./ Poises	Grind/ µm	Visc./ Poises	Grind/ µm	Visc./ Poise s	Grind/ µm	Visc./ Poise s	Grind/ µm	Visc./ Poises	Grind/ µm	Visc./ Poise s	Grind/ µm	Visc./ Poises	Grind/ µm	Visc./ Poise s	Grind/ µm
0	42.1	40	36.8	40	31.7	40	35.0	40	39.8	40	63.7	40	21.7	40	37.7	40	30.2	40
28	37.7	40	32.5	40	27.6	40	37.5	40	44.3	40	76.1	40	30.9	40	32.6	40	34.1	40
56	45.9	40	34.5	40	29.0	40	40.2	40	50.4	40	82.5	40	32.2	40	34.0	40	34.6	40
84	45.1	40	35.7	40	28.4	40	39.4	40	49.4	40	84.9	40	32.6	40	35.1	40	35.0	40
112	52.5	40	37.4	40	28.7	40	39.8	45	52.9	40	84.3	40	34.4	40	37.5	40	40.5	45
140	54.1	45	37.8	40	30.5	40	40.9	50	54.5	40	90.0	40	37.0	40	37.4	45	38.5	45

Table 10:36: Storage data for 2<sup>nd</sup> Generation MESQ paints at 23 °C

2<sup>nd</sup> Generation MESQ coatings storage data **Figure 3:34**

Days	MESQ(I)v2		MESQ(I)v3		MESQ(I)v4		MESQ(I)v5		MESQ(I)v6		MESQ(I)v7		MESQ(I)v8		MESQ(I)v9		MESQ(I)v10	
	Visc./ Poise s	Grind/ µm	Visc./ Poises	Grind/ µm	Visc./ Poises	Grind/ µm	Visc./ Poise s	Grind/ µm	Visc./ Poise s	Grind/ µm	Visc./ Poises	Grind/ µm	Visc./ Poise s	Grind/ µm	Visc./ Poises	Grind/ µm	Visc./ Poise s	Grind/ µm
0	42.1	40	36.8	40	31.7	40	35.0	40	39.8	40	63.7	40	21.7	40	37.7	40	30.2	40
28	26.0	40	24.3	40	18.9	40	27.5	40	28.6	40	51.3	50	10.4	40	11.5	40	18.4	40
56	23.6	60	22.7	60	17.3	70	26.3	50	25.3	60	57.3	50	11.3	60	11.5	80	15.3	70
84	24.1	100	22.0	100	18.3	100	27.0	100	29.4	100	56.8	100	11.6	100	13.0	100	16.6	100
112	24.5	-	24.7	-	19.7	-	29.9	-	31.8	-	62.5	-	12.4	-	14.8	-	16.1	-
140	27.2	-	25.7	-	23.2	-	31.5	-	35.2	-	64.3	-	11.8	-	15.7	-	17.3	-

**Table 10:37: Storage data for 2<sup>nd</sup> Generation MESQ paints at 45 °C**

AMPSQ storage data for **Figure 4:28**

Days	AMPSQv4		AMPSQv6		AMPSQv8		AMPSQv9		AMPSQv12		AMPSQ(II)v4	
	Visc./ Poises	Grind/ $\mu\text{m}$										
0	2.30		1.16		0.99		1.09		1.17		0.60	
	2.44	40	1.08	40	1.11	40	1.32	50	1.19	40	0.61	45
	1.99		1.29		1.10		1.32		1.14		0.61	
30	2.66		1.50		1.21		1.23		1.33		0.60	
	2.73	40	1.34	45	1.28	40	1.30	50	1.37	40	0.64	45
	2.76		1.38		1.17		1.29		1.45		0.63	
86	2.88		1.67		1.40		1.32		1.37		0.63	
	2.77	40	1.32	45	1.41	40	1.35	45	1.41	40	0.65	40
	2.91		1.34		1.62		1.35		1.35		0.64	
126	2.85		1.35		1.38		1.19		1.36		0.69	
	2.77	40	1.32	40	1.34	40	1.31	45	1.36	40	0.65	50
	2.63		1.47		1.37		1.45		1.42		0.63	
191	2.81		1.42		1.41		1.36		1.42		0.65	
	2.83	50	1.59	50	1.42	40	1.32	50	1.46	40	0.48	40
	2.88		1.36		1.44		1.33		1.45		0.69	

**Table 10:38: Storage data for AMPSQ paints at 5 °C**

AMPSQ storage data for **Figure 4:28**

Days	AMPSQv4		AMPSQv6		AMPSQv8		AMPSQv9		AMPSQv12		AMPSQ(II)v4	
	Visc./ Poises	Grind/ $\mu\text{m}$										
0	2.30		1.16		0.99		1.09		1.17		0.60	
	2.44	40	1.08	40	1.11	40	1.32	50	1.19	40	0.61	45
	1.99		1.29		1.10		1.32		1.14		0.61	
30	2.79		1.29		1.21		1.23		1.32		0.59	
	2.56	50	1.42	50	1.18	40	1.21	40	1.31	45	0.52	45
	2.40		1.29		1.40		1.23		1.28		0.38	
86	2.58		1.38		1.34		1.55		1.35		0.66	
	2.90	45	1.40	45	1.24	40	1.25	40	1.37	40	0.69	45
	2.71		1.39		1.30		1.38		1.38		0.53	
126	2.79		1.42		1.18		1.33		1.48		0.68	
	3.24	45	1.41	45	1.29	40	1.27	40	1.39	50	0.48	40
	2.70		1.31		1.35		1.32		1.33		0.56	
191	2.85		1.42		1.42		1.34		1.45		0.68	
	2.90	50	1.43	50	1.36	40	1.35	40	1.43	40	0.66	50
	3.03		1.48		1.30		1.35		1.41		0.65	

**Table 10:39: Storage data for AMPSQ paints at 23 °C**

AMPSQ storage data for **Figure 4:28**

<i>Days</i>	<i>AMPSQv4</i>		<i>AMPSQv6</i>		<i>AMPSQv8</i>		<i>AMPSQv9</i>		<i>AMPSQv12</i>		<i>AMPSQ(II)v4</i>	
	<i>Visc./ Poises</i>	<i>Grind/ µm</i>										
<b>0</b>	2.30		1.16		0.99		1.09		1.17		0.60	
	2.44	40	1.08	40	1.11	40	1.32	50	1.19	40	0.61	45
	1.99		1.29		1.10		1.32		1.14		0.61	
<b>30</b>	3.51		1.30		1.34		1.29		1.49		0.64	
	2.48	40	1.31	45	1.21	50	1.25	40	1.46	50	0.64	40
	2.46		1.31		1.31		1.34		1.41		0.64	
<b>86</b>	2.55		1.39		1.21		1.22		1.34		0.69	
	3.05	40	1.26	40	1.20	45	1.26	40	1.38	45	0.60	40
	3.03		1.28		1.24		1.24		1.36		0.68	
<b>126</b>	2.69		1.42		1.24		1.29		1.36		0.70	
	2.74	40	1.45	50	1.26	45	1.30	40	1.48	45	0.72	40
	3.57		1.28		1.34		1.32		1.77		0.71	
<b>191</b>	3.57		1.40		1.40		1.31		1.44		0.67	
	2.92	40	1.34	40	1.30	50	1.35	40	1.49	50	0.70	40
	2.97		1.46		1.39		1.39		1.46		0.76	

**Table 10:40: Storage data for AMPSQ paints at 45 °C**

## 10.5.10 Water absorption

Gravimetric Data, Data for Table 4:8

10 days

Paint	Initial Mass Slide 1/ g	Final Mass Slide 1/ g	$\Delta$ Mass Slide 1/ g	Initial Mass Slide 2/ g	Final Mass Slide 2/ g	$\Delta$ Mass Slide 2/ g
AMPSQ(I)v1	5.1080	5.1282	0.0202	5.1297	5.1515	0.0218
AMPSQ(I)v2	5.0864	5.1077	0.0213	5.1109	5.1317	0.0208
AMPSQ(I)v3	5.1049	5.1354	0.0305	5.1011	5.1310	0.0299
AMPSQ(I)v4	5.0974	5.1242	0.0268	5.0842	5.1108	0.0266
AMPSQ(I)v5	5.0721	5.0986	0.0265	5.0862	5.1106	0.0244
AMPSQ(I)v6	5.0879	5.1137	0.0258	5.1059	5.1306	0.0247
AMPSQ(I)v7	5.0852	5.1170	0.0318	5.1093	5.1415	0.0322
AMPSQ(I)v8	5.0716	5.1060	0.0344	5.0518	5.0885	0.0367
AMPSQ(I)v9	5.0605	5.0753	0.0148	5.0597	5.0753	0.0156
AMPSQ(I)v10	5.0411	5.0600	0.0189	5.0818	5.1003	0.0185
AMPSQ(I)v11	5.1239	5.1516	0.0277	5.0723	5.1010	0.0287
AMPSQ(I)v12	5.1011	5.1202	0.0191	5.0886	5.1079	0.0193
AMPSQ(II)v4	5.1254	5.1314	0.0060	5.1096	5.1208	0.0112

Table 10:41: Water absorption gravimetric - 10 days

Gravimetric Data, Data for Table 4:8

24 days

Paint	Initial Mass Slide 1/ g	Final Mass Slide 1/ g	$\Delta$ Mass Slide 1/ g	Initial Mass Slide 2/ g	Final Mass Slide 2/ g	$\Delta$ Mass Slide 2/ g
AMPSQ(I)v1	5.1080	5.1305	0.0225	5.1297	5.1490	0.0193
AMPSQ(I)v2	5.0864	5.1074	0.0210	5.1109	5.1300	0.0191
AMPSQ(I)v3	5.1049	5.1357	0.0308	5.1011	5.1310	0.0299
AMPSQ(I)v4	5.0974	5.1225	0.0251	5.0842	5.1073	0.0231
AMPSQ(I)v5	5.0721	5.0978	0.0257	5.0862	5.1093	0.0231
AMPSQ(I)v6	5.0879	5.1106	0.0227	5.1059	5.1285	0.0226
AMPSQ(I)v7	5.0852	5.1155	0.0303	5.1093	5.1377	0.0284
AMPSQ(I)v8	5.0716	5.1071	0.0355	5.0518	5.0840	0.0322
AMPSQ(I)v9	5.0605	5.0758	0.0153	5.0597	5.0738	0.0141
AMPSQ(I)v10	5.0411	5.0594	0.0183	5.0818	5.0984	0.0166
AMPSQ(I)v11	5.1239	5.1491	0.0252	5.0723	5.0944	0.0221
AMPSQ(I)v12	5.1011	5.1214	0.0203	5.0886	5.1059	0.0173
AMPSQ(II)v4	5.1254	5.1296	0.0042	5.1096	5.1144	0.0048

Table 10:42: Water absorption gravimetric - 24 days

Profilometry Data for **Table 4:8**

*10 Days*

<i>Paint</i>	<i>Initial thickness /<math>\mu\text{m}</math></i>	<i>Final thickness /<math>\mu\text{m}</math></i>	<i><math>\Delta</math> thickness strip 1 /<math>\mu\text{m}</math></i>	<i>Initial thickness /<math>\mu\text{m}</math></i>	<i>Final thickness /<math>\mu\text{m}</math></i>	<i><math>\Delta</math> thickness strip 2 /<math>\mu\text{m}</math></i>	<i>Initial thickness /<math>\mu\text{m}</math></i>	<i>Final thickness /<math>\mu\text{m}</math></i>	<i><math>\Delta</math> thickness strip 3 /<math>\mu\text{m}</math></i>
<i>AMPSQ(I)v1</i>	171.98	172.75	0.77	167.27	173.78	6.51	175.53	171.16	4.37
<i>AMPSQ(I)v2</i>	172.13	181.25	9.12	169.39	181.77	12.38	179.55	172.11	7.44
<i>AMPSQ(I)v3</i>	173.30	186.09	12.79	171.96	184.02	12.06	185.48	170.84	14.64
<i>AMPSQ(I)v4</i>	165.34	175.35	10.01	164.44	176.85	12.41	174.13	162.40	11.73
<i>AMPSQ(I)v5</i>	166.39	177.88	11.49	165.89	175.70	9.81	175.27	166.34	8.93
<i>AMPSQ(I)v6</i>	169.48	178.74	9.26	173.40	180.78	7.38	182.41	174.53	7.88
<i>AMPSQ(I)v7</i>	185.09	195.47	10.38	186.29	197.80	11.51	192.24	180.30	11.94
<i>AMPSQ(I)v8</i>	152.95	171.41	18.46	153.14	169.46	16.32	169.44	153.55	15.89
<i>AMPSQ(I)v9</i>	150.00	158.37	8.37	152.80	155.46	2.66	157.59	152.42	5.17
<i>AMPSQ(I)v10</i>	161.77	166.10	4.33	162.31	164.47	2.16	162.49	166.56	-4.07
<i>AMPSQ(I)v11</i>	151.01	168.21	17.20	157.90	167.44	9.54	166.37	161.18	5.19
<i>AMPSQ(I)v12</i>	158.02	171.92	13.90	158.82	170.26	11.44	170.49	160.72	9.77
<i>AMPSQ(II)v4</i>	161.71	166.42	4.71	163.17	169.04	5.87	170.91	165.10	5.81

**Table 10:43: Water absorption profilometry - 10 days**

Profilometry Data for **Table 4:8**

**24 Days**

<i>Paint</i>	<i>Initial thickness /<math>\mu\text{m}</math></i>	<i>Final thickness /<math>\mu\text{m}</math></i>	<i><math>\Delta</math> thickness strip 1 /<math>\mu\text{m}</math></i>	<i>Initial thickness /<math>\mu\text{m}</math></i>	<i>Final thickness /<math>\mu\text{m}</math></i>	<i><math>\Delta</math> thickness strip 2 /<math>\mu\text{m}</math></i>	<i>Initial thickness /<math>\mu\text{m}</math></i>	<i>Final thickness /<math>\mu\text{m}</math></i>	<i><math>\Delta</math> thickness strip 3 /<math>\mu\text{m}</math></i>
<i>AMPSQ(I)v1</i>	171.98	175.34	3.36	167.27	174.85	7.58	175.53	177.10	5.94
<i>AMPSQ(I)v2</i>	172.13	178.98	6.85	169.39	178.51	9.12	179.55	174.26	2.15
<i>AMPSQ(I)v3</i>	173.30	187.88	14.58	171.96	185.04	13.08	185.48	185.84	15.00
<i>AMPSQ(I)v4</i>	165.34	177.87	12.53	164.44	177.65	13.21	174.13	176.27	13.87
<i>AMPSQ(I)v5</i>	166.39	180.49	14.10	165.89	177.59	11.70	175.27	177.03	10.69
<i>AMPSQ(I)v6</i>	169.48	185.49	16.01	173.40	182.23	8.83	182.41	184.84	10.31
<i>AMPSQ(I)v7</i>	185.09	193.30	8.21	186.29	196.10	9.81	192.24	193.28	12.98
<i>AMPSQ(I)v8</i>	152.95	174.08	21.13	153.14	171.96	18.82	169.44	173.12	19.57
<i>AMPSQ(I)v9</i>	150.00	160.76	10.76	152.80	158.51	5.71	157.59	159.69	7.27
<i>AMPSQ(I)v10</i>	161.77	165.00	3.23	162.31	163.22	0.91	162.49	160.71	-5.85
<i>AMPSQ(I)v11</i>	151.01	164.34	13.33	157.90	158.80	0.90	166.37	158.54	-2.64
<i>AMPSQ(I)v12</i>	158.02	169.62	11.60	158.82	168.36	9.54	170.49	173.34	12.62
<i>AMPSQ(II)v4</i>	161.71	168.85	7.14	163.17	167.14	3.97	170.91	167.40	2.30

**Table 10:44: Water absorption profilometry - 24 days**

### 10.5.11 Antifouling Performance

61 × 61 × 6 cm marine plywood boards were coated with primer paint (Interprotect) and cured at ambient conditions for 24 hours. Once fully dry the boards were masked off into a 6 × 6 matrix pattern (Latin square statistical design; 36 individual squares) using masking tape. Each board contained 4 test coatings, an appropriate biocidal standard paint (Intersmooth 460) and a non-biocidal control (Primocon). The paints were arranged on the boards such that no paint/control appears in the same row/column twice, **Figure 10:3**. This arrangement attempted to minimise the effect of natural variability of the fouling challenge which the boards were subjected to.

	1	2	3	4	5	6
A	1	2	3	4	ST	CT
B	ST	CT	1	2	3	4
C	3	4	ST	CT	1	2
D	CT	1	2	3	4	ST
E	4	ST	CT	1	2	3
F	2	3	4	ST	CT	1

**Figure 10:3: Test Panel Layout Design**

The paints (4 test and standard) were applied by brush in 2 coats to ensure full coverage of each square. Following drying for 48 hours the masking tape was removed to reveal lines of primer paint. These lines were overcoated with a standard biocidal product (Trilux 33) with 2 coats ensuring that the extreme edges of the coated squares were covered. The finalised boards were then immersed in the marine environment.

During immersion of the boards, fouling assessments were carried out periodically during the period of immersion; nominally every three months. The fouling level of each of the 36 squares on a board was assessed by visually estimating its percentage fouling cover. The fouling was broken down into 4 categories:

- a). Micro-fouling (Slime)
- b). Weed
- c). Soft-bodied animal
- d). Hard-bodied animal (Shell)

Total fouling coverage was reported first (as a percentage of the total surface area of each trial square). The contribution of each fouling category to the total percentage was then estimated and recorded. Any additional observations or comments such as any peculiar fouling behaviour, or damage (blistering, cracking etc) to the coatings, were also noted.

The test boards were finally photographed (whole panel in one frame), preferably using a digital camera. Close-up photographs were also taken of interesting features (such as coating detachment, interesting fouling etc) as appropriate.

Assessment data was then transferred to International Paint's in-house panel database and the performance of each test coating statistical analysed. This analysis was then utilised to discern the antifouling performance of the test coatings relative to the standard paint.

Data for **Figure 2:13**

**Phoenix Anti-Fouling Immersion Test Data**

Phoenix Panel Number:		732F	Immersion Date:		27-May-09	Immersion Site:		Newton Ferrers	
Raft Panel Bay Number:		09304F	Assessment Date:		02-Sep-09	Country :		UK	
Trial	Row	Column	Coating	% Microfouling	% Weed	% Soft-Bodied Animal	% Hard-Bodied Animal	% Total Fouling	Foul Release
A1	1	1	2483	10				10	
A2	1	2	2428		3			3	
A3	1	3	2571	3				3	
A4	1	4	2422	6				6	
A5	1	5	ST	25				25	
A6	1	6	CT	69	15		1	85	
B1	2	1	ST	12				12	
B2	2	2	CT	20	20			40	
B3	2	3	2483	35				35	
B4	2	4	2428		1			1	
B5	2	5	2571	2				2	
B6	2	6	2422	10				10	
C1	3	1	2571	5				5	
C2	3	2	2422	10				10	
C3	3	3	ST	35				35	
C4	3	4	CT	9	11			20	
C5	3	5	2483	10				10	
C6	3	6	2428		2			2	
D1	4	1	CT	10	15			25	
D2	4	2	2483	30				30	
D3	4	3	2428		3			3	
D4	4	4	2571	8				8	
D5	4	5	2422	8				8	
D6	4	6	ST	15				15	
E1	5	1	2422	12				12	
E2	5	2	ST	45				45	
E3	5	3	CT	6	4			10	
E4	5	4	2483	13				13	
E5	5	5	2428		2			2	
E6	5	6	2571	4				4	
F1	6	1	2428		3			3	
F2	6	2	2571	15				15	
F3	6	3	2422	15				15	
F4	6	4	ST	15				15	
F5	6	5	CT	12	8		1	21	
F6	6	6	2483	15				15	

Data for Figure 2:14

**Phoenix Anti-Fouling Immersion Test Data**

Phoenix Panel Number:		732F	Immersion Date:		27-May-09	Immersion Site:		Newton Ferrers	
Raft Panel Bay Number:		09304F	Assessment Date:		14-Apr-10	Country :		UK	
Trial	Row	Column	Coating	% Microfouling	% Weed	% Soft-Bodied Animal	% Hard-Bodied Animal	% Total Fouling	Foul Release
A1	1	1	2483	90				90	
A2	1	2	2428	5		85		90	
A3	1	3	2571	85				85	
A4	1	4	2422	95				95	
A5	1	5	ST	95				95	
A6	1	6	CT	15		40	45	100	
B1	2	1	ST	90		5		95	
B2	2	2	CT	15		85		100	
B3	2	3	2483	90		5		95	
B4	2	4	2428	15		85		100	
B5	2	5	2571	100				100	
B6	2	6	2422	95				95	
C1	3	1	2571	95				95	
C2	3	2	2422	95				95	
C3	3	3	ST	98				98	
C4	3	4	CT	10		85		95	
C5	3	5	2483	95				95	
C6	3	6	2428	15		85		100	
D1	4	1	CT	15		85		100	
D2	4	2	2483	95				95	
D3	4	3	2428	15		70		85	
D4	4	4	2571	95				95	
D5	4	5	2422	80				80	
D6	4	6	ST	95				95	
E1	5	1	2422	80		10		90	
E2	5	2	ST	75		5		80	
E3	5	3	CT	5		95		100	
E4	5	4	2483	95				95	
E5	5	5	2428	10		85	5	100	
E6	5	6	2571	70			5	75	
F1	6	1	2428	10		85	5	100	
F2	6	2	2571	95				95	
F3	6	3	2422	15		85		100	
F4	6	4	ST	80				80	
F5	6	5	CT	45		5	50	100	
F6	6	6	2483	80				80	

Data for **Figure 3:10**

**Phoenix Anti-Fouling Immersion Test Data**

Phoenix Panel Number:		497F	Immersion Date:		06-Jul-07	Immersion Site:		Newton Ferrers	
Raft Panel Bay Number:		07319F	Assessment Date:		29-Oct-07	Country :		UK	
Trial	Row	Column	Coating	% Microfouling	% Weed	% Soft-Bodied Animal	% Hard-Bodied Animal	% Total Fouling	Foul Release
A1	1	1	1827	0	0	30	0	30	
A2	1	2	1828	0	0	10	0	10	
A3	1	3	1829	80	0	0	0	80	
A4	1	4	1830	75	0	0	0	75	
A5	1	5	ST	50	0	0	0	50	
A6	1	6	CT	35	0	25	0	60	
B1	2	1	ST	60	0	0	0	60	
B2	2	2	CT	19	0	10	1	30	
B3	2	3	1827	0	0	10	0	10	
B4	2	4	1828	0	0	3	0	3	
B5	2	5	1829	98	0	2	0	100	
B6	2	6	1830	99	0	1	0	100	
C1	3	1	1829	99	0	1	0	100	
C2	3	2	1830	49	0	1	0	50	
C3	3	3	ST	40	0	0	0	40	
C4	3	4	CT	0	0	25	0	25	
C5	3	5	1827	0	0	10	0	10	
C6	3	6	1828	0	0	8	0	8	
D1	4	1	CT	40	0	15	5	60	
D2	4	2	1827	0	0	5	0	5	
D3	4	3	1828	0	0	3	0	3	
D4	4	4	1829	89	0	1	0	90	
D5	4	5	1830	99	0	1	0	100	
D6	4	6	ST	50	0	0	0	50	
E1	5	1	1830	74	0	1	0	75	
E2	5	2	ST	70	0	0	0	70	
E3	5	3	CT	0	0	14	1	15	
E4	5	4	1827	0	0	10	0	10	
E5	5	5	1828	0	0	5	0	5	
E6	5	6	1829	42	0	3	0	45	
F1	6	1	1828	19	0	20	1	40	
F2	6	2	1829	99	0	1	0	100	
F3	6	3	1830	99	0	1	0	100	
F4	6	4	ST	30	0	0	0	30	
F5	6	5	CT	0	0	30	10	40	
F6	6	6	1827	0	0	40	0	40	

Data for **Figure 3:12**

**Phoenix Anti-Fouling Immersion Test Data**

Phoenix Panel Number:		474F	Immersion Date:		25-Apr-07	Immersion Site:		Newton Ferrers	
Raft Panel Bay Number:		07376F	Assessment Date:		06-Nov-07	Country :		UK	
Trial	Row	Column	Coating	% Microfouling	% Weed	% Soft-Bodied Animal	% Hard-Bodied Animal	% Total Fouling	Foul Release
A1	1	1	1772	2				2	
A2	1	2	1769	2				2	
A3	1	3	1771	20				20	
A4	1	4	1770	25				25	
A5	1	5	ST	25				25	
A6	1	6	CT	45	5	5	40	95	
B1	2	1	ST	1				1	
B2	2	2	CT	28	10	7	45	90	
B3	2	3	1772	1				1	
B4	2	4	1769	10				10	
B5	2	5	1771	50				50	
B6	2	6	1770	70				70	
C1	3	1	1771	40				40	
C2	3	2	1770	15				15	
C3	3	3	ST	1				1	
C4	3	4	CT	60			15	75	
C5	3	5	1772	25				25	
C6	3	6	1769	35				35	
D1	4	1	CT	25		15	30	70	
D2	4	2	1772	25				25	
D3	4	3	1769	10				10	
D4	4	4	1771	25			5	30	
D5	4	5	1770	35			1	36	
D6	4	6	ST	8				8	
E1	5	1	1770	12				12	
E2	5	2	ST	8				8	
E3	5	3	CT	25			25	50	
E4	5	4	1772	35				35	
E5	5	5	1769	26				26	
E6	5	6	1771	45			10	55	
F1	6	1	1769	2				2	
F2	6	2	1771	10			12	22	
F3	6	3	1770	8			12	20	
F4	6	4	ST	20				20	
F5	6	5	CT	20	3	5	52	80	
F6	6	6	1772	30				30	

Data for **Figure 3:13**

**Phoenix Anti-Fouling Immersion Test Data**

Phoenix Panel Number:		474F	Immersion Date:		25-Apr-07	Immersion Site:		Newton Ferrers	
Raft Panel Bay Number:		07376F	Assessment Date:		26-Mar-08	Country :		UK	
Trial	Row	Column	Coating	% Microfouling	% Weed	% Soft-Bodied Animal	% Hard-Bodied Animal	% Total Fouling	Foul Release
A1	1	1	1772	95				95	
A2	1	2	1769	95				95	
A3	1	3	1771	50				50	
A4	1	4	1770	88				88	
A5	1	5	ST	95				95	
A6	1	6	CT				100	100	
B1	2	1	ST	90				90	
B2	2	2	CT			85	5	90	
B3	2	3	1772	95				95	
B4	2	4	1769	98				98	
B5	2	5	1771	20				20	
B6	2	6	1770	98				98	
C1	3	1	1771	50				50	
C2	3	2	1770	95				95	
C3	3	3	ST	95				95	
C4	3	4	CT			85		85	
C5	3	5	1772	98				98	
C6	3	6	1769	99				99	
D1	4	1	CT	55			30	85	
D2	4	2	1772	98				98	
D3	4	3	1769	100				100	
D4	4	4	1771	50				50	
D5	4	5	1770	80				80	
D6	4	6	ST	100				100	
E1	5	1	1770	60				60	
E2	5	2	ST	80				80	
E3	5	3	CT			80	5	85	
E4	5	4	1772	90				90	
E5	5	5	1769	99				99	
E6	5	6	1771	30				30	
F1	6	1	1769	95				95	
F2	6	2	1771	84		1		85	
F3	6	3	1770	80		5		85	
F4	6	4	ST	80				80	
F5	6	5	CT	10		20	68	98	
F6	6	6	1772	30				30	

Data for **Figure 3:14**

**Phoenix Anti-Fouling Immersion Test Data**

Phoenix Panel Number:		474F	Immersion Date:		25-Apr-07	Immersion Site:		Newton Ferrers	
Raft Panel Bay Number:		07376F	Assessment Date:		30-Apr-09	Country :		UK	
Trial	Row	Column	Coating	% Microfouling	% Weed	% Soft-Bodied Animal	% Hard-Bodied Animal	% Total Fouling	Foul Release
A1	1	1	1772	58	2			60	
A2	1	2	1769	50				50	
A3	1	3	1771	93	5			98	
A4	1	4	1770	90	5			95	
A5	1	5	ST	5				5	
A6	1	6	CT		40		60	100	
B1	2	1	ST	50				50	
B2	2	2	CT				100	100	
B3	2	3	1772	75				75	
B4	2	4	1769	80				80	
B5	2	5	1771	73	2		25	100	
B6	2	6	1770	97	2			99	
C1	3	1	1771	70	20			90	
C2	3	2	1770	88	10	1		99	
C3	3	3	ST	98				98	
C4	3	4	CT				100	100	
C5	3	5	1772	93	2			95	
C6	3	6	1769	93	2			95	
D1	4	1	CT				100	100	
D2	4	2	1772	79	20			99	
D3	4	3	1769	97	2			99	
D4	4	4	1771	78	20			98	
D5	4	5	1770	80	10			90	
D6	4	6	ST	88	2			90	
E1	5	1	1770	73	25			98	
E2	5	2	ST	75				75	
E3	5	3	CT				100	100	
E4	5	4	1772				99	99	
E5	5	5	1769	93	5			98	
E6	5	6	1771	50	45			95	
F1	6	1	1769	65	10		25	100	
F2	6	2	1771	25	24		50	99	
F3	6	3	1770	70	20			90	
F4	6	4	ST	70	5			75	
F5	6	5	CT				100	100	
F6	6	6	1772	50	50			100	

Data for Figure 3:24

**Phoenix Anti-Fouling Immersion Test Data**

Phoenix Panel Number:				575F	Immersion Date:			22-Apr-08	Immersion Site:		Newton Ferrers
Raft Panel Bay Number:				08346F	Assessment Date:			19-Aug-08	Country :		UK
Trial	Row	Column	Coating	% Microfouling	% Weed	% Soft-Bodied Animal	% Hard-Bodied Animal	% Total Fouling	Foul Release		
A1	1	1	1827	80	5			85			
A2	1	2	2029	80	10			90			
A3	1	3	2030	70	15			85			
A4	1	4	2031		45			45			
A5	1	5	ST	25				25			
A6	1	6	CT	5	85			90			
B1	2	1	ST	10				10			
B2	2	2	CT	50	35			85			
B3	2	3	1827	50				50			
B4	2	4	2029	85				85			
B5	2	5	2030	50				50			
B6	2	6	2031	50	30			80			
C1	3	1	2030	50	5			55			
C2	3	2	2031	15	5			20			
C3	3	3	ST	30				30			
C4	3	4	CT		90			90			
C5	3	5	1827	70				70			
C6	3	6	2029	80	10			90			
D1	4	1	CT	60	30			90			
D2	4	2	1827	30	5			35			
D3	4	3	2029	85	5			90			
D4	4	4	2030	70				70			
D5	4	5	2031	55				55			
D6	4	6	ST	51				51			
E1	5	1	2031	25				25			
E2	5	2	ST	25				25			
E3	5	3	CT	10	20			30			
E4	5	4	1827	35				35			
E5	5	5	2029	95				95			
E6	5	6	2030	60	10			70			
F1	6	1	2029	90	5			95			
F2	6	2	2030	60	5			65			
F3	6	3	2031	10	10			20			
F4	6	4	ST	10				10			
F5	6	5	CT	20	10			30			
F6	6	6	1827	60				60			

Data for Figure 3:25

**Phoenix Anti-Fouling Immersion Test Data**

Phoenix Panel Number:		576F		Immersion Date:		22-Apr-08		Immersion Site:		Newton Ferrers	
Raft Panel Bay Number:		08349F		Assessment Date:		19-Aug-08		Country :		UK	
Trial	Row	Column	Coating	% Microfouling	% Weed	% Soft-Bodied Animal	% Hard-Bodied Animal	% Total Fouling	Foul Release		
A1	1	1	1827	60	2			62			
A2	1	2	2032	93	2			95			
A3	1	3	2033	60	5			65			
A4	1	4	2034	40	1			41			
A5	1	5	ST	2				2			
A6	1	6	CT	93	5			98			
B1	2	1	ST	5				5			
B2	2	2	CT	80	5			85			
B3	2	3	1827	20	5			25			
B4	2	4	2032	20	5			25			
B5	2	5	2033	50	5			55			
B6	2	6	2034	85	8			93			
C1	3	1	2033	40	5			45			
C2	3	2	2034	25				25			
C3	3	3	ST	10				10			
C4	3	4	CT	55	3			58			
C5	3	5	1827	40	2			42			
C6	3	6	2032	27				27			
D1	4	1	CT	93	3			96			
D2	4	2	1827	60	1			61			
D3	4	3	2032	20	1			21			
D4	4	4	2033	20	2			22			
D5	4	5	2034	10	1			11			
D6	4	6	ST	10				10			
E1	5	1	2034	75	3			78			
E2	5	2	ST	5				5			
E3	5	3	CT	50	2			52			
E4	5	4	1827	25				25			
E5	5	5	2032	15				15			
E6	5	6	2033	12				12			
F1	6	1	2032	43				43			
F2	6	2	2033	43	2			45			
F3	6	3	2034	36				36			
F4	6	4	ST	10				10			
F5	6	5	CT	45	1			46			
F6	6	6	1827	50	1			51			

Data for Figure 3:26

**Phoenix Anti-Fouling Immersion Test Data**

Phoenix Panel Number:				577F	Immersion Date:			22-Apr-08	Immersion Site:		Newton Ferrers
Raft Panel Bay Number:				08362F	Assessment Date:			19-Aug-08	Country :		UK
Trial	Row	Column	Coating	% Microfouling	% Weed	% Soft-Bodied Animal	% Hard-Bodied Animal	% Total Fouling	Foul Release		
A1	1	1	1827				80	80			
A2	1	2	2035				90	90			
A3	1	3	2036	90	5			95			
A4	1	4	2037				50	50			
A5	1	5	ST	5				5			
A6	1	6	CT		80		10	90			
B1	2	1	ST	1				1			
B2	2	2	CT	50	10			60			
B3	2	3	1827	10				10			
B4	2	4	2035	80	15			95			
B5	2	5	2036	90	5			95			
B6	2	6	2037	50	20			70			
C1	3	1	2036	95				95			
C2	3	2	2037	5			10	15			
C3	3	3	ST	1				1			
C4	3	4	CT	40	20		15	75			
C5	3	5	1827	30				30			
C6	3	6	2035	95				95			
D1	4	1	CT				90	90			
D2	4	2	1827	10				10			
D3	4	3	2035	95				95			
D4	4	4	2036	95				95			
D5	4	5	2037	25	10			35			
D6	4	6	ST	1				1			
E1	5	1	2037		10			10			
E2	5	2	ST	1				1			
E3	5	3	CT	25	25		1	51			
E4	5	4	1827	25	10			35			
E5	5	5	2035	90	5		5	100			
E6	5	6	2036	80	5		15	100			
F1	6	1	2035	80				80			
F2	6	2	2036	95				95			
F3	6	3	2037	20	5			25			
F4	6	4	ST	1				1			
F5	6	5	CT	25	20		5	50			
F6	6	6	1827	10	10			20			

Data for **Figure 3:27**

**Phoenix Anti-Fouling Immersion Test Data**

Phoenix Panel Number:				577F	Immersion Date:			22-Apr-08	Immersion Site:		Newton Ferrers
Raft Panel Bay Number:				08362F	Assessment Date:			07-Oct-08	Country :		UK
Trial	Row	Column	Coating	% Microfouling	% Weed	% Soft-Bodied Animal	% Hard-Bodied Animal	% Total Fouling	Foul Release		
A1	1	1	1827	50	30			80			
A2	1	2	2035	40	60			100			
A3	1	3	2036	70	10		5	85			
A4	1	4	2037		40		5	45			
A5	1	5	ST					0			
A6	1	6	CT	30			10	40			
B1	2	1	ST					0			
B2	2	2	CT		50		10	60			
B3	2	3	1827	20	8		2	30			
B4	2	4	2035	35	60		5	100			
B5	2	5	2036	75			5	80			
B6	2	6	2037	35			5	40			
C1	3	1	2036	90				90			
C2	3	2	2037	15	13		2	30			
C3	3	3	ST					0			
C4	3	4	CT	20	40		5	65			
C5	3	5	1827	40			5	45			
C6	3	6	2035		100			100			
D1	4	1	CT		55		25	80			
D2	4	2	1827	30			5	35			
D3	4	3	2035	60	28			88			
D4	4	4	2036	60	30			90			
D5	4	5	2037	18			2	20			
D6	4	6	ST					0			
E1	5	1	2037	35			5	40			
E2	5	2	ST					0			
E3	5	3	CT	50	40		10	100			
E4	5	4	1827	30	25		5	60			
E5	5	5	2035	60	30			90			
E6	5	6	2036	60	30			90			
F1	6	1	2035	55	40	5		100			
F2	6	2	2036	60	40			100			
F3	6	3	2037	22	8			30			
F4	6	4	ST					0			
F5	6	5	CT	40	25		15	80			
F6	6	6	1827	20	10		10	40			

Data for **Figure 3:28**

**Phoenix Anti-Fouling Immersion Test Data**

Phoenix Panel Number:				572F	Immersion Date:			22-Apr-08	Immersion Site:		Newton Ferrers
Raft Panel Bay Number:				08369F	Assessment Date:			07-Oct-08	Country :		UK
Trial	Row	Column	Coating	% Microfouling	% Weed	% Soft-Bodied Animal	% Hard-Bodied Animal	% Total Fouling	Foul Release		
A1	1	1	2019	90				90			
A2	1	2	2020	95				95			
A3	1	3	2021	90				90			
A4	1	4	2022	85				85			
A5	1	5	ST					0			
A6	1	6	CT	25	25	25	25	100			
B1	2	1	ST	15				15			
B2	2	2	CT	25	25	25	25	100			
B3	2	3	2019	80				80			
B4	2	4	2020	95				95			
B5	2	5	2021	85				85			
B6	2	6	2022	80				80			
C1	3	1	2021	75				75			
C2	3	2	2022	70				70			
C3	3	3	ST	10				10			
C4	3	4	CT	60	10	10	10	90			
C5	3	5	2019	80				80			
C6	3	6	2020	90				90			
D1	4	1	CT	25	25	25	25	100			
D2	4	2	2019	70				70			
D3	4	3	2020	75				75			
D4	4	4	2021	70				70			
D5	4	5	2022	75				75			
D6	4	6	ST	15				15			
E1	5	1	2022	60				60			
E2	5	2	ST	35				35			
E3	5	3	CT	50	20	10	10	90			
E4	5	4	2019	70				70			
E5	5	5	2020	70				70			
E6	5	6	2021	30				30			
F1	6	1	2020	85				85			
F2	6	2	2021	90				90			
F3	6	3	2022	80				80			
F4	6	4	ST	35				35			
F5	6	5	CT	25	25	25	25	100			
F6	6	6	2019	90				90			

Data for Figure 3:29

**Phoenix Anti-Fouling Immersion Test Data**

Phoenix Panel Number:		573F		Immersion Date:		22-Apr-08		Immersion Site:		Newton Ferrers	
Raft Panel Bay Number:		08360F		Assessment Date:		07-Oct-08		Country:		UK	
Trial	Row	Column	Coating	% Microfouling	% Weed	% Soft-Bodied Animal	% Hard-Bodied Animal	% Total Fouling	Foul Release		
A1	1	1	2019	20				20			
A2	1	2	2023	10				10			
A3	1	3	2024	10				10			
A4	1	4	2025	10				10			
A5	1	5	ST	40				40			
A6	1	6	CT	44	20		1	65			
B1	2	1	ST	100				100			
B2	2	2	CT	25	30			55			
B3	2	3	2019	80				80			
B4	2	4	2023	25				25			
B5	2	5	2024	25				25			
B6	2	6	2025	25				25			
C1	3	1	2024	2				2			
C2	3	2	2025	2				2			
C3	3	3	ST	15				15			
C4	3	4	CT	30	30			60			
C5	3	5	2019	60				60			
C6	3	6	2023	55				55			
D1	4	1	CT	20	25		15	60			
D2	4	2	2019	50				50			
D3	4	3	2023	25				25			
D4	4	4	2024	30				30			
D5	4	5	2025	30				30			
D6	4	6	ST	50				50			
E1	5	1	2025	30				30			
E2	5	2	ST	10				10			
E3	5	3	CT	30			2	32			
E4	5	4	2019	80				80			
E5	5	5	2023	40				40			
E6	5	6	2024	35				35			
F1	6	1	2023	50				50			
F2	6	2	2024	5				5			
F3	6	3	2025	35				35			
F4	6	4	ST	25				25			
F5	6	5	CT	10	40		10	60			
F6	6	6	2019	70				70			

Data for Figure 3:30

**Phoenix Anti-Fouling Immersion Test Data**

Phoenix Panel Number:				574F	Immersion Date:			22-Apr-08	Immersion Site:		Newton Ferrers
Raft Panel Bay Number:				08359F	Assessment Date:			07-Oct-08	Country:		UK
Trial	Row	Column	Coating	% Microfouling	% Weed	% Soft-Bodied Animal	% Hard-Bodied Animal	% Total Fouling	Foul Release		
A1	1	1	2019	40				40			
A2	1	2	2026	40				40			
A3	1	3	2027	45				45			
A4	1	4	2028	20				20			
A5	1	5	ST	35				35			
A6	1	6	CT	70	10	10		90			
B1	2	1	ST	40				40			
B2	2	2	CT	80				80			
B3	2	3	2019	25				25			
B4	2	4	2026	20				20			
B5	2	5	2027	20				20			
B6	2	6	2028	20				20			
C1	3	1	2027	45				45			
C2	3	2	2028	45				45			
C3	3	3	ST	30				30			
C4	3	4	CT	80				80			
C5	3	5	2019	70				70			
C6	3	6	2026	70				70			
D1	4	1	CT	85	5			90			
D2	4	2	2019	80				80			
D3	4	3	2026	55				55			
D4	4	4	2027	60				60			
D5	4	5	2028	60				60			
D6	4	6	ST	20				20			
E1	5	1	2028	70				70			
E2	5	2	ST	25				25			
E3	5	3	CT	90	5			95			
E4	5	4	2019	70				70			
E5	5	5	2026	75				75			
E6	5	6	2027	75				75			
F1	6	1	2026	85				85			
F2	6	2	2027	80				80			
F3	6	3	2028	6				6			
F4	6	4	ST	20				20			
F5	6	5	CT	90		5	5	100			
F6	6	6	2019	65				65			

Data for Figure 3:31

**Phoenix Anti-Fouling Immersion Test Data**

Phoenix Panel Number:				572F	Immersion Date:			22-Apr-08	Immersion Site:		Newton Ferrers
Raft Panel Bay Number:				08369F	Assessment Date:			30-Apr-09	Country :		UK
Trial	Row	Column	Coating	% Microfouling	% Weed	% Soft-Bodied Animal	% Hard-Bodied Animal	% Total Fouling	Foul Release		
A1	1	1	2019	80				80			
A2	1	2	2020	95				95			
A3	1	3	2021	95				95			
A4	1	4	2022	55				55			
A5	1	5	ST	0				0			
A6	1	6	CT	20	40		40	100			
B1	2	1	ST	95				95			
B2	2	2	CT	90	10			100			
B3	2	3	2019	70				70			
B4	2	4	2020	90				90			
B5	2	5	2021	60				60			
B6	2	6	2022	90				90			
C1	3	1	2021	90				90			
C2	3	2	2022	85				85			
C3	3	3	ST	75				75			
C4	3	4	CT	90	10			100			
C5	3	5	2019	65				65			
C6	3	6	2020	100				100			
D1	4	1	CT	10	30		60	100			
D2	4	2	2019	70				70			
D3	4	3	2020	95				95			
D4	4	4	2021	95				95			
D5	4	5	2022	80				80			
D6	4	6	ST	65				65			
E1	5	1	2022	80	5			85			
E2	5	2	ST	90				90			
E3	5	3	CT	40	60			100			
E4	5	4	2019	80				80			
E5	5	5	2020	100				100			
E6	5	6	2021	98				98			
F1	6	1	2020	100				100			
F2	6	2	2021	100				100			
F3	6	3	2022	80				80			
F4	6	4	ST	95				95			
F5	6	5	CT	20	10		70	100			
F6	6	6	2019	90				90			

Data for Figure 3:32

**Phoenix Anti-Fouling Immersion Test Data**

Phoenix Panel Number:				573F	Immersion Date:			22-Apr-08	Immersion Site:		Newton Ferrers
Raft Panel Bay Number:				08360F	Assessment Date:			30-Apr-09	Country :		UK
Trial	Row	Column	Coating	% Microfouling	% Weed	% Soft-Bodied Animal	% Hard-Bodied Animal	% Total Fouling	Foul Release		
A1	1	1	2019	90				90			
A2	1	2	2023	95				95			
A3	1	3	2024	90				90			
A4	1	4	2025	100				100			
A5	1	5	ST	90				90			
A6	1	6	CT	60	20		20	100			
B1	2	1	ST	80				80			
B2	2	2	CT	90	10			100			
B3	2	3	2019	85	10			95			
B4	2	4	2023	100				100			
B5	2	5	2024	95				95			
B6	2	6	2025	95				95			
C1	3	1	2024	90				90			
C2	3	2	2025	85				85			
C3	3	3	ST	95				95			
C4	3	4	CT	90	10			100			
C5	3	5	2019	60	10			70			
C6	3	6	2023	100				100			
D1	4	1	CT	40	10		50	100			
D2	4	2	2019	95				95			
D3	4	3	2023	95				95			
D4	4	4	2024	95				95			
D5	4	5	2025	85				85			
D6	4	6	ST	90				90			
E1	5	1	2025	95				95			
E2	5	2	ST	95				95			
E3	5	3	CT	75	10		5	90			
E4	5	4	2019	80				80			
E5	5	5	2023	90				90			
E6	5	6	2024	95				95			
F1	6	1	2023	95				95			
F2	6	2	2024	90				90			
F3	6	3	2025	85				85			
F4	6	4	ST	80				80			
F5	6	5	CT	50				50			
F6	6	6	2019	85				85			

Data for Figure 3:33

**Phoenix Anti-Fouling Immersion Test Data**

Phoenix Panel Number:		574F		Immersion Date:		22-Apr-08		Immersion Site:		Newton Ferrers	
Raft Panel Bay Number:		08359F		Assessment Date:		30-Apr-09		Country :		UK	
Trial	Row	Column	Coating	% Microfouling	% Weed	% Soft-Bodied Animal	% Hard-Bodied Animal	% Total Fouling	Foul Release		
A1	1	1	2019		100			100			
A2	1	2	2026	65	25			90			
A3	1	3	2027	50	50			100			
A4	1	4	2028	45	45			90			
A5	1	5	ST	70	20			90			
A6	1	6	CT	0	100			100			
B1	2	1	ST	25	50			75			
B2	2	2	CT	20	80			100			
B3	2	3	2019	20	70			90			
B4	2	4	2026	45	50			95			
B5	2	5	2027	50	50			100			
B6	2	6	2028	45	45			90			
C1	3	1	2027	50	50			100			
C2	3	2	2028	75	5			80			
C3	3	3	ST	93	5			98			
C4	3	4	CT	0	100			100			
C5	3	5	2019	60	30			90			
C6	3	6	2026	70	30			100			
D1	4	1	CT	10	65		25	100			
D2	4	2	2019	40	20			60			
D3	4	3	2026	50	40			90			
D4	4	4	2027	65	10			75			
D5	4	5	2028	35	5			40			
D6	4	6	ST	85	5			90			
E1	5	1	2028	38	2			40			
E2	5	2	ST	50	45			95			
E3	5	3	CT	0	95		5	100			
E4	5	4	2019	45	5			50			
E5	5	5	2026	70	25			95			
E6	5	6	2027	70	10			80			
F1	6	1	2026	78	20			98			
F2	6	2	2027	85	5			90			
F3	6	3	2028	29	1			30			
F4	6	4	ST	85	10			95			
F5	6	5	CT	0	10		90	100			
F6	6	6	2019	70	5			75			

Data for **Figure 4:12**

Panel Number	730F		Immersion Date	27/05/2009			
Raft Bay Number	9323F		Assessment Date	22/07/2009			
Immersion Site	Ferrers		No. Weeks Immersed	8			
Immersion Country	UK						
		<b>% fouling coverage</b>				<b>Total</b>	
<b>Square</b>	<b>Coating</b>	<b>Micro</b>	<b>Weed</b>	<b>Soft</b>	<b>Hard</b>	<b>% cover</b>	<b>H. Rating</b>
A1	v1	10	0	5	0	15	5
A2	v2	5	0	5	0	10	4
A3	v3	0	0	2	0	2	1
A4	v4	15	0	2	0	17	4
A5	Q(II)v4	15	0	5	0	20	6
A6	CT	15	0	20	1	36	17
B1	Q(II)v4	5	0	2	0	7	2
B2	CT	60	0	10	1	71	19
B3	v1	10	0	1	0	11	3
B4	v2	10	0	1	0	11	3
B5	v3	0	0	1	0	1	1
B6	v4	10	0	1	0	11	3
C1	v3	10	0	0	0	10	2
C2	v4	20	0	0	0	20	4
C3	Q(II)v4	15	0	2	0	17	4
C4	CT	50	0	15	1	66	20
C5	v1	20	0	1	0	21	5
C6	v2	15	0	0	0	15	3
D1	CT	40	0	25	1	66	25
D2	v1	15	0	0	0	15	3
D3	v2	30	0	0	0	30	6
D4	v3	10	0	0	0	10	2
D5	v4	20	0	1	0	21	5
D6	Q(II)v4	15	0	1	0	16	4
E1	v4	20	0	1	0	21	5
E2	Q(II)v4	10	1	1	0	12	3
E3	CT	40	0	20	0	60	21
E4	v1	10	0	2	0	12	3
E5	v2	15	0	1	0	16	4
E6	v3	5	0	1	0	6	2
F1	v2	20	0	2	0	22	5
F2	v3	5	0	2	0	7	2
F3	v4	15	0	2	0	17	4
F4	Q(II)v4	15	0	2	0	17	4
F5	CT	65	0	20	0	85	26
F6	v1	30	0	2	0	32	7

Data for **Figure 4:13**

Panel Number	<b>730B</b>		Immersion Date	<b>27/05/2009</b>				
Raft Bay Number	<b>09320B</b>		Assessment Date	<b>22/07/2009</b>				
Immersion Site	<b>Ferrers</b>		No. Weeks Immersed	<b>8</b>				
Immersion Country	<b>UK</b>							
			<b>% fouling coverage</b>				<b>Total</b>	
<b>Square</b>	<b>Coating</b>	<b>Micro</b>	<b>Weed</b>	<b>Soft</b>	<b>Hard</b>	<b>% cover</b>	<b>H. Rating</b>	
A1	v4	20	7	0	0	27	6	
A2	v5	20	2	0	0	22	5	
A3	v6	23	0	0	0	23	5	
A4	Bz quat	14	0	0	0	14	3	
A5	Q(II)v4	50	13	0	0	63	13	
A6	0	50	41	0	0	91	20	
B1	Q(II)v4	68	3	0	0	71	14	
B2	0	40	50	0	0	90	21	
B3	v4	23	0	0	0	23	5	
B4	v5	62	0	0	0	62	12	
B5	v6	50	0	0	0	50	10	
B6	Bz quat	11	7	0	0	18	4	
C1	v6	25	1	1	0	27	6	
C2	Bz quat	24	3	0	0	27	6	
C3	Q(II)v4	37	0	0	0	37	7	
C4	0	44	37	0	0	81	18	
C5	v4	35	0	0	0	35	7	
C6	v5	41	0	2	0	43	9	
D1	0	35	11	0	0	46	10	
D2	v4	19	2	3	0	24	6	
D3	v5	21	0	1	0	22	5	
D4	v6	11	2	0	0	13	3	
D5	Bz quat	26	0	0	0	26	5	
D6	Q(II)v4	26	4	0	0	30	6	
E1	Bz quat	20	5	4	0	29	8	
E2	Q(II)v4	28	4	0	0	32	7	
E3	0	40	31	0	0	71	16	
E4	v4	19	1	3	0	23	6	
E5	v5	48	0	0	0	48	10	
E6	v6	35	4	1	0	40	9	
F1	v5	31	3	0	0	34	7	
F2	v6	31	5	0	0	36	7	
F3	Bz quat	12	2	0	0	14	3	
F4	Q(II)v4	35	2	1	0	38	8	
F5	0	60	14	2	0	76	17	
F6	v4	30	3	2	0	35	8	

Data for **Figure 4:14**

Panel Number	730B		Immersion Date	27/05/2009				
Raft Bay Number	9323B		Assessment Date	22/07/2009				
Immersion Site	Ferrers		No. Weeks Immersed	8				
Immersion Country	UK							
			<b>% fouling coverage</b>				<b>Total</b>	
<b>Square</b>	<b>Coating</b>	<b>Micro</b>	<b>Weed</b>	<b>Soft</b>	<b>Hard</b>	<b>% cover</b>	<b>H. Rating</b>	
A1	v6	2	0	0	0	2	0	
A2	v7	10	0	0	0	10	2	
A3	v8	2	0	0	0	2	0	
A4	v9	20	0	0	0	20	4	
A5	Q(II)v4	40	0	0	0	40	8	
A6	CT	28	70	0	0	98	23	
B1	Q(II)v4	50	0	0	0	50	10	
B2	CT	20	10	0	0	30	7	
B3	v6	20	0	0	0	20	4	
B4	v7	20	0	0	0	20	4	
B5	v8	15	0	0	0	15	3	
B6	v9	45	0	0	0	45	9	
C1	v8	10	0	0	0	10	2	
C2	v9	15	0	0	0	15	3	
C3	Q(II)v4	15	0	0	0	15	3	
C4	CT	20	10	0	0	30	7	
C5	v6	25	0	0	0	25	5	
C6	v7	20	0	0	0	20	4	
D1	CT	20	5	0	0	25	5	
D2	v6	25	0	0	0	25	5	
D3	v7	20	0	0	0	20	4	
D4	v8	25	0	0	0	25	5	
D5	v9	40	0	0	0	40	8	
D6	Q(II)v4	18	0	2	0	20	5	
E1	v9	15	0	1	0	16	4	
E2	Q(II)v4	25	0	2	0	27	6	
E3	CT	20	0	2	0	22	5	
E4	v6	25	0	0	0	25	5	
E5	v7	30	0	0	0	30	6	
E6	v8	25	0	0	0	25	5	
F1	v7	35	0	5	0	40	10	
F2	v8	20	0	0	0	20	4	
F3	v9	25	0	2	0	27	6	
F4	Q(II)v4	30	0	1	0	31	7	
F5	CT	20	0	10	0	30	10	
F6	v6	20	0	1	0	21	5	

Data for **Figure 4:15**

Panel Number	731F		Immersion Date	27/05/2009				
Raft Bay Number	9313F		Assessment Date	22/07/2009				
Immersion Site	Ferrers		No. Weeks Immersed	8				
Immersion Country	UK							
		% fouling coverage					Total	
Square	Coating	Micro	Weed	Soft	Hard	% cover	H. Rating	
A1	v5	25	12	0	0	37	8	
A2	v10	41	10	0	0	51	11	
A3	v11	15	4	0	0	19	4	
A4	v12	30	10	0	0	40	9	
A5	Q(II)v4	19	37	0	0	56	13	
A6	CT	20	62	0	0	82	20	
B1	Q(II)v4	19	12	0	0	31	7	
B2	CT	40	58	0	0	98	23	
B3	v5	7	3	0	0	10	2	
B4	v10	7	4	0	0	11	2	
B5	v11	11	8	0	0	19	4	
B6	v12	15	10	2	0	27	7	
C1	v11	19	0	1	0	20	4	
C2	v12	4	0	1	0	5	1	
C3	Q(II)v4	15	12	4	0	31	9	
C4	CT	51	14	7	0	72	18	
C5	v5	12	0	8	0	20	7	
C6	v10	31	7	3	0	41	10	
D1	CT	30	34	10	6	80	27	
D2	v5	4	4	4	0	12	4	
D3	v10	11	9	0	0	20	4	
D4	v11	21	0	4	0	25	7	
D5	v12	23	0	3	0	26	6	
D6	Q(II)v4	38	0	7	0	45	12	
E1	v12	14	0	1	0	15	3	
E2	Q(II)v4	55	0	6	0	61	15	
E3	CT	53	45	0	0	98	22	
E4	v5	11	0	5	0	16	5	
E5	v10	20	2	0	0	22	5	
E6	v11	8	0	3	0	11	3	
F1	v10	11	5	2	1	19	6	
F2	v11	18	2	3	0	23	6	
F3	v12	10	2	2	0	14	4	
F4	Q(II)v4	19	8	1	0	28	6	
F5	CT	20	40	14	2	76	25	
F6	v5	10	21	3	0	34	9	

Data for **Figure 4:16**

Panel Number	<b>730B</b>		Immersion Date	<b>27/05/2009</b>				
Raft Bay Number	<b>09320B</b>		Assessment Date	<b>02/09/2009</b>				
Immersion Site	<b>Ferrers</b>		No. Weeks Immersed	<b>14</b>				
Immersion Country	<b>UK</b>							
		<b>% fouling coverage</b>					<b>Total</b>	
<b>Square</b>	<b>Coating</b>	<b>Micro</b>	<b>Weed</b>	<b>Soft</b>	<b>Hard</b>	<b>% cover</b>	<b>H. Rating</b>	
A1	v4	20	0	0	0	20	4	
A2	v5	15	5	0	0	20	4	
A3	v6	20	0	0	0	20	4	
A4	Bz quat	100	0	0	0	100	20	
A5	Q(II)v4	70	0	0	0	70	14	
A6	0	70	30	0	0	100	22	
B1	Q(II)v4	40	0	0	0	40	8	
B2	0	60	20	0	0	80	17	
B3	v4	20	0	0	0	20	4	
B4	v5	3	0	0	0	3	1	
B5	v6	10	0	0	0	10	2	
B6	Bz quat	80	0	0	0	80	16	
C1	v6	2	0	0	0	2	0	
C2	Bz quat	40	0	0	0	40	8	
C3	Q(II)v4	40	0	0	0	40	8	
C4	0	50	10	0	0	60	13	
C5	v4	10	5	0	0	15	3	
C6	v5	15	0	0	0	15	3	
D1	0	60	40	0	0	100	22	
D2	v4	5	0	0	0	5	1	
D3	v5	10	0	0	0	10	2	
D4	v6	2	0	0	0	2	0	
D5	Bz quat	60	0	0	0	60	12	
D6	Q(II)v4	60	0	0	0	60	12	
E1	Bz quat	60	0	0	0	60	12	
E2	Q(II)v4	60	0	0	0	60	12	
E3	0	40	10	0	0	50	11	
E4	v4	10	0	0	0	10	2	
E5	v5	15	0	0	0	15	3	
E6	v6	10	0	0	0	10	2	
F1	v5	40	0	0	0	40	8	
F2	v6	5	0	0	0	5	1	
F3	Bz quat	60	0	0	0	60	12	
F4	Q(II)v4	60	0	0	0	60	12	
F5	0	60	18	0	0	78	17	
F6	v4	25	0	0	0	25	5	

Data for **Figure 4:17**

Panel Number	730F		Immersion Date	27/05/2009				
Raft Bay Number	9323F		Assessment Date	02/09/2009				
Immersion Site	Ferrers		No. Weeks Immersed	14				
Immersion Country	UK							
			<b>% fouling coverage</b>				<b>Total</b>	
<b>Square</b>	<b>Coating</b>	<b>Micro</b>	<b>Weed</b>	<b>Soft</b>	<b>Hard</b>	<b>% cover</b>	<b>H. Rating</b>	
A1	v1	20	30	0	1	51	13	
A2	v2	2	0	0	0	2	0	
A3	v3	2	0	0	0	2	0	
A4	v4	2	0	0	0	2	0	
A5	Q(II)v4	50	0	0	0	50	10	
A6	CT	40	40	0	10	90	28	
B1	Q(II)v4	80	0	0	0	80	16	
B2	CT	40	45	0	5	90	24	
B3	v1	5	0	0	1	6	2	
B4	v2	3	0	0	0	3	1	
B5	v3	3	0	0	0	3	1	
B6	v4	20	0	0	0	20	4	
C1	v3	15	0	0	0	15	3	
C2	v4	8	0	0	0	8	2	
C3	Q(II)v4	49	0	0	1	50	11	
C4	CT	50	17	0	3	70	17	
C5	v1	5	0	0	0	5	1	
C6	v2	20	60	0	0	80	19	
D1	CT	30	32	0	3	65	17	
D2	v1	20	0	0	0	20	4	
D3	v2	20	0	0	1	21	5	
D4	v3	5	0	0	0	5	1	
D5	v4	10	0	0	0	10	2	
D6	Q(II)v4	40	0	0	0	40	8	
E1	v4	20	0	0	0	20	4	
E2	Q(II)v4	50	0	0	0	50	10	
E3	CT	75	5	0	0	80	16	
E4	v1	20	30	0	0	50	12	
E5	v2	15	0	0	0	15	3	
E6	v3	10	0	0	0	10	2	
F1	v2	40	0	0	1	41	9	
F2	v3	20	0	0	1	21	5	
F3	v4	10	0	0	1	11	3	
F4	Q(II)v4	40	0	0	1	41	9	
F5	CT	60	10	0	1	71	16	
F6	v1	70	0	0	0	70	14	

Data for **Figure 4:18**

Panel Number	<b>730B</b>		Immersion Date	<b>27/05/2009</b>				
Raft Bay Number	<b>9323B</b>		Assessment Date	<b>02/09/2009</b>				
Immersion Site	<b>Ferrers</b>		No. Weeks Immersed	<b>14</b>				
Immersion Country	<b>UK</b>							
			<b>% fouling coverage</b>				<b>Total</b>	
<b>Square</b>	<b>Coating</b>	<b>Micro</b>	<b>Weed</b>	<b>Soft</b>	<b>Hard</b>	<b>% cover</b>	<b>H. Rating</b>	
A1	v6	10	0	0	0	10	2	
A2	v7	10	0	0	0	10	2	
A3	v8	20	0	0	0	20	4	
A4	v9	10	5	0	0	15	3	
A5	Q(II)v4	20	0	0	0	20	4	
A6	CT	70	20	0	0	90	19	
B1	Q(II)v4	60	0	0	0	60	12	
B2	CT	30	2	0	3	35	10	
B3	v6	2	0	0	0	2	0	
B4	v7	2	0	0	0	2	0	
B5	v8	7	0	0	0	7	1	
B6	v9	10	60	0	0	70	17	
C1	v8	2	0	0	0	2	0	
C2	v9	2	0	0	0	2	0	
C3	Q(II)v4	40	0	0	0	40	8	
C4	CT	10	60	0	0	70	17	
C5	v6	2	0	0	0	2	0	
C6	v7	20	0	0	0	20	4	
D1	CT	40	0	0	2	42	10	
D2	v6	2	0	0	0	2	0	
D3	v7	2	0	0	0	2	0	
D4	v8	2	0	0	0	2	0	
D5	v9	2	0	0	0	2	0	
D6	Q(II)v4	40	60	0	0	100	23	
E1	v9	30	0	0	10	40	16	
E2	Q(II)v4	25	0	0	10	35	15	
E3	CT	5	0	0	10	15	11	
E4	v6	2	0	0	0	2	0	
E5	v7	0	0	0	10	10	10	
E6	v8	2	0	0	0	2	0	
F1	v7	0	0	0	10	10	10	
F2	v8	5	20	0	0	25	6	
F3	v9	5	20	0	0	25	6	
F4	Q(II)v4	20	5	0	10	35	15	
F5	CT	5	5	0	30	40	32	
F6	v6	3	0	0	0	3	1	

Data for **Figure 4:19**

Panel Number	731F		Immersion Date	27/05/2009				
Raft Bay Number	9313F		Assessment Date	02/09/2009				
Immersion Site	Ferrers		No. Weeks Immersed	14				
Immersion Country	UK							
			<b>% fouling coverage</b>				<b>Total</b>	
<b>Square</b>	<b>Coating</b>	<b>Micro</b>	<b>Weed</b>	<b>Soft</b>	<b>Hard</b>	<b>% cover</b>	<b>H. Rating</b>	
A1	v5	30	10	0	0	40	9	
A2	v10	25	0	0	0	25	5	
A3	v11	25	1	0	0	26	5	
A4	v12	25	1	0	0	26	5	
A5	Q(II)v4	25	0	0	0	25	5	
A6	CT	70	30	0	0	100	22	
B1	Q(II)v4	25	0	0	0	25	5	
B2	CT	70	30	0	0	100	22	
B3	v5	48	2	0	0	50	10	
B4	v10	15	2	0	0	17	4	
B5	v11	28	2	0	0	30	6	
B6	v12	20	0	0	0	20	4	
C1	v11	10	30	0	0	40	10	
C2	v12	15	0	0	0	15	3	
C3	Q(II)v4	25	0	0	0	25	5	
C4	CT	68	30	0	0	98	21	
C5	v5	25	0	0	0	25	5	
C6	v10	25	0	0	0	25	5	
D1	CT	60	40	0	0	100	22	
D2	v5	10	0	0	0	10	2	
D3	v10	5	0	0	0	5	1	
D4	v11	10	0	0	0	10	2	
D5	v12	30	0	0	0	30	6	
D6	Q(II)v4	30	0	0	0	30	6	
E1	v12	15	0	0	0	15	3	
E2	Q(II)v4	40	0	0	0	40	8	
E3	CT	70	10	0	0	80	17	
E4	v5	5	0	0	0	5	1	
E5	v10	5	0	0	0	5	1	
E6	v11	20	0	0	0	20	4	
F1	v10	70	0	0	0	70	14	
F2	v11	0	30	0	0	30	8	
F3	v12	20	0	0	0	20	4	
F4	Q(II)v4	30	0	0	0	30	6	
F5	CT	60	20	0	0	80	17	
F6	v5	50	0	0	0	50	10	

Data for **Figure 4:20**

Panel Number	<b>728F</b>		Immersion Date	<b>27/05/2009</b>				
Raft Bay Number	<b>09305F</b>		Assessment Date	<b>02/09/2009</b>				
Immersion Site	<b>Ferrers</b>		No. Weeks Immersed	<b>14</b>				
Immersion Country	<b>UK</b>							
		<b>% fouling coverage</b>					<b>Total</b>	
<b>Square</b>	<b>Coating</b>	<b>Micro</b>	<b>Weed</b>	<b>Soft</b>	<b>Hard</b>	<b>% cover</b>	<b>H. Rating</b>	
A1	v1	25	0	0	0	25	5	
A2	v2	30	0	0	0	30	6	
A3	v3	60	0	0	0	60	12	
A4	v4	50	0	0	0	50	10	
A5	Int 460	60	0	0	0	60	12	
A6	CT	55	15	0	0	70	15	
B1	Int 460	45	0	0	0	45	9	
B2	CT	45	5	0	0	50	10	
B3	v1	30	0	0	0	30	6	
B4	v2	15	0	0	0	15	3	
B5	v3	35	0	0	0	35	7	
B6	v4	10	0	0	0	10	2	
C1	v3	55	0	0	0	55	11	
C2	v4	30	0	0	0	30	6	
C3	Int 460	30	0	0	0	30	6	
C4	CT	55	15	0	0	70	15	
C5	v1	5	0	0	0	5	1	
C6	v2	5	0	0	0	5	1	
D1	CT	55	14	0	1	70	16	
D2	v1	25	0	0	0	25	5	
D3	v2	5	5	0	0	10	2	
D4	v3	50	0	0	0	50	10	
D5	v4	15	0	0	0	15	3	
D6	Int 460	15	0	0	0	15	3	
E1	v4	30	0	0	0	30	6	
E2	Int 460	25	0	0	0	25	5	
E3	CT	30	2	0	1	33	8	
E4	v1	5	0	0	0	5	1	
E5	v2	5	0	0	0	5	1	
E6	v3	25	0	0	0	25	5	
F1	v2	5	0	0	0	5	1	
F2	v3	25	0	0	0	25	5	
F3	v4	25	0	0	0	25	5	
F4	Int 460	45	0	0	0	45	9	
F5	CT	15	40	0	0	55	13	
F6	v1	15	0	0	0	15	3	

Data for **Figure 4:21**

Panel Number	<b>728B</b>		Immersion Date	<b>27/05/2009</b>				
Raft Bay Number	<b>09305B</b>		Assessment Date	<b>02/09/2009</b>				
Immersion Site	<b>Ferrers</b>		No. Weeks Immersed	<b>14</b>				
Immersion Country	<b>UK</b>							
			<b>% fouling coverage</b>				<b>Total</b>	
<b>Square</b>	<b>Coating</b>	<b>Micro</b>	<b>Weed</b>	<b>Soft</b>	<b>Hard</b>	<b>% cover</b>	<b>H. Rating</b>	
A1	v6	2	0	0	0	2	0	
A2	v7	5	0	0	0	5	1	
A3	v8	15	0	0	0	15	3	
A4	v9	5	0	0	0	5	1	
A5	Int 460	15	0	0	0	15	3	
A6	CT	85	5	0	0	90	18	
B1	Int 460	10	0	0	0	10	2	
B2	CT	40	50	0	0	90	21	
B3	v6	10	0	0	0	10	2	
B4	v7	10	0	0	0	10	2	
B5	v8	25	0	0	0	25	5	
B6	v9	2	0	0	0	2	0	
C1	v8	35	0	0	0	35	7	
C2	v9	15	0	0	0	15	3	
C3	Int 460	40	0	0	0	40	8	
C4	CT	70	10	0	0	80	17	
C5	v6	5	0	0	0	5	1	
C6	v7	5	0	0	0	5	1	
D1	CT	40	34	0	1	75	18	
D2	v6	3	0	0	0	3	1	
D3	v7	10	0	0	0	10	2	
D4	v8	25	0	0	0	25	5	
D5	v9	5	0	0	0	5	1	
D6	Int 460	20	0	0	0	20	4	
E1	v9	45	0	0	0	45	9	
E2	Int 460	35	0	0	0	35	7	
E3	CT	40	23	0	2	65	16	
E4	v6	2	0	0	0	2	0	
E5	v7	8	0	0	0	8	2	
E6	v8	15	0	0	0	15	3	
F1	v7	2	0	0	0	2	0	
F2	v8	60	0	0	0	60	12	
F3	v9	40	0	0	0	40	8	
F4	Int 460	60	0	0	0	60	12	
F5	CT	55	35	0	5	95	25	
F6	v6	8	0	0	0	8	2	

Data for **Figure 4:22**

Panel Number	<b>729F</b>		Immersion Date	<b>27/05/2009</b>				
Raft Bay Number	<b>9313F</b>		Assessment Date	<b>02/09/2009</b>				
Immersion Site	<b>Ferrers</b>		No. Weeks Immersed	<b>14</b>				
Immersion Country	<b>UK</b>							
			<b>% fouling coverage</b>				<b>Total</b>	
<b>Square</b>	<b>Coating</b>	<b>Micro</b>	<b>Weed</b>	<b>Soft</b>	<b>Hard</b>	<b>% cover</b>	<b>H. Rating</b>	
A1	v5	2	0	0	0	2	0	
A2	v10	4	0	0	0	4	1	
A3	v11	15	0	0	0	15	3	
A4	v12	4	0	0	0	4	1	
A5	Int 460	10	0	0	0	10	2	
A6	CT	50	40	0	0	90	20	
B1	Int 460	20	0	0	0	20	4	
B2	CT	35	40	0	0	75	17	
B3	v5	25	0	0	0	25	5	
B4	v10	5	0	0	0	5	1	
B5	v11	50	0	0	0	50	10	
B6	v12	5	0	0	0	5	1	
C1	v11	10	0	0	0	10	2	
C2	v12	10	0	0	0	10	2	
C3	Int 460	40	10	0	0	50	11	
C4	CT	25	25	0	0	50	11	
C5	v5	5	0	0	0	5	1	
C6	v10	5	50	0	0	55	14	
D1	CT	40	50	0	5	95	26	
D2	v5	8	0	0	0	8	2	
D3	v10	8	0	0	0	8	2	
D4	v11	5	0	0	0	5	1	
D5	v12	12	0	0	0	12	2	
D6	Int 460	40	0	0	0	40	8	
E1	v12	35	0	0	0	35	7	
E2	Int 460	50	0	0	0	50	10	
E3	CT	45	40	0	0	85	19	
E4	v5	5	0	0	0	5	1	
E5	v10	15	0	0	0	15	3	
E6	v11	10	0	0	0	10	2	
F1	v10	15	0	0	0	15	3	
F2	v11	10	0	0	0	10	2	
F3	v12	5	0	0	0	5	1	
F4	Int 460	40	0	0	0	40	8	
F5	CT	60	40	0	0	100	22	
F6	v5	25	0	0	0	25	5	

Data for **Figure 4:23**

Panel Number	<b>729B</b>		Immersion Date	<b>27/05/2009</b>				
Raft Bay Number	<b>09320B</b>		Assessment Date	<b>02/09/2009</b>				
Immersion Site	<b>Ferrers</b>		No. Weeks Immersed	<b>14</b>				
Immersion Country	<b>UK</b>							
			<b>% fouling coverage</b>				<b>Total</b>	
<b>Square</b>	<b>Coating</b>	<b>Micro</b>	<b>Weed</b>	<b>Soft</b>	<b>Hard</b>	<b>% cover</b>	<b>H. Rating</b>	
A1	v4	15	0	0	0	15	3	
A2	v5	15	0	0	0	15	3	
A3	v6	15	0	0	0	15	3	
A4	Q(II)v4	7	0	0	0	7	1	
A5	Int 460	30	0	0	0	30	6	
A6	CT	30	70	0	0	100	24	
B1	Int 460	40	0	0	0	40	8	
B2	CT	40	40	0	0	80	18	
B3	v4	30	0	0	0	30	6	
B4	v5	30	0	0	0	30	6	
B5	v6	30	0	0	0	30	6	
B6	Q(II)v4	30	0	0	0	30	6	
C1	v6	20	0	0	0	20	4	
C2	Q(II)v4	30	0	0	0	30	6	
C3	Int 460	60	0	0	0	60	12	
C4	CT	60	20	0	0	80	17	
C5	v4	10	0	0	0	10	2	
C6	v5	10	0	0	0	10	2	
D1	CT	40	50	0	0	90	21	
D2	v4	30	0	0	0	30	6	
D3	v5	20	0	0	0	20	4	
D4	v6	5	0	0	0	5	1	
D5	Q(II)v4	20	0	0	0	20	4	
D6	Int 460	50	0	0	0	50	10	
E1	Q(II)v4	10	0	0	0	10	2	
E2	Int 460	60	0	0	0	60	12	
E3	CT	40	40	0	0	80	18	
E4	v4	40	20	0	0	60	13	
E5	v5	5	0	0	0	5	1	
E6	v6	10	0	0	0	10	2	
F1	v5	5	0	0	0	5	1	
F2	v6	10	0	0	0	10	2	
F3	Q(II)v4	7	0	0	0	7	1	
F4	Int 460	37	0	0	0	37	7	
F5	CT	40	60	0	0	100	23	
F6	v4	10	0	0	0	10	2	

Data for **Figure 4:24**

Panel Number	<b>728F</b>		Immersion Date	<b>27/05/2009</b>				
Raft Bay Number	<b>09305F</b>		Assessment Date	<b>21/07/2010</b>				
Immersion Site	<b>Ferrers</b>		No. Weeks Immersed	<b>59</b>				
Immersion Country	<b>UK</b>							
			<b>% fouling coverage</b>				<b>Total</b>	
<b>Square</b>	<b>Coating</b>	<b>Micro</b>	<b>Weed</b>	<b>Soft</b>	<b>Hard</b>	<b>% cover</b>	<b>H. Rating</b>	
A1	v1	40				40	8	
A2	v2	25				25	5	
A3	v3	55				55	11	
A4	v4	60				60	12	
A5	Int 460	65				65	13	
A6	CT		5		95	100	96	
B1	Int 460	75				75	15	
B2	CT		5		95	100	96	
B3	v1	45				45	9	
B4	v2	50				50	10	
B5	v3	25				25	5	
B6	v4	25				25	5	
C1	v3	25				25	5	
C2	v4	40				40	8	
C3	Int 460	70				70	14	
C4	CT		5		95	100	96	
C5	v1	30				30	6	
C6	v2	50				50	10	
D1	CT				100	100	100	
D2	v1	20				20	4	
D3	v2	40				40	8	
D4	v3	50				50	10	
D5	v4	50				50	10	
D6	Int 460	60				60	12	
E1	v4	50				50	10	
E2	Int 460	80				80	16	
E3	CT				100	100	100	
E4	v1	50				50	10	
E5	v2	50				50	10	
E6	v3	50				50	10	
F1	v2	50				50	10	
F2	v3	20				20	4	
F3	v4	20				20	4	
F4	Int 460	100				100	20	
F5	CT				100	100	100	
F6	v1	75				75	15	

Data for **Figure 4:25**

Panel Number	<b>729B</b>		Immersion Date	<b>27/05/2009</b>				
Raft Bay Number	<b>09320B</b>		Assessment Date	<b>21/07/2010</b>				
Immersion Site	<b>Ferrers</b>		No. Weeks Immersed	<b>59</b>				
Immersion Country	<b>UK</b>							
			<b>% fouling coverage</b>				<b>Total</b>	
<b>Square</b>	<b>Coating</b>	<b>Micro</b>	<b>Weed</b>	<b>Soft</b>	<b>Hard</b>	<b>% cover</b>	<b>H. Rating</b>	
A1	v4	50				50	10	
A2	v5	20				20	4	
A3	v6	30				30	6	
A4	Q(II)v4	30				30	6	
A5	Int 460	60				60	12	
A6	CT				100	100	100	
B1	Int 460	50				50	10	
B2	CT				100	100	100	
B3	v4	20				20	4	
B4	v5	10				10	2	
B5	v6	10				10	2	
B6	Q(II)v4	10				10	2	
C1	v6	50				50	10	
C2	Q(II)v4	20				20	4	
C3	Int 460	80				80	16	
C4	CT		5	10	85	100	93	
C5	v4	30				30	6	
C6	v5	10				10	2	
D1	CT				100	100	100	
D2	v4	5				5	1	
D3	v5	10				10	2	
D4	v6	20				20	4	
D5	Q(II)v4	30				30	6	
D6	Int 460	60				60	12	
E1	Q(II)v4	50				50	10	
E2	Int 460	80				80	16	
E3	CT				100	100	100	
E4	v4	30				30	6	
E5	v5	5				5	1	
E6	v6	5				5	1	
F1	v5	30				30	6	
F2	v6	30				30	6	
F3	Q(II)v4	30				30	6	
F4	Int 460	60				60	12	
F5	CT				100	100	100	
F6	v4	10				10	2	

Data for **Figure 4:26**

Panel Number	<b>728B</b>		Immersion Date	<b>27/05/2009</b>				
Raft Bay Number	<b>09305B</b>		Assessment Date	<b>21/07/2010</b>				
Immersion Site	<b>Ferrers</b>		No. Weeks Immersed	<b>59</b>				
Immersion Country	<b>UK</b>							
			<b>% fouling coverage</b>				<b>Total</b>	
<b>Square</b>	<b>Coating</b>	<b>Micro</b>	<b>Weed</b>	<b>Soft</b>	<b>Hard</b>	<b>% cover</b>	<b>H. Rating</b>	
A1	v6	40				40	8	
A2	v7	5				5	1	
A3	v8	15				15	3	
A4	v9	90				90	18	
A5	Int 460	80				80	16	
A6	CT			20	80	100	93	
B1	Int 460	75				75	15	
B2	CT		5	10	85	100	93	
B3	v6	10				10	2	
B4	v7	25				25	5	
B5	v8	10				10	2	
B6	v9	10		5		15	5	
C1	v8	60				60	12	
C2	v9	75				75	15	
C3	Int 460	75				75	15	
C4	CT		5	10	85	100	93	
C5	v6	50				50	10	
C6	v7	40				40	8	
D1	CT		15		85	100	89	
D2	v6	25				25	5	
D3	v7	15				15	3	
D4	v8	20				20	4	
D5	v9	60				60	12	
D6	Int 460	80				80	16	
E1	v9	50				50	10	
E2	Int 460	90				90	18	
E3	CT	10			90	100	92	
E4	v6	10				10	2	
E5	v7	10				10	2	
E6	v8	20				20	4	
F1	v7	40				40	8	
F2	v8	3	5			8	2	
F3	v9	70				70	14	
F4	Int 460	8				8	2	
F5	CT				100	100	100	
F6	v6	20				20	4	

Data for **Figure 4:27**

Panel Number	<b>729F</b>		Immersion Date	<b>27/05/2009</b>				
Raft Bay Number	<b>9313F</b>		Assessment Date	<b>21/07/2010</b>				
Immersion Site	<b>Ferrers</b>		No. Weeks Immersed	<b>59</b>				
Immersion Country	<b>UK</b>							
			<b>% fouling coverage</b>				<b>Total</b>	
<b>Square</b>	<b>Coating</b>	<b>Micro</b>	<b>Weed</b>	<b>Soft</b>	<b>Hard</b>	<b>% cover</b>	<b>H. Rating</b>	
A1	v5	50				50	10	
A2	v10	40				40	8	
A3	v11	30				30	6	
A4	v12	30				30	6	
A5	Int 460	80				80	16	
A6	CT		25	5	70	100	79	
B1	Int 460	80				80	16	
B2	CT		20		80	100	85	
B3	v5	80				80	16	
B4	v10	65				65	13	
B5	v11	30				30	6	
B6	v12	40				40	8	
C1	v11	40				40	8	
C2	v12	40				40	8	
C3	Int 460	90				90	18	
C4	CT		5		95	100	96	
C5	v5	40				40	8	
C6	v10	60				60	12	
D1	CT				100	100	100	
D2	v5	60				60	12	
D3	v10	20				20	4	
D4	v11	40				40	8	
D5	v12	40				40	8	
D6	Int 460	60				60	12	
E1	v12	80				80	16	
E2	Int 460	5	10			15	4	
E3	CT			15	85	100	94	
E4	v5	35				35	7	
E5	v10	10			5	15	7	
E6	v11	30				30	6	
F1	v10	10			5	15	7	
F2	v11	20				20	4	
F3	v12	10			5	15	7	
F4	Int 460	60				60	12	
F5	CT				100	100	100	
F6	v5	70				70	14	

## 10.5.12 Leaching

### 10.5.12.1 Leaching SPE recovery

Data for Figure 5:9

<i>Days</i>	<i>didecyl-quat recovery (ppb)</i>				<i>benzyl-quat recovery (ppb)</i>			
	Replicate 1	Replicate 2	Replicate 3	Replicate 4	Replicate 1	Replicate 2	Replicate 3	Replicate 4
<b>0</b>	61	57	44	46	51	55	51	49
<b>3</b>	57	45	47	47	51	52	51	49
<b>7</b>	52	52	47	45	50	52	53	49
<b>10</b>	53	59	63	58	46	54	54	55

**Table 10:45: SPE recovery data for didecyl- and benzyl-quats**

## 10.5.12.2 Leaching Trial

Date for Figure 5:10

Date and Time Immersion  
30/11/2009 16:30

Sampling date and time	Time elapsed from initial immersion (days)	AMPSQ(I)v8 Paint [didecyl-quat] (ppb)	Actual leaching period (minutes)	[didecyl-quat]/per day (ppb)	AMPSQ(I)v8 Polymer [didecyl-quat] (ppb)	Actual leaching period (minutes)	[didecyl-quat]/per day (ppb)	AMPSQ(II)v4 + Bz quat Polymer [trioctyl-quat] (ppb)	Actual leaching period (minutes)	[trioctyl-quat]/per day (ppb)	AMPSQ(II)v4 + Bz quat Polymer [benzyl-quat] (ppb)	Actual leaching period (minutes)	[benzyl-quat]/per day (ppb)
01/12/2009 10:30	0.79	75	30	3600	271	15	26016	417	15	40032	1222	15	117312
04/12/2009 10:30	3.79	261	30	12528	120	15	11520	154	15	14784	95	15	9120
08/12/2009 10:30	7.79	133	30	6384	134	15	12864	88	15	8448	15	15	1440
17/12/2009 10:30	16.79	144	30	6912	100	15	9600	38	15	3648	0.01	15	1
23/12/2009 10:30	22.79	194	25	11174	234	25	13478	75	25	4320	0.001	25	0

Table 10:46: Leach rate measurements from initial leaching test

### 10.5.12.3 Leaching Data

Free association didecyl-quat Paint data for **Figure 6:7**

		PANEL 1						PANEL 2						PANEL 3						CALCULATIONS				
time	elapsed	SampleID	1	2	Leaching	[C10-quat]	[C10-quat]	SampleID	3	4	Leaching	[C10-quat]	[C10-quat]	SampleID	5	6	Leaching	[C10-quat]	[C10-quat]	C10-quat	C10-quat	C10-quat	C10-quat	C10-quat
date & time	immersion		[C10-quat]	[C10-quat]	Period	per day	per day		[C10-quat]	[C10-quat]	Period	per day	per day		[C10-quat]	[C10-quat]	Period	per day	per day	per day	per day	per day	per day	per day
	days		ppb	ppb	minutes	ppb	ppb		ppb	ppb	minutes	ppb	ppb		ppb	ppb	minutes	ppb	ppb	ppb	ppb	ppb	ppb	ppb
06/07/2010 09:20	0.76	1	72.91	88.52	15	7749	749.28	2	79.71	82.32	15	7777	125.28	3	98.19	101.16	15	9569	142.56	8365.0	1042.7	1297.9	133.8	21.30
07/07/2010 13:45	1.95	4	28.46	22.50	15	2446	286.08	5	24.84	29.86	15	2626	240.96	6	27.56	32.20	15	2868	222.72	2646.7	212.0	484.2	42.3	7.94
08/07/2010 10:50	2.83	7	33.59	37.44	30	1705	92.40	8	36.67	36.24	30	1750	10.32	9	39.78	37.21	30	1848	61.68	1767.4	73.1	133.4	28.3	2.19
09/07/2010 10:00	3.79	10	62.91	65.78	60	1544	34.44	11	61.75	60.20	60	1463	18.60	12	69.74	61.84	60	1579	94.80	1528.9	59.3	118.5	24.5	1.94
13/07/2010 09:40	7.78	13	52.25	43.78	60	1152	101.64	14	46.90	42.21	60	1069	56.28	15	40.54	39.12	60	956	17.04	1059.2	98.6	153.3	16.9	2.52
14/07/2010 13:45	8.95	16	22.24	22.84	30	1082	14.40	17	20.43	22.06	30	1020	39.12	18	17.50	15.87	35	686	33.53	929.4	212.7	219.3	14.9	3.60
16/07/2010 10:00	10.79	19	83.61	74.88	90	1268	69.84	20	49.67	43.08	90	742	52.72	21	37.48	41.94	90	635	35.68	881.8	338.6	351.6	14.1	5.77
03/08/2010 11:50	28.87	22	2.64	2.63	45	84	0.16	23	1.43	1.42	45	46	0.16	24	3.19	3.25	45	103	0.96	77.7	29.3	29.3	1.2	0.48
05/08/2010 11:35	30.86	25	4.74	5.41	80	91	6.03	26	3.79	3.78	80	68	0.09	27	5.47	5.02	230	33	1.41	64.1	29.5	30.1	1.0	0.49
15/09/2010 09:35	71.77	28	4.62	4.17	230	28	1.41	29	3.10	4.82	230	25	5.38	30	9.30	7.40	230	52	5.95	34.9	15.1	17.2	0.6	0.28

**Table 10:47: Final leach rate data for free association didecyl-quat paint**

AMPSQ(I)v10 Polymer data for **Figure 6:6**

		PANEL 1					PANEL 2					PANEL 3					CALCULATIONS								
time	elapsed	SampleID	1	2	Actual Leaching	average [C10-quat]	std dev [C10-quat]	SampleID	3	4	Actual Leaching	average [C10-quat]	std dev [C10-quat]	SampleID	5	6	Actual Leaching	average [C10-quat]	std dev [C10-quat]	average	std dev	std dev	average	SD	
sampling date & time	from initial immersion		[C10-quat]	[C10-quat]	Period	per day	per day		[C10-quat]	[C10-quat]	Period	per day	per day		[C10-quat]	[C10-quat]	Period	per day	per day	per day	per day	per day	per day	per day	per day
	days		ppb	ppb	minutes	ppb	ppb		ppb	ppb	minutes	ppb	ppb		ppb	ppb	minutes	ppb	ppb	ppb	ppb	ppb	per cm2	per cm2	
06/07/2010 13:33	0.94	1	110.48	116.44	16	10211	268.20	2	116.08	130.98	16	11118	670.50	3	113.25	127.24	16	10822	629.55	10717.1	462.2	1063.7	171.5	17.45	
07/07/2010 16:45	2.07	4	86.92	91.13	18	7122	168.40	5	101.85	98.57	18	8017	131.20	6	103.56	99.84	18	8136	148.80	7758.3	554.2	612.3	124.1	10.05	
08/07/2010 15:20	3.01	7	102.56	116.98	25	6323	415.30	8	111.38	109.98	25	6375	40.32	9	114.43	105.16	25	6324	266.98	6340.7	29.9	496.2	101.5	8.14	
09/07/2010 13:45	3.95	10	68.34	64.07	20	4767	153.72	11	58.36	57.00	20	4153	48.96	12	69.83	69.30	20	5009	19.08	4642.8	441.1	470.1	74.3	7.71	
13/07/2010 14:45	7.99	13	75.83	80.23	40	2809	79.20	14	99.82	86.51	40	3354	239.58	15	104.27	111.95	40	3892	138.24	3351.7	541.4	613.1	53.6	10.06	
14/07/2010 13:30	8.94	16	63.34	66.07	30	3106	65.52	17	78.36	72.43	30	3619	142.32	18	69.83	69.30	30	3339	12.72	3354.6	256.9	301.2	53.7	4.94	
16/07/2010 15:25	11.02	19	75.78	74.64	42	2579	19.54	20	84.44	93.06	42	3043	147.77	21	111.00	110.75	42	3801	4.29	3141.0	617.3	635.0	50.3	10.42	
03/08/2010 10:05	28.80	22	33.18	34.56	62	787	16.03	23	23.91	26.37	62	584	28.57	24	34.22	31.58	62	764	30.66	711.6	111.1	119.8	11.4	1.97	
05/08/2010 14:05	30.96	25	27.71	29.87	62	669	25.08	26	29.97	29.83	62	694	1.63	27	31.35	34.41	62	764	35.54	708.9	49.1	65.6	11.3	1.08	
14/09/2010 09:40	70.78	28	107.50	91.69	230	624	49.49	29	88.50	100.21	230	591	36.66	30	90.05	94.36	230	577	13.49	597.2	23.8	67.4	9.6	1.11	

Table 10:48: Final leach rate data for AMPSQ(I)v10 polymer

AMPSQ(I)v10 Paint data for **Figure 6:6**, **Figure 6:7** and **Figure 6:8**

		PANEL 1					PANEL 2					PANEL 3					CALCULATIONS								
time	elapsed	SampleID	1	2	Actual Leaching	average [C10-quat]	std dev [C10-quat]	SampleID	3	4	Actual Leaching	average [C10-quat]	std dev [C10-quat]	SampleID	5	6	Actual Leaching	average [C10-quat]	std dev [C10-quat]	average	std dev	std dev	average	SD	
sampling date & time	from initial immersion		[C10-quat]	[C10-quat]	Period	per day	per day		[C10-quat]	[C10-quat]	Period	per day	per day		[C10-quat]	[C10-quat]	Period	per day	per day	per day	per day	per day	per day	per day	per day
	days		ppb	ppb	minutes	ppb	ppb		ppb	ppb	minutes	ppb	ppb		ppb	ppb	minutes	ppb	ppb	ppb	ppb	ppb	per cm2	per cm2	
06/07/2010 11:13	0.84	1	104.19	106.58	15	10117	114.72	2	107.61	101.56	15	10040	290.40	3	96.21	84.01	15	8651	585.60	9602.6	825.3	1059.1	153.6	17.38	
07/07/2010 14:45	1.99	4	55.22	47.80	15	4945	356.16	5	56.80	63.49	15	5774	321.12	6	66.00	63.14	15	6199	137.28	5639.2	637.6	809.6	90.2	13.28	
08/07/2010 14:05	2.96	7	44.57	39.37	15	4029	249.60	8	53.27	48.56	15	4888	226.08	9	43.99	40.45	15	4053	169.92	4323.4	489.0	617.6	69.2	10.13	
09/07/2010 14:45	3.99	10	82.05	79.13	30	3868	70.08	11	86.53	87.40	30	4174	20.88	12	85.46	85.89	30	4112	10.32	4051.7	161.8	177.8	64.8	2.92	
13/07/2010 11:15	7.84	13	42.16	38.49	30	1936	88.08	14	53.95	55.39	30	2624	34.56	15	47.88	44.92	30	2227	71.04	2262.3	345.6	365.3	36.2	5.99	
14/07/2010 13:45	8.95	16	39.53	40.87	30	1930	32.16	17	45.29	48.47	30	2250	76.32	18	41.23	38.36	30	1910	68.88	2030.0	191.0	219.3	32.5	3.60	
16/07/2010 13:20	10.93	19	47.92	41.86	35	1847	124.66	20	43.39	40.83	35	1733	52.66	21	43.04	46.06	35	1833	62.13	1804.1	62.4	161.5	28.9	2.65	
03/08/2010 13:55	28.95	22	4.92	5.17	60	121	3.00	23	4.73	4.27	60	108	5.52	24	5.73	5.31	60	132	5.04	120.5	12.2	14.7	1.9	0.24	
05/08/2010 15:10	31.01	25	3.85	3.67	60	90	2.16	26	6.50	6.39	60	155	1.32	27	4.63	4.53	60	110	1.20	118.3	33.0	33.1	1.9	0.54	
15/09/2010 09:35	71.77	28	21.90	21.60	230	136	0.94	29	19.89	17.45	230	117	7.64	30	15.75	16.88	230	102	3.54	118.4	17.1	19.1	1.9	0.31	

Table 10:49: Final Leach rate data for AMPSQ(I)v10 paint

AMPSQ(I)v10 FB Paint data for **Figure 6:8**

		PANEL 1					PANEL 2					PANEL 3					CALCULATIONS							
time	elapsed	SampleID	1	2	Actual Leaching	average	std dev	SampleID	3	4	Actual Leaching	average	std dev	SampleID	5	6	Actual Leaching	average	std dev	3 panel average	3 panel std dev	overall std dev	3 panel average	SD
sampling date & time	from initial immersion		[C10-quat]	[C10-quat]	Period	per day	[C10-quat]		[C10-quat]	[C10-quat]	Period	per day	per day		[C10-quat]	[C10-quat]	Period	per day	per day	C10-quat	C10-quat	C10-quat	C10-quat	C10-quat
	days		ppb	ppb	minutes	ppb	ppb		ppb	ppb	minutes	ppb	ppb		ppb	ppb	minutes	ppb	ppb	ppb	ppb	ppb	per cm2	per cm2
06/07/2010 14:35	0.98	1	87.33	81.19	15	8089	294.72	2	91.57	80.78	15	8273	517.92	3	87.72	85.53	15	8316	105.12	8225.9	120.6	617.0	131.6	10.12
07/07/2010 15:45	2.03	4	42.41	49.26	15	4400	328.80	5	64.20	66.13	15	6256	92.64	6	63.38	67.33	15	6274	189.60	5643.4	1076.7	1145.4	90.3	18.79
08/07/2010 14:50	2.99	7	37.40	32.49	15	3355	235.68	8	45.45	48.78	15	4523	159.84	9	37.08	36.09	15	3512	47.52	3796.6	634.0	696.6	60.7	11.43
09/07/2010 16:45	4.07	10	54.23	57.80	30	2689	85.68	11	73.54	70.77	30	3463	66.48	12	81.78	79.61	30	3873	52.08	3341.8	601.6	613.5	53.5	10.07
13/07/2010 13:30	7.94	13	31.83	41.42	30	1758	230.16	14	49.76	50.48	30	2406	17.28	15	64.32	58.89	30	2957	130.32	2373.6	600.2	656.1	38.0	10.77
14/07/2010 13:30	8.94	16	48.78	50.27	35	2038	30.65	17	47.40	40.08	35	1800	150.58	18	39.53	41.38	35	1664	38.06	1833.9	188.9	246.5	29.3	4.04
16/07/2010 14:20	10.97	19	29.64	29.36	35	1214	5.76	20	33.83	29.97	35	1312	79.41	21	42.79	43.61	35	1777	16.87	1434.5	301.0	311.8	23.0	5.12
03/08/2010 15:00	29.00	22	1.92	1.97	60	47	0.60	23	1.96	2.31	60	51	4.20	24	2.43	2.49	60	59	0.72	52.3	6.3	7.6	0.8	0.12
05/08/2010 09:50	30.78	25	2.74	2.76	80	50	0.18	26	2.97	2.91	80	53	0.54	27	2.44	2.64	80	46	1.80	49.4	3.6	4.1	0.8	0.07
14/09/2010 09:40	70.78	28	5.19	4.56	210	33	2.16	29	4.17	3.84	210	27	1.13	30	6.43	6.15	210	43	0.96	34.7	7.9	8.3	0.6	0.14

**Table 10:50: Final leach rate data for AMPSQ(I)v10 FB paint**

Leaching Data supplied by Adrian Downer for free association coating containing seanine-211 for **Figure 6:7**

		PANEL 1					PANEL 2					PANEL 3					CALCULATIONS							
time	elapsed	SampleID	1	2	Actual Leaching	average	std dev	SampleID	3	4	Actual Leaching	average	std dev	SampleID	5	6	Actual Leaching	average	std dev	3 panel average	3 panel std dev	overall std dev	3 panel average	SD
sampling date & time	from initial immersion		[C9211]	[C9211]	Period	per day	[C9211]		[C9211]	[C9211]	Period	per day	per day		[C9211]	[C9211]	Period	per day	per day	C9211	C9211	C9211	C9211	C9211
	days		ppb	ppb	minutes	ppb	ppb		ppb	ppb	minutes	ppb	ppb		ppb	ppb	minutes	ppb	ppb	ppb	ppb	ppb	per cm2	per cm2
30/06/2010 13:02	0.94	1	752.77	756.08	90	12071	26.48	2	755.39	754.86	90	12082	4.24	3	763.40	749.41	90	12102	111.92	12085.1	16.1	116.2	73.6	0.71
02/07/2010 10:33	2.84	4	421.78	421.27	60	10117	6.12	5	403.23	400.46	60	9644	33.24	6	419.43	415.48	60	10019	47.40	9926.6	249.3	256.0	60.4	1.57
05/07/2010 11:03	5.86	7	299.94	303.51	60	7241	42.84	8	294.64	293.27	60	7055	16.44	9	262.79	261.69	60	6294	13.20	6863.4	502.0	504.3	41.8	3.10
09/07/2010 11:53	9.90	10	174.98	170.58	60	4147	52.80	11	153.07	150.85	60	3647	26.64	12	133.29	133.42	60	3201	1.56	3864.8	473.3	477.0	22.3	2.93
13/07/2010 11:55	13.90	13	99.00	99.76	60	2385	9.12	14	83.76	85.60	60	2032	22.08	15	72.38	72.11	60	1734	3.24	2050.4	326.0	326.9	12.5	2.01
16/07/2010 11:56	16.90	16	71.34	68.55	60	1679	33.48	17	58.62	59.39	60	1416	9.24	18	50.82	49.65	60	1206	14.04	1433.5	237.0	239.9	8.7	1.47
22/07/2010 14:17	23.00	19	41.74	43.36	60	1021	19.44	20	28.95	33.47	60	749	54.24	21	27.93	24.53	60	630	40.80	799.9	200.7	212.8	4.9	1.31
04/08/2010 14:00	35.98	22	18.37	19.18	120	225	4.86	23	16.07	14.43	120	183	9.84	24	11.55	13.84	120	152	13.74	186.9	36.6	40.6	1.1	0.25

**Table 10:51: Comparable leach rate data for free association coating containing seanine-211**

# 11 References

- <sup>1</sup>Lloyd's Register, Available at: [http://www.ihsfairplay.com/Maritime\\_data/PC\\_Register/PC\\_Register.html?product=PCReg&i=1](http://www.ihsfairplay.com/Maritime_data/PC_Register/PC_Register.html?product=PCReg&i=1) (Accessed: 10 August 2010).
- <sup>2</sup>Howden, D. (2007) 'Shipping pollution 'far more damaging than flying'', *The Independent*, 10 October, pp. 6.
- <sup>3</sup>European Community (2008) Available at: [http://ec.europa.eu/environment/climat/pdf/bali/post\\_2012.pdf](http://ec.europa.eu/environment/climat/pdf/bali/post_2012.pdf) (Accessed: 9 October 2008).
- <sup>4</sup>Woods Hole Oceanographic Institution United States (1952), 'Chapter 2: Ship Resistance' in *Marine fouling and its prevention*. Massachusetts Navy Department Bureau of Ships (United States Naval Institute) (<http://hdl.handle.net/1912/191>).
- <sup>5</sup>Omae, I. (2003) 'Organotin Antifouling Paints and their Alternatives', *Applied Organometallic Chemistry*, 17, pp. 81-105.
- <sup>6</sup>Lewis, J. (1998) 'Marine Biofouling and its Prevention on Underwater Surfaces', *Materials Forum*, 22, pp. 41-61.
- <sup>7</sup>Woods Hole Oceanographic Institution United States (1952), 'Chapter 11: The History of the Prevention of Fouling' in *Marine fouling and its prevention*. Massachusetts Navy Department Bureau of Ships (United States Naval Institute) (<http://hdl.handle.net/1912/191>).
- <sup>8</sup>International Paint (2004), 'Coatings Technology: Fouling' in "Propeller", March 2004 (17) pp. 3-5.
- <sup>9</sup>Wahl M., (1989) 'Marine Epibiosis I. Fouling and antifouling: some basic aspects', *Marine ecology progress series*, 58, pp. 175-189.
- <sup>10</sup>Di Cintio R., De Carolis G., (1993) 'Biofouling and corrosion', *Corrosion prevention and control*, pp. 104-107.
- <sup>11</sup>Maggs C., Callow, M. (2010) 'Algal Spores' in *Encyclopaedia of Life Sciences*, (2002) [Online]. Available at <http://www.els.net/> (Accessed 3 March 2010).
- <sup>12</sup>Thomason JC., Hills JM., (2003) 'The 'ghost of settlement past' determines mortality and fecundity in the barnacle, *Semibalanus balanoides*', *Oikos*, 101 (3), pp. 529-538.
- <sup>13</sup>Woods Hole Oceanographic Institution United States (1952), 'Chapter 8: Relations to Local Environments' in *Marine fouling and its prevention*. Massachusetts Navy Department Bureau of Ships (United States Naval Institute) (<http://hdl.handle.net/1912/191>).
- <sup>14</sup>Woods Hole Oceanographic Institution United States (1952), 'Chapter 5: The seasonal Sequence' in *Marine fouling and its prevention*. Massachusetts Navy Department Bureau of Ships (United States Naval Institute) (<http://hdl.handle.net/1912/191>).
- <sup>15</sup>National Aeronautics and Space Administration NASA (2002) *AMSR\_E First light images*. Available at: <http://library01.gsfc.nasa.gov/nix/nixImages/screenimage/GL-2002-001275.jpg> (Accessed: 15 October 2008).
- <sup>16</sup>Woods Hole Oceanographic Institution United States (1952), 'Chapter 13: Factors Influencing the Attachment and Adherence of Fouling Organisms' in *Marine fouling and its prevention*. Massachusetts Navy Department Bureau of Ships (United States Naval Institute) (<http://hdl.handle.net/1912/191>).
- <sup>17</sup>Candries M., (2000) *Paint systems for the Marine Industry*. Available at: [http://www.geocities.com/maxim\\_candries/Candries-Paint\\_Review.pdf](http://www.geocities.com/maxim_candries/Candries-Paint_Review.pdf) (Accessed: 9 October 2008).
- <sup>18</sup>Finnie A. (2009) E-mail to Paul Bassarab, 3 March 2009.
- <sup>19</sup>Hunt O., (1961) *Antifouling Research – Some Biological Aspects*. Available at International Paint.
- <sup>20</sup>International Paint (2002), 'Antifouling: Through the ages' in "Propeller", August 2002 (14), pp. 2-5.
- <sup>21</sup>Adams M., (2005) *Trafalgar's Lost Hero. Admiral Lord Collingwood and the defeat of Napoleon*. John Wiley & Sons.
- <sup>22</sup>Philips M., (no date) *Michael Philips Ships of the Old Navy: Royal Sovereign*. Available at: [www.ageofnelson.org/MichaelPhillips/info.php?ref=1930](http://www.ageofnelson.org/MichaelPhillips/info.php?ref=1930) (Accessed: 9 October 2008).
- <sup>23</sup>International Marine Organization (IMO) (2002), *Anti-fouling Systems*. Available at: [http://www.imo.org/includes/blastDataOnly.asp/data\\_id%3D7986?FOULING2003.pdf](http://www.imo.org/includes/blastDataOnly.asp/data_id%3D7986?FOULING2003.pdf) (Accessed: 28 September 2008).
- <sup>24</sup>Gitlitz, M. (1981) 'Recent developments in marine antifouling coatings', *Journal of Coatings Technology*, 53 (678), pp. 46-53.
- <sup>25</sup>Yebra, D., Kiil, S. & Joansen, K. (2004) 'Antifouling technology-past, present and future steps towards efficient and environmentally friendly antifouling coatings', *Progress in Organic Coatings*, 50 (2), pp. 75-104.
- <sup>26</sup>Lewis, J. (2003) 'TBT antifouling paints are now banned! What are the alternatives and what of the future?', *Surface Coatings Australia*, pp. 12-15.
- <sup>27</sup>Milne A., and Hails G. (1974) *Marine Paint*. UK Intellectual Property Office Patent no. GB1457590.
- <sup>28</sup>Milne A., (1991) 'Ablation and after: the law and the profits', *Polymers in a Marine Environment Conference*, 23-24 October 1991, pp. 139-144.

- <sup>29</sup>Anderson C., (1999) 'Developments in TBT-free Antifouling Technology', *Pittura e Vernici*, 75, pp.15-21.
- <sup>30</sup>Champ M., (2001) 'The status of the treaty to ban TBT in marine antifouling paints and alternatives', *the 24<sup>th</sup> UJNR (US/Japan Natural Resources) Marine Facilities Panel Meeting*, 7-8 November. Hawaii, pp. 1-7.
- <sup>31</sup>Ryle M., (1999) 'Are TBT alternatives as good?', *Motor Ship*, pp. 34-39.
- <sup>32</sup>Anderson C., (no date) *TBT Free Antifoulings and Foul Release Systems*. Available at: [http://www.international-marine.com/antifoulings/TBT\\_FreeAF\\_TechPaper.pdf](http://www.international-marine.com/antifoulings/TBT_FreeAF_TechPaper.pdf) (Accessed: 15 October 2008).
- <sup>33</sup>Baier R., (1980), 'Chapter 2: Substrata Influences on Adhesion of Microorganisms and Their Resultant New Surface Properties' in Bitton G., and Marshall K., (eds.) *Mechanisms Involved in sorption of Microorganisms to Solid Surfaces*. John Wiley & Sons, pp. 59-104.
- <sup>34</sup>International Paint (2010) *Intersleek: Better for the environment. Better for your business*. Available at: <http://www.international-marine.com/Literature/Intersleekbrouchure.pdf> (Accessed 29 September 2010)/
- <sup>35</sup>Health and Safety Commission (2006) *Biocidal Products Directive/Regulations*. Available at: <http://www.hse.gov.uk/biocides/bpd/index.htm> (Accessed: 17 October 2008).
- <sup>36</sup>Thomas K., (2001) 'The Environmental Fate and Behaviour of Antifouling Paint Booster Biocides: A Review', *Biofouling*, 17, pp.73-86.
- <sup>37</sup>European Community (1998) 'Biocidal Product Directive 98/98/EC', *Official Journal of European Communication*, L123/1. Available at: [http://ec.europa.eu/environment/biocides/pdf/List\\_participants\\_applicants\\_prod.pdf](http://ec.europa.eu/environment/biocides/pdf/List_participants_applicants_prod.pdf) (Accessed: 17 October 2008).
- <sup>38</sup>Konstantinou I., Hela D., Lambropoulou D., Sakkas V., (2002) 'Comparison of the performance of analytical methods based on solid-phase microextraction for the Determination of Antifouling Booster Biocides in Natural Waters', *Chromatographia*, 56, pp. 745-751.
- <sup>39</sup>Sundberg D., Vasishtha N., Zimmerman R., (1997), 'Chapter 7: Selection, Design and Delivery of Environmentally Benign Antifouling Agents' in *Naval Research Reviews*. Office of Naval Research, 49, pp. 51-59.
- <sup>40</sup>Health and Safety Executive (no date) *Safe: Use of Tin-free, Marine Anti-fouling Coatings*. Available at: [http://www.hse.gov.uk/fod/infodocs/730\\_15id.pdf](http://www.hse.gov.uk/fod/infodocs/730_15id.pdf) (Accessed: 28 September 2008).
- <sup>41</sup>Voulvoulis N., Scrimshaw M., Lester J., (2002) 'Comparative environmental assessment of biocides used in antifouling paints', *Chemosphere*, 47, pp. 789-795.
- <sup>42</sup>Omae, I. (2003) 'General Aspects of Tin-free Antifouling Paint', *Chemical Review*, 103, pp. 3431-3448.
- <sup>43</sup>Bertram V., (2000) 'Past, Present and Prospects of Antifouling', *32<sup>nd</sup> WEGEMT school: Marine coatings*. Plymouth July. London: WEGEMT, pp. 85-98.
- <sup>44</sup>Speedo *Fastskin® FSII*. Available at: [http://www.speedo.com/aqualab\\_technologies/aqualab/racing\\_suits\\_fastskin\\_fsii/index.html](http://www.speedo.com/aqualab_technologies/aqualab/racing_suits_fastskin_fsii/index.html) (Accessed: 3 March 2010).
- <sup>45</sup>Sharklet Technologies Inc. (2010). Available at: <http://www.sharklet.com> (Accessed: 3 March 2010).
- <sup>46</sup>Fusetani N., (2004) 'Biofouling and antifouling', *Natural Product Reports*, 21, pp. 94-104.
- <sup>47</sup>Lomax E., (1997) 'Cationic Surfactants' in *Surfactant Dictionary and Encyclopaedia*. Speciality Training, pp. 5-10.
- <sup>48</sup>Kenawy E., Mahmoud Y., (2003) 'Synthesis and Antimicrobial activity of some linear copolymers with Quaternary Ammonium and Phosphonium groups', *Micromolecular Bioscience*, 3, pp. 107-116.
- <sup>49</sup>Merianos J.J., (1991) 'Chapter 13: Quaternary Ammonium Antimicrobial Compounds' in Block, S. (ed.) *Disinfection, Sterilization and Preservation*. Lea and Febiger, PA, pp. 225-255.
- <sup>50</sup>Menschutkin N., (1890) 'Beiträgen zur kenntnis der affinitätskoeffizienten der alkylhaloide und der organischen amine', *Zeitschrift für Physikalische Chemie*, 5, pp. 589-601.
- <sup>51</sup>Parhizkari G., Delker G., Miller RB., Chen C., (1995) 'A stability-indicating HPLC method for the determination of Benzalkonium chloride in 0.5% Tramadol Ophthalmic solution' *Chromatographia*, 40, (3/4), pp. 155-158.
- <sup>52</sup>Li X., Geng Yu., (2004) 'Application of ionic liquids for electrostatic control in wood', *Holzforschung*, 58, pp. 280-285.
- <sup>53</sup>Wu H., Liu C., Lin Y., (2002) 'Extraction of Halide Quaternary salts in an Organic solvent/water system: Hydrodynamics and Mass transfer', *The Canadian Journal of Chemical Engineering*, 80, pp. 421-431.
- <sup>54</sup>Pernak J., Smiglak M., (2006) 'Long chain quaternary ammonium-based ionic liquids and potential applications', *Green Chemistry*, 8, pp. 786-806.
- <sup>55</sup>Wasserscheid P., Wilhelm K., (2000) 'Ionic liquids-New "Solutions" for Transition Metal Catalysis', *Angewandte Chemie International Edition*, 39, pp. 3772-3789.
- <sup>56</sup>Ding X., Mou S., Zhao S., (2004) 'Analysis of benzyldimethyldodecylammonium bromide in chemical disinfectants by liquids chromatography and capillary electrophoresis', *Journal of Chromatography A*, 1039, pp. 209-213.
- <sup>57</sup>Ibáñez M., Picó Y., Mañes J., (1997) 'On-line determination of Bipyridylum Herbicides in water by HPLC', *Chromatographia*, 45, pp. 402-407.

- <sup>58</sup>Vallejo-Freire A., Riberio O., (1954) 'Quaternary Ammonium Compounds as Molluscicides', *Science*, 119, pp. 470-472.
- <sup>59</sup>Smith M., Adam G., (2002) 'The effect of cationic surfactants on Marine Biofilm Growth on Hydrogels', *Estuarine, Coastal, and Shelf Science*, 55, pp. 361-367.
- <sup>60</sup>British Pharmacopoeia (2007) 'Benzalkonium Chloride', *British Pharmacopoeia Commission Stationary Office*, vol I, pp. 178-179.
- <sup>61</sup>Prince SJ., McLaury HJ., Allen LV., McLaury P (1999) 'Analysis of benzalkonium chloride and its homologs: HPLC versus HPCE', *Journal of Pharmaceutical and Biomedical Analysis*, 19, pp. 877-882.
- <sup>62</sup>Majumdar P., Lee E., Patel N., Ward K., (2008) 'Combinatorial materials research applied to the development of new surface coatings IX: An investigation of novel antifouling/fouling-release coatings containing quaternary ammonium salt groups', *Biofouling*, 24 (3), pp. 185-200.
- <sup>63</sup>Sauvet G., Dupond S., Kazmierski K., (2000) 'Biocidal polymers active by contact V: Synthesis of polysiloxanes with biocidal activity', *Journal of Applied Polymer Science*, 75, pp. 1005-1012.
- <sup>64</sup>Harney M., Pant R., Fulmer P., (2009) 'Surface self-concentrating amphiphilic quaternary ammonium biocides as coating additives', *Applied Materials and Interfaces*, 1 (1), pp. 39-41.
- <sup>65</sup>Franklin T., Snow G., (1981) 'Antiseptics, Antibiotics and the Cell membrane' in *Biochemistry of Antimicrobial Action*, 3<sup>rd</sup> ed. Chapman & Hall Ltd., London, pp 58-78.
- <sup>66</sup>Kügler R., Bouloussa O., Rondelez F., (2005) 'Evidence of a Charge-density threshold for optimum efficiency of biocidal cationic surfaces', *Microbiology*, 151, pp. 1341-1348.
- <sup>67</sup>Milovic N., Wang J., Lewis K., Kilbanov A., (2005) 'Immobilized N-Alkylated polyethylenimine avidly kills bacteria by disrupting cell membranes with no resistance developed', *Biotechnology and Bioengineering*, 90 (6), pp. 715-722.
- <sup>68</sup>Jiang S., Wang L., Yu H., Chen Y., (2005) 'Preparation of crosslinked polystyrenes with quaternary ammonium and their antibacterial behaviour', *Reactive and Functional Polymer*, 62, pp. 209-213.
- <sup>69</sup>Valko E.I., DuBois A.S., (1945) 'Correlation Between Antibacterial power and Chemical Structure of Higher Alkyl Ammonium Ions', *Journal of Bacteriology*, 50, pp. 481-490.
- <sup>70</sup>Lu G., Wu D., Fu., (2007) 'Studies on the synthesis and antimicrobial activities of polymeric quaternary ammonium salts from dimethylaminoethyl methacrylate', *Reactive and Functional Polymers*, 67, pp. 355-366.
- <sup>71</sup>Ayfer B., Dizman B., Elasri M., Mathias L., Avci D., (2005) 'Synthesis and antibacterial activities of new quaternary ammonium monomers', *Designed Monomers and Polymers*, 8 (5), pp. 437-451.
- <sup>72</sup>Kenawy E., Abdel-Hay F., El-Raheem A., El-Shanshoury R., (1998) 'Biological active polymers: synthesis and antimicrobial activity of modified glycidyl methacrylate polymers having a quaternary ammonium and phosphonium groups', *Journal of Controlled Release*, 50, pp. 145-152.
- <sup>73</sup>Oosterhof J., Buijessen K., Busscher H., (2006) 'Effect of Quaternary ammonium silane coatings on mixed fungal and bacterial biofilms on Tracheoesophageal shut prostheses', *Applied and Environmental Microbiology*, 72 (5), pp. 3673-2677.
- <sup>74</sup>Walters P., Abbott E., Isquith A., (1973) 'Algicidal Activity of a surface-bonded Organosilicon Quaternary Ammonium Chloride', *Applied Microbiology*, 25 (2), pp. 253-256.
- <sup>75</sup>Lin J., Qiu S., Lewis K., Klivanov A., (2003) 'Mechanism of bactericidal and fungicidal activities of textiles covalently modified with Alkylated Polyethylenimine', *Biotechnology and Bioengineering*, 83 (2), pp. 168-172.
- <sup>76</sup>Kouvai H., (1989) 'Part XIV: Relationship between hydrophobicity of bacterial cell surface and drug susceptibility to alkylpyridinium iodides', *Journal of Antibacterial and Antifungal Agents*, 17, pp. 119-128.
- <sup>77</sup>Daoud N., (1983) 'Antimicrobial activity and physio-chemical properties of some alkyl dimethylammonium chlorides', *Microbios*, 37, pp. 73-85.
- <sup>78</sup>Daoud N., (1983) 'Determination of benzalkonium chlorides by chemical ionisation mass spectrometry', *Journal of Pharmaceutical Sciences*, 72, pp. 290-292.
- <sup>79</sup>Tomlinson E., (1977) 'Effect of colloidal association on the measured activity of alkyl dimethylbenzylammonium chlorides against *Pseudomonas aeruginosa*', *Journal of Medicinal Chemistry*, 20, pp. 1277-1282.
- <sup>80</sup>Ikeda T., Yamaguchi H., Tazuke S., (1984) 'New polymeric biocides: Synthesis and antibacterial activities of polycations with pendant biquanide groups', *Antimicrobial Agents and Chemotherapy*, 26 (2), pp. 139-144.
- <sup>81</sup>Tiller J., Liao C., Klivanov A., (2001) 'Designing surfaces that kill bacteria on contact', *Proceedings of the National Academy of Sciences of the United States of America*, 98 (11), pp. 5981-5985.
- <sup>82</sup>Lin J., Tiller J., Lee S., Lewis K., Klivanov A., (2002) 'Insights into bacterial action of surface-attached poly(vinyl-N-hexalpyridinium) chains', *Biotechnology Letters*, 24, pp. 801-805.
- <sup>83</sup>Lin J., Murthy S., Olsen B., Gleason K., Klivanov A., (2003) 'Making thin polymeric materials, including fabrics, microbicidal and also water-repellent', *Biotechnology Letters*, 25, pp. 1661-1665.

- <sup>84</sup>Lin J., Qiu S., Lewis K., Klibanov A., (2002) 'Bactericidal Properties of flat surfaces and Nanoparticles derivatized with alkylated polyethylenimines', *Biotechnology Progress*, 18, pp.1082-1086.
- <sup>85</sup>Sambhy V., Hoar J., Peterson B., Sen A., (2007) 'Effect of spatial relationship between positive charge and alkyl tail on the biocidal activity of pyridinium polymers', *Polymeric Materials: Science and Engineering*, 96, pp. 345.
- <sup>86</sup>Murata H., Koepsel R., Matyjaszewski K., Russell A., (2007) 'Permanent, non-leaching antibacterial surfaces - 2: How high density cationic surfaces kill bacteria', *Biomaterials*, 28, pp. 4870-4879.
- <sup>87</sup>Cen L., Neoh G., Kang E., (2003) 'Surface functionalization techniques for conferring antibacterial Properties to Polymeric and Cellulosic Surfaces', *Langmuir*, 19, pp. 10295-10303.
- <sup>88</sup>Brass J., (1986) 'The cell envelope of gram-negative bacteria: new aspects of its function in transport and chemotaxis', *Current Topics in Microbiology and Immunology*, 129, pp. 1-92.
- <sup>89</sup>Balson T., Felix M., (1995) 'The biodegradation of non-ionic surfactants' in Karsa D. R., Porter M. R., (Eds.), *Biodegradation of surfactants*, Blackie Academic and Professional, pp. 204-230.
- <sup>90</sup>Ying G., (2006) 'Fate, Behaviour and Effects of surfactants and their Degradation products in the Environment', *Environment International*, 32, pp. 417-431.
- <sup>91</sup>Scott M., Jones M., (2000) 'The biodegradation of surfactants in the Environment', *Biochimica et Biophysica Acta*, 1508, pp. 235-251.
- <sup>92</sup>Nishiyama N., Toshima Y., Ikeda Y., (1995) 'Biodegradation of alkyltrimethylammonium salts in activated sludge', *Chemosphere*, 30, pp. 594-603.
- <sup>93</sup>van Ginkel C., Kolvenbach M., (1991) 'Relations between the Structure of Quaternary Alkyl Ammonium salts and their Biodegradability', *Chemosphere*, 23 (3), pp. 281-289.
- <sup>94</sup>Yoshimura K., Machida S., Masuda F., (1980) 'Biodegradation of long chain alkylamines', *Journal of the American Oil Chemists' Society*, 57 (7), pp. 238-240.
- <sup>95</sup>Swisher R., (1987) *Surfactant Biodegradation*, in "Surfactant Science Series", 18, 2<sup>nd</sup> Edition, New York: Marcel Dekker.
- <sup>96</sup>Garcia M., Ribosa I., Guindulain T., Sanchez-Leal J., (2001) 'Fate and effect of monoalkyl quaternary ammonium surfactants in the aquatic environment', *Environmental Pollution*, 111, pp. 167-175.
- <sup>97</sup>Games L., King J., Larson R., (1982) 'Fate and distribution of a quaternary ammonium surfactant, octadecyltrimethylammonium chloride (OTAC) in wastewater treatment', *Environmental Science and Technology*, 16, pp. 483-488.
- <sup>98</sup>Garcia M., Campos E., Sanchez-Leal J., Ribosa I., (1999) 'Effect of the Alkyl chain length on the anaerobic biodegradation and toxicity of Quaternary Ammonium Surfactants', *Chemosphere*, 38 (15), pp. 3473-3483.
- <sup>99</sup>Battersby N., Wilson V., (1989) 'Survey of the anaerobic biodegradation potential of organic chemicals in digesting sludge', *Applied and Environmental Microbiology*, 55, pp. 433-430.
- <sup>100</sup>Larson R., Vashon R., (1983) 'Adsorption and biodegradation of cationic surfactants in laboratory and environmental systems', *Developments in Industrial Microbiology series*, 24, pp. 425 – 434.
- <sup>101</sup>Weber J., Coble H., (1968) 'Microbial decomposition of diquat adsorbed on montmorillonites and kaolinite clay', *Journal of Agriculture and Food Chemistry*, 16, pp. 475 – 478.
- <sup>102</sup>Barbaro R., Hunter J., (1965) 'The effect of clay minerals on surfactants biodegradability', *Proceeding of the 20<sup>th</sup> Industrial Waste Conference*, Purdue University, 49 (4), pp. 189-196.
- <sup>103</sup>Moraru V., (2001) 'Structure formation of alkylammonium montmorillonites in organic media', *Applied Clay Science*, 19, pp. 11-26.
- <sup>104</sup>Lewis M., (1990) 'Chronic Toxicities of surfactants and Detergent Builders to Algae: A Review and Risk Assessment', *Ecotoxicology and Environmental Safety*, 20, pp. 123-140.
- <sup>105</sup>Lewis M., (1991) 'Chronic and Sublethal toxicities of surfactants to Aquatic animals: A Review and Risk Assessment', *Water Research*, 25 (1), pp. 101-113.
- <sup>106</sup>Lewis M., (1992) 'The effect of mixtures and other Environmental Modifying factors on the Toxicities of surfactants to Freshwater and Marine Life', *Water Research*, 26 (8), pp. 1013-1023.
- <sup>107</sup>Sanchez-Leal J., Gonzalez J., Kaiser K., Palabrica V., (1994) 'On the toxicity and biodegradation of Cationic surfactants', *Acta Hydrochimica et Hydrobiologica*, 22 (1), pp. 13-18.
- <sup>108</sup>Baudrion F., Perichaud A., Vacelet E., (2000) 'Influence of Concentration and Structure of Quaternary Ammonium Salts on their Antifouling Efficiency Tested against a Community of Marine Bacteria', *Biofouling*, 14 (4), pp. 317-331.
- <sup>109</sup>Ferks F., Misik M., Hoelzl C., Uhl M., (2007) 'Benzalkonium Chloride (BAC) and dimethyldioctadecylammonium bromide (DDAB), two common quaternary ammonium compounds, cause genotoxic effects in mammalian and plant cells at environmentally relevant concentrations', *Mutagenesis*, 22 (6), pp. 363-370.
- <sup>110</sup>Auerbach M., (1943) 'Germicidal Ammonium Salts in Dilute Solution. A colorimetric Assay Methods', *Industrial and Engineering Chemistry, Analytical Edition*, 15, pp. 492 – 493.
- <sup>111</sup>Epton R., (1947) 'A rapid method of analysis for certain surface-active Agents', *Nature*, 160, pp. 795-796.

- <sup>112</sup>Piera E., Erra P., Infante M., (1997) 'Analysis of cationic surfactants by capillary electrophoresis', *Journal of Chromatography A*, 757, pp. 275-280.
- <sup>113</sup>Metcalfe LD., (1963) 'The Direct Gas Chromatographic Analysis of long Chain Quaternary Ammonium Compounds', *Journal of the American Oil Chemists' Society*, 40, pp. 25-27.
- <sup>114</sup>Dudkiewicz-Wilczyńska J., Tautt J., Roman I., (2004) 'Application of the HPLC method for benzalkonium chloride determination in aerosol preparations', *Journal of Pharmaceutical and Biomedical Analysis*, 34, pp. 909-920.
- <sup>115</sup>Taylor RB., Toasaksiri S., Reid RG (1998) 'Determination of antibacterial quaternary ammonium compounds in lozenges by capillary electrophoresis', *Journal of Chromatography A*, 798, pp. 335-343.
- <sup>116</sup>Hou YH, Wu CY, Ding WH (2002) 'Development and validation of a capillary zone electrophoresis method for the determination of benzalkonium chlorides in ophthalmic solutions', *Journal of Chromatography A*, 976, pp. 207-213.
- <sup>117</sup>Jimidar M., Beyns I., Rome R., Peeters R., Musch G., (1998) 'Determination of Benzalkonium Chloride in Drug Formulations by Capillary Electrophoresis (CE)', *Biomedical Chromatography*, 12, pp. 128-130.
- <sup>118</sup>Altria K., Elgey J., Howells J., (1996) 'Validated capillary electrophoretic methods for the quantitative analysis of histamine acid phosphate and/or benzalkonium chloride', *Journal of Chromatography B*, 686, pp. 111-117.
- <sup>119</sup>Gardner WP, Girard JE (2000) 'Analysis of common household cleaner-disinfectants by capillary electrophoresis', *Journal of Chemical Education*, 77 (10), pp. 1335-1338.
- <sup>120</sup>Carneiro MC., Puignou L., Galceran MT (1994) 'Comparison of capillary electrophoresis and reversed-phase ion-pair high-performance liquid chromatography for the determination of paraquat, diquat and difenzoquat', *Journal of Chromatography A*, 669, pp. 217-224.
- <sup>121</sup>So, T. S.K & Huie C. W (2000) 'Investigation of the effect of cyclodextrins and organic solvents on the separation of cationic surfactants in capillary electrophoresis', *Journal of Chromatography A*, 872, pp. 269-278.
- <sup>122</sup>Herrero-Martínez JM., Simó-Alfonso E., Mongay-Fernández C., Ramis-Ramos G., (2000) 'Determination of cationic surfactants by capillary zone electrophoresis and micellar electrokinetic chromatography with deoxycholate micelles in the presence of large organic solvent concentrations', *Journal of Chromatography A*, 895, pp. 227-235.
- <sup>123</sup>Heinig K., Vogt C., (1999) 'Determination of surfactants by capillary electrophoresis', *Electrophoresis*, 20, pp. 3311-3328.
- <sup>124</sup>Heinig K., Vogt C., Werner G., (1997) 'Determination of cationic surfactants by capillary electrophoresis', *Journal of Analytical Chemistry*, 358, pp. 500-505.
- <sup>125</sup>Lin C. E, Chiou WC, Lin CW (1996) 'Capillary zone electrophoretic separation of alkylbenzyl quaternary ammonium compounds: effect of organic modifier', *Journal of Chromatography A*, 722, pp. 345-352.
- <sup>126</sup>Pohlmann J., Cohan S., (1977) 'Simplified Detection of Quaternary Ammonium Compounds by Gas Chromatography', *Journal of Chromatography*, 131, pp. 297-301.
- <sup>127</sup>Abidi SL., (1981) 'Speciation of Aryoxyethoxyethyl benzyl dimethyl ammonium salts by glass capillary gas chromatography and high-performance liquid chromatography', *Journal of Chromatography*, 213, pp. 463-474.
- <sup>128</sup> Fressenden R., & Fressenden J., (1994) *Organic Chemistry*, 5<sup>th</sup> Edition. Thomason Brooks/Cole, pp. 770.
- <sup>129</sup>Piedra L., Tejedor A., Hernando M., Aguera A., (2000) 'Screening of Antifouling Pesticides in seawater samples at low ppt levels by GC-MS and LC-MS', *Chromatographia*, 52, pp. 631-638.
- <sup>130</sup>Miller RB., Chen C., Sherwood CH (1993) 'High-Performance Liquid Chromatographic determination of Benzalkonium Chloride in vasocidin ophthalmic Solution', *Journal of Liquid Chromatography*, 16 (17), 3801-3811.
- <sup>131</sup>Bernal J., del Nozel M., Martín MT., Diez-Masa J., Cifuentes A., (1998) 'Quantitation of active ingredients and excipients in nasal sprays by high-performance liquid chromatography, capillary electrophoresis and UV spectroscopy', *Journal of Chromatography A*, 823, pp. 423-431.
- <sup>132</sup>Itagaki T., Lai S., Binder S., (1997) 'A rapid monitoring method of paraquat and diquat in serum and urine using ion-pairing bare-silica stationary phase HPLC following a single acidification step of sample pretreatment', *Journal of Liquid Chromatography and Related Technology* 20 (20), pp. 3339-3350.
- <sup>133</sup>Gonzalez S., Petrovic M., Barcelo D., (2007) 'Advanced liquid chromatography-mass spectrometry (LC-MS) methods applied to wastewater removal and the fate of surfactants in the environment', *Trends in Analytical Chemistry*, 26 (2), pp. 116-124.
- <sup>134</sup>Ferrer I., Furlong ET., (2002) 'Accelerated solvent extraction followed by on-line solid-phase extraction coupled to Ion trap LC/MS/MS for Analysis of Benzalkonium Chloride in sediment samples', *Analytical Chemistry*, 74, pp. 1275-1280.

- <sup>135</sup>Marr JC., King JB., (1997) 'A simple High Performance Liquid Chromatography/Ionspray Tandem Mass Spectrometry method for the Direct Determination of Paraquat and Diquat in water', *Rapid communications in mass spectrometry*, 11, pp. 479-483.
- <sup>136</sup>Giovannelli D., Abballe F., (2005) 'Aliphatic long chain quaternary ammonium compounds analysis by ion-pair chromatography coupled with suppressed conductivity and UV detection in lysing reagent for blood cell analysis', *Journal of Chromatography A*, 1085, pp. 86-90.
- <sup>137</sup>Liu X., Pohl C., Dionex Corporation (2006) 'Analysis of cationic surfactants using Acclaim® surfactant column' in *The application notebook*. February 2006, pp. 17.
- <sup>138</sup>Bluhm LH., Li T., (1999) 'Effect of Analogue Ions in Normal-Phase Ion-pair Chromatography of Quaternary Ammonium Compounds', *Journal of Chromatographic science*, 37, pp. 273-276.
- <sup>139</sup>Bluhm LH., Li T., (2003) 'The role of Analogue Ions in the Ion-pair Reversed-Phase Chromatography of Quaternary Ammonium Compounds', *Journal of Chromatographic Science*, 41, pp. 6-9.
- <sup>140</sup>Nakae A., Kunihiro K., Muto G., (1997) 'Separation of homologous alkylbenzyltrimethylammonium chlorides and alkylpyridinium halides by High-performance liquid Chromatography', *Journal of Chromatography*, 134, pp. 459-466.
- <sup>141</sup>Ambrus G., Takahashi L., Marty P., (1987) 'Direct determination of Benzalkonium Chloride in Ophthalmic systems by Reversed-phase High-performance liquid chromatography', *Journal of Pharmaceutical Sciences*, 76 (2), pp. 174-176.
- <sup>142</sup>Valladao M., Sandine W., (1994) 'Quaternary Ammonium Compounds in Milk: Detection by Reverse-phase High-Performance Liquid Chromatography and their Effects on Starter Growth', *Journal of Dairy Science*, 77, pp. 1509-1514.
- <sup>143</sup>Parhizkari G., Miller RB., Chen C., (1993) 'A stability-indicating HPLC method for the determination of Benzalkonium chloride in phenylephrine HCL 10% ophthalmic solution', *Journal of Liquid Chromatography*, 18 (3), pp. 553-563.
- <sup>144</sup>Taylor RB., Toasaksiri S., Reid RG., Wood D., (1997) 'Determination of the Quaternary Ammonium Compounds Dequalinium and Cetylpyridinium Chloride in candy-based Lozenges by HPLC', *Analysts*, 122, pp. 973-976.
- <sup>145</sup>Shibukawa M., Eto R., Kira A., Miura F., Oguma K., (1999) 'Separation and determination of quaternary ammonium compounds by high-performance liquid chromatography with a hydrophilic polymer column and conductometric detection', *Journal of Chromatography A*, 830, pp. 321-328.
- <sup>146</sup>Restek (2006) 'Simple, Sensitive HPLC/UV analysis for Paraquat and Diquat'.
- <sup>147</sup>Paul GJ., Maracotte I., Anastassopoulou J., Theophanides T., (1996) 'Investigation of the Clustering Processes occurring in Liquid secondary Ion Mass Spectrometry for alkyl Quaternary ammonium Bromides', *Journal of Mass spectrometry*, 31, pp. 95-100.
- <sup>148</sup>Kambhampati I., Roinestad K., Hartman T., Rosen J., (1994) 'Determination of diquat and paraquat in water using high-performance liquid chromatography with confirmation by liquid chromatography-particle beam mass spectrometry', *Journal of Chromatography A*, 688, pp. 67-73.
- <sup>149</sup>Fernández P., Alder A., Suter M., Giger W., (1996) 'Determination of the Quaternary Ammonium Surfactants Ditalowdimethylammonium in Digested Sludges and Marine sediments by supercritical fluid extraction and Liquid Chromatography with Postcolumn Ion-pair formation', *Analytical Chemistry*, 68, pp. 921-929.
- <sup>150</sup>van der HoevenR., Reewijk H., Tjaden U., (1996) 'Analysis of quaternary ammonium drugs by thermospray liquid chromatography-mass spectrometry using resin-based stationary phase', *Journal of Chromatography A*, 742, pp. 75-84.
- <sup>151</sup>Vahl M., Graven A., Juhler R., (1998) 'Analysis of Chlormequat residues in grain using liquid chromatography-mass spectrometry (LC-MS/MS)', *Journal of Analytical Chemistry*, 361, pp. 817-820.
- <sup>152</sup>Radke M., Behrends T., Förster J., Herrmann R., (1999) 'Analysis of cationic surfactants by microbore High-Performance Liquid Chromatography-Electrospray Mass spectrometry', *Analytical Chemistry*, 71, pp. 5362-5366.
- <sup>153</sup>Castro R., Moyano E., Galceran MT., (1999) 'Ion-pair liquid chromatography-atmospheric pressure ionization mass spectrometry for the determination of quaternary ammonium herbicides', *Journal of Chromatography A*, 830, pp. 145-154.
- <sup>154</sup>Ferrer I., Furlong ET., (2001) 'Identification of alkylbenzyltrimethylammonium surfactants in water samples by solid-phase extraction followed by ion Trap LC/MS and LC/MS/MS', *Environmental Science Technology*, 35, pp. 2583-2588.
- <sup>155</sup>Ford MJ., Tetler LW., White J., (2002) 'Determination of alkyl benzyl and dialkyl dimethyl quaternary ammonium biocides in occupational hygiene and environmental media by liquid chromatography with electrospray ionisation mass spectrometry and tandem mass spectrometry', *Journal of Chromatography A*, 952, pp. 165-172.

- <sup>156</sup>Merino F., Rubio S., Pérez-Bendito D., (2003) 'Mixed aggregate-based acid-induced cloud-point extraction and ion-trap liquid chromatography-mass spectrometry for the determination of cationic surfactants in sewage sludge', *Journal of Chromatography A*, 998, pp. 143-154.
- <sup>157</sup>Martínez Vidal JL., Belmonte Vega A., Sánchez López FJ., Garrido Frenich A., (2004) 'Application of internal quality control to analysis of quaternary ammonium compounds in surface and groundwater from Andalusia (Spain) by liquid chromatography with mass spectrometry', *Journal of Chromatography A*, 1050, pp. 170-184.
- <sup>158</sup>Núñez O., Moyano E., Galceran MT., (2004) 'Determination of quaternary ammonium biocides by liquid chromatography-mass spectrometry', *Journal of Chromatography A*, 1058, pp. 89-95.
- <sup>159</sup>Martínez-Carballo E., Sitka A., Gonzalez-Barreiro C., (2007) 'Determination of selected quaternary ammonium compounds by liquid chromatography with mass spectrometry. Part I. Application to surface, waste and indirect discharge water samples in Austria', *Environmental Pollution*, 145, pp. 489-496.
- <sup>160</sup>Castro R., Moyano E., Galceran MT., (2000) 'On-line ion-pair solid-phase extraction-liquid chromatography-mass spectrometry for the analysis of quaternary ammonium herbicides', *Journal of Chromatography A*, 869, pp. 441-449.
- <sup>161</sup>Picó Y., Font G., Moltó JC., Mañes J., (2000) 'Solid-phase extraction of quaternary ammonium herbicides', *Journal of Chromatography A*, 885, pp. 251-271.
- <sup>162</sup>Carneiro MC., Puignou L., Galceran MT., (2000) 'Comparison of silica and porous graphitic carbon as solid-phase extraction materials for the analysis', *Analytica Chimica Acta*, 408, pp. 263-269.
- <sup>163</sup>Núñez O., Moyano E., Galceran MT., (2002) 'Solid-phase extraction and sample stacking-capillary electrophoresis for the determination of quaternary ammonium herbicides in drinking water', *Journal of Chromatography A*, 946, pp. 275-282.
- <sup>164</sup>American Standard Method of Test (2007) 'D 6903-07: Standard test method for determination of Organic Biocide release rate from Antifouling coatings in substitute Ocean water', London: British Standard Institution SMT.
- <sup>165</sup>Rogers J., Sesso M., (1967) *Coating composition*. United States Patent Office Patent no. 3 308 078.
- <sup>166</sup>Earl G., Weisshaar D., Paulson D., Hanson M., (2004) 'Quaternary methyl carbonates: Novel agents for fabric conditioning', *Journal of Surfactants and Detergents*, 8 (2), pp. 325-329.
- <sup>167</sup>Watson C., (2002) *Standard method of test 26L: Brookfield viscometer*. Available at International Paint.
- <sup>168</sup>Cameron C., (2008) *Standard method of test 14: Determination of non-volatile content*. Available at International Paint.
- <sup>169</sup>Craighead L., (2009) *Standard method of test 25B: Relative density – Pressure weight per gallon cu*. Available at International Paint.
- <sup>170</sup>Voulvoulis N., Scrimshaw M., and Lester J., (1999) 'Alternative antifouling biocides', *Applied Organometallic Chemistry*, 13, pp. 135-143.
- <sup>171</sup>Wang J., Wang F., Yu J and Zhuang Y., (2008) 'A survey analysis of heavy metals bio-accumulation in internal organs of sea shells animal affected by the sustainable pollution of antifouling paints used for ships anchored at some domestic maritime spaces', *Chinese Science Bulletin*, 53 (6), pp. 2471-2475.
- <sup>172</sup>Craighead L., (2007) *Standard method of test 28A: Determination of fineness of grind*. Available at International Paint.
- <sup>173</sup>Watson C., (1997) *Standard method of test 56J: Semi rapid boot top cycling*. Available at International Paint.
- <sup>174</sup>Stenson P., (2009) *Standard method of test 56A: Polishing rate determination – Rotating disk method*. Available at International Paint.
- <sup>175</sup>Lee A., and Williams D., (2005) *Standard method of test 38: Statistical antifouling assessments*. Available at International Paint.
- <sup>176</sup>Thomason J., Hills J., (1998) *Immersion trials at Newtons Ferrers: Optimising facilities and procedures*. Available at International Paint.
- <sup>177</sup>Brown C., (2005) 'Epifaunal colonization of the Loch Linnhe artificial reef: Influence of substratum on epifaunal assemblage structure', *Biofouling*, 21 (2), pp. 73-85.
- <sup>178</sup>Craighead L., (2008) *Standard method of test 44: Determination of storage properties*. Available at International Paint.
- <sup>179</sup>Price C., (2002) *Milestone II Report: Development of self polishing copolymer system based on quaternary ammonium capped acid functional copolymer*. Available at International Paint.
- <sup>180</sup>Sigmaaldrich (no date) *Thermal transitions of Homopolymers: Glass transitions and Melting point*. Available at [http://www.sigmaaldrich.com/etc/medialib/docs/Aldrich/General Information/thermal transitions of homopolymers.Par.0001.File.tmp/thermal transitions of homopolymers.pdf](http://www.sigmaaldrich.com/etc/medialib/docs/Aldrich/General%20Information/thermal%20transitions%20of%20homopolymers.Par.0001.File.tmp/thermal%20transitions%20of%20homopolymers.pdf) (Accessed: 9 January 2008).
- <sup>181</sup>Wills T., (2008) *Standard operating procedure C176: Netzsch DSC 200 F3 Maia*. Available at International Paint.

- 
- <sup>182</sup>Wills T., (2008) Conversation with Paul Bassarab, 15 January.
- <sup>183</sup>Price C., (2004) *Anti-fouling compositions comprising a polymer with salt group*. World Intellectual Patent Organisation Patent no. WO/2004/018533.
- <sup>184</sup>McLearie J., Finnie A., and Andrews A., (1991) *Anti-fouling coating compositions*. World Intellectual Patent Organisation Patent no. WO/1991/009915.
- <sup>185</sup>Willett K., (2003) *Contact Angle Apparatus*. Available at International Paint.
- <sup>186</sup>Mittal K., (2003) 'Chapter 12: Characterization of surface free energies and surface chemistry of solids' in *Contact and angle, wettability and adhesion: vol 3*. VSP.
- <sup>187</sup>James M., (2009) 'Chapter 43: Nylon 6,6' in *Polymer data handbook*, 2<sup>nd</sup> ed. Oxford University Press.
- <sup>188</sup>Ko Y., Ratner B., Hoffman A., (1981) 'Characterisation of hydrophilic-hydrophobic polymer surfaces by contact angle', *Journal of Colloid and Interface Science*, 82 (1), pp. 25-37.
- <sup>189</sup>Kinlock A., (1987) 'Effect of surface roughness' in *Adhesion and Adhesive: science and technology*, Chapman and Hall.
- <sup>190</sup>ALOGPS 2.1 [computer program]. Available at Virtual computational chemistry laboratory; [www.vcclab.org](http://www.vcclab.org) (Accessed: 2 August 2010).
- <sup>191</sup>Schultz M., Finlay J., Callow M., Callow J., (2003) 'Three models to relate detachment of low form fouling at laboratory and ship scale', *Biofouling*, 19, pp 17-26.
- <sup>192</sup>Schultz M., (2007) 'Effects of coating roughness and biofouling on ships resistance and powering', *Biofouling*, 23 (5), pp 331-341.
- <sup>193</sup>European Community (2006) 'Registration, Evaluation and Authorisation of Chemicals EC 1907/2006', *Official Journal of European Communication*, L396/1.
- <sup>194</sup>European Community (2000) 'Water Framework Directive 2000/60/EC', *Official Journal of European Communication*, L327/1.
- <sup>195</sup>Ketchum B., Ferry J., and Redfield A., (1945) 'Evaluation of antifouling paints by leaching rate determinations', *Industrial and Engineering Chemistry*, 37 (5), pp. 456-460.
- <sup>196</sup>American Standard Method of Test (2007) 'D 6442-05: Test method for determination of copper release rates from antifouling coating systems in artificial seawater', London: British Standard Institution SMT.
- <sup>197</sup>Bassarab P., (2007) *Quaternary ammonium quantification method development*. Available at International Paint.
- <sup>198</sup>Fattori M., (1996) *FlowCalc* (Version A.02.07) [Computer program]. Available at Hewlett Packard.
- <sup>199</sup>Soler C., Mañes J, Picó Y (2005) 'Comparison of liquid chromatography using triple quadrupole and quadrupole ion trap mass analyzers to determine pesticide residues in oranges', *Journal of Chromatography A*, 1067, pp. 115-125.
- <sup>200</sup>Bassarab P., Williams D., Dean J., Ludkin E., Perry J., (2011) 'Determination of quaternary ammonium compounds in seawater samples by solid-phase extraction and liquid chromatography-mass spectrometry', *Journal of Chromatography A*, 1218, pp. 673-677.

---

*“A thesis has to be presentable...but don’t attach too much importance to it. If you do succeed in the sciences, you will do later on better things, and it will be of little note. If you don’t succeed...it doesn’t matter at all.”*

Paul Ehrenfest (1985) *Leidraad*, vol 2.